MASS-SPRING MODELLING OF VAULT SPRINGBOARD CONTACT

by

Michael John Harwood

A Doctoral Thesis

Submitted in partial fulfilment of the requirements for the award of
Doctor of Philosophy of Loughborough University

April 1999

ABSTRACT

MASS-SPRING MODELLING OF VAULT SPRINGBOARD CONTACT

Michael John Harwood

Loughborough University, 1999.

Vaulting is a discipline in Men's and Women's Artistic Gymnastics. While the springboard contact is not judged, the success of the rest of the vault is underpinned by it. The purpose of this study was to develop an understanding of the mechanics of the springboard contact phase of gymnastic vaulting.

An analysis of hopping in place, forward hopping and running jumps on a force platform showed that the force-mass centre displacement relationship during ground contact approximated that of a mass rebounding on a linear spring. Subsequently, two mass-spring models were developed using a symbolic mathematics package. Both models represented the gymnast as a rigid cylinder, with personalized linear and angular inertia characteristics, connected at its mass centre to a linear spring. A one spring model combined the springiness of the gymnast and the springboard in a single linear spring, while a two spring model treated them as separate linear springs.

Handspring vaults performed by an elite male gymnast at a range of approach speeds and springboard settings were analysed to provide model inputs. Springboard properties were empirically determined and revealed that the springboard stiffness varied appreciably depending upon feet contact position. Given the touchdown kinematics and takeoff angle of the gymnast, the models estimated spring stiffness and linear and angular takeoff velocities, the spring stiffness and takeoff vertical velocity estimates showing some sensitivity to spring angle at touchdown. Simulations in which the touchdown kinematics and spring stiffnesses were systematically adjusted, identified their influence on takeoff kinematics and provided an insight into the mechanics of springboard contact.

Estimated (leg) spring stiffnesses were consistent with those reported in the literature for other activities and simulation results showed that simple rebounds accounted for the majority of the takeoff velocities. Spring angle at touchdown was found to be most effective at modifying each of the takeoff variables, however to produce a selective effect on takeoff required a combination of adjustments to the touchdown. In proposing strategies for gymnasts, their ability to control each of the touchdown variables has to be considered.

Loughborough University Loughborough Leicestershire LE11 3TU UK
Switchboard: +44 (0)1509 263171 Fax: +44 (0)1509 223905

Loughborough University

CERTIFICATE OF ORIGINALITY

This is to certify that I am responsible for the work submitted in this thesis, that the original work is my own except as specified in acknowledgments or in footnotes, and that neither the thesis nor the original work contained therein has been submitted to this or any other institution for a higher degree.

M Harwood ..... (Signed)

1 April 1999 ..... (Date)

PUBLICATIONS

Refereed published abstracts

Challis, J. H., Harwood, M. J. and Kerwin, D. G. (1994) A multi-phase DLT based solution to calibrating a large volume. *Journal of Sports Sciences*, **12**, 169.

Harwood, M. J., Kerwin, D. G. and Challis, J. H. (1995) Leg spring linearity in forward hopping and running jumping by humans. In Hakkinen, K., Keskinen, K. L., Komi, P. V. and Mero, A. (Eds.) *XVth Congress of the International Society of Biomechanics Book of Abstracts* (pp.366-367). Gummerus Printing, Jyvaskyla, Finland.

ACKNOWLEDGEMENTS

I wish to express my thanks to:

My supervisor, Dr David Kerwin for his friendship, advice, encouragement and example.

Dr John Challis, for his friendship, good sense and insightful comments.

My subjects, for their efforts, time and patience.

Dr Fred Yeadon and the Loughborough biomechanics research group (past and present), for their help and support.

Gymnova, for the use of their springboard.

British Gymnastics, for the use of the National Gymnastics Centre, Lilleshall.

The staff in the Department of Civil and Building Engineering at Loughborough University, who provided assistance with the servo jack springboard testing.

My family and friends, for their encouragement and confidence in me.

DEDICATION

To my wife, Sue.

TABLE OF CONTENTS

LIST OF FIGURES

LIST OF TABLES

CHAPTER ONE
INTRODUCTION

1.1 THE AREA OF STUDY

As one might expect of a sport which has its roots in ancient Egypt and Greece (Gajdos, 1997), much has been written on the subject of artistic gymnastics. This is also true of the vault, which has been a competitive activity in a form which would be recognised today, including the springboard, since at least the 1870's (Gajdos, 1997). Springboard contact in gymnastic vaulting comes at the culmination of an approach run of up to 20 metres and sets up the entire vault. Following the final step of the run-up, the gymnast performs a low flight onto the springboard (known as the hurdle step) during which the feet are brought together for the landing on the springboard (or reuther board). The gymnast's momentum is altered during the board contact and the gymnast takes off from the board with the linear and angular momenta which go a long way to determining the success of the vault. Although the springboard contact and the flight from springboard to horse (known as the preflight) are not specifically scored by the judges, they are critical to the vault. Smith (1982, page 144) said: '...vault take-off is probably the most important 0.1 to 0.15 seconds in gymnastics.'

A survey of coaching literature (see Chapter Two, section 2.1) relating to vaulting, reveals that whilst many authors acknowledge the importance of the board contact phase, the advice to gymnasts can be imprecise and at times contradicts the results of quantitative studies. For example, the orientation of the body at touchdown with the board has been given as leaning back slightly (George, 1980; Sands, 1982), upright/vertical (Loken and Willoughby, 1977; Pflughoeft, 1989), and from leaning back to leaning forward depending on the required preflight (Stuart and Sommerville, 1980). Researchers have found that gymnasts typically contact the springboard with their bodies leaning back at about 30° to the vertical (e.g. Dillman, Cheetham and Smith, 1985; Takei, 1991).

Researchers of the mechanics of the vault have on a number of occasions noted the importance of the board contact in producing a desirable preflight, but only a small amount of research has actually focused on the board contact phase specifically. Brüggemann (1994, page 88) said of the springboard contact phase:

> Although there are detailed biomechanical studies on the vault, this most important phase in which angular momentum and quantity and direction of linear momentum are determined from the run-up momentum has received little attention.

As the quest for more difficult, and therefore potentially higher scoring, vaults continues, it is increasingly important to understand the mechanics of springboard contact, the foundation upon which the rest of the vault is built. The lack of consensus in the coaching literature on the subject of board contact technique leaves questions such as "How would a faster approach to the board affect preflight?", or "When does an increase in approach velocity become detrimental to performance?", and "If the touchdown velocity and the board stayed the same, what effect would an increased blocking angle have on preflight?" unanswered.

1.2 MODELLING PHILOSOPHY

Finding the answers to these questions by trial and error in the gymnasium can be time consuming and runs the risk of injury; furthermore, precise control over the variables would be very difficult to achieve, even with the most skilled gymnast. However, a modelling approach is ideally suited to answering such questions. A mathematical model allows control over each of the variables included in it, thereby enabling them to be adjusted independently and in combination. Identification of the influence of each variable is then possible, revealing the mechanical principles underpinning the activity and permitting specific questions to be addressed. It is important however, to evaluate the output of a model against real performances prior to its application, so that any limitations of the model predictions become apparent.

Many types of mathematical model are possible, the choice of which to adopt being dependent on the activity to be modelled and the intended use of the model. The decision to use a mass-spring system as the basis for the model of springboard contact was founded on several factors. The most obvious was the nature of the springboard, but Stuart and Sommerville (1980) also lent support for the notion of treating springboard contact as a rebound when they said 'The action [of the gymnast during board contact] is not of jumping, but of bouncing' (page 99). In addition, several studies have demonstrated similarities between aspects of the kinematics of human motion and that of mass-spring systems. For example, consideration of the mass centre kinetic and potential energy changes during running led Cavagna, Saibene and Margaria (1964) to propose a bouncing model of the human runner, and Ker, Bennett, Bibby, Kester and Alexander (1987) showed that the arches of the feet compress and recoil like a spring due to the elastic properties of the ligaments in them. Furthermore, Cavagna (1970) found that the supporting structures of the body possessed a natural frequency of vibration which he modelled as a damped spring, and in a later study he and his co-workers found that the force-mass centre displacement history

during ground contact in running was linear, like that of a Hookean spring (Cavagna, Franzetti, Heglund and Willems, 1988).

Mass-spring models of the human body have in fact already been used, for example by McMahon and his co-workers to study running (e.g. McMahon, Valiant and Frederick, 1987, McMahon and Cheng, 1990) and by Farley and her co-workers to study hopping (e.g. Farley, Blickhan, Saito and Taylor, 1991, Farley, Blickhan, and Taylor, 1985). However, these studies have generally been confined to the special case of rebounding activities where the path of the mass centre is symmetrical about the vertical, such that the body leaves the ground at the same speed at which contact was made and at the same angle past the vertical as the angle that it contacted before the vertical. This clearly is not the case in vault springboard contact, nor during the majority of rebound actions in sport and only approximately true for running. Blickhan, Friedrichs, Rebhan, Schmalz and Wank (1995) extended the mass-spring modelling approach to long jump takeoffs, but their model does not account for angular motion which is so important in gymnastic vaulting.

None of the preceding remarks are meant to imply that the gymnast and board are simply coupled masses and springs, but rather that their combined motion could be considered to behave in a way similar to such a system, and that a mass-spring system might be an appropriate simplification of the real situation. The attraction of this approach was its conceptual simplicity, which it was hoped would result in an understanding of the mechanics of the activity and make the findings readily useful to gymnasts and coaches. Throughout the thesis, the term 'rebound' or 'simple rebound' is used to indicate simulations of springboard contact in which the takeoff is solely the result of the motion of a mass-spring system on the basis of given touchdown conditions.

Vaulting springboards are manufactured to conform with Fédération Internationale de Gymnastique (FIG) specifications (FIG, 1994), but differences between the materials from which they are constructed, age and the ambient conditions at a specific venue and time, result in variations to which gymnasts have to adapt. Gymnasts subjectively assess the 'springiness' of a board before using it, but in competition they are limited to a brief practice period. A model for vault springboard contact could lead to an improved comprehension of the interaction of gymnasts and springboards, enabling ways in which gymnasts might compensate for springboard variations to be predicted. The insight gained could also enable the identification ways of achieving specific enhancements to the takeoffs in order to improve vaults or to progress to more demanding vaults.

1.3 STATEMENT OF PURPOSE AND QUESTIONS

The purpose of this study was to develop an understanding of the mechanics of the springboard contact phase of gymnastic vaulting. Using a combination of analysing real vaults and modelling of the springboard contact as a mass-spring system, the aim was to explore the relationships between hurdle and preflight kinematics as modified by the springboard contact. With this knowledge it was anticipated that the strategies a gymnast might employ to achieve desired springboard takeoffs could be predicted.

The following questions were addressed by conducting mass-spring model simulations using input data based on real vaults:

What proportion of a gymnast's linear and angular velocities at takeoff from the springboard can be accounted for by a simple rebound?

During springboard contact gymnasts extend at the ankles, knees and hips, and can use their arms to influence their takeoff. Nevertheless it was anticipated that most of the linear and angular velocities at takeoff would be produced as a result of the (predominantly horizontal) momentum of the approach run being modified by a simple rebound from the board.

To what extent does springboard stiffness affect takeoff kinematics?

Gymnasts subjectively assess, and have some control over, the stiffnesses of the springboards they use in training and competition. An evaluation of the possible magnitude of the effect of these stiffness alterations on the takeoff from the springboard was performed.

How does changing the kinematics at springboard touchdown affect the takeoff from the board?

By altering the approach to the springboard, gymnasts can alter their takeoff. The influence on takeoff of adjusting approach speed and blocking angle, independently and in combination, was investigated.

What effect does the gymnast's stiffness during springboard contact have on the takeoff from the board?

Research into running and hopping has shown that humans can adjust the overall stiffness of their legs. The extent to which the leg stiffness of the gymnast could affect the takeoff was assessed.

How can gymnasts compensate for springboard stiffness differences?

When vaulting from a springboard which has a different stiffness from those that a gymnast is used to, some alteration to the approach or board contact may be necessary in order to

achieve the desired takeoff from the board. Different mechanisms for achieving this compensation were explored.

What modifications to a gymnast's approach to and contact with the springboard would be most effective for achieving specific changes to preflight?
Whilst a number of methods for changing the takeoff from the springboard may be possible, the most effective for modifying each of the takeoff velocities was sought. The practical issues involved with these changes were also considered.

1.4 ORGANIZATION OF THE CHAPTERS

Chapter Two reviews the literature related to the theoretical and practical aspects of the study.

Chapter Three details a study conducted to evaluate the suitability of using a linear spring to represent the lower limbs in a model of rebounding activities.

Chapter Four describes the formulation of two mass-spring models: a one spring model in which the springiness of the gymnast and the springboard are treated as one, and a two spring model in which they are treated separately.

Chapter Five concerns the collection and analysis of vaulting and springboard data, which were to be used in the simulations.

Chapter Six describes the evaluation and application of the models. A series of simulations were performed to explore the mechanics of vault springboard contact and to enable the questions posed in Chapter One to be answered.

Chapter Seven discusses and summarizes the results of the study and suggests some directions for future investigations.

CHAPTER TWO
REVIEW OF LITERATURE

This chapter is divided into four main sections. The first covers the literature in coaching and research publications which concerns the springboard contact phase of gymnastic vaulting. This also includes studies of the springboard itself and studies of vaulting in general which contain specific information about the board contact phase. The second section reviews the modelling of rebound activities, from the evidence which suggested a mass-spring approach for modelling these activities, to the models themselves and the results obtained from their use. In the third section, evidence concerning the accommodation by subjects to changes in surface stiffness is reviewed, before the final section considers the variety of methods of investigation in use in biomechanics which relate to this study.

2.1 VAULT SPRINGBOARD CONTACT

Advice regarding springboard contact for vaults in coaching books and articles is based mainly on experience and observation. A brief summary of a selection from the coaching literature serves to highlight the major coaching points. These do not relate to specific vaults and span a number of years during which the scoring of vaults, regulations for run up, hand positions on the horse and flight, as well as the springboards themselves have changed (Takei, 1991).

The consensus on the hurdle step to the board is that it should be low and fast (e.g. Readhead, 1987; George, 1980; Pflughoeft, 1989). Sands (1982) also specified that the body should be rising at contact. This last point is however contradicted by the results of studies of elite gymnasts, which have found that the mass centre is falling at the point of touchdown with the springboard at slightly more than 1 $m.s^{-1}$ (see for example Takei, 1988, 1989; Takei and Kim, 1990). Foot contact position has received a variety of descriptions which apparently refer to a similar point: Warren (1972) and Loken and Willoughby (1977) talked of the point of maximum spring of the board, Sands (1982) referred to the 'sweet spot' and George (1971, page 22) elaborated a little more with '...the balls of the feet contact the "belly" of the reuter board (centre of oscillation) so that the maximum restitutional coefficient of the board can be realized'. However, neither precise details of the location of this point nor how it could be determined were given. Readhead (1987) made no mention of the point of contact with the springboard but he stressed the need to achieve consistency in the hurdle step.

According to George (1980) and Sands (1982), at springboard touchdown, the body should be leaning back slightly, while Loken and Willoughby (1977) and Pflughoeft (1989) suggested a vertical position. Warren (1972) and Stuart and Sommerville (1980) explained that the body angle at contact with the springboard determines the shape of the preflight such that leaning back leads to a slow, high trajectory, while an upright or forward leaning position leads to a fast, low flight. Mechanically, touching down at or past the vertical seems unlikely to be adopted in practice as the possibility of generating vertical velocity would be very limited and no studies of elite male gymnasts have reported body angles at springboard touchdown which were vertical or past vertical. Dillman, Cheetham and Smith (1985) reported a mean of 27.5° before the vertical for both handspring (standard deviation 3.24°) and Tsukahara vaults (standard deviation 2.29°), while Takei (1991) found that gymnasts performing handspring and salto forward tucked vaults were leaning back at 33° before the vertical (standard deviation 3°).

The patterns of arm swing and body action on the springboard seem to be fairly well agreed within the coaching literature. Arm swing should be forward and upward, although recommended timing varies, and any flexion at the ankle, knee and hip should be vigorously extended up to takeoff; Sands (1982) even suggested that the gymnast should anticipate contact and begin extension slightly before contact. Stuart and Sommerville (1980) and Pflughoeft (1989) emphasised a tensing of the body to receive the recoil of the springboard, while White (1989) advised a more active 'jump with the recoil' of the board. This latter suggestion may be useful as a coaching point but the implied notion of waiting for the recoil and then jumping with it would be difficult to achieve in a contact which lasts only around 0.10 to 0.14 seconds. Furthermore the extension of the body would increase the force applied by the gymnast to the board and hence would add to the compression or at least delay the recoil. Gymnasts could however pre-program their movements if they have knowledge of the board's performance. Good extension of the body at takeoff is generally recommended and Taylor, Bajin and Zivic (1972) found that takeoff usually occurred with the body at about ten degrees past the vertical, Takei (1991) reported approximately fifteen degrees past vertical for handspring and salto forward tucked vaults and in a study of handspring with full twist vaults (Takei, Blucker, Dunn, Myers, and Fortney, 1996) 30 to 35 degrees past vertical was common.

Hay (1993, page 314) described takeoff from the springboard as 'the most critical phase of the vault' and Smith (1982, page 144) said '...vault takeoff is probably the most important 0.1 to 0.15 seconds in gymnastics.' yet little research into the mechanics of takeoff from springboard has been reported in the scientific research literature.

Kreighbaum (1974) analysed the interaction of vaulters with a springboard which had undergone a static load-deflection calibration. Cine-film from the side view and an electro-mechanically derived deflection-time traces were recorded for eight women vaulters performing sidehorse (horse at right angles to the direction of motion) handspring vaults. Kinematic and kinetic data were calculated including estimates of segmental angular velocities and accelerations and joint torques (though precise details of the methods used were not included). Means and ranges of kinematic parameters of the mass centre are presented and the kinematics of the body segments are discussed. The deflection-time traces showed an initial peak in the first half of contact which equated to vertical forces of between 5262 and 9632 N, while second peaks were estimated to reflect forces of 2453 to 4682 N. A drawback of the study was that the estimated external forces from the board deflection traces were taken to act vertically and no estimates of the horizontal forces were made, therefore the accuracy of calculated joint torques and the total impulses must be in doubt. This is highlighted by the fact that the total impulses calculated were found not to be correlated to the vaulters' change in velocity during board contact. Furthermore the suggestion that the joint extensions should be completed **prior to** the maximum deflection of the springboard, ignores the fact that the joint extensions themselves contribute to the deflection of the board and contradicts the results of the study itself, which found that the gymnasts were at their lowest position at the peak deflection and that the submaximal peak coincided with extension of the hip, knee and ankle joints.

In a second study Kreighbaum (1979) filmed at a rate of 400 frames per second to look in detail at the undulations of the board and the foot placements when one male and one female nationally ranked American gymnast performed handsprings. The difference between the mean board contact times of the two gymnasts was reported to be 'approximately one tenth of a second' (page 26) which is rather imprecise, given the framing rate, and large, given the total springboard contact times of between 0.10 and 0.16 seconds reported in other studies for both men and women performing handspring type vaults (e.g. Nelson, Gross and Street. 1985; Takei, 1989). Qualitative descriptions of the board deflection patterns for the variety of foot placements observed, illustrated the complex nature of the board's movements. especially when contact was not made in the centre of the board. A smooth deflection pattern was assumed to indicate more efficient [*sic*] board use and this was observed when an even foot placement in the mid-region of the board was achieved. However, it is clear from the study that neither gymnast seemed able to reproduce foot contact positions consistently.

The Fédération Internationale de Gymnastique (FIG) have developed a series testing procedures for gymnastic equipment to which manufacturers must subject their products

before they may be used in FIG competition (Schweizer, 1985; FIG, 1994). For the vault springboard the test consists of dropping a 20 kg testing body with a 0.10 m contact diameter, from a height of 0.80 m (or slightly more, in order to achieve an impact velocity of -3.96 $m.s^{-1}$, equivalent to a frictionless drop from 0.80 m) using a custom built testing rig. Ten drops are made in each of five locations on the mid-line of the board surface, 0.75 to 0.95 m from the run-up (near) end of the board in 0.05 m intervals (positions 1 to 5). A further ten drops are made at each of two locations 0.15 m each side of the board's mid-line, 0.95 m from the near end (positions 6 and 7). During the testing the ambient temperature must be 20 ± 2° Celsius. A Kistler accelerometer is attached to the test body and the springboard itself is placed on two Kistler force plates, however the precise mounting details and sampling information are not detailed.

Three parameters are measured for the FIG norm test: the deformation of the board, the height of rebound of the test body and the maximum force during the impact. These are calculated from the accelerometer and the force plate records, although other than the fact that the mean values from drops 3 to 10 in each position are used, no details of the calculations are given. The results for each parameter from all seven positions must conform to set criteria and the results must not vary between positions by more than set amounts (Table 2.1). The three parameters are an attempt to quantify in a general way acceptable board stiffness and damping: the maximum force and deformation are facets of stiffness, while rebound height gives some information about damping. It is noted that for vaulting springboards a high rebound height is required (low damping), while the stiffness should be such that the stress on the gymnast is not great. While the norms do not quote stiffness in standard units, estimates can be made by dividing the maximum allowable impact force by the extremes of the range of allowable deformations; these calculations give a stiffness range of approximately 57 to 65 $kN.m^{-1}$. A damping estimate is not so easily obtained but the range of acceptable rebound heights indicate a loss of energy of between 49 and 64%, which seems to be rather high.

Kerwin & Littlechild (1989) examined the potential for energy storage and return by springboards using a static loading/unloading protocol. They devised a cantilever system for producing loads up to 6000 N in 125 N increments while measuring the board deflection, in three different positions along the middle of the surface (0.75, 0.85 and 0.95 m from the near edge of the springboard), similar to the FIG testing procedure (FIG, 1994). They found that approximately 300 J were stored at the full loading, though there was some hysteresis which meant that not all of this energy was returned (20% lost for loading-unloading up to 5000 N, but not quantified for the 6000 N loadings). This is considerably better than the FIG norms

Table 2.1. FIG springboard norm testing criteria (FIG, 1994).

	Deformation (m)	Rebound height (m)	Max. impact force (N)
Norm for positions 1-5	0.070-0.080	0.285-0.405	< 4550
Difference between positions 1-5	< 0.015	< 0.120	---
Difference between positions 6 & 7	< 0.004	< 0.025	< 150

would suggest should be the case under dynamic conditions (FIG, 1994). They also found that the load-deflection curves were linear up to around 3500 N and showed some non-linearity above this load, though the degree was dependent on the loading position (only the loading position 0.95 m from the near end of the board demonstrated a substantial increase in slope). Estimates from their load-deflection graphs indicate board stiffness of around 60.00 to 68.75 $kN.m^{-1}$ which is in agreement with estimates from the FIG norms (FIG, 1994).

Other studies into vaulting have not focused specifically on springboard contact but several have reported information on springboard touchdown and takeoff kinematics, and some of these have noted the importance of the springboard takeoff to overall success. The studies of Handspring and Handspring-based vaults by Takei (1988, 1989 and 1991), Takei and Kim (1990) and Takei *et al.* (1996) are the most comprehensive yet into the kinematics of men's vaulting. Takei (1988,1989) and Takei and Kim (1990) developed a deterministic model of vaulting based on the method of Hay and Reid (1982) which was used to identify mechanical factors determining performance and these factors were then measured during competitions using film analysis. Correlations were then performed between each measured variable and the judged score of the vault. The later studies (Takei, 1991; Takei *et al.*, 1996) compared the best and worst performers of the compulsory vault at the 1988 and 1992 Olympic Games respectively to determine which factors were significantly different between the groups.

In all of these studies by Takei and his colleagues, the horizontal velocity of the gymnast's mass centre at board takeoff was found to be significantly correlated with score (Takei, 1988, 1989; Takei and Kim, 1990) or significantly higher for the higher scoring gymnasts (Takei, 1991; Takei *et al.*, 1996). Horizontal velocity in the hurdle and angular momentum in preflight were also identified as being of importance in several of the studies. Takei *et al.* (1996) stated their belief that performance differences in the latter phases of the vaults were

caused by differences in the technique used in the earlier phases. Brüggemann and Nissinen (1981, cited in Brüggemann, 1987) found that the horizontal velocity of the centre of mass during the approach was directly related to performance, as was high angular momentum at board takeoff and a short preflight. As part of his review of gymnastics research Brüggemann (1994, page 88) nicely summarized the importance of the springboard contact by stating:

> The takeoff from the board becomes the performance limiting instant in which the kinetic energy provided in the run-up is transformed into the linear and angular requirements.

Care must however be exercised when interpreting the results of statistical studies within homogeneous groups and applying them to other groups. Important factors contributing to high scores within an elite group may be less important to less skilled gymnasts and the fundamental features of successful vaults should be so well established in the elite performer so as not to vary greatly within the elite group and therefore not correlate highly with score. This could be true of the studies by Takei (1988, 1989) and Takei and Kim (1990), although they might argue that they studied the full range of abilities within a large (but still elite) population (41, 40 and 51 gymnasts respectively in each of the studies). Brüggemann and Nissinen (1981, cited in Brüggemann, 1987) did not have this problem because they looked at the mean values of the measured variables of three groups of differing ability and compared them with the group's ranking. Another problem is that the overall score takes into account factors other than those that were measured in these studies, such as risk, originality and virtuosity. The studies by Takei and his colleagues mentioned this explicitly when developing their deterministic model of performance and Dainis (1979) took this into account by having the vaults studied scored independently only on the basis of variables which were measured. Other studies (e.g. Cheetham, 1982, Draper, 1981) performed correlations with postflight height and/or distance, which were assumed to indicate the overall score.

Dainis (1981) developed a mathematical model for handspring vaulting covering the period from springboard takeoff to landing following the postflight. The model was evaluated using the results of an analysis of four vaults by advanced female gymnasts. The results of varying a range of selected parameters in the model indicated that the takeoff velocity from the springboard and preflight distance (springboard takeoff to horse touchdown) were the principal variables influencing the outcome of the vaults.

2.1.1 SUMMARY OF VAULT SPRINGBOARD CONTACT

The advice found in coaching books and articles regarding springboard contact is rather vague and at times contradicts the findings published in scientific papers. This should not be that surprising since the duration of contact with the board is typically only 0.10 to 0.14 seconds, making direct observation of the detail impossible. Few researchers have investigated the properties of springboards, though a protocol for the testing of springboards has been developed, and most studies of vaulting have focused on the preflight, horse contact and postflight rather than board contact. Nevertheless, several authors have noted the importance of the board contact phase to the overall success of the vault.

2.2 MODELLING REBOUND ACTIVITIES

The possibility of storage and recovery of elastic energy in the legs of animals during locomotion has been recognized for many years. This, along with the fact that the pattern of motion of the mass centre in running and hopping is like that of a bouncing ball (Cavagna, Saibene and Margaria, 1964), has led to the development of a number of models which represent the movement patterns of these activities as rebounding mass-spring systems. This section reviews the evidence that has led to the development of mass-spring models of rebound activities and the models themselves.

2.2.1 EVIDENCE FOR MODELLING WITH SPRINGS

2.2.1.1 Muscle and tendon studies

Research into the operation of muscle and tendon in a variety of animals has suggested the sites for energy storage and given an indication of the magnitude of the energy stored and then returned.

Alexander (1974) conducted a detailed study of the mechanics of jumping by a dog and Alexander and Vernon (1975) used similar techniques to study hopping by kangaroos and wallabies. By using dissection and X-radiography in conjunction with cine-film and force plate data they were able to perform inverse dynamics calculations of the force-length relationships of the plantaris and gastrocnemius muscle-tendon complexes during ground contact. These relationships were reasonably linear with the force the muscles exerted rising as the muscles and tendons lengthened and then falling as they shortened, in much the same way as a linear spring being stretched and allowed to recoil. Alexander and Vernon (1975) noted that the overall compliance of the muscle-tendon complex could be considered the sum of the compliance of the truly elastic materials (mainly tendon) and the 'pseudocompliance' of the muscles as they actively lengthened and then shortened. Furthermore, Alexander and

Vernon (1975) estimated that the elastic recoil of the tendons could supply around 40% of the positive work required by a wallaby during the contact phase at 'moderate speeds'.

Morgan, Proske and Warren (1978) attempted to determine directly whether the tendons and muscles involved in hopping (in this case by wallabies) behaved as elastic structures, as had previously been suggested (e.g. Alexander and Vernon, 1975). Using an anaesthetized wallaby they separated the medial head of the gastrocnemius muscle and tendon from the surrounding tissue to allow them to measure tension and length changes during a rapid stretches of the muscle while they stimulated it to tetanus. When measuring length changes involving the whole muscle-tendon complex, they estimated approximately eight times as much stretch in the tendon as in the muscle tissue for maximal isometric activity. The tendon length-tension relationship was linear over a wide range of forces, however they found that muscle tissue did not follow this pattern once the stretch of the muscle exceeded about 1 mm. In fact they estimated approximately 40% energy dissipation due to forced cross-bridge detachment during the eccentric phase of the ground contact in their study.

Drawing together results from previous studies Alexander and Bennet-Clark (1977) estimated that for humans running, the Achilles tendon could store five to ten times as much strain energy as the knee and ankle extensor muscles themselves (running at 3.9 $m.s^{-1}$), and for wallabies hopping at 2.4 $m.s^{-1}$ the ratio was similar, at between six and thirteen to one. These estimates, however, assumed a linear length-tension relationship for both tendon and muscle which the results of Morgan *et al.* (1978) would not support for large stretches of the muscle. Alexander and Bennet-Clark (1977) were unable to estimate the storage in the human patellar tendon but expected it also to be substantial, thereby increasing the difference in energy storage between the tendons and muscles of the legs. However by 1988 Alexander had changed his mind about the role of the patellar tendon when he stated that he suspected that 'it may be relatively unimportant' (Alexander, 1988, page 20).

Ker, Bennett, Bibby, Kester and Alexander (1987) revised downward the estimate by Alexander and Bennet-Clark (1977) of the strain energy stored in the Achilles tendon during running (from 42 to 35 J per step), but Ker *et al.*'s results from studies of amputated human feet showed that the longitudinal arch had elastic properties which could contribute to the energy efficiency of locomotion. Combining the estimated energy storage in the arch of the foot (17 J) and the revised storage by the Achilles tendon gave a higher total than Alexander and Bennet-Clark's original estimate and amounted to approximately 52% of the energy required in each step (although the method of calculating the energy required per step could affect this figure; see section 2.2.1.2).

Griffiths (1989) studied the medial head of the gastrocnemius muscle and its tendon in freely hopping wallabies. He found the musculo-tendinous force-length graph to be linear over a variety of hopping speeds in agreement with previous studies (e.g. Alexander and Vernon, 1975; Morgan *et al.*, 1978). However he calculated that while the amount of energy stored in the tendon increased as hopping speed increased, the *proportion* of the positive work performed by the return of stored elastic energy did not increase. Nevertheless a considerable amount of energy was stored and returned, estimated to be 41% in this case, comparable with the 39% estimated by Alexander and Vernon (1975).

Roberts, Marsh, Weyand and Taylor (1997) measured directly the tendon force and muscle fibre length in the lateral gastrocnemius of turkeys during level running. They found that the muscle shortened little during ground contact, providing less than 40% of the positive work done by the muscle-tendon complex and deduced therefore that energy stored and then released by the tendon (including aponeurosis) did in excess of 60% of the work. This conclusion seems to fit very well with the estimate by Morgan *et al.* (1978) of 40% energy loss due to work being done on muscle during the eccentric phase of ground contact in hopping wallabies, although Alexander and Vernon (1975) and Griffiths (1989) estimated only about 40% return of stored energy for hopping wallabies.

While the species, methodologies and absolute figures have varied in the above studies, a number of points of consensus emerge:

- there is considerable scope for the storage and return of energy by muscle and tendon, though primarily by tendon;
- this stored and returned energy could account for between 40% and 60% of the positive work done in a ground contact;
- the force-length relationship of combined muscle and tendon is, in some muscles at least, linear over a range of speeds of locomotion.

A question may be raised regarding whether human muscle and tendon can be assumed to behave as do those of other animals, but there are precedents for this assumption. A great deal of the research performed to elucidate the function of muscle and tendon has been conducted for example on frog, toad and cat tissue (e.g. Hill, 1950; Wilkie, 1956; Griffiths, 1991), but the findings are still generalized to the performance of other vertebrates, including humans. Alexander (1984) clearly supports the idea for tendon similarity by stating, `The properties of tendon are more or less the same in all mammals` (page 353).

Assuming a reasonable degree of similarity of the properties of muscle and tendon between vertebrates, a more important issue is the proportion of each type of tissue in the muscle-tendon units involved in locomotion. Given the preceding evidence for tendon being better able to store and return energy than muscle, muscle-tendon units which have relatively short muscle fibres and long tendons are better able to store energy, providing that they are stretched during the first part of ground contact and recoil as the body rises to leave the ground (Alexander and Bennet-Clark, 1977). In humans the knee and ankle extensors do just this (Alexander, 1984), though as previously mentioned the potential of the knee extensors is debatable. The ligaments in the arches of the feet also contribute to storing and returning elastic energy. Morgan *et al.* (1978) artificially reduced the tendon length of the medial gastrocnemius in wallabies and found that muscle length changes accounted for proportionately more of the movement than tendon during stretching when compared with stretches of the normal length muscle-tendon complex. The result was greater energy dissipation by the muscle and therefore the longer the tendon in relation to the muscle, the greater the potential efficiency of locomotion.

2.2.1.2 Efficiency studies

Studies of the mechanical efficiency of humans and other animals have shown that the nature of the activity affects the efficiency of the subject. For example, humans are more efficient when they run normally than when they walk or cycle normally. Some researchers have concluded that this efficiency improvement is due to the storage and return of energy by elastic structures within the body which is only possible in certain activities.

Cavagna, Saibene and Margaria (1964) calculated the mechanical efficiency of positive work in running at up to 5.6 $m.s^{-1}$ to be between 0.4 and 0.5, compared with values of 0.25 found in earlier uphill walking studies (by Margaria). This led them to conclude that in running, up to half of the positive mechanical work was being contributed by the liberation of elastic strain energy. This energy is stored in the legs during the first part of the stance, when the hip, knee and ankle flex, and then released as the legs extend.

Cavagna (1970) performed a study to calculate the amount of elastic energy stored in human legs when subjects made small jumps to land on the balls of their feet with stiff, straight legs and ankles plantarflexed. The subjects made one and two legged landings onto a force plate and the stiffness and damping of the hypothesized elastic structures were calculated from the vertical force traces, which were modelled as damped harmonic oscillations. The results of calculations when the load on the legs approximated those in running indicated that an appreciable part (anything from 43% to 75%) of the positive external work of level running

might be stored and returned by elasticity in the legs. However the force traces look similar to those which might be obtained in any landing, without being constrained in the way that they were in this study. There is no indication that restrictions were placed on arm movements during landing and some of the oscillation would undoubtedly have been derived from the motion of the soft tissue of the body, not just the 'springiness' of the elastic structures at the ankle.

Thys, Faraggiana and Margaria (1972) measured the positive mechanical work done on the mass centre and the oxygen consumption when subjects performed a standing deep knee flexion-extension exercise. Two conditions were studied over continuous 6 minute periods: one in which extension immediately followed flexion ('rebound'), and one in which flexion and extension were separated by an interval of 1.5 seconds. A standing pause was necessary in the rebound condition so that the frequency of the movements was the same in both conditions (20 cycles per minute), and therefore the total amount of mechanical work done was approximately equivalent. Their results showed that the oxygen consumption was on average 22% less in the rebound condition, an average increase in efficiency of 37%, and the absolute efficiency values were 0.26 and 0.19 for the rebound and no rebound cases respectively. The rebound efficiency of 0.26 might have been expected to be higher in the light of the value of 0.4 to 0.5 found in running by Cavagna *et al.* (1964), but Thys *et al.* (1972) suggested that this difference was due to the range and rate of movement being less than optimal in their experiment. It is also likely that the oxygen expenditure during the pauses (approximately 70-80% of the duration of the cycle) would reduce the efficiency estimate as it increases the denominator in the calculation. Nevertheless, the improved efficiency in the rebound condition was interpreted as supporting the contention that some positive work was being derived from the release of energy stored in elastic structures of the leg when shortening immediately followed stretching.

Dawson and Taylor (1973) investigated the energetic cost of locomotion by kangaroos at speeds up to 22 $km.h^{-1}$ (6.1 $m.s^{-1}$), by measuring their rate of oxygen consumption while hopping on a motorized treadmill. The characteristic bipedal hopping commenced at between 6 and 7 $km.h^{-1}$ (1.7 to 1.9 $m.s^{-1}$) and oxygen consumption showed slight decreases as hopping speeds increased from 7 to 22 $km.h^{-1}$ (1.9 to 6.1 $m.s^{-1}$). Since the oxygen consumptions rapidly reached constant levels at each speed and there was a lack of an appreciable oxygen debt following the runs, Dawson and Taylor (1973) assumed that steady state had been achieved and that all energy needs were being met aerobically. Over the range of speeds, the hopping frequency remained approximately constant, so the increases in speed were achieved by increasing the distance per hop. Therefore, despite the increased speed, the

energy cost per hop was nearly constant, and it was suggested that this was due to increasing amounts of energy storage and recovery in elastic structures at higher speeds. Similarly, Cavagna and Kaneko (1977) found that the efficiency of positive work increased with the speed when humans run. Their subjects ran over short distances at speeds up to 9.17 $m.s^{-1}$ and the efficiencies reached 0.70 to 0.80 at the highest speeds, which they took to suggest that most of the positive work was coming from the release of stored elastic energy. However, at these higher speeds it is inconceivable that the subjects would be deriving their energy requirements solely from aerobic metabolism (in any case, Cavagna and Kaneko only estimated the metabolic costs), which makes the efficiency calculation dubious.

Alexander and Vernon (1975) suggested that the slight fall in oxygen consumption as hopping speed increased found by Dawson and Taylor (1973) might be explained by the fact that as the speed increases the muscle-tendon forces increase and the energy which can be stored in linearly elastic materials increases in proportion to the square of the force the materials are exerting. Therefore much more energy should be available from elastic storage at higher speeds of locomotion, limiting the rise in metabolic cost, or even reducing it. This hypothesis would also apply to the results of Cavagna and Kaneko (1977). However the discovery by Griffiths (1989) that, in the medial gastrocnemius of hopping wallabies at least, the proportion of the positive work performed by the return of stored elastic energy did not increase as hopping speed increased, even though the total amount of energy stored in the tendon did increase, casts doubts on this hypothesis.

A problem with comparing mechanical efficiency studies is the variety of methods used for the calculations; both the numerator, mechanical work done, and the denominator, metabolic cost, have been calculated in different ways. Williams and Cavanagh (1983) provided a detailed review of the methods which had been used in various studies and calculated mechanical work and power in distance running using a selection of calculation methods and found efficiencies ranging between 0.31 and 1.97! In 1985, Cavanagh and Kram introduced a symposium of papers in Medicine and Science in Sports and Exercise on human efficiency estimation that identified the issues and some solutions to the problem (Volume 17, Number 3).

Many studies have estimated only the positive mechanical work done in the activity. Thys, Faraggiana and Margaria (1972) in fact only measured the positive work done on the mass centre, thus neglecting any negative, internal and non-vertical positive work (though in their knee bend activity the latter two were likely to be small contributions). Studies by Cavagna and his colleagues (e.g. Cavagna, Saibene and Margaria, 1964; Cavagna and Kaneko, 1977) also calculated only the positive mechanical work though they did estimate both external and

internal positive work. However their methods were not entirely rigorous in that they measured internal energy changes with respect to the proximal joints of the limbs rather than an inertia reference frame (Smith, 1975) and did not calculate metabolic cost concurrently, but used data from previous studies.

The extent to which energy can flow between segments and thereby influence the estimate of the mechanical work done is also an issue. Cavagna, Saibene and Margaria (1964) did not consider the effect of allowing total transfer between segments to be appreciable (although it amounted to differences of 10 to 25%). Williams and Cavanagh (1983) however found that in a cycle of running allowing no energy transfer within or between segments gave a total mechanical work done nearly four and a half times greater than when complete energy transfer was allowed. Willems, Cavagna and Heglund (1995) considered that only energy transfer within segment and between segments of the same limb should be included when estimating total mechanical work done.

Despite the difficulty of calculating mechanical efficiency accurately, where studies that have used the same methods reveal efficiency differences, the notion that an elastic mechanism might be the reason for the efficiency improvements in some activities is still attractive. However, the role of elastic elements has been questioned. Ingen Schenau (1984) stated that while he did not question the existence of elastic elements, he was not convinced of the significance of their contribution to performance. He proposed a model which saw the role of pre-stretch in an activity as being to take up any slack in the cross-bridges of the muscle rather than to store energy by stretching elastic tissues. The question of the role of elastic energy was debated at length in a target issue of the Journal of Applied Biomechanics (Volume 13, Number 4, 1997).

Although there is a debate over whether efficiency improvements are attributable to elastic energy storage and return, it is still the case that the studies which led to the proposal of this mechanism were behind the idea of mass-spring models for running and hopping. These models have subsequently proved useful in investigating the mechanics of these activities.

2.2.1.3 Whole body studies

Despite the evidence of an elastic mechanism based on energy expenditure studies, Cavagna, Franzetti, Heglund and Willems (1988, page 82) noted that, 'Although the bouncing mechanism of running is now widely accepted, it is poorly substantiated by experimental evidence.' To attempt to rectify this situation they analysed men and other animals running, trotting or hopping over a force plate. Some doubt exists over the precision of their data since they admit to considerable noise in their force plate records and went through a rather

convoluted route to obtain their acceleration and displacement data. Bearing this in mind, they found the relationship between the mass centre vertical acceleration and vertical displacement during the 'effective contact time' (the period between maximum downward vertical velocity and maximum upward vertical velocity) to be approximately linear, thereby supporting the contention that the vertical stiffness of the body could be represented as a Hookean spring. The slope of the acceleration-displacement graph during the effective contact time they then termed the 'effective vertical stiffness'. For humans running, the mean stiffness for the subjects was found to be approximately constant (very roughly 25 $kN.m^{-1}$, estimating from their graphs) up to about 11 $km.h^{-1}$ (3 $m.s^{-1}$) and then to increase with speed (up to, again roughly, 75 $kN.m^{-1}$ at 7 $m.s^{-1}$).

In a similar way Farley, Blickhan, Saito and Taylor (1991) investigated two-footed stationary hopping, two-footed stationary hopping at maximum height and two-footed forward hopping. They found that graphs of vertical ground reaction force against mass centre displacement during ground contact were approximately linear for hopping at and above their subjects' preferred frequency (all chose about 2.2 hops per second) and over the full range of forward hopping speeds (0.5 to 3.0 $m.s^{-1}$). Unlike Cavagna *et al.* (1988) they calculated the vertical stiffnesses, k, of the subjects by modelling them as linear mass-spring systems and using the vertical ground reaction force histories to determine the half period, $T/2$, of the oscillation (i.e. the time for which the force exceeded body weight, $m.g$):

$$k = m.\omega^2$$

$$\text{where } \omega = \frac{2.\pi}{T}$$

Vertical stiffness increased with frequency in stationary hopping and with speed in forward hopping, the range in both cases being from around 18 $kN.m^{-1}$ to 50 $kN.m^{-1}$ at each frequency/speed of the activities.

He, Kram and McMahon (1991) produced vertical force-displacement graphs for subjects running on a treadmill at speeds ranging from 2 to 6 $m.s^{-1}$ and at 3 $m.s^{-1}$ under simulated low gravity conditions (0.2 to 1.0 times normal gravity). Under all conditions, they found the force-displacement graphs to be approximately linear, particularly from mid-stance to takeoff. When the proportion of gravity was varied, the slopes of the graphs (i.e. the effective stiffness) remained reasonably constant, while as running speed was increased the slopes increased. Farley and González (1996) presented vertical force-displacement graphs for subjects running on a treadmill at one speed (2.5 $m.s^{-1}$) but a range of stride frequencies

(from 26% below to 36% above the subjects' preferred frequencies), which again were approximately linear, though the slopes (stiffnesses) increased as stride frequency increased.

A number of studies have therefore presented data derived from the vertical motion of the whole body which supports the principle of representing at least the vertical component of human running and hopping as a mass bouncing on a linear spring. For hopping this model would seem only to be valid when the hopping frequency is above about 2 Hz (Farley *et al.*, 1991) and it is likely that if very slow running stride frequencies/speeds were investigated a similar deviation from the linear spring model would be observed (since the ground contacts would be unlike a pre-programmed rebound and more under conscious control).

2.2.2 MASS-SPRING MODELS

A number of studies have been conducted in which the mechanics of the whole body while hopping and/or running has been investigated with the aid of simple models. Based on the evidence presented above, most of these models have been simple mass-spring systems comprising a point mass representing the whole body mass and a massless linear spring representing the leg or legs in contact with the ground. In some models the spring has been considered only to act vertically (whether the mass moves forward or not) in which case the terms vertical spring and vertical stiffness have been used, while other models have had the spring act along a line from the mass to the point of contact with the ground, calling the spring in this case the leg spring and talking of the leg stiffness. Some studies have considered both the vertical and leg springs, while for stationary hopping the two are identical.

Mass-spring models usually require estimates of the spring stiffness and a number of methods have been used to make these estimates. As previously mentioned, Cavagna *et al.* (1988) calculated the slope of the mass centre vertical displacement-acceleration graph during the effective contact time to estimate the vertical stiffness of the subjects, while Farley *et al.* (1991) used the force history to determine the natural half period of the assumed mass-spring system and calculated the vertical stiffness from this.

Greene and McMahon (1979) calculated vertical stiffness values for human subjects over a range of fixed knee angles and while supporting additional loads on their shoulders. The subjects' stiffnesses were calculated by numerical solution of an equation representing the oscillation of a two mass, two spring system (the man being one mass-spring, and the board being the other), using input data obtained when subjects performed small amplitude oscillations while standing on spruce boards of known stiffness supported at each end. They found that while subject stiffness was independent of the stiffness of the supporting boards, it

decreased as the knees were bent more, and increased slightly with increasing load. However they noted that bouncing on boards at a relatively fixed knee angle was not necessarily comparable to running where the knee angle changes continuously.

McMahon, Valiant and Frederick (1987) overcame this shortcoming by calculating vertical stiffness during running. They were interested in how man's vertical stiffness affected parameters such as foot contact time, step length and vertical ground reaction force at mid-stance. Subjects ran over a force plate at a variety of speeds and with varying amounts of maximum knee flexion. The amount of knee flexion, as measured by the maximum thigh angle (the angle between the thigh and the horizontal at mid-stance), was used in an attempt to control vertical stiffness. Stiffness estimates were obtained by numerical solution of equations of motion representing a mass-spring system, given the initial vertical landing velocity and time of ground contact which were obtained from the force history. They found that increasing the amount of knee flexion reduced the vertical stiffness of the body, but to get good agreement between the theoretical and the experimentally observed vertical stiffness-thigh angle relationship, the model was augmented with a constant stiffness spring at the hip, in series with the leg spring. This second spring accounted for the part of vertical stiffness not affected by thigh angle (also noted by Greene & McMahon, 1979).

Siegler, Seliktar and Hyman (1982) proposed that the stiffness of the leg could be calculated by dividing the change in ground reaction force by the corresponding change in hip to foot distance. They were studying walking (not really a rebounding type of activity) and found this stiffness to vary throughout ground contact, so they calculated the average as a representative value. In a similar way Farley, Blickhan and Taylor (1985) used the peak ground reaction force-maximum mass centre displacement ratio to calculate what was essentially the vertical spring stiffness for a linear mass-spring model of human hopping in place. Where the force-displacement relationship is approximately linear (as in hopping, but less so in walking), this method is likely to give similar results to the linear regression method of Cavagna *et al.* (1988). Farley *et al.* (1991), Farley, Glasheen and McMahon (1993), and Farley and González (1996) calculated **leg** stiffness in a similar way, by dividing the change in leg length from touchdown to mid-stance (when the hip is vertically above the point of contact) by peak vertical ground reaction force.

McMahon and his co-workers have regularly used mass-spring models to investigate running gaits in man and other mammals. McMahon (1985) applied such a model to a number of patterns of biped and quadruped locomotion. The model was used to make predictions regarding which gait should be preferred if criteria, for example improving smoothness of ride, travelling at a given speed, or reducing energy cost, were chosen. Although the model

contained a number of gross simplifications and only represented vertical motion, its predictions were not greatly affected when modifications were made to imitate more closely real conditions.

McMahon and Cheng (1990) investigated the relationship between leg spring stiffness and forward running speed, using an undamped, linear mass-spring model. As with most models of running and hopping, their model assumed the ground contact to be symmetrical about mid-stance (i.e. at takeoff compared with touchdown: the mass centre vertical velocity was exactly reversed, the mass centre horizontal velocity was exactly the same and the mid-foot to mass centre line was as far past the vertical as it had been to the vertical). They explained that for given touchdown velocity and spring angle only one **leg** stiffness would result in the correct takeoff velocity and angle (too stiff and takeoff occurs too soon, too soft and takeoff occurs too late). The model equations of motion were solved numerically and the appropriate leg stiffness was found by iteration. Simulations based on an 'average' man illustrated the effects on one variable if another was systematically varied, while the others were fixed. The model predicted leg stiffness to be an approximately linear function of touchdown horizontal and vertical velocities when the touchdown and takeoff leg angle was held constant. However, a *constant* leg stiffness could account for the patterns of stride and step length changes as running speed increased, if other parameters (e.g. initial leg angle) were allowed to change. Alexander (1990a) also suggested that if suitable leg angles were chosen for a given speed, a constant tendon stiffness may be found which allowed leg muscles to act isometrically throughout ground contact. McMahon and Cheng (1990) evaluated their model by comparing predictions with the experimental results from the literature, showing that the model displayed 'generally good agreement' with mass centre vertical acceleration-displacement graphs of Cavagna *et al.* (1988), and that the ground contact time predictions as knee flexion and vertical velocity at touchdown were altered were 'in agreement with' the findings of McMahon *et al.* (1987). The level of agreement was not actually quantified.

He, Kram and McMahon (1991) developed a crude method of simulating low gravity conditions (the trunk was partially supported, but the limbs were not) to see how leg spring stiffness changed as speed and 'gravity' varied. They calculated the vertical leg stiffness by dividing the change in vertical force by the change in vertical mass centre displacement, and leg stiffness from the maximum vertical force divided by the change in leg length. In common with McMahon and Cheng (1990) they found **leg** stiffness to be roughly constant regardless of speed and they also found it to be unaffected by the fraction of 'gravity' acting, though as mentioned previously, the **vertical** stiffness was constant over different fractions of gravity but increased as running speed increased. Farley *et al.* (1993) also found leg

stiffness to be independent of speed for dogs, goats, horses and red kangaroos trotting or hopping.

Several studies of human hopping and running have been conducted by Farley and her colleagues in which the body was modelled as a linear mass-spring system (Farley, Blickhan and Taylor, 1985; Farley *et al.*, 1991; Farley and González, 1996; Ferris and Farley, 1997). These studies have investigated the mechanics of hopping and running, and in particular how hopping/stride frequency is dependent on the spring-like behaviour of the musculo-skeletal system of the legs. They also confirmed the ability of humans to alter appreciably their stiffness: over a range of about 18 to 50 $kN.m^{-1}$ in stationary and forward hopping (Farley *et al.*, 1991), 7 to 16.3 $kN.m^{-1}$ in running at different stride frequencies (Farley and González, 1996) and 20 to 55 $kN.m^{-1}$ when hopping at 2 Hz on a surface with variable stiffness (Ferris and Farley, 1997). In hopping at 3.2 Hz on a compliant surface Ferris and Farley (1997) found that leg stiffness could reach in excess of 120 $kN.m^{-1}$ (see section2.3 below). While these studies modelled humans as mass-spring systems, they did not use the models to make predictions, only as a basis for the estimation of the stiffnesses.

Blickhan (1989) used a simple mass-spring model of hopping and running to show that despite the variety of theoretically possible bouncing patterns, the constraints imposed by the human body (e.g. peak ground reaction forces, maximum vertical displacement of the mass centre during ground contact) make hopping and running only possible within quite a narrow parameter space. The model predictions were compared with data from the literature: for example for stationary hopping the contact time, peak ground reaction force, maximum mass centre displacement during contact and stiffness agreed to within 20% with the results of Farley *et al.* (1985), while for running the predicted stiffnesses are 'of the correct magnitude' when compared with McMahon *et al.* (1987) and the mass centre energetics are said to be predicted correctly (though this is not quantified). Blickhan (1989) makes the point that the predictions for hopping in place:

> ... do not depend on finding a linear elastic spring in the musculo-skeletal system. It is sufficient that the control of the musculo-skeletal system results in a nearly spring-like behaviour during ground contact. (page 1222)

Blickhan and his colleagues have more recently extended the application of mass-spring models to investigate long jumping (Blickhan, Friedrichs, Rebhan, Schmalz and Wank, 1995; Seyfarth, Friedrichs, Wank and Blickhan, 1996). Blickhan *et al.* (1995) allowed the spring stiffness to vary during contact by making the natural length of the spring a function of leg angle, while Seyfarth *et al.* (1996) added a second mass which was connected to the

leg by a frictionless joint and non-linear damped spring element. The variable spring seems to have enabled the takeoff position of the mass centre to match that of real long jumpers better and the additional mass was included to improve the fit of the predicted ground reaction forces to observed data. These studies have only been published as abstracts, therefore details are incomplete.

Alexander and Vernon (1975) developed a model to look at the energetics of hopping by kangaroos in order to investigate hopping technique. Rather than calculating the spring stiffness from force plate data or by trial and error (e.g. Farley *et al.*, 1991; McMahon and Cheng, 1990) they modelled the vertical ground reaction force as a sinusoidal function of time. This mimicked quite well actual force histories and stiffness could be calculated directly from the mass centre kinematics. Some evaluation of the model was attempted by comparing the predicted and actual mass centre accelerations graphically, and the positive energy changes during a hop numerically (from perfect agreement to a 33% discrepancy). The larger discrepancy was explained by the fact that the trunk of the animal is not rigid as had been assumed for modelling purposes. Luhtanen and Komi (1980) used Alexander and Vernon's model when investigating running, long jumping and triple jumping, though they calculated separate stiffnesses for the first (eccentric) and second (concentric) parts of the ground contacts to account for the lack of symmetry, particularly in the jumps. They found that while the concentric stiffnesses where approximately constant, the eccentric stiffnesses increased with speed and were always greater than those in the concentric phase.

Table 2.2 summarizes the stiffnesses which have been calculated for humans in the studies above. In many cases these have been estimated from graphs in these papers and may represent mean rather than individual data. It is interesting to note that with one exception (the eccentric leg stiffness for long jumping calculated by Luhtanen and Komi, 1980) all stiffnesses are of about the same order of magnitude.

The use of mass-spring models for rebounding activities has not been entirely restricted to modelling the whole body, they have also been used to represent the surfaces with which athletes interact. For example, McMahon and Greene (1979) modelled the running track as mass-spring system when looking at the influence of track stiffness on running performance. Empirical load-deflection graphs of the different tracks they constructed for the study were non-linear so representative track stiffnesses were estimated by finding the slope of the curves at the estimated mean load during foot contact and at one body weight. The influence of track mass on the results of the study was theoretically demonstrated to be negligible and was therefore ignored. In this study the runners were also modelled as mass-spring systems

Table 2.2. Summary of leg and vertical stiffnesses reported in the literature.

Study	Activity	Stiffness ($kN.m^{-1}$)	Leg or vertical
McMahon & Greene (1979)	running	56 to 112	vertical
Luhtanen & Komi (1980)	running @ 4.2 to 9.7 $m.s^{-1}$	35 to 73	leg (ecc.)
Luhtanen & Komi (1980)	running @ 4.2 to 9.7 $m.s^{-1}$	10 to 11	leg (conc.)
Luhtanen & Komi (1980)	long jump	1087	leg (ecc.)
Luhtanen & Komi (1980)	long jump	8	leg (conc.)
McMahon *et al.* (1987)	running @ 2.5 to 4 $m.s^{-1}$	ca. 12 to 30	vertical
Cavagna *et al.* (1988)	running @ 3 $m.s^{-1}$	ca. 25	vertical
Cavagna *et al.* (1988)	running @ 7 $m.s^{-1}$	ca. 75	vertical
He *et al.* (1991)	running @ 2 to 6 $m.s^{-1}$	ca. 22 to 45	vertical
He *et al.* (1991)	running @ 2 to 6 $m.s^{-1}$	ca. 12	leg
Farley *et al.* (1991)	hopping (2 legs)	ca. 18 to 50	vertical
Farley & González (1996)	running @ 2.5 $m.s^{-1}$	7 to 16.3	leg
Seyfarth *et al.* (1996)	long jump	11 to 20	leg
Ferris & Farley (1997)	hopping (2 legs)	ca. 20 to 120	leg

N.B. The data from He *et al.* (1991) are those for normal gravity.

with the runners' stiffnesses assumed to be constant providing they were running at maximum effort, however this assumption was not investigated and it is possible that subjects adjust their stiffness to accommodate surface stiffness changes (see section 2.3).

Vaughan (1980) modelled the trampolinist as a rigid body and the trampoline as a Hookean body (i.e. equivalent to a massless undamped linear spring) in an analysis of basic trampoline stunts. While he acknowledged that energy is dissipated by the trampoline during the rebound, he made the point that the trampolinist can compensate for this by extending at the ankles, knees and hips. Good agreement was found between predicted and actual displacement-, velocity- and acceleration-time graphs, showing that modelling the system in this way was effective, however it is not clear that this was an independent evaluation since the constants in the equations may well have been determined from the trial with which the predictions were compared. In a similar way, Sprigings and Watson (1985) modelled a diving springboard as a massless undamped linear spring in their search for the optimal timing of the arm-swing in diving. They modelled the diver as two rigid segments (arms and the rest of the body) between which a force could be exerted, but allowed for no contribution from the legs.

In a later study, Sprigings, Stilling and Watson (1989) conducted a finite element analysis of a diving springboard and found that a single undamped linear spring model of the board was indeed adequate, but that an effective mass for the board should also be included. However their analyses were conducted on an unloaded springboard; once the mass of a diver is added to the system, the effective board mass might no longer be of importance. In fact the contribution of the inertial force from the board (the product of effective board mass and board acceleration) to the total force applied to a diver's feet by the board was estimated to be at least three orders of magnitude less than the spring force component, again suggesting that the effective board mass was of little practical significance. The board stiffness and effective mass were found to depend on both the point of loading along the board length and the position of the adjustable fulcrum of the board.

In addition to the studies of running which have modelled the whole body as a mass-spring system, some studies have modelled the foot as a second mass-spring body. These have investigated only the impact peak (e.g. Bahlsen and Nigg, 1987; Ker, Bennett, Alexander and Kester,1989; Kim, Voloshin and Johnson, 1994) not the general rebounding nature of the activity.

2.2.3 SUMMARY OF MODELLING REBOUND ACTIVITIES

Evidence from studies of humans and other animals has been reviewed which provides support for the idea of modelling rebound activities as mass-spring systems. The mass-spring models which have subsequently been developed to represent whole body rebounding activities have been considered and the estimates made for leg spring stiffness have been summarized. The majority of these models have been used to investigate hopping and constant speed running, where a certain degree of kinematic symmetry about the middle of the stance phase has been assumed, and a few models of springy surfaces have been reported. However very little attention has been paid to activities like board contact in vaulting, in which takeoff does not mirror touchdown, and no models have been presented of this activity. Similarly no models which enable the investigation of subjects' interactions with springy surfaces have been presented, however the following section considers the evidence relating to the ways in which subjects may adjust to changes in surface.

2.3 ACCOMMODATING SURFACE CHANGES

Following their study of the control of stepping and hopping, Melvill Jones and Watt (1971) stressed the importance of pre-programming the muscular activity used to control landings. They found that the force produced by the gastrocnemius muscle in response to a stretch takes in excess of 150 ms to appear, far too long for it to be effective in halting the descent of the body in a landing. Therefore they concluded that the muscular response required in landing must be pre-programmed based on previous experience. Their study was conducted in such a way that no visual information was available to the subjects, but in normal conditions subjects would be able to use visual cues to anticipate landing and so help in the preparation of a suitable landing strategy. Nevertheless the stretch reflex would still be ineffective and when landing on a surface with an unusual or unexpected consistency modifications to the pattern of muscular force required would presumably take even longer than 150 ms to be effected. In ground contacts of around 150 ms or less, the pattern of motor activity for landings on a surface with an unexpected consistency should be the same as for landings on the expected surface.

Studies of subjects' responses to drop landings onto different surfaces have shown that with practice they altered their leg joint kinematics but that the peak vertical ground reaction forces and time to this peak did not always change (e.g. Fukuda, Miyashita and Fukuoka, 1987; McNitt-Gray, Yokoi and Millward, 1993; McNitt-Gray, Yokoi and Millward, 1994). McMahon and Greene (1979) found empirically and predicted using a mass-spring model, that foot contact time and average vertical ground reaction force were approximately constant for running on tracks as stiff as and stiffer than their subjects' own stiffnesses.

Similarly in some studies, running in shoes with different sole cushioning has been found not to affect vertical ground reaction forces significantly (e.g. Clarke, Frederick and Cooper, 1982; Nigg, Herzog and Read, 1988) and it has been suggested that the lack of influence of sole cushioning may be due to compensatory adjustments to the body's kinematics (Gagnon and Bourassa, 1987; Clarke, Frederick and Cooper, 1983, cited in Frederick, 1986).

Presumably the same process of adjustment might occur in other ground contact situations where the surface stiffness has been altered. In the case of drop landings, McNitt-Gray *et al.* (1994) found that when landing on stiffer surfaces the 'stiffness index' (the ratio of peak vertical force to change in knee angle during landing) of the subjects decreased; this led them to suggest that 'gymnasts may fix the combined stiffness of the body/surface system' (page 247). Ferris and Farley (1997) also demonstrated that hopping humans modified their leg stiffness to compensate for surface stiffness changes, with the result that 'many aspects of the hopping mechanics remained remarkably similar' (page 15), in particular the combined stiffness of the subject and surface was almost constant over more than a thousand-fold change in surface stiffness (35 000 $kN.m^{-1}$ down to 26.1 $kN.m^{-1}$). In their study the peak vertical force decreased gradually as surface stiffness decreased but the surface contact time remained the same. In part of their study they required the subjects to maintain the same hopping frequency (2 Hz) in all trials, which might have effectively forced the subjects to keep the combined stiffness constant regardless of the surface stiffness. However in the second part, subjects hopped at a range of frequencies (2.0, 2.4, 2.8 and 3.2 Hz) on two surfaces with different stiffnesses (35 000 $kN.m^{-1}$ and 50.1 $kN.m^{-1}$) and at all frequencies the combined stiffness remained approximately the same between surfaces (though it increased with hopping frequency).

It would appear that combined stiffness may be the factor which subjects are subconsciously controlling when accommodating surface alterations, though peak vertical reaction force and other factors may also be unchanged. For example, for a given peak vertical ground reaction force on two different surfaces, the combined stiffness would be the same providing the combined deflection was the same (the proportions of the deflection contributed by the surface and the subject would be different).

Studies of maximal drop jumping from a stiff and a sprung surface (Sanders and Wilson, 1992; Sanders and Allen, 1993) revealed that subjects reduced the flexion of their ankle, knee and hip joints and altered the timing of the joint torques in order to compensate for the switch to a sprung surface. The reduction in joint flexion again suggests an increased lower limb stiffness in response to a reduction in surface stiffness, though from the reported results it is not possible to say whether the combined stiffness actually remained constant. The

increase in peak vertical force and decrease in contact time would suggest that overall stiffness was not constant, but interestingly adjustments to accommodate to the reduced surface stiffness were still taking place after the 190 jumps the subjects were allowed on the softer surface, in line with the implications of the results of Melvill Jones and Watt (1971). This has potential implications for athletes in sports in which the playing surface stiffness can vary, although it is unlikely that the range of stiffnesses encountered in a sporting environment would be as great as in Sanders and Wilson (1992) and Sanders and Allen (1993) (their sprung surface had a stiffness of 22.95 $kN.m^{-1}$ and while they gave no stiffness for the force plate acting as their stiff surface, Ferris and Farley (1997) reported another force plate's stiffness to be 35 000 $kN.m^{-1}$).

Springboard diving is a good example of a sport where the surface stiffness can be changed deliberately by the competitor. Jones and Miller (1996) found that springboard divers altered their lower limb kinematics in response to alterations of the springboard fulcrum position, but found that they needed only four to six practices at the new fulcrum settings before they felt comfortable. They did not report the actual changes in springboard stiffness, but Sprigings, Stilling, Watson and Dorotich (1990) tested the same type of springboard and found a maximum range of stiffnesses of between approximately 5 and 17.5 $kN.m^{-1}$, substantially less than the range used by Sanders and Wilson (1992) and Sanders and Allen (1993) for drop jumps, and perhaps explaining the small number of practices required at the new stiffnesses. Ferris and Farley (1997) allowed their subjects as much time as needed to achieve the required hopping frequency and good 'balance' when switching to hopping on a compliant surface.

2.3.1 SUMMARY OF ACCOMMODATING SURFACE CHANGES

From the research reviewed in this section, it would seem that subjects do change their movement patterns when faced with a surface stiffness change. One possibility is that they might make these adjustments in order to keep the combined stiffness of their legs and the surface approximately constant. How long or how much practice subjects might need in order to make this accommodation is not clear and may vary depending upon the magnitude of the change in the surface stiffness.

2.4 METHODS OF INVESTIGATION

This section reviews the methods commonly used in the biomechanical analysis of sporting performance, focusing especially on those used in this study. These can be categorized as visual data capture and analysis, the determination of body segment inertia parameters, force data collection and analysis, and modelling and simulation.

2.4.1 VISUAL DATA CAPTURE AND ANALYSIS

2.4.1.1 Data collection

The collection and analysis of moving images of subjects is common in sport biomechanics (Yeadon and Challis, 1994). Increasingly video is replacing 16 mm cinefilm as the medium for recording the images owing to the relative cheapness and simplicity of the process, the improving quality of video images and the immediacy of the resulting record (Kennedy, Wright and Smith, 1989; Angulo and Dapena, 1992). Film is still used where higher picture rates than the 50/60 per second commonly recorded on video are required, but high-speed video is also now more readily available. The picture rate should 'ideally be 8 to 10 times the highest frequency expected in the sampled signal' (Challis, Bartlett and Yeadon, 1997, page 11), with a minimum rate greater than twice the highest frequency content of the signal.

Despite concerns over the resolution of video systems, a number of studies have found them almost as accurate as 16 mm film in practical terms. Kennedy *et al.* (1989) calculated the mean error (as a percentage of the calibrated field width) to be 0.29% for video and 0.24% for film. Angulo and Dapena (1992) calculated relative errors (as a percentage of surveyed lengths) for distances within and outside a calibrated volume of 0.3% and 1.3% respectively for video and 0.1% and 1.0% respectively for film. Kerwin (1994) reported a result of 0.2% error from video digitization using a custom built system with improved resolution of the frame grabber over the Peak Performance Technologies systems used in the previous studies. This was the same as results from film analysis, though this was a two-dimensional study of a planar array of landmarks as opposed to the three-dimensional studies of Kennedy *et al.* (1989) and Angulo and Dapena (1992), and the width of field was only 1.170 m which would be small for a sport biomechanics application. Video camera resolution also has an influence and Tan, Kerwin and Yeadon (1995) found Hi 8 recordings to reduce errors by up to 34% compared with VHS recordings. With the reduced cost and increased availability of digital video cameras, there should be further improvements in the quality of data from video recordings.

Whether using video or cinefilm the basic steps in collecting and analysing the records are the same:

- the images must be obtained, paying due attention to the positioning of the camera(s), calibration, lighting and camera field of view, focusing, shutter speed and aperture
- the images must be digitized to provide image-space coordinate data

- the image-space coordinates are (usually) smoothed and then transformed to object-space (real world) coordinates (sometimes the data are transformed and then smoothed)

- the object-space coordinates can then be used in the analysis of the activity, either in isolation or in conjunction with other data (e.g. body segment inertia parameters, force data).

Challis *et al.* (1997) presented a good summary of the practical issues involved in data collection.

Where more than one camera is being used or other data are being recorded simultaneously (e.g. force data) all recording instruments must be synchronized, or a method for post-collection synchronization must have been considered. Cameras can often be synchronized physically by phase- or gen-locking, but where this is impossible common events in all cameras' fields of view can give nearest field/frame synchronization; better still a single timing device in all views allows more precise post-recording analytical synchronization by enabling data from other cameras to be interpolated over the timebase of a 'master' camera (Yeadon, 1990a). Yeadon (1989) devised a novel alternative method for synchronizing two cameras filming ski-jumping which was based on the point of intersection of a ray from one camera to the jumper's mass centre at one instant, with a line joining the positions of the mass centre in frames either side of this instant as determined from the other camera. Common-event synchronization is also often possible when other forms of data are being recorded, for example an LED switched on in the field(s) of view when force collection commences, though some form of mechanical or electrical synchronization is preferable. Methods of improving the synchronization of cameras with other data have been described which have recorded the vertical blanking pulse from a video camera (O'Connor, Yack and White, 1995) or the shutter pulse from a cine-camera (Rome, 1995) alongside the data from other instruments.

2.4.1.2 Smoothing and differentiating

Any data obtained from the digitization of a visual record contains some errors in addition to the true data. Experience and good practise can eliminate or reduce the magnitude of some systematic errors, while others (such as lens distortions) can be adjusted for during the data transformation. Undetectable or unremovable systematic errors may remain but these are likely to be small. Random errors are assumed to be a stationary, uncorrelated, normally distributed, zero mean addition to the true displacement data (Hatze, 1990). Random errors are spread across the frequency spectrum but their amplitude is usually small, therefore they

are generally insignificant in relation to the position data. However differentiation of this 'noisy' data has the effect of preferentially amplifying the high frequencies so that they may mask the true data (Wood, 1982), which for human movement (excluding impacts) are generally low frequency. In order to reduce this problem some form of data filtering or smoothing is necessary prior to the determination of derivatives.

Occasionally in biomechanics the nature of the digitized signal is known, for example while airborne mass centre horizontal velocity is constant and mass centre vertical velocity is a quadratic function of time (if air resistance is negligible). In such cases a straightforward approach such as least squares linear or quadratic curve fitting to the mass centre position data is appropriate (McLaughlin, Dillman and Lardner, 1977). Usually however, this is not the case and a more general approach to noise removal is required. The three main categories of noise removal technique are digital filtering, Fourier series truncation and spline fitting (Challis *et al.*, 1997).

Digital filters selectively reject certain frequencies within the signal while, ideally, leaving the other frequencies unaltered (Winter, 1990). For the filtering of position data from human motion analysis this means rejecting frequencies higher than a specified cut-off. A recursive second order Butterworth filter has often been used, with a cut-off selected on the basis of an analysis of the frequency spectrum of the signal (Winter, Sidwall and Hobson, 1974) or residual analysis (Winter, 1990). Digital filters are best suited to cyclic signals and have the disadvantages of requiring equispaced data and distorting the signal close to the boundaries of the data set, though Smith (1989) found that 'padding' the ends of the data set could overcome this last problem. A further drawback of digital filters is that they do not generate a function which can be differentiated analytically, therefore derivatives must be calculated separately, for example by the use of finite difference techniques or splines. However some finite difference techniques for determining derivatives also attenuate noise (Lees, 1980). Lees (1980) described the issues surrounding routines for filtering followed by differentiation, in particular the choice of an appropriate sampling frequency, and presented a method for the selection of routines.

Fourier analysis models a set of data as a function comprising a series of sine and cosine waves with different frequencies and amplitudes. In Fourier series truncation, noise is removed by deleting the terms with frequencies higher than a prescribed cut-off, this cut-off being determined either subjectively, by systematic residual analysis (e.g. Jackson, 1979) or by means of optimal regularization (Hatze, 1981). The truncated Fourier series can be differentiated analytically but, as with digital filters, Fourier analysis requires equispaced data. In principle, Fourier analysis should only be used for cyclic data, though this is

sometimes ignored; alternatively it is possible to 'detrend' the data to force it to appear cyclic, but this leads to zero endpoints in second derivatives (Challis *et al.*, 1997).

Spline functions are piecewise polynomials of degree *n*, with each piece joined at a *knot* and constrained such that the function and its first *n-1* derivatives are continuous (Wold, 1974). The piecewise nature of the spline means that the fit to one part of the data set only influences the fit of the immediately neighbouring part of the data (due to the continuity constraint), unlike fitting normal polynomials. Splines also have the advantage, like truncated Fourier series, of being analytically differentiable. Most spline fitting is currently done using natural splines based on the work of Reinsch (1967, 1971) with knots at every data point (Challis *et al.*, 1997), the amount of smoothing being controlled by the value given to the smoothing parameter (based on the maximum acceptable least squares error and the estimated error in the data). Increasing the smoothing parameter results in a smoother fit and vice versa, while setting it to zero results in an interpolating spline (McLaughlin *et al.*, 1977).

Cubic ($n = 3$) and quintic ($n = 5$) natural splines have both been used in biomechanics, but quintic splines have several advantages:

- their derivatives are continuous up to the fourth derivative, rather than the second for cubics,
- their first three derivatives are smooth, whereas the second and third derivatives of cubics consist of linear pieces (a step function in the case of the third derivative),
- the endpoints of only the third and higher derivatives are constrained to zero, as opposed to the second and third derivatives for cubics (Wood and Jennings, 1979).

Several authors have investigated solutions to the zero acceleration endpoint problem of cubic splines based on padding the data with dummy values at each end (Zernicke *et al.*, 1976; McLaughlin *et al.*, 1977; Phillips and Roberts, 1983) but the use of quintic splines would seem to be the most sensible solution if accelerations are required. A number of methods for choosing an appropriate smoothing parameter have been proposed based on the estimated error present in the raw data (e.g. Reinsch, 1967) and/or a combination of subjective analysis of residuals and the smoothness of the second derivative of the spline (e.g. Zernicke *et al.*, 1976). Objective methods for determining the degree of smoothing have been proposed based on the technique of cross validation (e.g. Wahba and Wold, 1975; Woltring, 1986) thereby removing any operator intervention or the need to estimate the error in the raw data.

All three of the main techniques have been used in biomechanics and have their devotees, but the case for using cross-validated (quintic) splines is strong. Challis and Kerwin (1988) compared cubic and quintic splines, truncated Fourier series and Butterworth digital filters for filtering a variety of mathematically derived data. The quintic splines performed best in most cases, with the truncated Fourier series also performing well with data to which it was particularly suited (i.e. cyclic functions). Challis, Yeadon and Kerwin (1991) also found the generalized cross validated quintic spline (Woltring, 1986) to be superior to a recursive second order Butterworth filter followed by finite difference differentiation when calculating second derivatives of a variety of noisy data sets. Vint and Hinrichs (1996) examined the effect of padding data sets on the endpoint problems associated with Butterworth digital filters, Fourier series and cubic and quintic splines. They found that quintic splines without data padding performed consistently better than the other techniques. Splines also have the advantage of not requiring equispaced data; indeed the ability to perform interpolation with splines is another benefit which allows them to be used to make estimates for regions where data are missing (e.g. when markers become obscured during digitization of film or video).

Wood (1982) advised that the main consideration when selecting a noise removal technique is to choose one which is valid for the data of the specific motion being analysed and both Hatze (1990) and Challis *et al.* (1997) recommended choosing a technique which provides an objective method for determining the optimal degree of smoothing. In most cases, cross-validated quintic splines meet these criteria.

2.4.1.3 Data reconstruction

All sports activities take place in a three-dimensional world, but very often they are treated as though they were two-dimensional. Studies of gymnastic vaults have usually ignored or considered to be negligible movements out of the vertical plane passing through the centre of the horse and the runway, therefore 2-D analysis techniques have been adopted (e.g. Dainis, 1979; Dillman *et al.*, 1985; Takei, 1991). Ideally this entails positioning the camera with its optical axis perpendicular to the movement plane and providing horizontal and vertical references which enable scaling of the image space coordinates to object space coordinates. Sometimes, particularly when filming in the field, such positioning of the camera is impossible, in which case a method such as the 2-D direct linear transformation (DLT) can be adopted (Challis *et al.*, 1997); Challis and Kerwin (1989) found that the 2-D DLT was more accurate than direct scaling even when ideal camera positioning was possible. An alternative is to use a suitable 3-D reconstruction technique to determine the kinematics of motion in a particular plane (e.g. Kwon, Fortney and Shin, 1990; Kerwin, Harwood and Yeadon, 1993).

An approximately inverse relationship exists between computational and practical complexity with regards to methods of performing 3-D reconstruction, in that the simplest computationally require the most painstaking preparation for data collection (e.g. camera positioning, surveying) and vice versa. Martin and Pongratz (1974) presented a method based on the geometry of similar triangles which was computationally straightforward but which required two cameras to be positioned with their optical axes intersecting at ninety degrees and the camera to intersection distances to be known. Approaches which allowed more flexible camera positioning have been devised, though some of these have still required knowledge of camera position, focal length and/or that the optical axes of the cameras intersect (e.g. Bergemann, 1974; van Gheluwe, 1974).

The most popular 3-D reconstruction method currently in use (Challis *et al.*, 1997; Hinrichs and McLean, 1995) is the DLT, based on the work of Abdel-Aziz and Karara (1971). In this method camera positioning is almost entirely flexible, requiring only that a suitable arrangement of control points be recorded by all cameras and that the camera positions (and focal lengths) remain fixed during the data collection. At least six control points with known locations are required in order to determine the eleven parameters (per camera) necessary to enable the reconstruction, though Chen, Armstrong and Raftopoulos (1994) found that the mean reconstruction error halved as the number of control points increased from eight to sixteen. Ideally the control points should surround the movement volume thereby improving accuracy (Challis and Kerwin, 1992) and avoiding the need for the reconstruction of unknown points which lie outside the calibrated volume, which has been shown to increase the reconstruction error (Wood and Marshall, 1986; Hinrichs and McLean, 1995). Usually the control points are located on a rigid frame, however this can be impractical with relatively large movement volumes, such as in gymnastics, so several studies have used a series of calibration poles in measured positions surrounding the volume (e.g. Kwon, Fortney and Shin, 1990; Kerwin *et al.*, 1993; Takei, Blucker, Dunn, Myers, and Fortney, 1996).

Another DLT-based solution to calibrating larger volumes has been to record a (relatively) small calibration frame in several positions (e.g. Ball and Pierrynowski, 1988; Challis, 1995). The calibration frame is first recorded in a position which defines the inertial reference frame for the calibration volume, then the frame is moved to and recorded in new positions which encompass the movement volume. The control points in the new calibration frame positions are then determined in terms of the inertial reference frame, thereby providing a number of control points which cover the proposed movement volume. Using these control points (or a selection from them) enables DLT reconstruction to be performed as though a much larger calibration frame had been used. Other techniques for performing

3-D reconstruction in large volumes have also been proposed (e.g. Woltring, 1980; Dapena, Harman and Miller, 1982; Yeadon, 1989), but for gymnastic vaulting the DLT has been preferred.

2.4.2 BODY SEGMENT INERTIA PARAMETERS

The mass, mass centre location and moments of inertia of the whole body and individual segments are often required in biomechanical studies. Only the mass of the whole body is easily measured for the living subject (providing one has direct access to the subject), while the whole body mass centre location and moments of inertia are usually calculated from information about the separate segments. The segment inertia parameters can be determined by one or more of an array of methods, which may be broadly categorized as experimental, regression equation and geometric model.

2.4.2.1 Experimental determination

Much of the body segment inertia parameter (BSIP) data in use today are in some way based on the cadaver studies of Dempster (1955), Clauser, McConville and Young (1969), or Chandler, Clauser, McConville, Reynolds and Young (1975). Dempster (1955) dissected eight male Caucasian cadavers aged between 52 and 83 years from which mass, volume, density, mass centre position and moments of inertia were measured. However, the small number and age of the cadavers present a problem for the use of these data where accurate data are required for the subjects typically studied in sports biomechanics. Clauser *et al.* (1969) conducted a similar study of 13 male Caucasian cadavers aged between 24 and 78 years, and included stepwise regression equations for predicting BSIP, but they did not determine the moments of inertia of the segments. Chandler *et al.* (1975) conducted a study to add detailed moment of inertia information to the other data already available. They studied six male Caucasian cadavers aged between 45 and 65 years, reporting principal moment of inertia data as well as other anthropometric data on the segments.

There are a number of problems common to the data from cadaver studies such as the small, skewed sample (on the whole elderly Caucasian males), differences between the methodologies adopted (segment boundaries for example), differences between living and embalmed bodies and the fact that the BSIP of the cadavers and the causes of death might be related in some way (e.g. obesity, sedentary lifestyle). These issues make the results of extrapolating cadaver data to healthy, highly trained athletes, especially females and/or non-Caucasians, rather uncertain. A solution to these problems would clearly be to make measurements on the subjects directly, or at least a matched group. However those studies which have been conducted have generally been limited to measuring a few parameters each

and have been rather time consuming. For example measurements of whole body mass centre position (Swearingen, 1962) and principal moments of inertia (e.g. Santschi, DuBois and Omoto, 1963; Matsuo, Ozawa, Goda and Fukunaga, 1995) have been made on subjects in fixed positions, immersion techniques have been used to determine segment mass, mass centre locations (e.g. Plagenhoef, Evans and Abdelnour, 1983), and the 'quick-release' method has been used to find the moment of inertia of the distal limb segments (e.g. Bouisset and Pertuzon, 1968; Cavanagh and Gregor, 1974). Drillis and Contini (1966) reviewed the range of experimental measurement techniques then available for use on living subjects and selected a battery of them to measure the BSIP of twenty males aged 20 to 40 years, which while quite thorough was again time consuming and complicated.

Perhaps the most promising methods for determining subject specific BSIP are those which utilize Gamma radiation (Brooks and Jacobs, 1975; Zatsiorsky and Seluyanov, 1983; Zatsiorsky, Seluyanov and Chugunova, 1990), Computerized Tomography (CT) scanning (Huang and Wu, 1976; Huang and Suarez, 1983; Ackland, Henson and Bailey, 1988), or Magnetic Resonance Imaging (MRI; Martin, Mungiole, Marzke and Longhill, 1989; Mungiole and Martin, 1990). MRI seems to be the most promising method, being at least as accurate as CT and gamma scanning (Nigg, 1994a), offering better imaging than CT and not being based on irradiation, in contrast with both CT and gamma scanning (Mungiole and Martin, 1990). However all of these techniques require expensive equipment, are time consuming and are subject to strict controls which make them unlikely to be used directly in sports biomechanics in the near future.

2.4.2.2 Regression equations

The use of regression equations to estimate BSIP is long established, including a number of studies which have reported results simply as proportions of body mass, stature or segment length (e.g. Dempster, 1955; Plagenhoef *et al.* 1983; Zatsiorsky and Seluyanov, 1983). Barter (1957) re-analysed the results from the cadaver studies of Braune and Fischer (1889, cited by Barter, 1957), Fischer (1906, cited by Barter, 1957) and Dempster (1955) and calculated regression equations for the prediction of segment masses from whole body mass. This was problematic due to the different dissection methods used and the equations are not appropriate for use with young, healthy athletes, especially non-Caucasians and females, because of the small, skewed sample of cadavers.

Clauser *et al.* (1969) presented equations for estimating segment masses, volumes and mass centre positions, and found that regression equations with three predictor variables were better than those with one or two. Chandler *et al.* (1975) produced two sets of regression

equations using single predictor variables, body mass or segment volume (the more accurate of the two), to estimate segment mass and moment of inertia. As noted in the previous section, these studies were also conducted on a small, skewed sample of cadavers which makes them of dubious validity for use with young athletic subjects, indeed Chandler *et al.* (1975) warned against using their data for estimating population parameters. Hinrichs (1985) revisited Chandler *et al.*'s data and produced further regression equations for predicting segment moments of inertia from anthropometric dimensions (e.g. segment lengths and circumferences). He added a caution against using his equations for predicting outside the range of anthropometric dimensions of the cadavers, not just their age and race. Hinrichs later (1990) adjusted the Clauser *et al.* (1969) segment mass centre position proportions to use joint centres rather than the original bony landmarks. Yeadon and Morlock (1989) and Challis (1996) also revisited the moment of inertia data of Chandler *et al.* (1975) and demonstrated that non-linear regression equations were superior to linear equations when estimating BSIP (Challis focussed on limb moments of inertia) for subjects with segment dimensions both within and outside the range of anthropometric dimensions of the original cadavers.

Zatsiorsky and Seluyanov (1983, 1985) presented regression equations based on the BSIP of 100 young men (aged 23.8 ± 6.2 years) determined by a gamma scanning technique. These data are the only comprehensive results from a large scale study of young, healthy subjects and as such are more suited to application to male athletes, even though the sample was probably still skewed in terms of race (details not reported). Zatsiorsky and Seluyanov (1983) gave both mean proportions and regression equations using body mass and stature as predictors, while in 1985 they published best predictive regression equations using three or four predictors which consisted of various anthropometric measures (e.g. perimeters, lengths, widths). A drawback to these studies is that the segmentation of the bodies followed the traditional cadaver dissection boundaries, rather than the joint centres which are typically digitized by researchers, and the 1985 study presented insufficient detail regarding where measurements should be taken.

2.4.2.3 Geometric models

A number of researchers have developed models of the human body which consist of a series of simple geometric solids. These models enable the determination of customized BSIP for individual subjects if the requisite measurements of the subject are made and segment densities are known. The differences between these models lie mainly in the way that the body is segmented, the number of solids used and consequently the measurements required. Most models assume a uniform density within each segment, which has been supported by

direct measurements by Ackland, Henson and Bailey, (1988) using CT and Mungiole and Martin (1990) using MRI. In addition, the results from Chandler *et al.* (1975) supported the assumption often made in geometric models that each limb segment can be considered symmetrical about its longitudinal axis.

The Hanavan model (Hanavan, 1964, summarized by Nigg, 1994a) consisted of fifteen solids (circular ellipsoids, elliptical cylinders, frustra of circular cones and a sphere) and required 25 measurements to be made on the subject. Segment masses were determined from Barter's (1957) regression equations and the solids were used to determine the mass centre position within the segments and segment moments of inertia. The segment masses were naturally affected by the shortcomings of the Barter regression equations, which Miller and Morrison (1975) sought to address by calculating segment masses for Hanavan's model using the regression equations presented by Clauser *et al.* (1969). Miller and Morrison found that the using the new equations led to an overestimate of the whole body mass of the subjects by 4.59% compared with an underestimate of 2.03% using the original equations. The BSIP were also at variance, but in the absence of a criterion Miller and Morrison had more confidence in the estimates using Clauser *et al.*'s equations because of the larger cadaver sample size and a dissection method which was not only the same for all cadavers but which more closely matched the segment boundaries of the Hanavan model.
Nevertheless the shortcomings of Clauser *et al.*'s sample noted previously would also have an adverse affect if the model were used to predict BSIP for young athletes, furthermore Reid and Jensen (1990) considered the Hanavan model to oversimplify the segment shapes and not to be very accurate.

Jensen (1978) proposed a model which divided the body into sixteen segments (later revised to fifteen by treating the head and neck as one segment; Jensen and Fletcher, 1994) each comprising a series of 2 cm thick elliptical zones. Measurements of the major and minor axes of the ellipses at each division were made from photographic records of the front and side views of the subject. This made the procedure very quick for the subjects (approximately 10 minutes) but it took the researcher up to 2 hours to digitize the images manually (the revised method reduced the time taken to 15 to 20 minutes: Jensen and Fletcher, 1994). Uniform segment densities were assumed, using the density data from Dempster (1955) (Clauser *et al.*'s density data (1969) were used for all but the trunk segment in some later applications), and the whole body mass was estimated to within 2 % of the measured values for three boys (aged 8 to 10 years). Jensen's model has been used in a number of studies by Jensen himself and co-workers (e.g. Jensen, 1986; Jensen and Nassas, 1988; Jensen and Fletcher, 1994) and by others (e.g. Yokoi, Shibukawa, Ae, Ishijima and

Hashihari, 1985; Ackland, Blanksby and Bloomfield. 1988) particularly in investigating BSIP of children and adolescents, and more recently the elderly and pregnant.

Hatze (1980) presented the most detailed geometric model, consisting of 17 segments, including the shoulders separately, and allowing segment density and shape to be varied to suit the subject. The penalty for this degree of customization was the 242 anthropometric measurements required directly from the subject, which Hatze (1980) and Sprigings, Burko, Watson and Laverty (1987) found to take an average of 80 minutes. However, Baca (1996) reported an automated method for determining 220 of the dimensions required for the Hatze model directly from video images of the subject and computing the remaining 22. It is worth noting that while segment density values may be customized in this model, the detailed density data must be available; typically this means using cadaver data with its associated problems, although in future an increase in the availability of such data from CT or MRI would help. Researchers should also consider whether the effort required to obtain such highly individualized BSIP will be justified in the final analysis, but this can only be determined in the light of the precision and accuracy of other data collected and the purpose of the analysis.

Yeadon (1990b) presented a geometric model primarily for the simulation of aerial movement consisting of 40 solids which defined 20 body segments, although typically several of these were combined to produce BSIP for an 11 segment model of the body. Thus while the head and neck, hands, and feet were modelled separately, it was assumed that no movement occurred at the neck, wrists and ankles (the ankles were treated as being plantarflexed, as is typically the case in aerial movements in gymnastics, diving and similar activities). A distinctive feature of Yeadon's model was the representation of the segments comprising the trunk as 'stadium solids', that is solids bounded proximally and distally by parallel surfaces shaped like an athletic stadium (a rectangle with semi-circles at each end of its width). The stadium shape was demonstrated to match the typical cross-section of the trunk better than an ellipse (as employed by Jensen, 1978 and Hatze, 1980). It was estimated that the 95 measurements required took between 20 and 30 minutes with the subject, though Yeadon, Challis and Ng (1994) reported some success with reducing this to 26 measurements in combination with regression equations to generate the remaining dimensions. Density values from Dempster (1955) were used because they were the only data available which corresponded to the segmentation of Yeadon's model. As with other uses of cadaver data this is a shortcoming, however Yeadon (1990b) noted that the BSIP were designed as inputs to a simulation model, so in the light of the fit of the simulation to actual performances adjustment of the inertia data was possible.

2.4.2.4 Selection of a method for BSIP determination

Validation of the various methods for determining BSIP can at best be only partial since few of the parameters are directly measurable in living subjects (Cappozzo and Berme, 1990). Sprigings *et al.* (1987) compared the geometric model of Hatze (1980) and the average segmental percentages of Dempster (1955) and Clauser *et al.* (1969) for calculating whole body mass centre position. They used each method to estimate subjects' mass centre positions during free fall, then calculated the mass centre accelerations and compared them with the expected value of 9.81 $m.s^{-2}$. Hatze's model proved to be the most accurate of the three. Kwon (1996) compared ten methods for determining BSIP and found that while the method chosen affected the estimated magnitude of angular momentum in full twisting double back dismounts from high bar, each method produced angular momentum values which fluctuated by about the same amount (e.g. 7-8% of mean somersaulting angular momentum). No criterion was available but had one method produced estimates which were more nearly constant (as should be expected in flight) it might be presumed to be more accurate; as it was the fluctuations were more likely due to other experimental errors (Kwon, 1996).

The findings of Kwon (1996) and the demonstration by Challis (1996) that the influence of the accuracy of limb moment of inertia values on resultant joint moments can be small, suggests that the most complex method for determining BSIP might not be necessary to achieve acceptable results, especially if the accuracy or precision of other data is limited. Nevertheless, researchers will usually want to obtain the best estimates possible which, given that a direct measurement technique such as MRI is unlikely to be readily available to most, probably means using a geometric model.

Yeadon and Challis (1994) pointed out the difficulties of restricted access to subjects (e.g. at competition) which might make it impossible to take measurements from subjects, in which case regression equations might have to be used. Furthermore, if the subjects of a study match (in terms of age, sex, race and anthropometry) those from whom regression equations or normative data have been derived the use of these methods might prove preferable. However in general 'because of individual differences it is preferable to use a mathematical model' (Reid and Jensen, 1990, page 237), a view supported by other surveys of available techniques (Cappozzo and Berme, 1990; Nigg, 1994a).

2.4.3 FORCE DATA CAPTURE AND ANALYSIS

The two most commonly used types of force transducer are based on piezoelectric or strain gauge technology (Nigg, 1994b), both working on the principle that a load will cause

deformation of the transducer which in turn will result in a change of output (Berme, 1990). Ideally, force transducer systems should have minimal crosstalk, high linearity, low drift, high frequency response, high natural frequency, low hysteresis and low threshold. Nigg (1994b) summarized a selection of the main performance characteristics for different types of force transducers which showed that there is little to choose between piezoelectric and strain gauge transducers, with piezoelectric having a slight edge in terms of linearity, hysteresis and threshold, while strain gauge are cheaper and do not suffer from drift (making them better for longer duration recordings).

Both piezoelectric and strain gauge transducers are capable of recording forces over a very large range of values. The analogue output from the transducer is usually converted to a digital signal using an analogue to digital converter (ADC) which can only resolve a discrete number of different levels (e.g. 4096 for a twelve-bit ADC). To maximise the accuracy of the recording system it is necessary to adjust its operating range to match as closely as possible the expected range of forces in a given trial (Bartlett, 1977). Failure to do this will result in inaccuracy either due to 'overloading' the transducer (if a force is applied which is larger than anticipated) or low sensitivity (if only small forces are recorded when a large range has been set).

Force plates incorporate one or more force transducers (typically four) supporting a rigid top plate (Winter, 1990). Where more than one transducer is used the output from each is usually combined to provide three orthogonal components of a single resultant force and the point at which that force can be considered to act (centre of force, also known as centre of pressure or point of force application). Moments of force can also be determined. While force plates based on both strain gauge and piezoelectric technology are available, Bartlett, Messenger and Lindsay (1997) suggested that piezoelectric plates are still preferred for sport and exercise biomechanics owing to their ability to measure rapidly changing forces accurately, despite the recent improvements of strain gauge plates in this regard.

Force plates are most often mounted in the ground. Care must be taken to mount the plate so as to minimize the effects of vibrations from the surrounding environment (Kerwin and Chapman, 1988a), which is usually achieved by attaching the plate to a large concrete block (Bartlett *et al.*, 1997). Bartlett (1997) noted that strain gauge plates are considered to be easier to install while piezoelectric plates are less susceptible to changes in temperature and therefore need calibrating less frequently. Biewener and Full (1992) and Hall, Fleming, Dolan, Millbank and Paul (1996) described similar methods for calibrating force plates. Hall *et al.* particularly noted the difficulties of quantifying crosstalk, also making the point that even if plates perform to manufacturers specifications (e.g. $\leq \pm 1\%$), the crosstalk from a

channel reading a large force (e.g. vertical force at mid-stance in running) can have a substantial effect on channels simultaneously reading small forces (e.g. medio-lateral forces).

When suitably installed, calibrated and operated, force plates can yield very accurate force measurements, however centre of force estimation can be more problematic. Bobbert and Schamhardt (1990) evaluated the accuracy of this measure for a piezoelectric force plate and found errors of up to 20 mm at the plate edges. They developed correction algorithms which achieved reductions in these errors of at least 50% and, more typically, over 75%. They also demonstrated theoretically that the errors were due to slight (but necessary) bending of the top plate. The plates they were using had a larger surface than is typical, consequently the errors might be smaller for smaller plates (Challis, 1997). It should be noted that large errors in the location of the centre of force can occur on any force plate when the resultant vertical force approaches zero, as this value is a denominator in the equations for the calculation of centre of force (Nigg, 1994b; see page 217 for equations).

Integration of force data with respect to time enables the calculation of changes in momentum and hence changes in velocity if divided by the subject mass. A further integration gives displacement, while knowledge of initial/final velocity and position allows absolute velocity and position to be determined. Bartlett *et al.* (1997) noted that Simpson's rule or the trapezoidal rule can be used for numerical integration of force histories, or an analytic function could be fitted to the data which could then be integrated analytically. The trapezoidal rule effectively joins consecutive ordinates with a straight line and calculates the area of the trapezium formed, while Simpson's 1/3 rule effectively joins three consecutive ordinates with a quadratic and finds the bounded area (Simpson's 3/8 rule puts a cubic through four consecutive values). It has been shown (e.g. de Vahl Davis, 1986) that in general circumstances Simpson's rule is more accurate than the trapezoidal rule, however without modification it only gives integrals for double time steps (Bartlett *et al.*, 1997). Furthermore, when the force is varying fairly slowly but a high sampling rate is being used (which, apart from impact transients, is usually the case in vertical and anterio-posterior ground reaction force records; Kerwin and Chapman, 1988b) the linear approximation used in the trapezoidal rule is likely to be adequate.

2.4.4 MODELLING AND SIMULATION

In general a model may be described as 'an attempt to represent reality' (Nigg, 1994c, page 368), though for the purposes of this thesis, mathematical models are the specific interest. Giordano and Weir (1985) defined a mathematical model as 'a mathematical construct designed to study a particular real-world system or phenomenon' (page 32). Apart from

providing a definition, this quotation also indicates that the model is not the goal, but the tool with which to conduct a study. Vaughan (1984) made the useful distinction between a (computer) model and (computer) simulation, defining simulation as: 'the use of a validated computer model to carry out "experiments", under carefully controlled conditions' (page 373). The use of the term 'computer' is now largely redundant since using computers to perform mathematical modelling and simulation is the norm.

The use of models in biomechanics enables the 'what if?' questions (Bratley, Fox and Schrage, 1987; Vaughan, 1984; Yeadon, 1994), and also the 'why?' questions (Yeadon, 1994) to be addressed. Attempting to answer 'what if?' questions by asking athletes to modify their technique is fraught with ethical and practical problems. Furthermore, without some evidence to suggest that the modifications will be advantageous, the biomechanist is likely to be met with some reluctance and suspicion by the athletes and their coaches. The use of appropriate models to conduct simulations means that answers can be suggested without risking athlete safety, minimizing the time and cost involved, and perhaps arriving at an optimized technique (or at least rejecting unpromising modifications) before athletes need to be involved (Vaughan, 1984). Models are useful for answering 'why?' questions because they are simplifications which allow attention to be focused on the fundamental factors and enable a level of control of these factors which would rarely be possible in a traditional biomechanical study. However Vaughan (1984) also drew attention to some of the drawbacks of modelling and simulation: difficulty in validating (evaluating) models (see below), the level of mathematical knowledge required (or conversely the lack of knowledge required if a 'black box' approach is taken) and the difficulty sometimes encountered in making the results of simulations accessible to athletes and coaches.

Numerous authors have described the stages involved in the development and use of mathematical models (e.g. Mihram, 1972; Giordano and Weir, 1985; Edwards and Hamson, 1989; Nigg, 1994c). Although their precise stages differ, a common general approach can be identified. Initially a study of the subject or activity to be modelled is necessary along with the questions or issues to be addressed. At this point, the type of model (e.g. deterministic or stochastic, inverse or direct dynamics) may be selected and some simplifying assumptions made. Formulation of the mathematical equations which make up the model and an attempt at their solution follows; increasingly this is done using simulation or symbolic mathematics packages (Meerschaert, 1993; Soest, Schwab, Bobbert and Ingen Schenau, 1992; Yeadon and Challis, 1994). Before making use of the model in simulations which attempt to answer the questions posed, the model should be verified (to ensure that the model program executes correctly) and evaluated (to ensure that what it does corresponds to reality). Once some

answers have been found it is then important that these be communicated appropriately to the intended audience.

Modelling is an iterative process: at any point it may be necessary to go back to an earlier stage, perhaps to simplify a model which is too complex to formulate mathematically, or maybe to increase the complexity in the event of a poor evaluation. Miller (1975) suggested that the aim was to achieve an optimal combination of accuracy and simplicity, while Hubbard (1993) proposed the rule of thumb 'always begin with the simplest possible model which captures the essence of the task being studied' (page 55). Alexander has often made a case for and demonstrated the benefits of simple models (e.g. Alexander, 1989, 1990b, 1991a). In fact he devoted a paper (Alexander, 1992) to encouraging the use of models which are 'as simple as is consistent with [their] task' (page 5) because they highlight basic principles. Hatze (1981) on the other hand presented one of the most complex models for the simulation of human motion, on the basis that this made it 'more powerful in its predictive capabilities' (page 135). The penalty for such complexity is likely to be in a lack of ease of use and a difficulty in understanding the results: 'The primary purpose of computer simulation is to increase the understanding of a particular phenomenon, not to simply replicate it.' (Sprigings and Yeadon, 1997, page 518).

Confusion arising from the numerous interpretations of the term 'validation' led Nigg (1994c) to propose using the term 'evaluation' to mean the process of establishing whether a model is 'strong and powerful for the purpose for which it was intended' (page 373). He identified three ways of evaluating a model: direct, indirect and trend measurements. Direct evaluation is the ideal, since the model results are compared with direct measurement of the variable of interest. However direct evaluation cannot always be performed since the variable may not be measurable in the real system, nevertheless it may be possible to compare other model results with corresponding real values, thereby indirectly evaluating the model. Trend measurement compares the general behaviour of the model with that of the real system, without great concern over the specific values predicted.

Panjabi (1979) also stressed the need to evaluate (validate in his terms) models since 'a mathematical model is only a set of equations' (page 238). However he noted the key problem with the notion of evaluation, that is to say that while model results may compare favourably with real data, one of the main uses of models is to make predictions about situations for which no data exist. Therefore the predictions may not be as accurate as the evaluation would suggest.

It is possible that more than one model may be formulated and may prove to be adequate for the purpose based on whatever criteria are chosen. Murthy, Page and Rodin (1990) suggested that in this case the selection of a model to use may be made on the basis of parsimony (i.e. a model with fewer parameters is best) and/or parameter sensitivity (i.e. less sensitivity is better). Sensitivity analysis establishes the influence of the uncertainty in the values used as inputs to the model on the model predictions. Where it is not possible to perform sensitivity analyses on all parameters, those about which there is most uncertainty should be focused upon (Meerschaert, 1993).

Nigg (1994c) pointed out that a model might produce accurate results without the conceptual construction corresponding to reality. This situation may exist for models of humans as mass-spring systems, since there is no actual spring but a series of joints, muscles and ligaments which together act reasonably like a spring in some circumstances. Nevertheless the model may be adequate for the purpose for which it was developed. Another possibility is that a model might not be expected to match reality. For example Sprigings and Yeadon (1997) used a very simple model of horse contact in Hecht vaulting to determine how much reversal of rotation might be possible without the use of torques at the shoulder joint. That the model produced 70% of the actual change in angular velocity was seen as a positive indication, not as a shortcoming. Indeed demonstrating the limitations of a particular model may be useful, since it can stimulate the search for a better understanding of the system being modelled.

2.4.5 SUMMARY OF METHODS OF INVESTIGATION

This section was divided into four main areas: visual data capture and analysis, the determination of body segment inertia parameters, force data collection and analysis, and modelling and simulation. It was argued that video is now comparable to cinefilm in terms of the quality of the data which can be derived from it, that cross-validated quintic splines provide a good general method for smoothing and differentiating position data, and that the DLT provides a flexible method for reconstructing raw position data. From the array of techniques available for determining BSIP, geometric modelling based on anthropometric measurements made on the subject is usually the best technique available providing at least some access to the subject is possible. For measuring ground reaction forces piezoelectric force plates are the most common in sports biomechanics, providing accurate data if they are mounted, calibrated and operated carefully, though some care needs to be taken when estimating the centre of force position. For integrating force data, the trapezoidal rule has the advantage over Simpson's rule of providing integrals at every interval and it may be as accurate depending upon the nature of the data. The process of modelling and simulation has

been summarized, the idea that simple rather than complex models may be more revealing has been proposed and the importance, but difficulty of evaluating models before they are used for simulation has been noted.

2.5 SUMMARY

This chapter has reviewed literature relating to this study under four main headings: vault springboard contact, modelling rebound activities, accommodating surface changes and methods of investigation. Little research has focused directly upon the springboard contact in vaulting, but mass-spring modelling, to date used mainly to investigate running and hopping, provides a promising route for developing the understanding of this activity, including the effects of springboard stiffness variations and how they might be accommodated. The review of methods of investigation has identified suitable approaches to collecting and analysing data for this study.

CHAPTER THREE
INVESTIGATING THE SUITABILITY OF A LINEAR SPRING

3.1 INTRODUCTION

A number of researchers have used a simple mass on a linear spring system to model human activities such as hopping and running (e.g. Blickhan, 1989; Farley, Blickhan, Saito and Taylor, 1991; McMahon and Cheng, 1990). As discussed in the previous chapter, the rationale for adopting such a model comes in part from the roughly linear vertical ground reaction force-mass centre displacement relationships found in these activities, which match the force-displacement relationship for a linear spring (Cavagna, Franzetti, Heglund and Willems, 1988; Farley *et al.*, 1991; Farley and González, 1996; He, Kram and McMahon, 1991).

The main purpose of the study reported in this chapter was to evaluate further the suitability of a mass-linear spring model for rebounding activities. In particular the study progressed to an activity in which, unlike hopping and running, the mass centre motion was not symmetrical about the middle of the ground contact, in other words an activity more like the springboard contact in gymnastic vaulting. To achieve this the ground reaction force-mass centre displacement relationships of four activities were analysed. The four activities were: hopping in place at the subject's preferred frequency, hopping in place at a higher frequency, two-footed forward hopping, and a running two-footed jump up onto a raised platform. A secondary purpose of the study was to enable the comparison of the two-dimensional Direct Linear Transformation (2-D DLT) method with the three-dimensional DLT (3-D DLT) method for obtaining sagittal plane data and to investigate the effect of different body segment inertia parameter estimates on mass centre position and velocity.

3.2 DATA COLLECTION

3.2.1 SUBJECT PREPARATION

A male athlete (mass 70.75 kg, height 1.79 m) agreed to be the subject and gave informed consent prior to the data collection (Appendix A.1). Ninety-five anthropometric measurements were made using tapes and callipers and were then entered into the geometric solid model developed by Yeadon (1990b). These measurements consisted of lengths, widths and perimeters at various points on the body which defined a 14 segment model made up of geometric solids. The segments were the hands, forearms, upper arms, thighs, shanks and feet for both left and right sides of the body, the trunk and the head. The human

body segmental density data reported by Dempster (1955) are used in the model, assuming the density of each segment to be uniform. The model output provided body segment inertia parameters (BSIP) for the subject, from which the segment masses and proximal ratios (distances from proximal segment endpoints to segment mass centres as a proportion of segment length) were later used to find the whole body mass centre position. The forearm and hand segments were combined to form a single segment (assuming a wrist flexion angle of zero and using the wrist as the distal endpoint) in order to avoid having to estimate finger positions when digitizing the film as occasionally these were blurred.

While the use of a geometric solid model such as Yeadon's is a way of tailoring BSIP estimations to the individual, if access to the subject is restricted (e.g. when only film data have been obtained at a sports competition) it is not always possible to make the anthropometric measurements required. In this case, a less sophisticated method of estimating BSIP must be used. To assess the influence of using perhaps the simplest method of mass centre position estimation, the ratio data of Dempster (1955) (as summarized in Winter, 1990) were also used. Appendix A.2 contains the subject's BSIP derived from the geometric solid model and the ratio data.

To aid the process of digitization the subject wore only swimming briefs and had 10 mm black adhesive tape placed around the perimeters of the metatarso-phalangeal joints, ankles, knees, hips, elbows, and wrists. These perimeters corresponded to the ends of the segments of the inertia model (Yeadon, 1990b) which were considered beneficial and practical to mark based on a pilot study. Taping perimeters was chosen since it provided guidance when digitizing segment extremities regardless of limb orientation or camera view.

Before data collection the subject, who was familiar with the laboratory and the experimental protocol, was allowed to warm up and then practice the four trial conditions. All trials were completed bare footed.

3.2.2 VISUAL DATA

The DLT method of reconstruction was chosen for this study because of the flexibility with which cameras may be positioned, the modest volume in which the activities were to take place and the ability to perform both 2-D and 3-D DLTs. Two-dimensional reconstruction of position data from film requires only one view of the activity to be recorded, whilst three-dimensional reconstruction normally requires a minimum of two simultaneously recorded views of the activity. By suitably positioning two cameras, the 2-D DLT was performed by selecting one of the views, whilst both views were used for the 3-D DLT.

The cameras used were a Redlake Locam II (model 51) with a Schneider-Kreuznach 13 972 262 Variogon 1.8 10-100 mm zoom lens running at 100 frames per second (fps) and a Bolex H16 EBM with a Switar 1:1.8 16 mm H16 RX lens running at 50 fps. Both cameras were battery powered. The film exposure times were $1/300^{th}$ second for the Locam (variable shutter opening set to 1/3) and $1/140^{th}$ second for the Bolex (fixed shutter) with Eastman Ektrachrome 7250 colour reversal high speed tungsten film (400 ASA tungsten rating) being used in both cameras. Daylight illumination was available through the laboratory windows but it was necessary to supplement this with 5 kW of flood lighting. Due to changes in the daylight illumination, light readings were taken frequently and lens apertures adjusted accordingly. Phase locking of the cameras was not possible so a high-rise LED timing light unit which displayed time down to milliseconds was positioned such that it could be clearly seen by both cameras. This enabled the synchronization of the resulting data from each view to be performed at the analysis stage (see below).

A 1.0 x 0.6 x 1.0 m calibration object consisting of 12 mm diameter steel tubing painted matt black and with a total of fifty centrally drilled coloured golf balls positioned throughout the volume was used in this study. The locations of the balls were determined using a civil engineering laser surveying system. A root mean square error (RMSE) of 0.8 mm was found for the consistency of locating the balls and a mean difference of 0.58 mm (±0.45 mm) was determined for the accuracy of ball location. The arrangement of the balls on the calibration object was such that by careful selection, control points which satisfied the calibration requirements of both the 2-D and 3-D DLTs could be found (Figure 3.1a).

In order for the calibration to cover the volume of interest while using this calibration object, the multiphase DLT approach was used (Challis, 1995). Initially the calibration object was placed centrally on the force plate and filmed, then it was raised 0.725 m so that the bottom layer of balls lay within the original volume and filmed again (Figure 3.1b). Preliminary calibration using only the object in the lower position enabled the positions of the bottom layer of control points of the object in its raised position to be determined and hence the position of all of the other control points in the raised position were determined. Calibration of the space for the activities was then performed using control points from the object in both positions, increasing the total volume covered by control points by approximately 75%. After filming the calibration object in the two positions with both cameras, the cameras were not moved, zoomed nor re-focused.

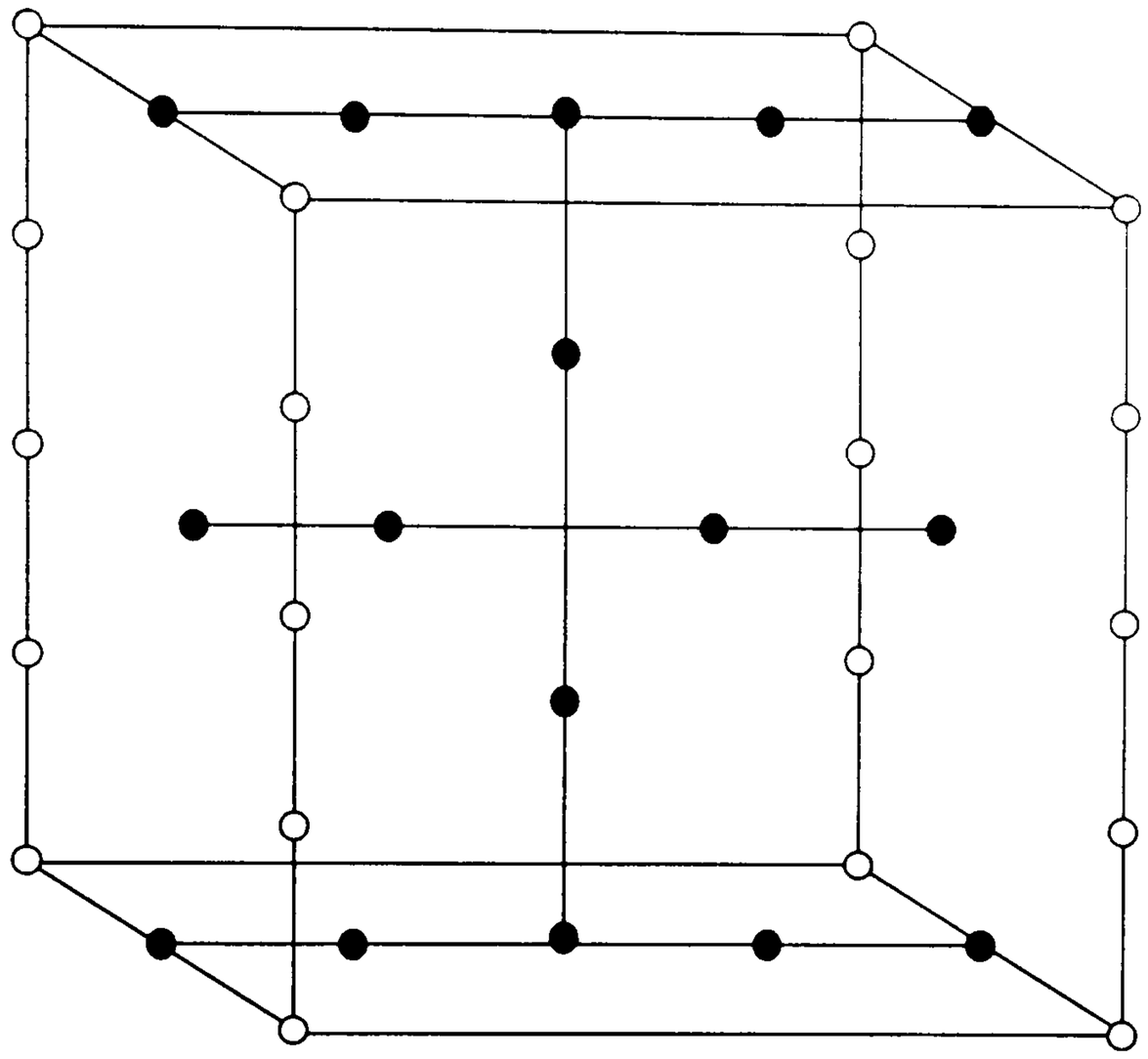

Figure 3.1a. The calibration object. Empty circles represent those balls digitized for 3D calibration; filled circles are those balls digitized for 2D calibration.

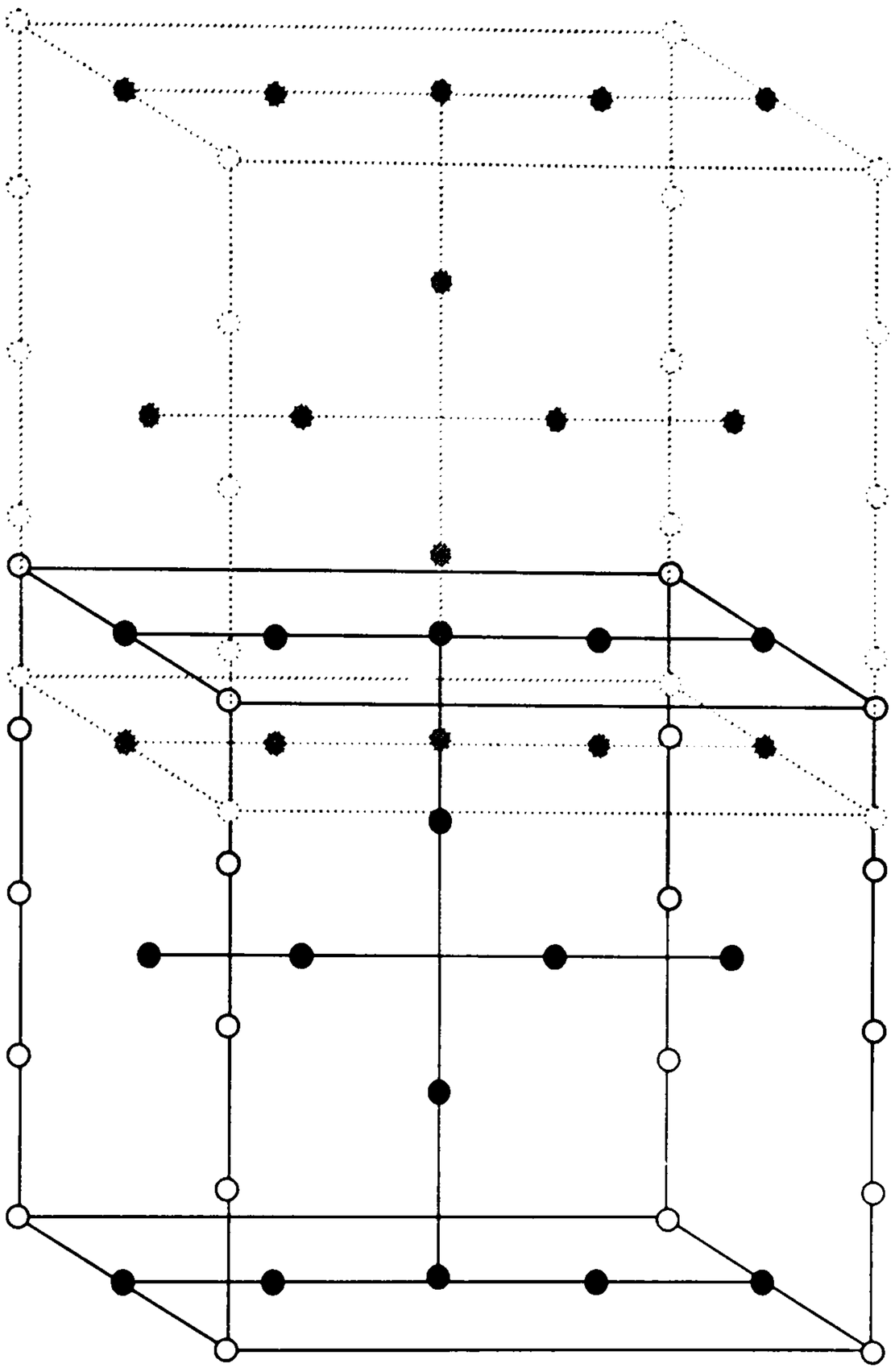

Figure 3.1b. An illustration of the multiphase DLT calibration. The black figure is the original position of the frame, the dotted figure is the second position.

For the 3-D reconstruction of the data the five control points on each of the four corner uprights of the calibration object were chosen based on the recommendation of Challis and Kerwin (1992). This gave a total of forty control points when the two calibration object positions were combined. The 2-D DLT requires control points to be distributed in a 'calibration plane', so the sixteen control points in the middle plane of the structure (approximately the plane of the activity) were chosen, giving thirty-two control points when the two calibration object positions were combined. Figure 3.1b illustrates the calibration object control points selected for each of the reconstructions.

A pilot study to establish suitable camera positions found that with both cameras on the same side of the subject and at an oblique angle to the sagittal plane of the activity, all necessary control points on the calibration object could be seen from both cameras. Furthermore, in the subsequent dynamic data collection, segment endpoints on both the near and far limbs of the subject could be seen by both cameras almost all of the time. The 2-D DLT allows flexible positioning of the camera, so filming from an oblique angle to obtain the sagittal plane data of the activity was not problematic. The camera positions chosen were such that each camera was at an angle of approximately 53° to the sagittal plane, giving an angle of 74° between the optical axes of the cameras. Each camera was mounted on a rigid tripod at a distance of 7.5 m from the centre of the force plate (reference origin) and the lens focal lengths were 18 mm for the Locam and 16 mm for the Bolex. Figure 3.2 shows the arrangement of the cameras with respect to the force plate. The cameras were levelled and the centres of both camera lenses were 0.96 m above the force plate surface.

Three markers were positioned horizontally at intervals of three metres on a wall two metres to the far side of the plane of activity from the cameras, at approximately camera height to act as reference points. Two of these points were visible in each camera view and enabled any camera wobble to be corrected for within the reconstruction software.

3.2.3 FORCE DATA

Horizontal and vertical ground reaction forces (GRF) and the centre of force were measured with a Kistler 9281-B12 force plate interfaced to an Acorn A440 Archimedes microcomputer via a CED 1401 analogue to digital converter. The vertical full scale deflection was set to 5 kN for all trials and the horizontal full scale deflection was set to 1 kN for hopping in place and forward hopping trials, and to 2 kN for running two-footed jump trials (see section 3.2.4). Burst sampling was performed at a rate of 1 kHz for one second for all trials.

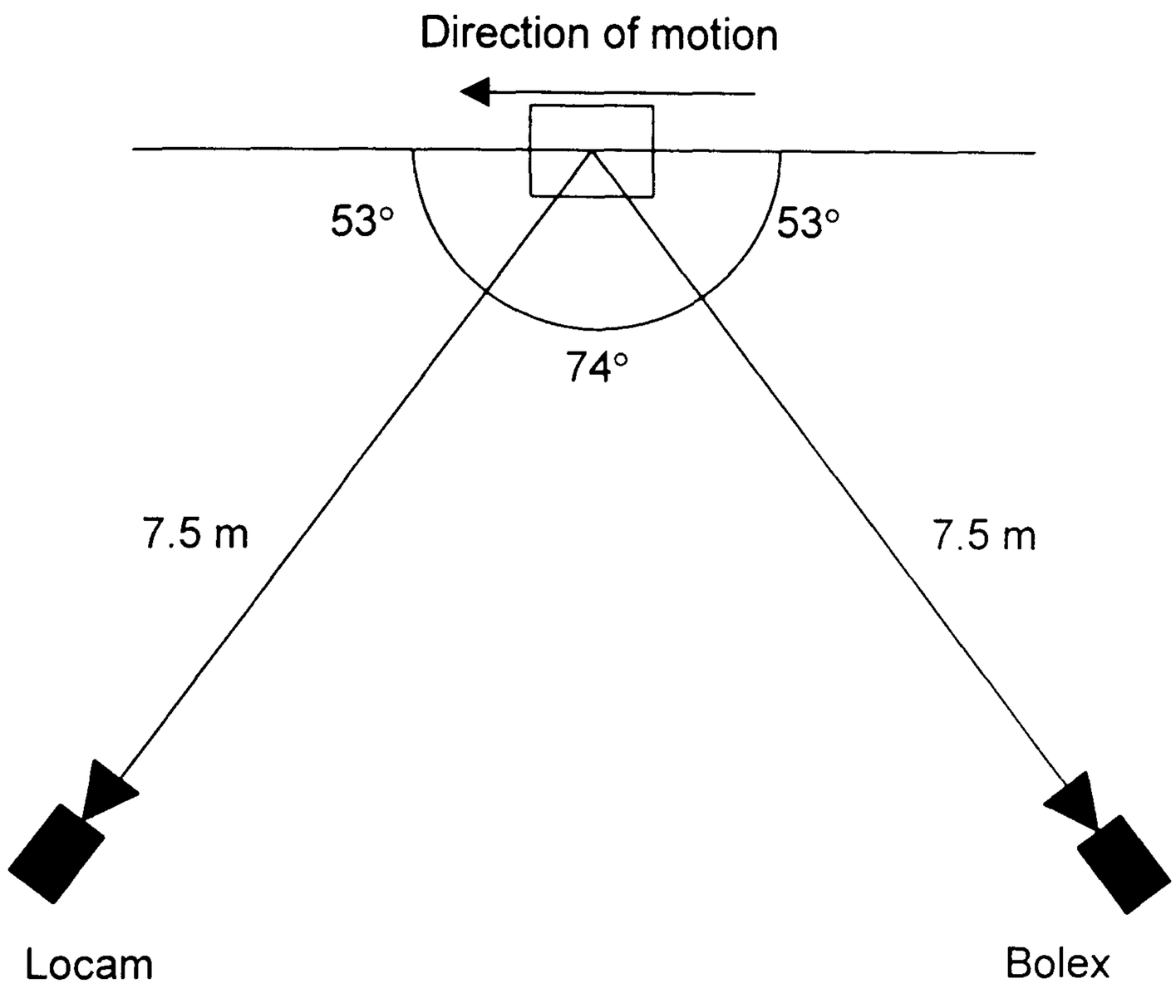

Figure 3.2. Plan view of camera positions relative to the force plate.

Nearest frame synchronization of film and force plate data is theoretically possible by noting plate contact and takeoff in both film and force data records. However in practice this can be problematic from the film records as the exact frames of contact and takeoff are often difficult to see clearly (a similar problem has also been demonstrated in the context of detecting loss of contact with the high bar in men's artistic gymnastics by Kerwin, Yeadon and Harwood, 1993). To improve on this, a high-rise LED in view of the Locam was switched on by the same signal which triggered the force plate thereby clearly locating the commencement of the force data record in the timescale of the cameras.

3.2.4 PROCEDURE

Four trial conditions were investigated:

1. Two footed hopping in place in the middle of the plate at preferred frequency.

2. As 1 but at a subject-selected higher frequency.

3. Two footed forward hopping at a subject-selected pace (subject contacted force plate after about four hops and continued hopping forwards after plate contact).

4. Running two-footed jump from the force plate onto a 0.3 m high platform positioned approximately 0.6 m from the centre of the plate (the subject took 3 or 4 strides prior to plate contact).

Arm movements were not restricted in any trial.

Each trial was identified by a unique number that was displayed in the view of both cameras and incorporated into the filename of the force data record. In all trials the force plate was triggered after the cameras to allow the cameras time reach the desired frame rates. For hopping in place trials, the data were collected after the subject had achieved a steady rhythm. The forward hopping and running jump trials required the subject to start hopping/running forward on an audible cue. Filming commenced prior to the ground contact *preceding* contact with the plate and the force data collection then started shortly after the cameras started running.

3.3 DATA ANALYSIS

3.3.1 TRIAL SELECTION

At least ten trials of each of the four activities were recorded. Where the force data capture had been successful (i.e. both feet completely on the plate, the whole contact period

recorded, and the plate not having been over-ranged), the film from each camera was inspected and possible trials to analyse were identified based on the following criteria:

- the LED synchronization event from the force plate trigger occurred after the cameras were up to speed (judged from the millisecond timing lights),
- the cameras were up to speed prior to the takeoff from the ground before the force plate contact of interest,
- both feet contacted the force plate approximately centrally,
- the cameras were still running when the ground contact after the one of interest occurred.

Despite the previously mentioned difficulty in locating the exact frames of touchdown and takeoff from visual records, it was found that for the trials which met the above criteria the duration of plate contact, as estimated from film and force data, corresponded to within 0.02 s. Inspection of the force data records revealed that within each group of trials there was very little variation in duration of contact with the plate (t_c), peak vertical force (Fz_{max}), percentage of t_c to reach Fz_{max} (tFz_{max}), vertical impulse (Imp_z), and horizontal impulse (Imp_y; only evaluated for the forward hopping and jumping trials), as shown in Table 3.1. This is illustrated in Figure 3.3 which shows the force histories from each of the trials. Therefore it was decided to select one trial at random from each of the four conditions to be analysed in detail.

Table 3.1. Summary of force data for each group of trials.

Trial		t_c (s)	Fz_{max} (N)	tFz_{max} (%)	Imp_z (N.s)	Imp_y (N.s)
PREF	mean	0.297	2235	53	192	-
	SD	0.016	145	2	7	-
HIGH	mean	0.185	2689	46	166	-
	SD	0.006	34	1	5	-
FWD	mean	0.207	2883	41	202	+5
	SD	0.005	87	2	8	6
JUMP	mean	0.174	3345	43	262	-65
	SD	0.008	155	2	7	2

(a)

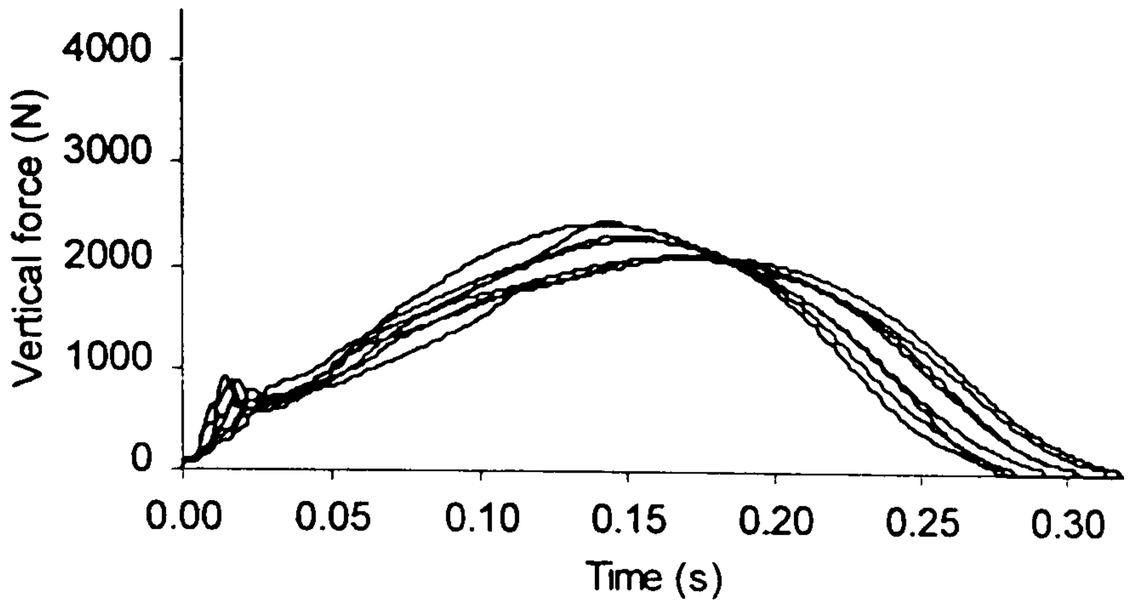

(b)

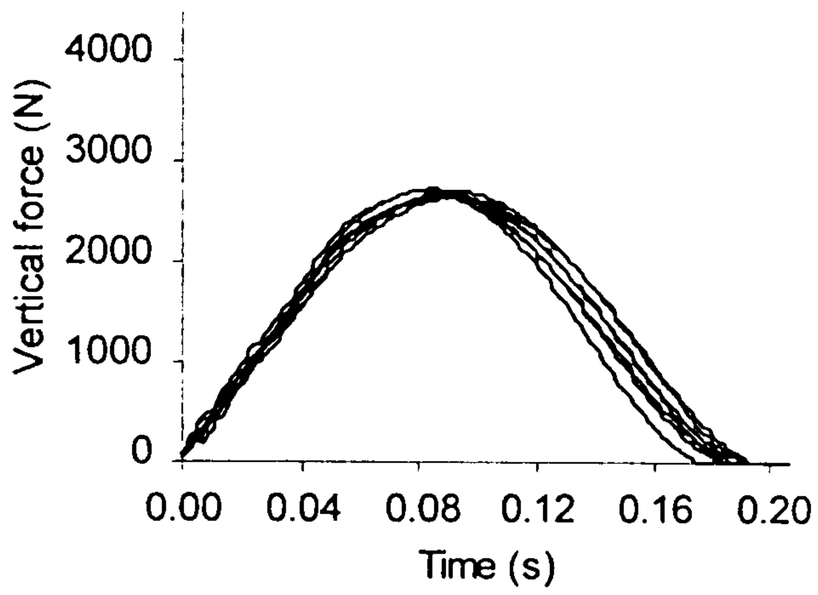

(c)

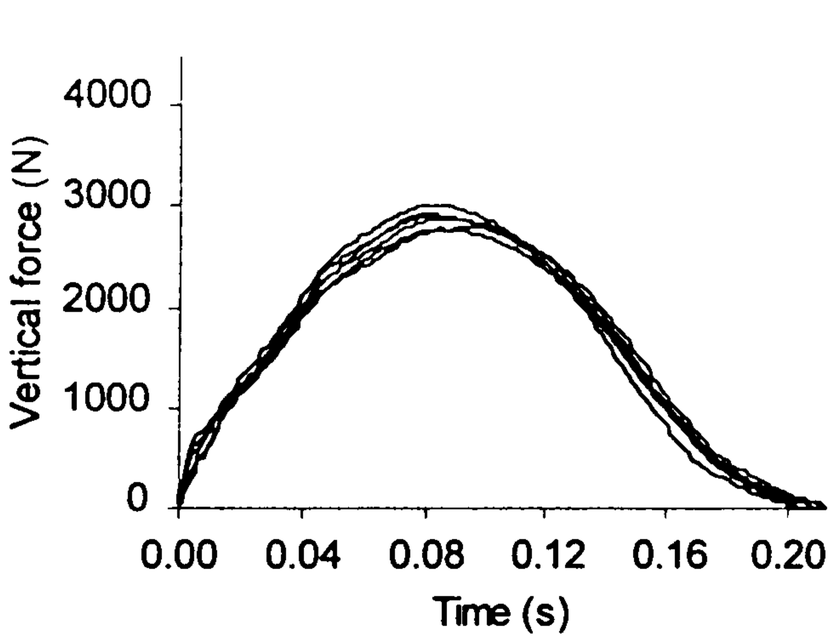

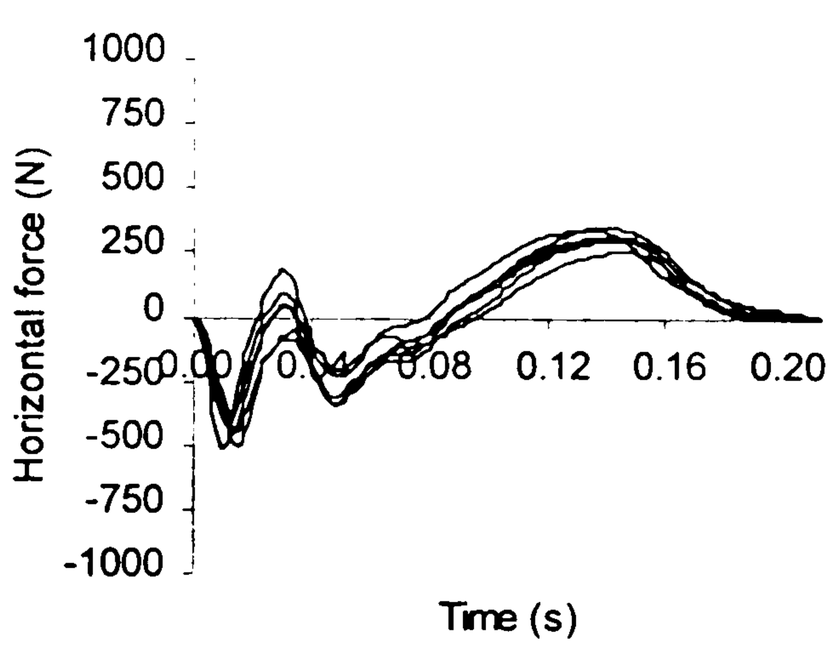

(d)

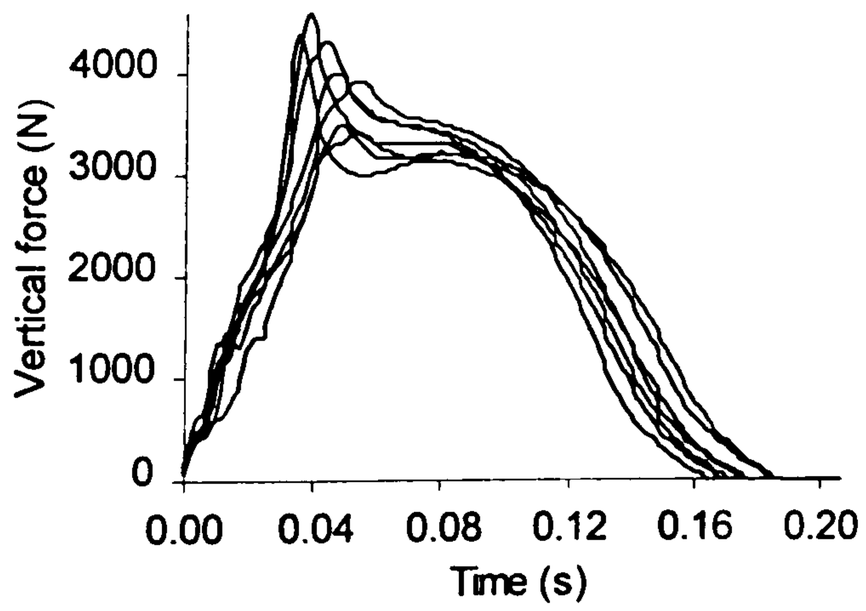

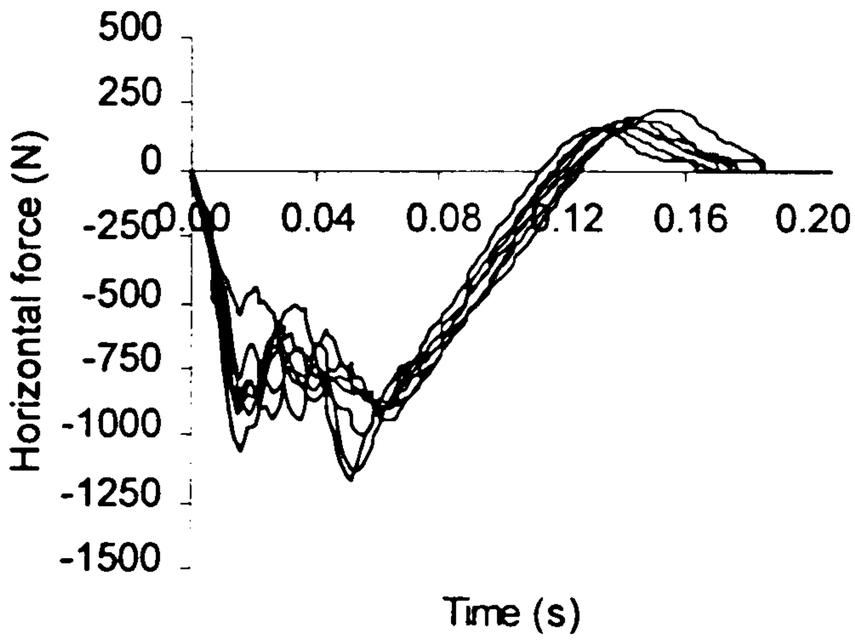

Figure 3.3. Force histories for each of the trials: (a) two-footed hopping in place at preferred frequency, (b) two-footed hopping in place at higher frequency, (c) two-footed forward hopping and (d) two-footed running jump.

3.3.2 IMAGE DATA ANALYSIS

All digitization was performed by projecting the film using an NAC Analysis Projector with a 50 mm lens onto a Terminal Display Systems HR48 tablet (active area 1.20 m x 0.90 m, resolution 0.025 mm) which was interfaced to an Acorn A3000 microcomputer. Standard laboratory software logged the digitized coordinates from the film images and then spooled the data to an ASCII format file. Despite the fact that the projector had an internal fan to control its temperature, before digitization commenced the projector was allowed to warm up to reduce the risk of inaccuracies due to possible film distortion when warming up.

From both camera views, the film of the forty control points for the 3-D DLT reconstruction and two of the three reference points on the wall were digitized ten times. The Locam view was used for the 2-D analysis and the thirty-two control points for the 2-D DLT reconstruction plus two reference points were digitized ten times. The mean digitized coordinates were later used for the reconstruction. Since the film in the cameras had to be changed during the data collection, which may have moved the cameras slightly, the calibration object was positioned and filmed again. Therefore the control point digitization was repeated to enable new DLT parameters to be calculated for the trials filmed after the film change.

To investigate the GRF-mass centre displacement relationship, the information required from film was the subject's mass centre position and velocity immediately before plate contact. Mass centre displacement during ground contact could then be estimated by combining these data with the GRF history. The mass centre velocity at touchdown was calculated using equations of constantly accelerated motion, therefore only the mass centre positions at each end of the airborne phase before plate contact and the duration of this phase were needed. In order to calculate the mass centre positions the image space coordinates of the subject's middle metatarso-phalangeal joints, ankles, knees, hips, elbows, shoulders and wrists and the centre of his head were required from both cameras.

To reduce the random error inherent in raw digitized data, the use of the mean data from repeated digitizations was investigated. This process reduces the magnitude of the random error by a factor of the square root of the number of digitizations used, but is not normally used owing to the time overhead when a large number of frames are to be digitized. In this study, the small number of frames digitized from each camera per trial meant that repeated digitization was viable.

To quantify the effect of repeated digitizations, one jump trial was digitized ten times from the Locam view and a 2-D DLT reconstruction was performed on each digitization. Mean values for the sagittal plane coordinates based on two, three, four, five, seven and all ten digitizations were calculated, then the precision with which these points could be located was estimated. This was achieved by determining the standard error for each point (Barford, 1985). The standard error of the mass centre location was also calculated for each combination of digitizations since the mass centre location was the main interest rather than the individual segment endpoints. The results for the last frame in flight before contact with the plate are summarized in Table 3.2.

On the whole, increasing the number of digitizations only slightly improved the precision with which the points were located (to three decimal places) and the precision for each endpoint was 0.01 m or better even for two digitizations. Since the mass centre position (a weighted mean of fifteen points) was the main information required and the precision for this point was of the order of a few millimetres it was decided that it would be sufficient simply to digitize each trial once.

The segment endpoints listed above and the reference points on the wall behind the plane of action were digitized from both camera views for the four selected trials. The time at exposure was read from the millisecond timer and entered manually for each frame digitized. This enabled synchronization of the two sets of film data by matching the Locam data (100 fps) as closely as possible to the Bolex data (50 fps), giving a synchronization error of no more than 0.005 s.

The digitized data for each trial were reconstructed using both the 2-D and 3-D DLTs to obtain sagittal plane position data. The mass centre position in each frame digitized was then calculated using the segment mass and segment proximal ratio data obtained from both the geometric model of Yeadon (1990b) and standard ratio data of Dempster (1955).

Equation 3.1 shows how the y coordinate of the mass centre in a given frame was calculated; the calculation of the z coordinate has the same form. In this equation Y is the horizontal coordinate of the mass centre, M is the whole body mass, y_{p_i} and y_{d_i} are the horizontal coordinates of the proximal and distal endpoints of segment i, r_{p_i} and m_i are the proximal ratio and the mass for segment i, and N is the number of segments comprising the body.

$$Y = \frac{1}{M}\sum_{i=1}^{N}\left[\left(y_{p_i} + (y_{d_i} - y_{p_i}).r_{p_i}\right)m_i\right] \qquad 3.1$$

Table 3.2. Overall (combined horizontal and vertical) standard errors in metres for each of the points digitized and the mass centre, over two to ten digitizations.

	Number of digitizations					
	2	3	4	5	7	10
Left toe	0.010	0.006	0.005	0.004	0.003	0.002
Left ankle	0.003	0.002	0.002	0.002	0.001	0.001
Left knee	0.002	0.003	0.003	0.002	0.003	0.002
Left hip	0.008	0.006	0.004	0.004	0.003	0.002
Left shoulder	0.003	0.002	0.002	0.002	0.002	0.001
Left elbow	0.009	0.007	0.005	0.004	0.003	0.002
Left wrist	0.003	0.002	0.002	0.001	0.001	0.001
Right toe	0.002	0.002	0.002	0.003	0.002	0.002
Right ankle	0.003	0.002	0.002	0.002	0.001	0.001
Right knee	0.004	0.004	0.003	0.002	0.002	0.002
Right hip	0.003	0.004	0.004	0.003	0.002	0.002
Right shoulder	0.008	0.008	0.006	0.005	0.003	0.003
Right elbow	0.003	0.003	0.002	0.002	0.001	0.001
Right wrist	0.004	0.002	0.002	0.002	0.001	0.001
Ear	0.004	0.003	0.003	0.003	0.002	0.002
Mass Centre	0.001	0.002	0.002	0.001	0.001	0.001

For each of the four combinations of BSIP and reconstruction methods, touchdown velocities were calculated for each trial. This was done using the equations of uniformly accelerated motion and mass centre displacements during the flight phases preceding touchdown as follows:

Horizontally,

$$v_y = \frac{s_y}{t} \qquad 3.2$$

Vertically,

$$u_z = v_z - a_z.t \qquad 3.3$$

$$s_z = u_z.t + {}^1\!/_2.a_z.t^2 \qquad 3.4$$

Substituting from 3.3 into 3.4,

$$s_z = v_z.t - a_z.t^2 + {}^1\!/_2.a_z.t^2$$
$$s_z = v_z.t - {}^1\!/_2.a_z.t^2$$

and rearranging,

$$v_z = \frac{s_z + {}^1\!/_2.a_z.t^2}{t} \qquad 3.5$$

In the above equations u_z is the mass centre vertical velocity at the beginning of the airborne phase, v_y and v_z are respectively the horizontal and vertical mass centre velocities at the end of the airborne phase, s_y and s_z are respectively the horizontal and vertical mass centre displacements during the airborne phase, a_z is the acceleration due to gravity and t is the duration of the airborne phase.

Table 3.3 summarizes the mass centre positions and velocities at touchdown for each of the four trials and four combinations of methods, and gives the root mean squared difference for each variable. Only small differences were found between methods for both mass centre positions and velocity estimates for a given trial. Closer comparison of the mass centre position data calculated from the ratio data and geometric model based data revealed a systematic difference of approaching 0.05 m in the vertical direction. This is approximately only five percent of the mass centre displacement from the ground and is not propagated to the velocity data (being a systematic difference). Therefore it was unlikely to have much influence on the investigation of the GRF-mass centre displacement relationship. Without a

Table 3.3. Horizontal and vertical mass centre position and velocity at touchdown for each of the four trial conditions (PREF, HIGH, FWD, JUMP) and combinations of reconstruction (2D, 3D) and BSIP (Dempster, D, and Yeadon, Y).

	Position		Velocity	
	y (m)	z (m)	v_y (m.s^{-1})	v_z (m.s^{-1})
PREF2DD	1.422	1.131	0.00	-1.08
PREF2DY	1.417	1.082	0.00	-1.08
PREF3DD	1.420	1.126	0.05	-1.12
PREF3DY	1.414	1.077	0.05	-1.13
RMSD	0.003	0.028	0.03	0.03
HIGH2DD	1.376	1.090	0.01	-1.14
HIGH2DY	1.369	1.041	0.00	-1.14
HIGH3DD	1.395	1.088	0.05	-1.09
HIGH3DY	1.389	1.038	0.05	-1.08
RMSD	0.012	0.029	0.03	0.03
FWD2DD	1.254	1.075	1.72	-1.53
FWD2DY	1.250	1.024	1.73	-1.52
FWD3DD	1.286	1.067	1.76	-1.48
FWD3DY	1.281	1.018	1.75	-1.47
RMSD	0.018	0.029	0.02	0.03
JUMP2DD	1.064	1.027	2.95	-1.62
JUMP2DY	1.066	0.980	2.95	-1.62
JUMP3DD	1.069	1.040	2.94	-1.57
JUMP3DY	1.072	0.992	2.95	-1.57
RMSD	0.004	0.028	0.01	0.03

N.B. 'RMSD' indicates the root mean squared deviations from the mean of the four estimates.

clear case for or against any one of the four methods of obtaining mass centre position data, it was decided that the simplest of the four methods, i.e. the 2-D reconstruction and standard BSIP, was satisfactory for the analyses which followed.

3.3.3 FORCE DATA ANALYSIS

For each of the four trials, the subject's vertical mass centre velocity and displacement during force plate contact were calculated by combining the force and visual data as follows:

- for every force sample the subject's body weight was subtracted from the vertical force (F_z),
- these were then divided by the subject's body mass to give the net vertical acceleration of the mass centre,
- the acceleration history was then integrated twice from touchdown to takeoff, using the mass centre positions and velocities just prior to touchdown obtained from the visual data as initial conditions.

Three methods of performing the numerical integration were tried on the trials. These methods were rectangle rule (simply treating each data point as a rectangle with the width of the inter-sample period, i.e. 0.001 s), trapezoidal rule, and Simpson's 1/3 rule. Table 3.4 shows the effect on the vertical mass centre position at takeoff of these different methods of integration. None of the three integration methods resulted in more than a 0.002 m difference in mass centre position at takeoff. Therefore it was decided that the rectangle rule was the most suitable of the three since it does not suffer from the loss of data at the ends of the sequence, as do the other methods.

Also shown in Table 3.4 are the effects on the vertical mass centre position at takeoff of over- and under-estimating the touchdown vertical velocity by 0.05 $m.s^{-1}$ (the largest variation between touchdown velocities calculated for any trial by the four different combinations of reconstruction method and BSIP). The largest difference caused by this perturbation was 0.016 m, less than two percent of the vertical mass centre displacement.

For the forward hopping and jumping trials, the sagittal plane horizontal force data (F_y) were divided by the subject's mass and numerically integrated twice using the rectangle rule, to generate the mass centre displacement histories for each of the trials during plate contact. The horizontal mass centre positions and velocities just prior to touchdown, as determined from the visual data, were again used as the initial conditions for the integrations.

Table 3.4. The vertical mass centre displacement at takeoff as calculated by each of the three integration methods and the effect on this displacement of a vertical velocity perturbation of 0.05 $m.s^{-1}$.

	Integration method			Velocity perturbation
	Rectangle	Trapezium	Simpson's	± 0.05 $m.s^{-1}$
PREF	1.187 m	1.188 m	1.188 m	± 0.016 m
HIGH	1.105 m	1.106 m	1.106 m	± 0.009 m
FWD	1.160 m	1.161 m	1.162 m	± 0.010 m
JUMP	1.122 m	1.122 m	1.121 m	± 0.009 m

Perturbation of the horizontal mass centre velocities by ±0.05 $m.s^{-1}$ (more than the largest variation between horizontal touchdown velocities calculated for any trial between the four different combinations of reconstruction method and BSIP) resulted in a change of mass centre position at takeoff from the plate of ±0.01 m in both trials. This was approximately 3 percent of the mass centre horizontal displacement during plate contact and as such was unlikely to affect the outcome of the subsequent investigation.

The distance between the mass centre and the mid metatarso-phalangeal joint (called the 'spring length') was calculated throughout force plate contact for each trial. The angle between a line joining these two points and the vertical (called the 'spring angle') was also calculated for the forward hopping and running jump trials, as was the angle of the resultant GRF vector to the vertical (called the 'force angle').

3.4 LINEAR SPRING SUITABILITY

Despite the overall complexity of the structures involved in supporting the body during various activities, evidence from Cavagna, Franzetti, Heglund and Willems (1988) and that of studies of the musculo-tendinous system of the lower limbs (e.g. Ker, Bennett, Bibby, Kester and Alexander, 1987; Alexander, 1991b), suggested that a single linear supporting spring may be a suitable model for these structures, at least for the vertical component of the motion. Following the work of Cavagna *et al.* (1988), this study used the shape of the force-mass centre displacement graphs during ground contact to establish empirically the suitability of using a linear spring model. In this study however, this investigation was conducted not only on the vertical component of the motion but also on the overall sagittal plane motion, thereby adding the forward component.

3.4.1 VERTICAL MOTION

The vertical GRF-mass centre displacement graphs during ground contact in all four activities (Figures 3.4 a-d) show reasonable linearity, supporting the use of a linear spring for modelling the vertical motion. The graph of the preferred frequency hopping trial shows that the loading (from touchdown to minimum displacement) and unloading (from minimum displacement to takeoff) phases do not overlap which is contrary to the results of Farley, Blickhan, Saito and Taylor (1991), who found that at the preferred frequency there was a very good overlap of these phases of the graphs. However, the preferred frequency in that study was around 2.2 hops.s^{-1}, whereas the subject in this study preferred a lower frequency of 1.7 hops.s^{-1}. At this frequency it is possible that rather than simply 'rebounding' the subject may have been hopping more like a series of small, slow jumps, in which case the legs may not act in a very spring-like way. The *most* linear of the graphs are for the higher frequency hopping in place (Figure 3.4b) and the forward hopping trial (Figure 3.4c), where the hopping frequencies were 2.4 and 2.1 hops.s^{-1}, in better agreement with Farley *et al.* (1991).

In the jumping trial (Figure 3.4d), the GRF-mass centre displacement relationship is markedly affected by the spike in the vertical force record due to the initial impact with the plate. All trials took place with the force plate uncovered by any protective material and with the subject in bare feet; it is possible that if the subject had worn running shoes or if the plate had been covered by even a thin crumb gymnastic mat that this spike would have been attenuated and the graph may have appeared more like that of an ideal linear spring. However this would also have had other effects on the force-displacement history which would have been undesirable for this study, since it would insert a damping element between the 'leg spring' and the ground.

Linear least squares fits to each of the four sets of data resulted in correlation coefficients (r values displayed in Figures 3.4 a-d) of between -0.89 for the running two-footed jump and -0.99 for the high frequency hopping, indicating that for all four activities, a linear spring would be a reasonable approximation. Linear least squares fits to the data limited to the period of 'effective contact' (Cavagna, Franzetti, Heglund and Willems, 1988), that is when the vertical GRF is greater than body weight, resulted in correlation coefficients (r(e) values displayed in Figures 3.4 a-d) which were of similar or slightly lower magnitude than for the complete data sets. Where the correlation coefficients were lower, this might be explained by the greater influence of the initial impact peaks on the shortened data sets.

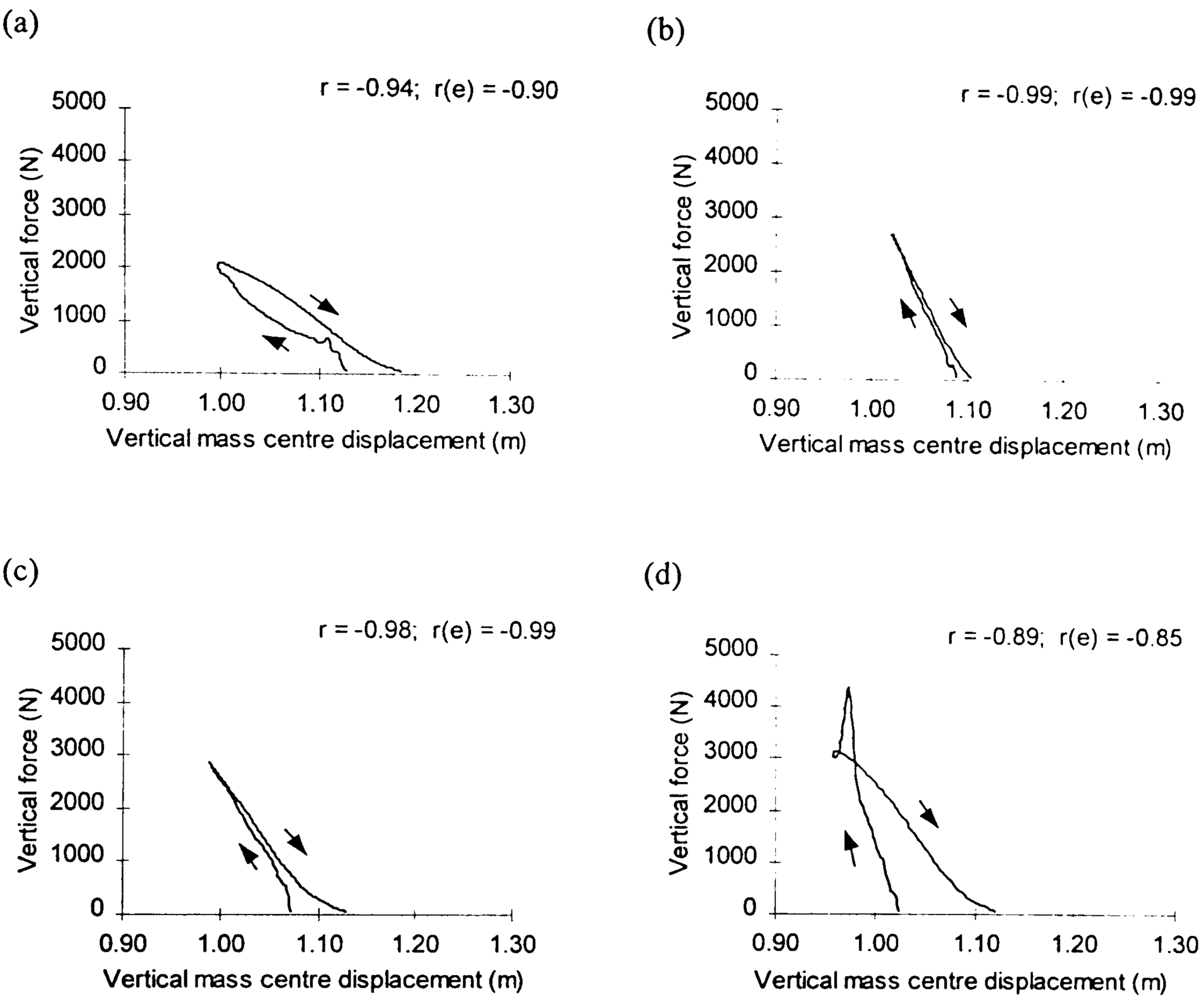

Figure 3.4. Vertical force-mass centre displacement relationships during force plate contact for (a) preferred frequency two-footed hopping in place, (b) high frequency two-footed hopping in place, (c) forward two-footed hopping and (d) running two-footed jump.

N.B. Arrows indicate the loading and unloading portions of the curve. Linear correlation coefficients are for the whole contact period (r) and the effective contact period (r(e)).

3.4.2 FORWARD MOTION

In previous studies (Blickhan, 1989; McMahon and Cheng; 1990), the suitability of a linear 'leg spring' for models of forward motion appears to have been assumed based on the evidence from studying the *vertical* motion of the mass centre during running and hopping activities, or because the use of a linear leg spring in a model produces reasonable agreement with the real world. In these models the spring runs from the mass centre to the 'foot' of the model and contacts the ground at some non-zero angle before the vertical, then leaves the ground at the same angle past the vertical (Figure 3.5). The magnitudes of the mass centre velocity at touchdown and takeoff were also the same, so the ground contact could be termed symmetrical. An implicit assumption is that in the real performance the GRF vector acts from the point of contact through the mass centre. In this study, the suitability of a linear spring for modelling forward motion was investigated explicitly.

The spring angle for the forward hopping trial was 8.8° before the vertical at touchdown and 8.2° past the vertical at takeoff, while the magnitude of the mass centre velocity at these times was 2.30 and 2.26 $m.s^{-1}$ respectively. The spring angles at the corresponding instants for the running jump trial were 19.1° before the vertical and 2.7° past, and the magnitude of the mass centre velocity at these times was 3.36 and 2.83 $m.s^{-1}$ respectively. The very close

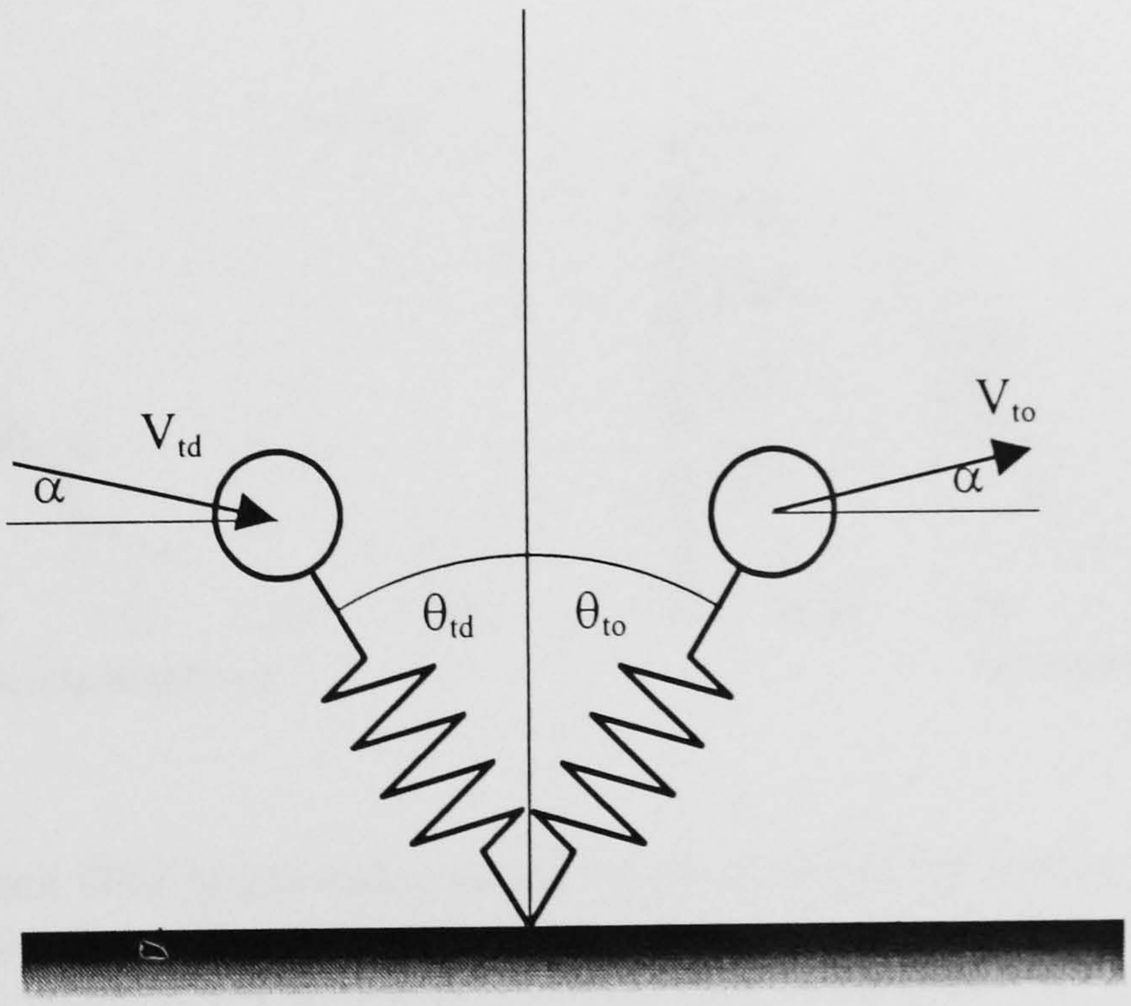

Figure 3.5. Symmetrical ground contact.
N.B. $\theta_{td} = \theta_{to}$ and $|V_{td}| = |V_{to}|$.

similarity between the touchdown and takeoff angles and speeds for the forward hopping, particularly when compared with the marked differences in the running jump, support the categorization of the forward hopping trial as a symmetrical ground contact. The jump trial was therefore considered to be an asymmetrical ground contact.

Considering the spring angle and the force angles (i.e. the angle of the resultant GRF), the difference between the two was less than fifteen degrees for 96% of ground contact for forward hopping and 90% for the running jump. The greatest difference between the two angles was 17.9° for the forward hopping trial and 19.4° for the jump trial, with the root mean squared differences being 6.24° and 7.94° respectively. Thus for these activities the GRF was indeed acting close to the mid-toe to mass centre line during ground contact.

To assess the linearity of the GRF-mass centre relationship in these trials, the magnitude of the GRF was plotted against the spring length and, as with the vertical motion, linear least squares fits to the data were calculated (Figures 3.6 a & b). The correlation coefficients were -0.99 for the forward hopping and -0.94 for the jump, again justifying the adoption of a linear spring to model this type of activity. It was found that calculating the component of the GRF acting directly along the mid-toe to mass centre line and performing least squares fits with these force data resulted in negligible differences in the correlation coefficients.

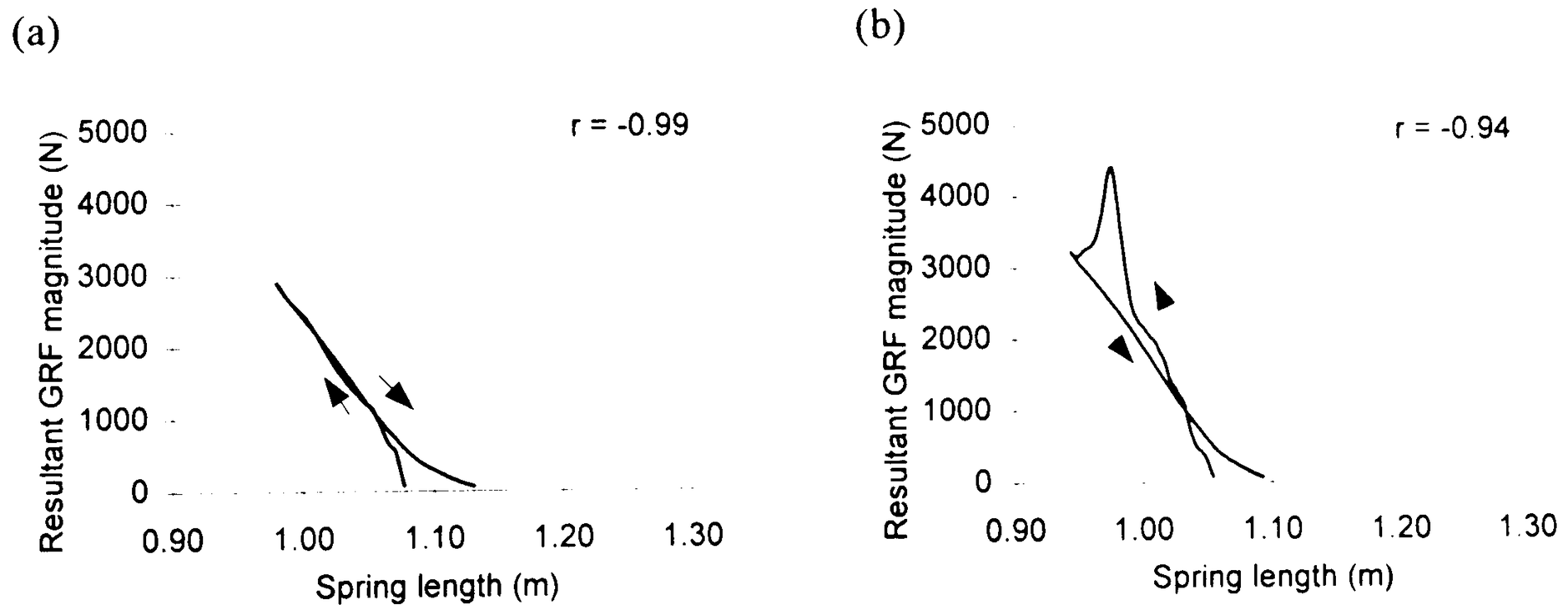

Figure 3.6. Resultant GRF magnitude-spring length relationship during force plate contact for: (a) forward two-footed hopping and (b) running two-footed jump.

N.B. Arrows indicate the loading and unloading portions of the curve. Linear correlation coefficient (r) is for the whole contact period.

3.5 SUMMARY

The main purpose of the study reported in this chapter was to evaluate further the suitability of using a linear spring for a mass-spring representation of human rebounding activities, including those where the mass centre motion was not symmetrical about the middle of the ground contact. This was achieved by recording four different types of rebounding activity using cine film and a force plate, then investigating the derived GRF-mass centre displacement relationships.

The vertical GRF-mass centre displacement graphs during the ground contact phase of a subject hopping and performing a running two-footed jump were found to be reasonably linear, thereby supporting the use of a linear spring for modelling the vertical motion of the mass centre in such activities. This finding was in agreement with that of Cavagna *et al* (1988), Farley, Blickhan, Saito and Taylor (1991), Farley and González (1996) and He, Kram and McMahon (1991). It was also found that for the forward hopping and running jump trials, the GRF-spring length graphs (i.e. not just the vertical components and not just symmetrical ground contacts) were sufficiently linear to support the use of a linear spring in a simple mass-spring model of this type of activity.

The secondary purpose of the study was to enable the comparison of the 2-D and 3-D DLT methods for obtaining sagittal plane data and to investigate the effect of different body segment inertia parameter estimates on mass centre position and velocity. For reconstructing the sagittal plane position data, the 2-D DLT was found to compare very favourably with the 3-D DLT. The difference in the whole body mass centre position when calculated using Dempster's (1955) ratio data compared with its position when using BSIP obtained using the geometric solid model of Yeadon (1990b) was found to be less than 0.01 m in the horizontal direction and a systematic 0.05 m vertically. Consequently, the differences in the mass centre velocities were also negligibly different. The four combinations of the two reconstruction methods and the two BSIP estimates for calculating whole body mass centre position and velocity, resulted in values which were sufficiently similar for the decision to be made to use the 2-D DLT with the BSIP from Dempster's ratio data for the analyses in this chapter.

Whilst the linearity of the GRF-mass centre displacement relationships in this study were not perfect, it must be remembered that the nature of a model is that it is a simplification of the system involved. Therefore the use of a linear spring would appear to be appropriate in the search for an adequate model of human rebounding activities like vault springboard takeoff which are asymmetrical in the ground contact phase. The following chapter describes the development of two such models.

CHAPTER FOUR
MODEL DEVELOPMENT

4.1 INTRODUCTION

The springboard takeoff in gymnastic vaulting can be affected by a number of biomechanical variables such as approach speed, body angle at contact with the board (commonly known as the blocking angle) and lower limb muscle activity. A systematic investigation of the influence of these variables requires either that they be under the control of the investigator, or that a very large sample of vaults be analysed in the hope of finding springboard contacts where some variables are (virtually) unchanged while one variable alters. Given that it is very difficult for even the most skilled and willing gymnasts to alter just one aspect of technique to order and that analysing a large number of vaults in the hope that the desired variety had been performed is unrealistic, this type of problem is ideally suited to a modelling approach.

This chapter describes the formulation of two mass-spring models and the methods used to program and solve the resulting equations. The decision to use a mass-spring model was based on the rebounding nature of the activity, the spring-like surface and the successful use by other researchers of mass-spring systems to model the kinematics of hopping, running and long jumping. The results of the previous chapter supported the adoption of a linear spring to represent the lower limbs. There were two modes of operation for each model:

- parameter estimation- determining a model leg stiffness value which satisfied given touchdown and takeoff conditions;
- simulation- calculating linear and angular velocities at springboard takeoff in response to given touchdown conditions, when the model leg stiffness was known.

The ability to determine leg stiffness from actual vault data was necessary in order to establish the likely range of stiffnesses which may be adopted by gymnasts during vaulting. Although a number of methods for estimating leg stiffness have been proposed in the literature (see Chapter Two, section 2.2.2), they have usually assumed a symmetrical ground contact and required ground reaction force information (e.g. Siegler, Seliktar and Hyman, 1982; Cavagna, Franzetti, Heglund and Willems, 1988; Farley and González, 1996; He, Kram and McMahon, 1991). However the method used by McMahon and Cheng (1990), where the model's leg stiffness was adjusted iteratively until the desired takeoff conditions were produced could be used.

With an estimate of the range of leg spring stiffnesses adopted in vaulting, it would then be possible to explore systematically the effect of variations to leg spring stiffness, board spring stiffness and initial conditions (such as approach speed and blocking angle) by a series of simulations. This would allow the mechanics of springboard contact to be investigated and a better understanding of the interrelationships among the key variables to be sought. This application of the models is described in Chapter Six.

4.2 THE MODELS

The simplest form of mass-spring model is a point mass attached to a massless linear spring and such an arrangement has formed the basis of models used previously to investigate hopping, running and jumping (e.g. Blickhan, 1989; Blickhan, Friedrichs, Rebhan, Schmalz and Wank, 1995; Farley and González, 1996; Farley, Blickhan, Saito and Taylor, 1991; McMahon and Cheng, 1990). Most of these models assumed that the ground contact was symmetrical about the mid-point, in other words, that the takeoff speed equalled touchdown speed, and that angles before the vertical of the leg spring and velocity vector at touchdown were the same as the angles past the vertical at takeoff. This is not the case in vault takeoffs and furthermore, point mass on a spring models only consider the linear motion of the mass centre, ignoring the rotational motion of the system which is an important factor in gymnastic vaulting (Readhead, 1987). The asymmetry of the ground contact and the rotational motion of the system were therefore addressed in this study.

To include angular motion in the model some account had to be taken of the rotational inertia of the system. A straightforward way to achieve this was to model the gymnast as a uniform rigid cylinder inside which ran a massless spring, attached at the mass centre of the cylinder and projecting slightly from the 'foot' end of the cylinder (Figure 4.1). The inside of the cylinder was considered to be smooth, therefore there was no friction between the spring and the cylinder. This cylinder and spring arrangement formed the basis of the two models that were developed.

The asymmetry of the ground contact was quite easily modelled. For a forward hopping mass-spring model to achieve perfect symmetry at a given speed of progression and touchdown angle, only one spring stiffness will suffice. That is to say, should the spring be too stiff the model will takeoff before the spring reaches the desired angle, or if too soft it will takeoff when the spring has passed the desired angle (or not takeoff at all). This principle was used by McMahon and Cheng (1990) for symmetrical ground contact, but the principle that only one stiffness will do applies to any other takeoff angle required. Therefore if the touchdown kinematics and takeoff spring angle are known, a unique spring

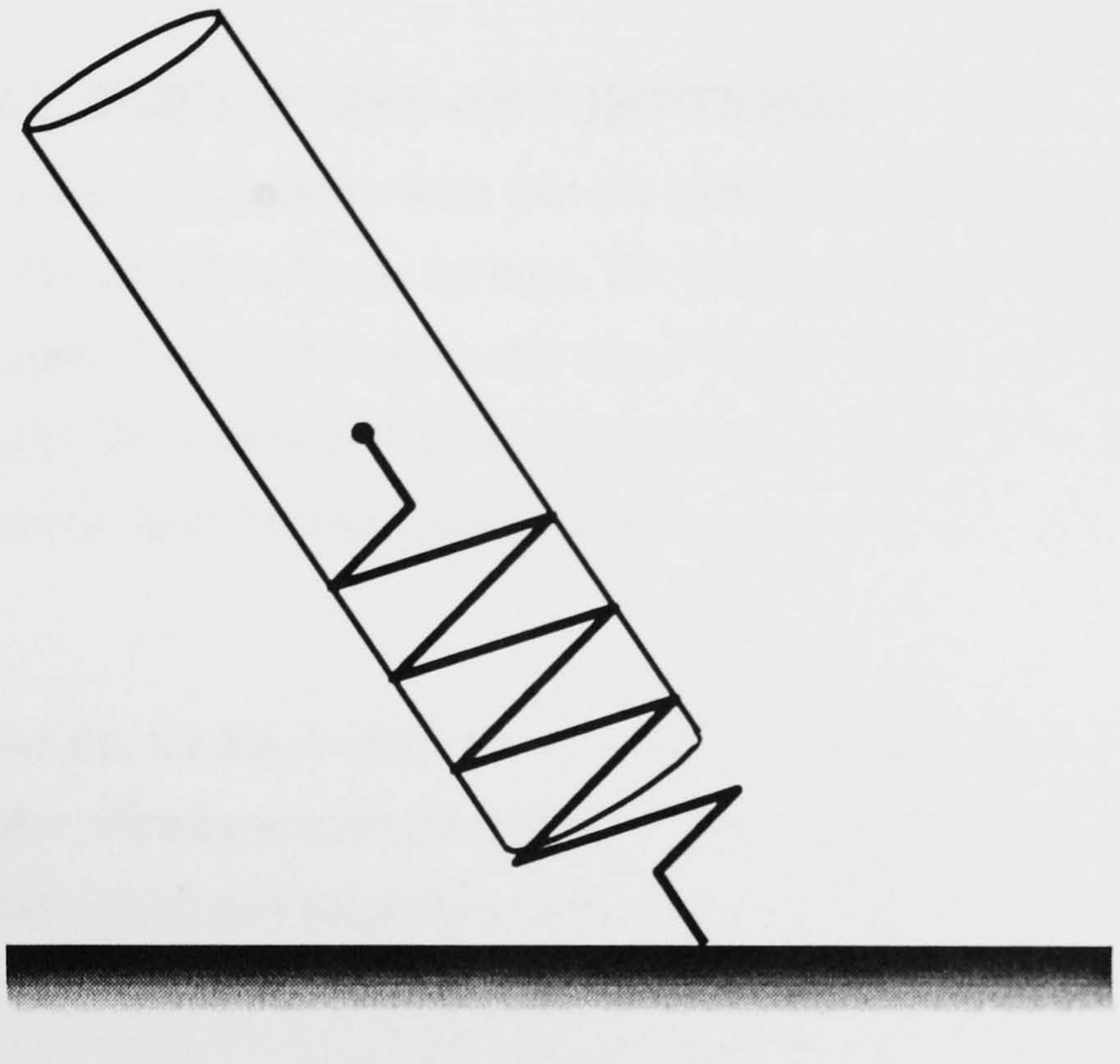

Figure 4.1. Schematic illustration of the one spring model.

stiffness can be found to satisfy these conditions. In the mode of operation where the leg spring stiffness was estimated for a particular vault trial this logic was applied. In other words, given the linear and angular velocities, body angle and transverse moment of inertia at springboard touchdown, and the corresponding body angle at springboard takeoff, iterations were performed with different stiffnesses until the model spring angle at takeoff matched the criterion. When using the models in the mode where the leg spring stiffness was specified the takeoff angle was not constrained.

4.2.1 GENERAL SIMPLIFYING ASSUMPTIONS

The major simplifying assumptions were that the gymnast's legs and springboard could be considered to act like massless linear springs. The former assumption was supported by the literature (see Chapter Two) and empirically (see Chapter Three), and the latter was investigated directly, the results of which are reported in Chapter Five. In the one spring model it was assumed that one linear spring could represent both the gymnast and the springboard.

It was assumed that the inertia characteristics of the gymnast could be represented by a single rigid cylinder, thereby ignoring moment of inertia variations and the increase in mass centre to feet distance between touchdown and takeoff as gymnasts raise their arms and extend their legs.

4.2.2 NOMENCLATURE

The following symbols are used in the development of the model equations which follows:

m = cylinder mass/(cylinder - feet) mass in two spring model

m_f = feet mass

g = acceleration due to gravity

L = natural length of the leg spring

x = change in leg spring length

y = change in board spring - damper length

θ = angle the leg spring makes with the horizontal

K_l = stiffness coefficient of the leg spring

K_b = stiffness coefficient of the board spring - damper

C_b = damping coefficient of the board spring - damper

R_t = transverse component of the ground/board reaction force

(excluding the transverse board spring - damper component)

R_r = radial component of the ground/board reaction force

R_z = vertical component of the ground/board reaction force

I_G = moment of inertia about cylinder mass centre

T_G = torque about the cylinder mass centre

First and second derivatives with respect to time were denoted using the standard single and double dot notation.

4.2.3 THE ONE SPRING MODEL

While the gymnast-springboard system suggests the existence of two springs, spring theory demonstrates that linear springs in series can be represented by a single spring. The stiffness of the single spring, say k_3, can be calculated from the stiffnesses of the series of springs, say k_1 and k_2, using the following relationship (note that the reciprocal of stiffness is called compliance):

$$\frac{1}{k_3} = \frac{1}{k_1} + \frac{1}{k_2}$$

Therefore

$$k_3 = \frac{k_1 . k_2}{k_1 + k_2} \qquad 4.1$$

A cylinder model was formulated which had only one linear spring to represent both the gymnast and the springboard. The base of the spring (BoS) was assumed to be at the lowest point that the gymnast's feet reached during board contact, which therefore required knowledge of the motion of the gymnast's feet during board contact.

The magnitude of the force exerted by the spring was equal to the product of the spring stiffness and the change in spring length, in accordance with Hooke's Law. The convention adopted for both the one and two spring models was that shortening (i.e. compression) of a spring was treated as a negative change in length. Therefore the force exerted by a spring while it was shortened was directed positively, i.e. $F = -k.x$ where k is the spring stiffness coefficient and x is the change in length.

The forces acting on the model were weight, $m.g$, and the ground reaction force, with radial and transverse components R_r and R_t respectively (see Figure 4.2). Note that the positive senses of R_r and R_t were in the direction of the arrows in Figure 4.2 and the positive sense

of the angle, θ, was taken to be clockwise. The radial component of the ground reaction force was equal to the force in the leg spring, $-K_l.x$.

Medley (1982, pages 49 and 50) showed that the transverse and radial components of the acceleration (a_t and a_r) of a point with polar coordinates (r,θ), rotating in a plane are $a_t = 2.\dot{r}\dot{\theta} + r\ddot{\theta}$ and $a_r = \ddot{r} - r\dot{\theta}^2$. For the mass centre of the model rotating in a plane while attached to the origin by the spring, the displacement of the mass from the origin, r, is given by $r = L + x$. Note that L is a constant, so differentiating r gives $\dot{r} = \dot{x}$ and a second differentiation gives $\ddot{r} = \ddot{x}$. Therefore, substituting for r, $\dot{r}$ and $\ddot{r}$ in the expressions for a_t and a_r gives $a_t = 2.\dot{x}\dot{\theta} + (L + x)\ddot{\theta}$ and $a_r = \ddot{x} - (L + x)\dot{\theta}^2$.

Applying Newton's Second Law, the equations of motion for the model were as follows-

Angularly (about the mass centre):

$$T_G = \frac{d}{dt}\left(I_G\dot{\theta}\right)$$

$$-R_t.(L + x) = \left(I_G\ddot{\theta} + \dot{I}_G\dot{\theta}\right)$$

$$R_t = \frac{-\left(I_G\ddot{\theta} + \dot{I}_G\dot{\theta}\right)}{(L + x)} \qquad 4.2$$

Transversely:

$$F_t = m.a_t$$

$$R_t - m.g.\cos\theta = m.\left(2.\dot{x}\dot{\theta} + (L + x)\ddot{\theta}\right) \qquad 4.3$$

Radially:

$$F_r = m.a_r$$

$$R_r - m.g.\sin\theta = m.\left(\ddot{x} - (L + x)\dot{\theta}^2\right)$$

$$-K_l.x - m.g.\sin\theta = m.\left(\ddot{x} - (L + x)\dot{\theta}^2\right)$$

$$\therefore \ddot{x} = (L + x)\dot{\theta}^2 - \frac{K_l.x}{m} - g.\sin\theta \qquad 4.4$$

Substituting 4.2 into 4.3 and rearranging:

$$\frac{-\left(I_G\ddot{\theta}+\dot{I}_G\dot{\theta}\right)}{(L+x)}-m.g.\cos\theta=m.\left(2.\dot{x}\dot{\theta}+(L+x)\ddot{\theta}\right)$$

$$\left(I_G\ddot{\theta}+\dot{I}_G\dot{\theta}\right)=-m.(L+x)\left(2.\dot{x}\dot{\theta}+(L+x)\ddot{\theta}+g.\cos\theta\right)$$

$$I_G\ddot{\theta}+m.(L+x)^2\ddot{\theta}=-m.(L+x)\left(2.\dot{x}\dot{\theta}+g.\cos\theta\right)-\dot{I}_G\dot{\theta}$$

$$\ddot{\theta}=\frac{-m.(L+x)\left(2.\dot{x}\dot{\theta}+g.\cos\theta\right)-\dot{I}_G\dot{\theta}}{I_G+m.(L+x)^2} \qquad 4.5$$

Takeoff occurs when the vertical ground reaction force falls to zero. This was determined from the following:

$$R_z=R_t.\cos\theta+P_r.\sin\theta$$

$$=m.\left(2.\dot{x}\dot{\theta}+(L+x)\ddot{\theta}+g.\cos\theta\right).\cos\theta-K_1.x.\sin\theta \qquad 4.6$$

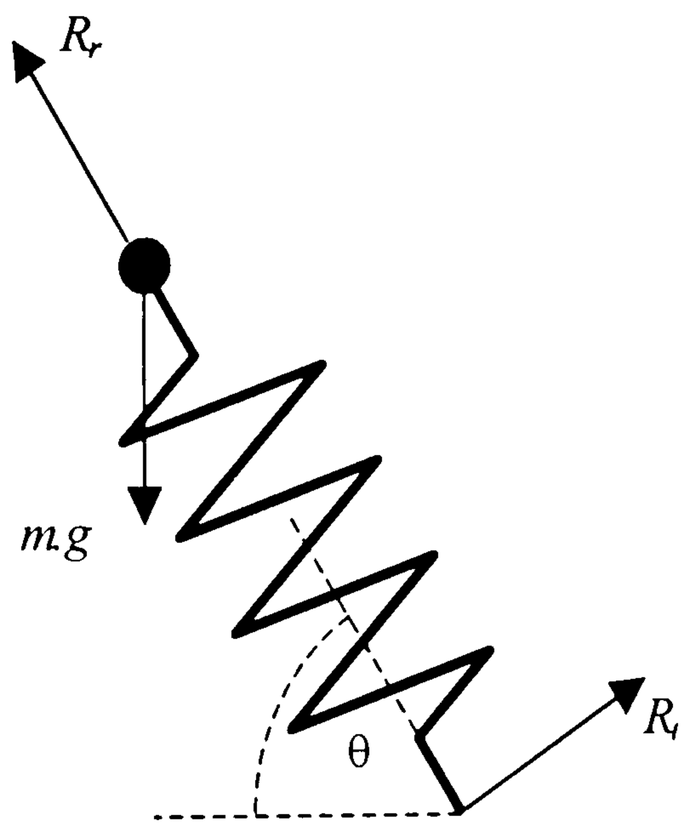

Figure 4.2. Free body diagram for the one spring model.

N.B. R_r and R_t are the radial and transverse components respectively of the ground reaction force and $m.g$ is the weight of the cylinder.

4.2.4 THE TWO SPRING MODEL

The second model incorporated a separate element to represent the springboard. This was modelled as a spring constrained to move vertically and coupled in parallel to a linear damper to form a spring-damper. The damper exerted an additional force proportional, but in the opposite direction, to the velocity of the spring length change. The overall force of the board spring-damper was therefore $-K_b.y - C_b.\dot{y}$, where K_b is the stiffness coefficient, C_b is the damping coefficient, y is the change (increase) in length and $\dot{y}$ is the velocity of the length change. The gymnast was again represented by the cylinder and spring arrangement described previously. Figure 4.3 illustrates the two spring model.

The addition of the board spring-damper introduced a further degree of freedom to the system (only one since it was constrained to move vertically). There was also the additional force of the board spring-damper and mass at the feet to be considered (Figure 4.4). A total of four equations of motion were needed to specify the model.

The equation of **angular** motion for the cylinder (about its mass centre) was similar to Equation 4.2 but with the addition of the torque due to the board spring-damper:

$$R_t + \left(-K_b.y - C_b.\dot{y}\right).\cos\theta = -\frac{\left(I_G.\ddot{\theta} + \dot{I}_G.\dot{\theta}\right)}{(L+x)} \qquad 4.7$$

The equation of **transverse** motion of the cylinder mass centre included an acceleration and a force term due to the board spring-damper, but was similar to Equation 4.3:

$$R_t + \left(-K_b.y - C_b.\dot{y}\right).\cos\theta - m.g.\cos\theta = m.\left(2.\dot{x}\dot{\theta} + (L+x)\ddot{\theta} + \ddot{y}.\cos\theta\right) \qquad 4.8$$

Radially there was an additional acceleration term due to the effect of the acceleration of the base of the leg spring but there was no explicit additional force term since any radial force component from the board manifested itself implicitly in the force in the leg spring. The equation of motion of the cylinder mass centre therefore became:

$$\ddot{x} = (L+x)\dot{\theta}^2 - \frac{K_l.x}{m} - g.\sin\theta - \ddot{y}.\sin\theta \qquad 4.9$$

The equation of **vertical** motion for the feet mass was:

$$\left(-K_b.y - C_b.\dot{y}\right) - \left(-K_l.x.\sin\theta\right) - \left(R_t + \left(-K_b.y - C_b.\dot{y}\right).\cos\theta\right).\cos\theta - m_f.g = m_f.\ddot{y} \qquad 4.10$$

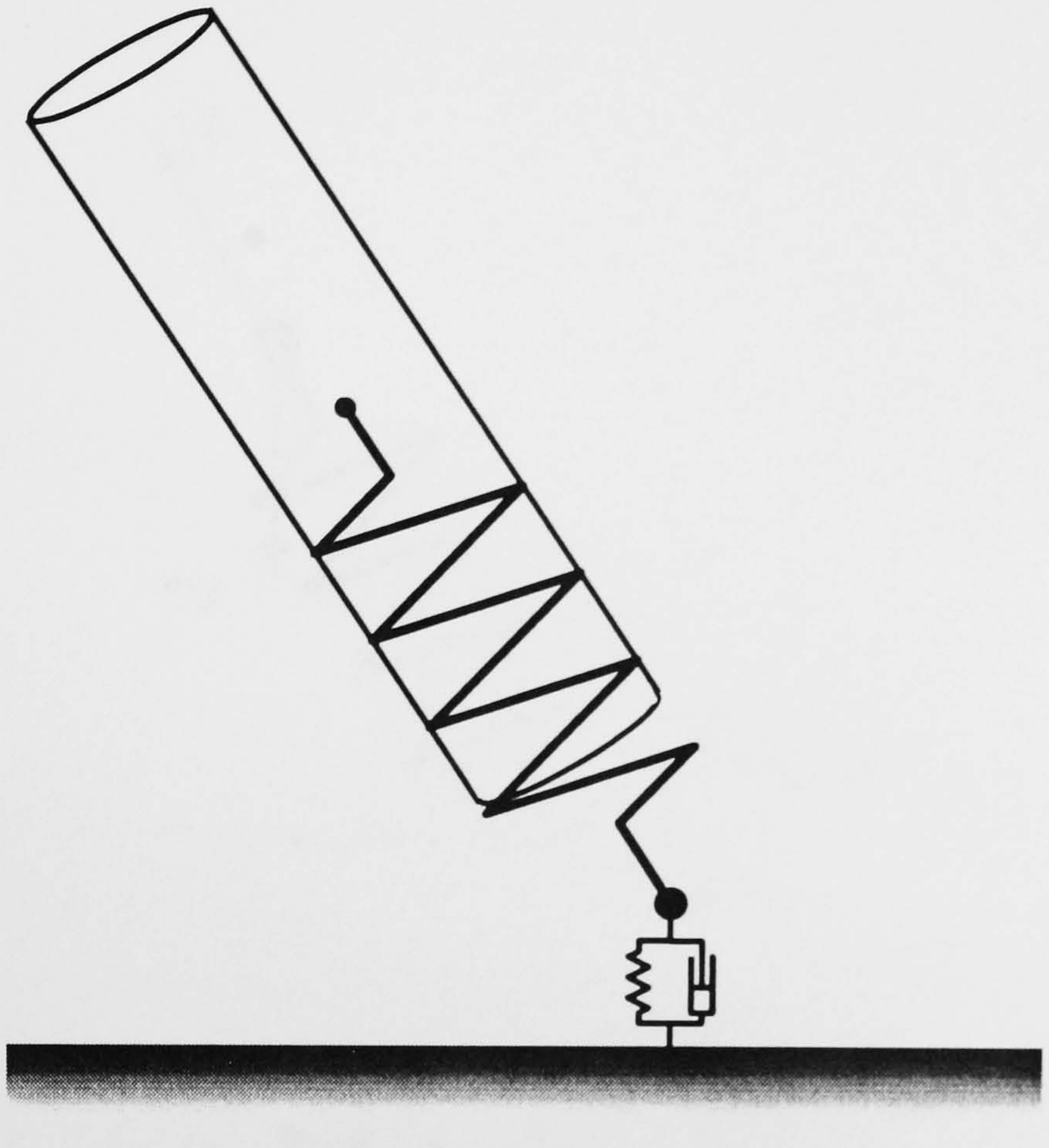

Figure 4.3. Schematic illustration of the two spring model.

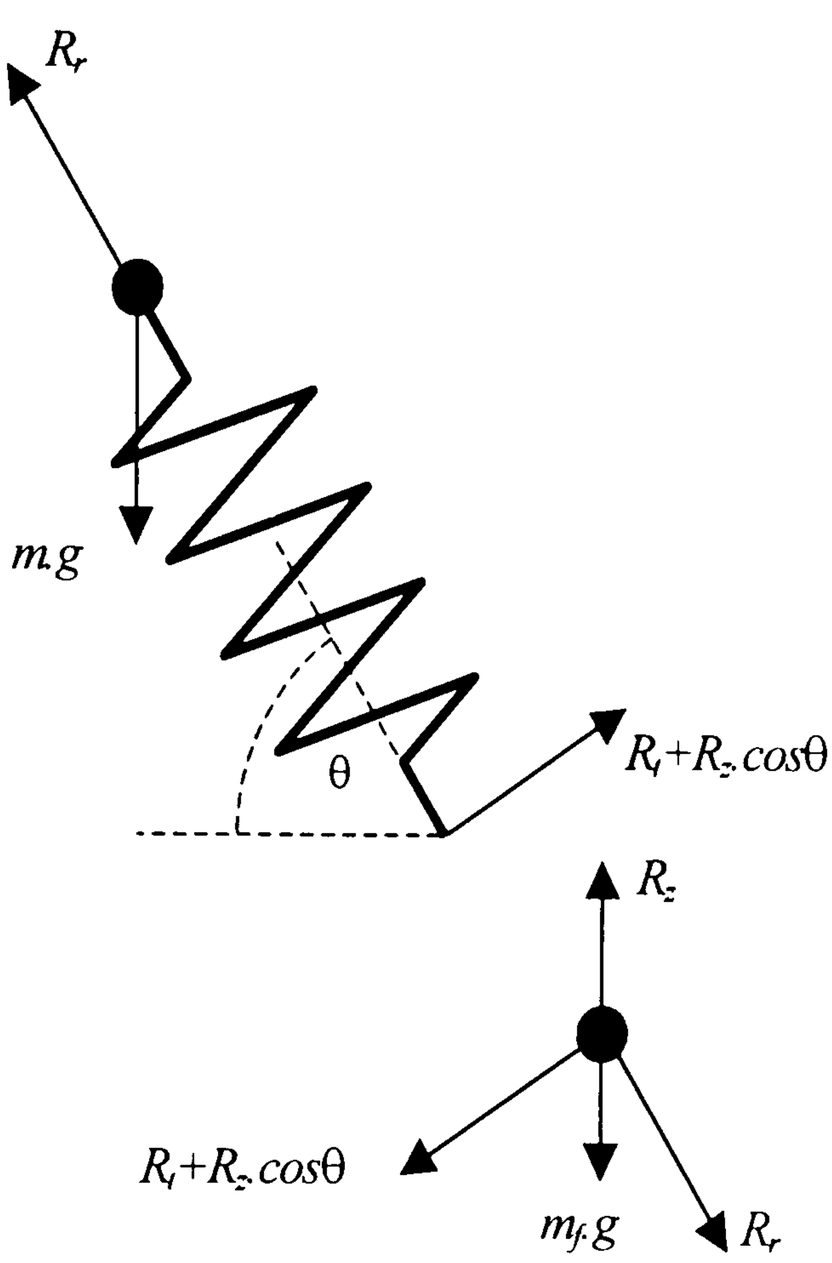

Figure 4.4. Free body diagrams for the two spring model.

N.B. R_z is the board spring-damper force, R_r is the component of the board reaction force acting radially along the leg spring, R_t is the transverse component of the board reaction force excluding the component due to R_z, $m_f.g$ is the weight of the feet and $m.g$ is the weight of the cylinder excluding m_f.

Substituting Equation 4.7 into Equation 4.8 and rearranging:

$$-\frac{\left(I_G\ddot{\theta}+\dot{I}_G\dot{\theta}\right)}{(L+x)}-m.g.\cos\theta=m.\left(2.\dot{x}\dot{\theta}+(L+x)\ddot{\theta}+\ddot{y}.\cos\theta\right)$$

$$\ddot{y}=\left(-\frac{\left(I_G\ddot{\theta}+\dot{I}_G\dot{\theta}\right)}{m.(L+x)}-g.\cos\theta-2.\dot{x}\dot{\theta}-(L+x)\ddot{\theta}\right).\sec\theta \qquad 4.11$$

Substituting Equation 4.7 into Equation 4.10 and rearranging:

$$\left(-K_b.y-C_b.\dot{y}\right)-\left(-K_l.x.\sin\theta\right)+\frac{\left(I_G\ddot{\theta}+\dot{I}_G\dot{\theta}\right)}{(L+x)}.\cos\theta-m_f.g=m_f.\ddot{y}$$

$$\frac{\left(I_G\ddot{\theta}+\dot{I}_G\dot{\theta}\right)}{(L+x)}.\cos\theta=\left(K_b.y+C_b.\dot{y}\right)-K_l.x.\sin\theta+m_f.(g+\ddot{y})$$

$$\ddot{\theta}=\frac{(L+x).\sec\theta.\left(K_b.y+C_b.\dot{y}-K_l.x.\sin\theta+m_f.(g+\ddot{y})\right)-\dot{I}_G\dot{\theta}}{I_G} \qquad 4.12$$

The force exerted by the board spring-damper was a Newton's Third Law reaction to the force acting down on the spring-damper from the feet mass (which in turn was affected by the force in the leg spring). Takeoff occurred when the spring-damper force fell to zero which was therefore when the force exerted on the feet mass by the board spring-damper became zero. In an undamped spring this would be when the spring returned to its natural (unextended/uncompressed) length. When damping *is* present, the force from the spring-damper will reach zero before the natural length is regained. This is due to the fact that once the spring-damper has passed the point of maximum compression, the force component from the damper has the opposite sign to that from the spring, i.e. the spring force is positive because the spring is still compressed but since the change in length velocity is then positive, the damper force is negative.

The point of takeoff was therefore determined from the equation for the force in the spring-damper:

$$R_z=-K_b.y-C_b.\dot{y} \qquad 4.13$$

4.3 MODEL IMPLEMENTATION

4.3.1 MODEL CODING AND SOLUTION

The one and two spring models were each programmed using the Maple™ V symbolic mathematics package (Waterloo Maple Software) running on an IBM compatible personal computer. This package allowed the equations of motion derived in sections 4.2.3 and 4.2.4 to be defined and solved subject to the initial conditions and other inputs outlined in section 4.3.2. For both models two modes of operation were coded: one which calculated the appropriate leg spring stiffness value to satisfy specified touchdown and takeoff conditions, and another which calculated the takeoff conditions given specific touchdown kinematics and leg spring stiffness. (Inputs other than leg spring stiffness, including the board stiffness and damping, were determined as described in Chapter Five). The procedures described below were the same for both the one and two spring models. All procedures were custom written in the Maple programming language, with the exception of the procedure to solve differential equations, dsolve, which is part of the Maple library of procedures.

The system of simultaneous differential equations for each model was non-linear and exact solutions were not possible, therefore a numerical solution method was required. The numerical solution of the differential equations was achieved using the Maple implementation of a subroutine based on the Fehlberg fourth-fifth order Runge-Kutta method, RKF45 (Forsythe, Malcolm and Moler, 1977). This method incorporates automatic step-size control, requiring only an error tolerance to be set; the Maple default value for the error tolerance was used in all cases as reducing the error tolerance was found only to affect the output of the model beyond the precision of the empirical data reported in Chapter Five.[1]

When the leg spring stiffness was *preset* this constituted a straightforward initial value problem. In other words, the conditions at touchdown were all known and the differential equations could be solved forwards in time without reference to the takeoff conditions. Once solved, the time of takeoff was determined (when the ground reaction force/springboard force fell below one newton) and the takeoff kinematics were calculated. Figure 4.5 is a flow diagram that represents the main steps in the model. The procedure for finding the point of takeoff was the same for both modes of operation and is described in more detail below.

---

[1] The RKF45 implementation in Maple includes full warning and error flagging (for example if the method is having to work very hard to achieve the requested accuracy). However, in the simulations performed none of these errors or warnings occurred.

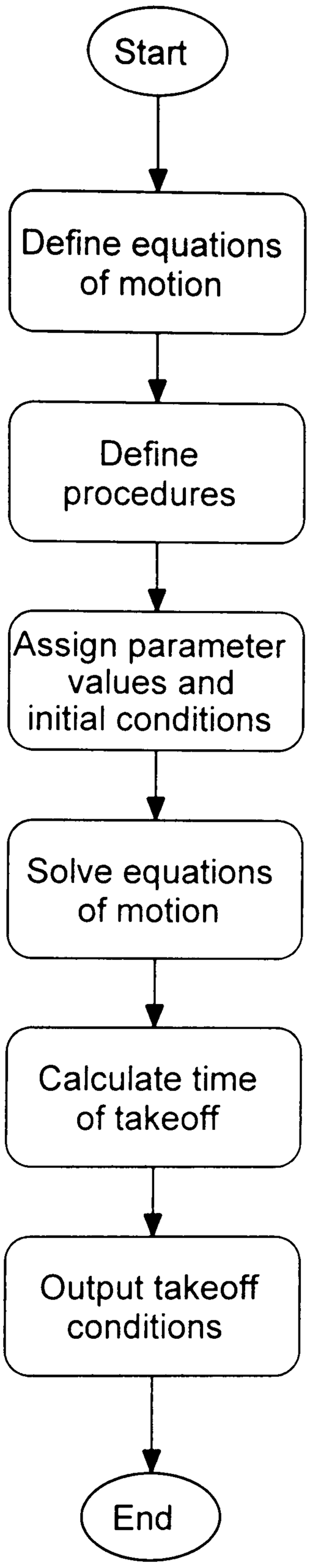

Figure 4.5. The main steps in the model when the leg spring stiffness is known. The procedure to calculate the time of takeoff is expanded upon in Figure 4.8.

When the leg spring stiffness was being *sought* the situation was slightly different in that reference to the takeoff conditions was necessary to assess the suitability of the stiffness estimate. If the spring was too stiff takeoff occurred before the required takeoff angle had been reached (this was defined as a negative angle error), while if it was too soft takeoff occurred past the required takeoff angle or not at all (a positive angle error). Figure 4.6 shows a flow diagram of the main steps in the model. The leg spring stiffness was found by an iterative procedure (Findk) which used the gymnast's body angle at takeoff from the springboard as the criterion. An initial stiffness estimate and a search interval were passed to the procedure from where the Bisection method was used to find the stiffness which resulted in an angle error of less than 0.0005 radians. The name of this method comes from the way in which the interval containing the required value is successively halved until the solution is found. Figure 4.7 illustrates the procedure Findk.

The Bisection technique is an example of a simple shooting method. Shooting methods are ways of calculating the roots of an equation, i.e. where the function equals zero. In this case, the problem was to find the stiffness value that resulted in an angle error of zero (or more precisely within 0.0005 radians of zero). These techniques can be compared on the basis of their speed to find a solution, but some of the faster algorithms can suffer from divergence problems, that is to say in certain circumstances successive estimates rapidly get further from the solution rather than converging towards it. Methods which converge more rapidly also require more information about the function, in particular its derivative at the point of each estimate, which may not be readily available. Bisection methods are robust, having the advantage that they will always find a solution once an interval containing one is identified, but they can take longer to find the solution than other methods. However in this study the length of time for one simulation to run rarely exceeded a few minutes, including the time for each solution of the differential equations, so this shortcoming was not considered critical. The same stiffness values were estimated by the program regardless of the starting point and step size for the search. The shooting method known as secant iteration is a faster converging technique which is often used, but when tried in this particular application it was found to suffer from divergence. More information on these numerical methods is available in many texts, for example Borse (1991) and de Vahl Davis (1986).

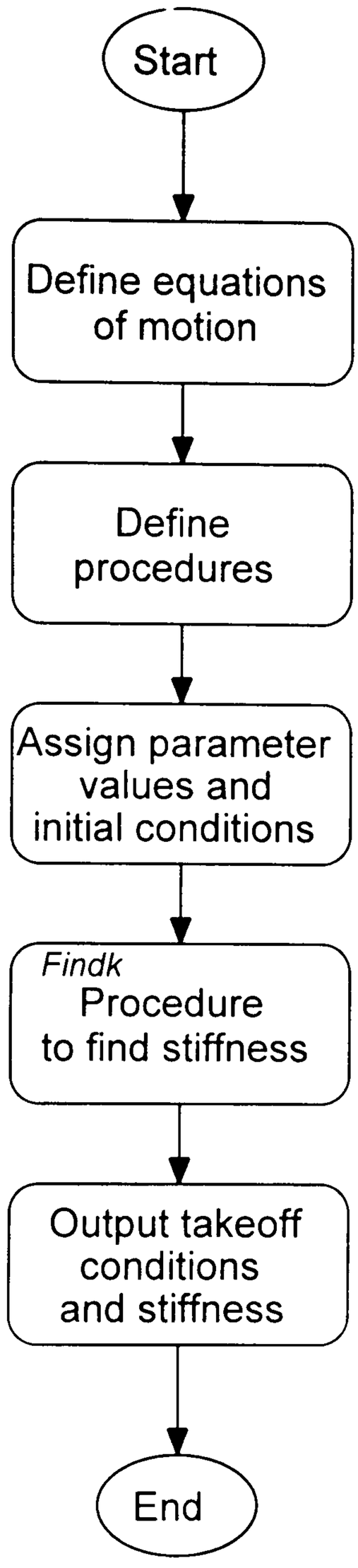

Figure 4.6. The main steps in the model when the leg spring stiffness is not known. The procedure to find the spring stiffness (Findk) is expanded upon in Figure 4.7.

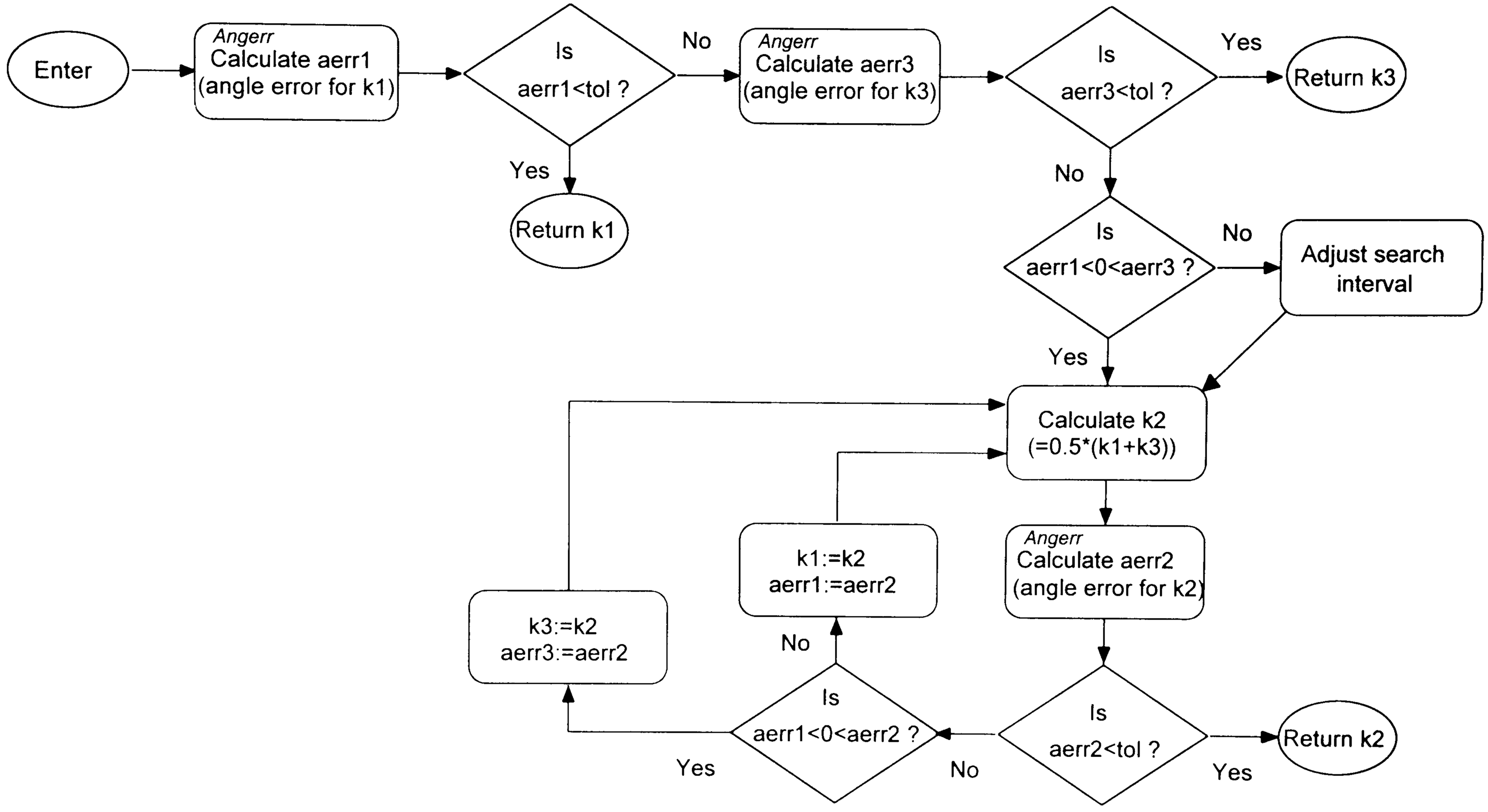

Figure 4.7. Flow diagram of procedure **Findk** which calculates the leg spring stiffness. k1, k2, k3, aerr1, aerr2 and aerr3 are local variables and **tol** is the maximum permitted angle error (0.0005 rad). Interval adjustment is necessary only if the required stiffness is outside of the initial search interval.

Within the procedure Findk another procedure, Angerr, solved the differential equations and calculated the angle error for each stiffness estimate. Angerr calls the Maple differential equation solver and then procedure Takeoffs to determine the time of takeoff. Equations 4.6 and 4.13 were used to calculate the ground/board reaction force (R_z) at the base of the leg spring for the one and two spring models respectively. Takeoff was deemed to have occurred when R_z fell to below one newton and the time when this happened was found using secant iteration to adjust the initial time estimate passed from Angerr. (Secant iteration proved to be successful in this situation, not suffering from the divergence problems experienced when used to find the leg spring stiffness). The time at takeoff was used in calculating the takeoff angle error in the search for the correct leg spring stiffness and in calculating the model output. Figure 4.8 outlines the procedure to calculate the angle error and incorporates the flow diagram for the process of finding the time at takeoff.

Output from both the one and two spring models consisted of the radial and angular velocities of the cylinder, the leg spring change in length and angle at takeoff, and when required, the calculated leg spring stiffness. The board spring-damper length change and rate of length change were also output by the two spring model. The cylinder mass centre horizontal and vertical velocities were then calculated using the following equations:

Vertically:

$$V_v = \dot{x}.\sin\theta + (L+x)\dot{\theta}.\cos\theta \qquad \text{for the one spring model, or}$$

$$V_v = \dot{x}.\sin\theta + (L+x)\dot{\theta}.\cos\theta + \dot{y} \qquad \text{for the two spring model}$$

and horizontally

$$V_h = (L+x)\dot{\theta}.\sin\theta - \dot{x}.\cos\theta$$

Appendix B contains listings of the Maple programs.

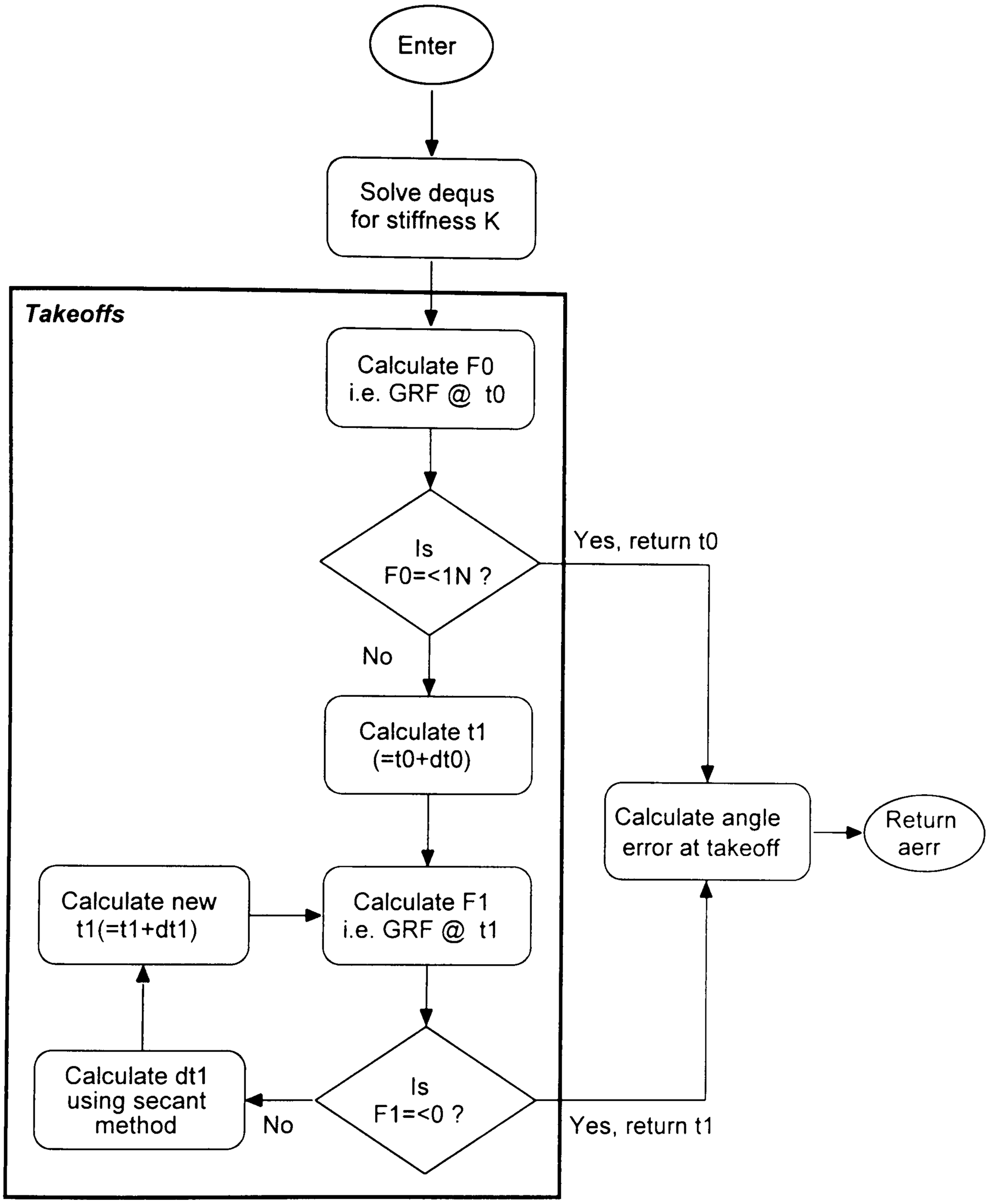

Figure 4.8. Flow diagram for the procedure Angerr which calculates the angle error at takeoff and incorporates the procedure Takeoffs.

K, t0 and dt0 are initial estimates, F0, F1, t1, and dt1 are local variables, and aerr is the angle error returned by the procedure.

4.3.2 MODEL INPUTS

For both models the information required to specify the touchdown conditions (i.e. the initial conditions for the equations of motion) was:

- the mass centre to BoS distance (i.e. the natural length of the spring),
- initial extension/compression of the spring (always considered to be zero),
- the cylinder/spring angle with respect to the horizontal,
- the mass centre radial velocity,
- and the cylinder angular velocity.

The two spring model also required the initial extension/compression of the board spring-damper (again, always considered to be zero) and the initial velocity of the board spring-damper to be known. Three ways of modelling the initial board velocity were considered:

1. If there is no mass at the base of the leg spring the initial board velocity is zero, since there is no force exerted by the leg spring until it has begun to compress;
2. If there is a foot mass and a board mass there will be an impact and the conservation of momentum must be applied to determine the initial board velocity;
3. If there is a foot mass but no board mass, the board's initial velocity will be that of the vertical component of the velocity of the foot mass.

The first option was not sufficiently realistic since inspection of video of vaulting suggests that the contact between feet and board clearly involves an impulsive acceleration of the board. Option two would allow for this but would demand that the effective board mass be determined in some way. McMahon and Greene (1979) demonstrated that the effective mass of the running track could be ignored in their mass-spring model of running and while Sprigings, Stilling and Watson (1989) modelled a diving springboard with mass, the inertial force from the board was found to be three orders of magnitude less than the spring force component (see Chapter Two, section 2.2.2). It was therefore assumed that the effective mass of the vaulting springboard was unlikely to have a large effect on the system, so the third option offered the best solution.

A number of other values were required as inputs to the models:

- cylinder mass (the mass of the gymnast, minus the mass of his feet in the two spring model),
- cylinder moment of inertia (the gymnast's transverse moment of inertia at touchdown),
- foot mass (for two spring model only),
- leg spring stiffness (when this was known in advance),
- board spring-damper stiffness and damping (for two spring model only).

When using the models to establish suitable leg spring stiffness values, the takeoff angle was also needed as a criterion.

The determination of these data is described and the values reported in Chapter Five.

4.4 SUMMARY

The principles behind and the development of one spring and two spring models for gymnastic springboard takeoffs have been described in this chapter. The models allow the determination of a leg spring stiffness where both the touchdown and takeoff kinematics are known, and the determination of the takeoff kinematics if the touchdown kinematics and leg spring stiffness are given. The distinct difference between these models and previous models of human rebounding is their ability to represent the angular motion of the body, which is a key feature of vaulting.

Also in this chapter, the derivation of the equations defining the motion of the systems was explained, along with a description of the computer methods used for their solution and the production of the required output data.

The following chapter details the collection and analysis of springboard and vaulting data which formed the input for the models and provided a basis for the evaluation and application of the models.

CHAPTER FIVE
DETERMINATION OF VAULTING AND SPRINGBOARD DATA

5.1. INTRODUCTION

In order to evaluate and apply the models described in Chapter Four it was necessary to record and analyse a number of vaults and to examine the springboard from which the gymnast vaulted. This chapter details the methods and presents the results of three studies performed to provide the required model inputs. In the first, kinematic data at touchdown and takeoff from the springboard for a series of handspring vaults by an elite male gymnast were collected, along with anthropometric data which were used to estimate his body segment inertia parameters. The second and third were studies of the springboard, to determine its stiffness and damping characteristics.

5.2. VAULTING

The aim was to collect data on trials performed by a single gymnast at a range of approach speeds and springboard settings. A Gymnova model 2170 adjustable springboard was generously loaned by the manufacturers for the study. Springboard adjustment was achieved by varying the position of a pair of steel springs under the wooden top leaf of the board and holding them in this position using a grub screw tightened using a knurled knob. The range of adjustment was designed to cover the full performance range of the company's other springboards, from 'initiation to competition', i.e. softer for training and beginners, to stiffer for competition. The data collection was performed at the Lilleshall National Sports Centre with the cooperation of the British Gymnastics Association.

5.2.1. VIDEO RECORDING

Before videoing the vaults, three 2.3 m poles each with three control points marked clearly at one metre intervals (0.13, 1.13 and 2.13 m from the bottom of the base) were positioned in the plane of motion. Their locations were measured and they were then videoed. The position of all three poles coincided with the middle of the runway and the long axis of the vaulting horse; one at each end of the horse and the third 2.82 m along the runway from the pole at the near end of the horse (Figure 5.1). These poles provided nine calibration points for the subsequent performance of a 2D DLT on the digitized data. As viewed from the camera, the origin was chosen to be the inside (right) edge of the left horse leg base, with the positive Y-axis from left to right and the positive Z-axis vertically upward. Once the

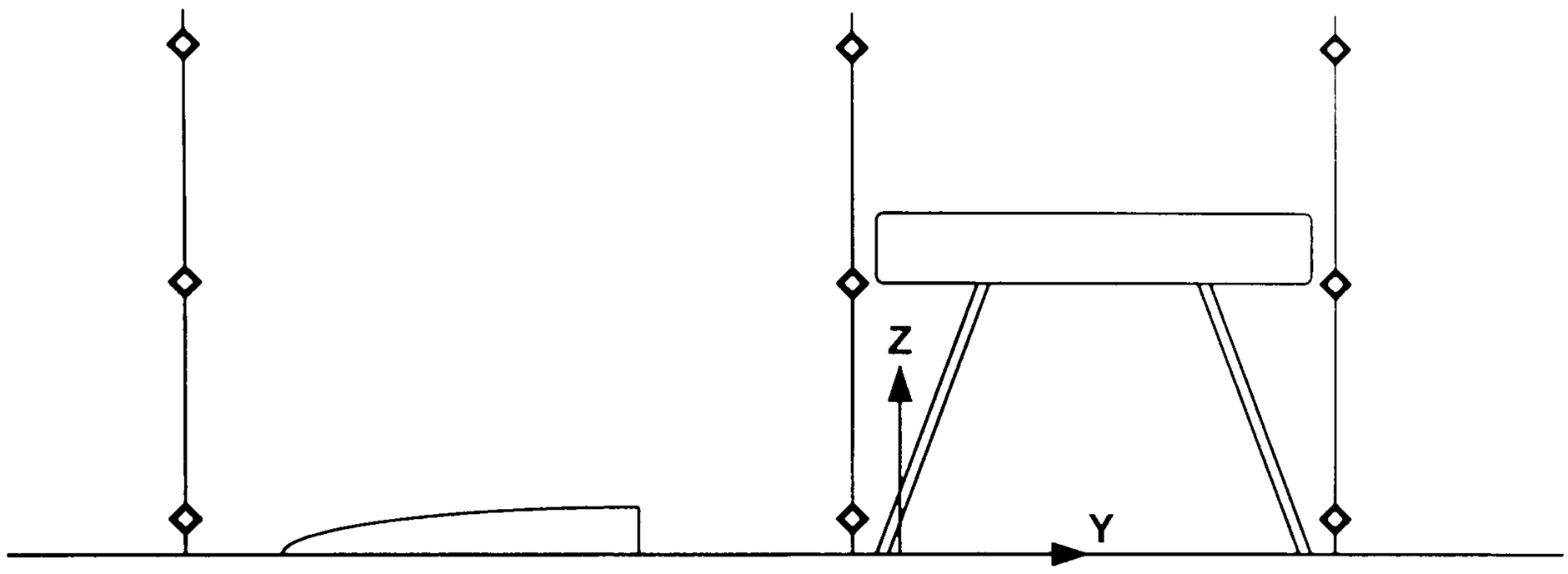

Figure 5.1. Side elevation of the calibration pole arrangement in relation to the springboard and vaulting horse, also showing the reference frame orientation.

poles had been recorded in position they were removed. No camera adjustments were made following the recording of the calibration poles.

Twelve handspring vaults were videoed as performed by one elite British male gymnast, who had given informed consent (Appendix C.1). Five were performed at the gymnast's preferred run up speed, and notionally at the 'competition' springboard setting. However, it was subsequently found that in the course of trials 4 to 9 the springboard setting changed slightly. Trials 6 through 9 were performed at a range of slower approach speeds, including the slowest at which the gymnast felt comfortable, effectively with an intermediate springboard setting due to the unintended board setting change. The last three trials were performed with the springboard at its 'initiation' setting, one at three-quarter pace and two at normal speed.

All trials were recorded using a Sony Hyper HAD Hi-8 video camera positioned on a balcony approximately 20 m from the plane of motion and 4.8 m above the gymnasium floor. This camera recorded 50 fields per second with an exposure of $1/250^{th}$ s. Inspection of the video showed that the minimum number of fields recorded during the hurdle (flight onto the springboard) or preflight (between leaving the springboard and contact with the horse) was eight, with ten or eleven being more usual.

The anthropometric measurements required for the inertia model of Yeadon (1990b) were made of the subject using tapes and callipers. The model provided estimates of the gymnast's body segment inertia parameters (BSIP) based on a 14 segment model of the human body. These segments were the hands, forearms, upper arms, thighs, shanks and feet for both left and right sides of the body, the trunk and the head. The BSIP can be found in Appendix C.2.

5.2.2. VIDEO DIGITIZATION AND TRANSFORMATION

A Peak Performance Technologies Inc. 'Peak 5' video digitizer was used to generate raw 2D data files which were exported to be processed in custom written software. This software used the mean of ten digitizations of the control points to perform 2D Direct Linear Transformations (DLT) on the raw data. The DLT calibration check assessed the transformation accuracy and found that the average root mean squared error was 4.5 mm horizontally and 5.1 mm vertically.

One trial was digitized four times to estimate the uncertainty involved in digitizing the gymnast. In every field the wrists, elbows, shoulders, hips, knees, ankles, mid-metatarso-phalangeal joints, mid-neck and top of the head were digitized (16 points). Both sides of the

body were digitized in order to account for any asymmetries in the limb movements: this was mainly relevant to the arms, shanks and feet during the first part of the hurdle phase. Combined hand and forearm segments were constructed which assumed a zero wrist flexion angle and used the wrist as the distal endpoint, thus avoiding having to estimate the fingertip points which were occasionally blurred. Otherwise the points digitized coincided with segment endpoints used in the inertia model (Yeadon, 1990b).

The transformed data from each digitization of this trial were combined with the segment masses and proximal ratios determined from the inertia model, to calculate the mass centre locations of each segment throughout the vault. The whole body mass centre position was then calculated for every field in each digitization. Equation 5.1 summarizes this calculation for the y coordinate of the mass centre in any given field; the calculation of the z coordinate has the same form. In this equation Y is the horizontal coordinate of the mass centre, M is the whole body mass, y_{p_i} and y_{d_i} are the horizontal coordinates of the proximal and distal endpoints of segment i, r_{p_i} and m_i are the proximal ratio and the mass for segment i, and N is the number of segments comprising the body.

$$Y = \frac{1}{M}\sum_{i=1}^{N}\left[\left(y_{p_i} + (y_{d_i} - y_{p_i}).r_{p_i}\right)m_i\right] \qquad 5.1$$

Standard errors of the mass centre and segment endpoint locations were calculated for two, three and four digitizations. The results indicated that there was little benefit in digitizing the trials more than twice (see section 5.4.1 below), therefore two digitizations were performed on each of the remaining 11 trials and the digitized coordinates were then transformed using a 2D DLT.

5.2.3. ANALYSIS

The purpose of analysing the vaults was to provide the data which were required for model evaluation and use. These were the mass centre velocity, whole body angular velocity and moment of inertia about the transverse axis through the mass centre, spring length and spring angle. These data were required at springboard touchdown and takeoff. For the two spring model, an estimate of the vertical velocity of the feet at touchdown was also needed.

The last instant before the feet contacted the springboard and the first instant after they left the springboard were used to define touchdown and takeoff respectively. To improve the precision with which these times were determined, the mean of the two digitizations of the

mid-metatarso-phalangeal joints of both feet were interpolated over a 250 Hz timebase using a generalized cross validated quintic spline (GCVQS). The effect of the springboard contact on the spline interpolation was assessed by comparing the raw and interpolated vertical coordinates throughout a trial. It was found that the difference between the two estimates was slightly greater immediately before and after impact than the root mean square (RMS) difference over the whole trial (0.011 m compared with 0.007 m). This discrepancy was of the same order of magnitude as the uncertainty in locating the mid-metatarso-phalangeal joints, therefore the interpolated data were considered to be reliable. Using these data, the times of springboard touchdown and takeoff were determined by locating the last and first times respectively when the mean of the two mid-metatarso-phalangeal joint vertical coordinates were above the level of the springboard (the board height with respect to the ground having been measured during data collection).

Calculations on the transformed data from each of the two digitizations and the subject's BSIP were performed using Microsoft Excel. Two estimates of the segment and whole body mass centre locations, segment orientation angles and segment mass centre to whole body mass centre angles were computed. The mass centre locations were calculated as described above and coordinate geometry was used to determine the angles. The mean and standard error values for each of these variables and for the segment endpoint locations were then calculated.

Mass centre linear positions and velocities

A least squares quadratic curve and a least squares straight line were fitted to the vertical and horizontal whole body mass centre position data respectively for each hurdle and preflight separately. The whole body mass centre position at springboard touchdown and takeoff was then calculated by evaluating these equations at the times of touchdown and takeoff. Touchdown and takeoff velocities were calculated by evaluating the first derivatives of the equations at the times of touchdown and takeoff.

Moment of inertia and angular velocity

The segment endpoint positions at springboard touchdown and takeoff were determined, using a GCVQS to interpolate the mean of the two digitizations of each trial over the same 250 Hz timebase previously used to find the times of touchdown and takeoff. The individual segment mass centre to whole body mass centre distances were calculated using the subject's BSIP in conjunction with these segment endpoint positions (Equations 5.2 and 5.3).

$$y_c = y_p + (y_d - y_p) r_p \qquad 5.2$$

Here y_c is the horizontal coordinate of the mass centre of the segment, y_p and y_d are the proximal and distal horizontal coordinates of the segment endpoints and r_p is the proximal ratio for the segment. The vertical coordinate of the mass centre (z_c) was found in the same way.

$$d = \sqrt{(y_c - Y)^2 + (z_c - Z)^2} \qquad 5.3$$

Here Y and Z are the horizontal and vertical coordinates of the whole body mass centre, y_c and z_c are as previously defined, and d is the distance between the segment mass centre and the whole body mass centre.

The moment of inertia for each segment about its principal transverse axis was given directly by the inertia model. The parallel axis theorem was then used to find each segment's moment of inertia relative to the whole body mass centre and these were summed for all segments to find the whole body moment of inertia about the transverse axis through the mass centre at touchdown and takeoff.

The whole body angular momentum about the transverse axis through the mass centre was determined throughout hurdle and preflight phases by summing the local and remote angular momentum terms for all of the body segments about the whole body mass centre, Equation 5.4 (Hay, Wilson, Dapena and Woodworth, 1977). The segment angular velocities and the angular velocities of the segment mass centres about the whole body mass centre used in this calculation were given by the first derivatives of a GCVQS fitted to the segment orientation angles and segment mass centre to whole body mass centre angles (mean angles from the two digitizations).

$$L = \sum_{i=1}^{N} \left(I_i \omega_i + m_i . d_i^2 \omega_{i/G} \right) \qquad 5.4$$

Here L is the whole body angular momentum, I_i is the moment of inertia of segment i, ω_i is its angular velocity, m_i is the segment mass, d_i is the distance of the segment mass centre to the whole body mass centre and $\omega_{i/G}$ is the angular velocity of the segment`s mass centre about the whole body mass centre. N is the total number of segments comprising the body.

Whole body angular velocity about the transverse axis through the mass centre at springboard touchdown was determined by dividing the mean whole body angular momentum about the transverse axis during the hurdle by the body's moment of inertia

about this axis at touchdown. The angular velocity at springboard takeoff was calculated in a similar fashion, using the mean angular momentum during preflight and the takeoff moment of inertia.

Leg spring length and angle

For the two spring model the leg spring length was taken to be the whole body mass centre to mid-metatarso-phalangeal joint distance at touchdown, and the leg spring angles at touchdown and takeoff were taken to be the angle that a line joining these two points at these times made with the left horizontal (negative Y) axis.

In order to estimate a point that represented the base of the spring (BoS) for the one spring model, the mid-points of the left and right mid-metatarso-phalangeal joint digitizations were calculated during the springboard contact phase. These data were interpolated using a quintic spline to provide three intermediate points between pictures (i.e. number of samples increased by a factor of four) and then a GCVQS was fitted. The point with the smallest vertical cocoordinate was taken to be the base of the spring for the spring length and spring angle calculations. These values were then calculated (at touchdown and takeoff) using geometry, on the assumption that the spring in the one spring model connected the mass centre of the gymnast to the BoS.

Error analysis

Estimates of the uncertainty in the kinematic data were calculated to determine the confidence which could be placed in them and to provide data with which model sensitivity could be estimated. The estimates were made as follows:

Position- From multiple digitization, the standard error for each digitized landmark and the calculated mass centre position were calculated.

Mass centre velocity- The estimated error in mass centre position was added to the measured displacements and new velocity values calculated. Mean relative error values over all trials were calculated for the touchdown and takeoff velocities separately.

Spring length and angle- Estimated errors in the mass centre and BoS position were combined using error propagation formulae (Barford, 1985) to determine the mean relative error over all trials.

Moment of inertia- The mean relative error from multiple digitization of the springboard contact phase of trial 1 was calculated.

Angular momentum- Assuming constant angular momentum during the airborne phases, the standard error of the angular momentum estimates in the hurdle and preflight phases for each trial were calculated. The mean values for hurdle and preflight over all trials were then calculated.

Angular velocity- Uncertainties in the moment of inertia and angular momentum estimates were combined using error propagation formulae (Barford, 1985) to determine the standard errors at touchdown and takeoff.

5.2.4. MODEL INPUTS

The input data required were the mass and touchdown moment of inertia, leg spring length and angle, mass centre radial velocity (i.e. the initial rate of shortening of the leg spring) and system angular velocity. The two spring model additionally required the mass allocated to the feet, the initial vertical velocity of this mass and the board stiffness and damping values. Inertia parameters were available directly from the inertia model (Yeadon, 1990b) and the spring length and angle values were calculated directly from the video data analysis as described previously, assuming that the length and angle values would not change during the instant of impact. Mass centre radial velocity, feet mass velocity and system angular velocity immediately after impact required additional calculation (see below), while the board data were determined in a series of tests described in section 5.3.

In both the one and two spring models, the mass of the system (excluding the mass of the feet in the two spring model) had its radial motion constrained by the leg spring. Since this spring was modelled to be at its natural length at the point of impact and the impact was considered to be instantaneous, there was no impulse applied radially on the mass during the impact and hence the initial radial velocity was unchanged. For the one spring model its value was calculated as follows:

$$v_r = -v_h.\cos\theta + v_v.\sin\theta \qquad 5.5$$

where v_r, v_h and v_v are the radial, horizontal and vertical components of the mass centre velocity respectively and θ is the mass centre to BoS angle, all at the last moment in the hurdle. For the two spring model the radial velocity was calculated with respect to the feet mass. This mass was assumed to have been brought to rest in the horizontal direction instantly upon impact with the board spring-damper (which was constrained to move vertically), while in the vertical direction, the assumption that the board spring-damper was massless meant that the vertical velocity of the feet mass was unchanged. Hence:

$$v_r = -v_h.\cos\theta + (v_v - \dot{y}).\sin\theta \qquad 5.6$$

where $\dot{y}$ is the vertical velocity of the board spring-damper/feet mass, calculated from the vertical velocity of the mass centre and the angular velocity of the system using the equation:

$$\dot{y} = v_v - L\dot{\theta}.\cos\theta \qquad 5.7$$

where θ is the angular velocity and other symbols are as previously defined. In the two spring model the combined mass of the gymnast's feet (1.6 kg) was used for the feet mass value.

The assumed instantaneous nature of the impact meant that there was negligible torque acting about the mass centre of the gymnast. Hence the angular velocity of the body at touchdown was calculated by applying the principle of conservation of angular momentum:

$$\begin{aligned} I_G\dot{\theta}_0 + m.v_{t0}.L &= I_G\dot{\theta}_1 + m.v_{t1}.L \\ &= I_G\dot{\theta}_1 + m.L^2\dot{\theta}_1 \end{aligned}$$

$$\therefore \dot{\theta}_1 = \frac{I_G\dot{\theta}_0 + m.v_{t0}.L}{I_G + m.L^2} \qquad 5.8$$

where subscripts 0 and 1 indicate instants immediately before and after impact respectively, m is the gymnast's body mass, I_G is the transverse moment of inertia through the mass centre, L is the mass centre to feet distance and v_t is the transverse velocity of the mass centre (other symbols are as previously defined). The transverse velocity of the mass centre was calculated as follows:

$$v_t = v_h.\sin\theta + v_v.\cos\theta \qquad 5.9$$

5.3. SPRINGBOARD TESTING

For the two spring model, estimates of the board stiffness and damping were required. It was anticipated that the point of contact with the springboard as well as the springboard adjustment would affect the stiffness and damping characteristics of the springboard. Therefore, to decide upon the details for the springboard calibration, the video of the vault trials was analysed. In the first field where springboard contact occurred in each trial, four points were digitized five times each. These points were the near and far ends of the vaulting area of the springboard surface, the middle of the metatarso-phalangeal joints, and the adjustment knob position (see Figures 5.2a and 5.2b). Mean values for these points were

then calculated and transformed using a 2D DLT, and the foot contact position and adjustment knob position with respect to the near end of the springboard (i.e. the end from which the gymnast approached) were calculated.

On the basis of these data three foot contact points and three springboard adjustment knob positions were chosen at which to conduct the calibration tests, giving a total of nine test conditions. The contact positions chosen were at 0.75, 0.90 and 1.05 m and the adjuster positions were at 0.96, 1.04 and 1.28 m (Figures 5.2a and 5.2b). The first and last of these adjuster positions corresponded approximately to the manufacturer's description of stiffest (competition) and softest settings respectively. The vaulting area lengths calculated from the transformed points were compared with the measured length in order to estimate the transformation accuracy.[1]

In order to estimate the stiffness and damping values two tests of the springboard were conducted. One was based closely on Fédération Internationale de Gymnastique (FIG) testing procedures (FIG, 1994) and entailed dropping a mass onto the springboard (Drop test), from which the velocity of the mass at touchdown and takeoff, and the duration of contact with the board were calculated. These data enabled the calculation of springboard stiffness and damping estimates using a simple mathematical mass-spring model. The second springboard test involved the use of a servo jacking rig, which measured the load applied to the springboard and the deflection of its surface, enabling stiffness to be calculated (Servo jack test).

5.3.1. DROP TEST

Video recording

Prior to testing, three calibration poles were positioned 0.6 m apart in the plane that would correspond to the long axis of the springboard. The three control points on each pole were 0.13, 0.63 and 1.13 m above the ground. A spirit level was used to level the pole stands, thus making the poles vertical. The control points were identified by white squares in the centre of black squares positioned on the poles with their diagonals pointing vertically and horizontally. The poles were videoed using a Sony Hyper HAD Hi-8 camera recording on

---

[1] For safety the springboard used had overall surface dimensions of 1.50 x 0.75 m while the actual *vaulting area* was the standard 1.20 x 0.60 m, thus giving a 0.30 m border at the far end and a 0.075 m border at each side of the springboard. The borders were coloured to contrast strongly with the vaulting area, as indicated in Figure 5.2b.

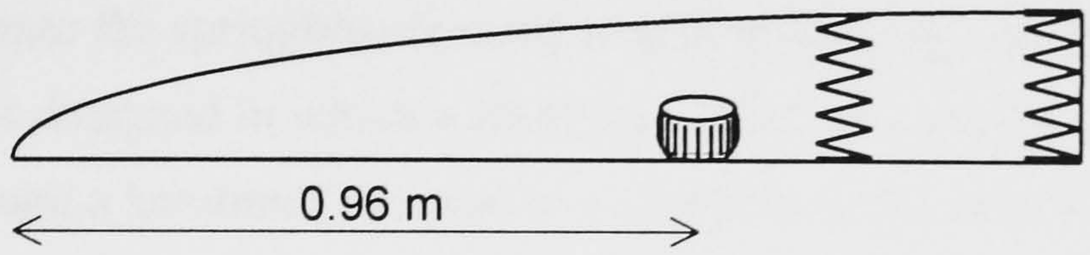

Figure 5.2a. Side elevation of the springboard showing the adjuster 0.96 m from the near end of the board, one of the three test positions.

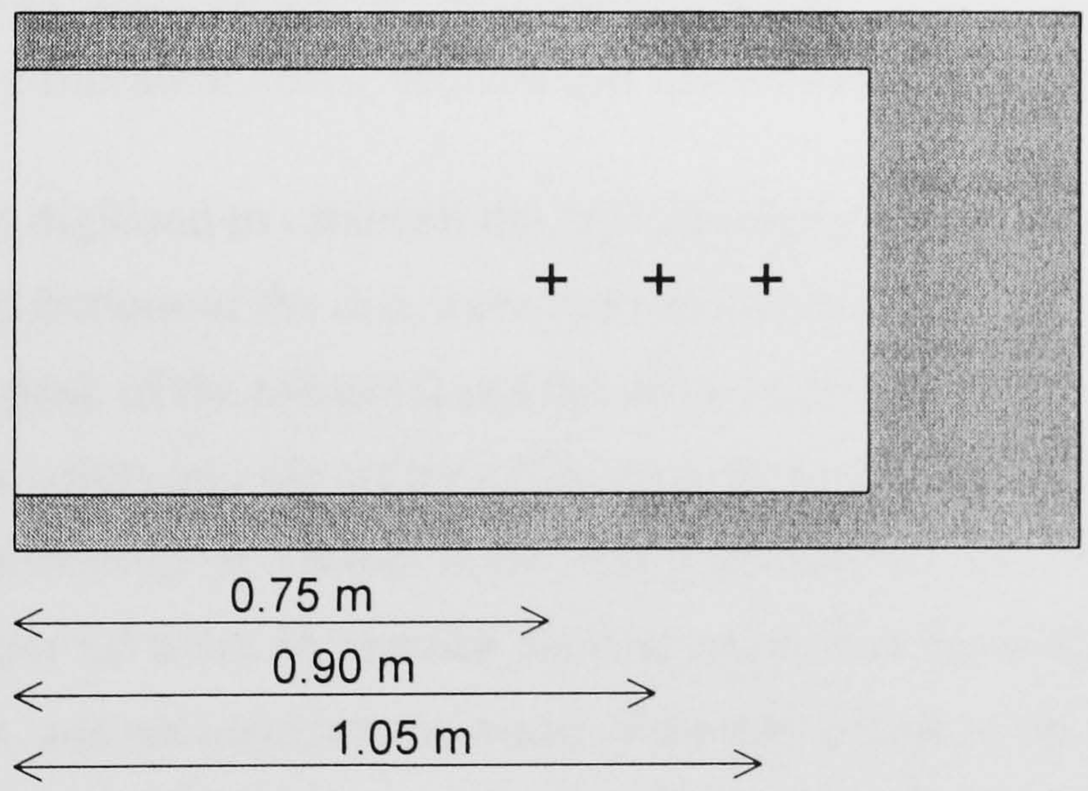

Figure 5.2b. Plan elevation of the springboard showing the three foot contact points tested.

N.B. The white area is the standard vaulting area, while the shaded area indicates the additional border that was present on the springboard tested.

sVHS videotape, positioned 4.5 m from the plane of the poles, with the optical axis of the camera approximately perpendicular to the axis down which the mass would be dropped. The poles were then removed and the springboard put into position. The camera was not moved nor adjusted following the recording of the calibration poles.

The FIG springboard testing procedures (FIG, 1994) consist of dropping a 20 kg mass from a height of 0.8 m onto the springboards using a custom built rig. For this study a similar testing method was designed in which a 20.45 kg barbell disc was suspended by a rope which passed through a karabiner attached to a roof joist in the laboratory. The disc was raised to 0.8 m above the surface of the springboard, steadied, then released and allowed to rebound from the board. Ten repeats at each of the nine combinations of the three board contact positions and three board adjustment settings previously identified were conducted. Contact with the springboard was always along its long axis.

Digitization and transformation

As for the vaulting digitization, a Peak 5 video digitizer (Peak Performance Technologies Inc.) was used. The mean of sixteen digitizations of the nine calibration points were used in order to perform a 2D DLT on the raw digitized coordinate data of the drop test. The mean RMS error for the calibration check was 0.9 mm horizontally and 1.5 mm vertically.

Initially trial 1 was digitized to establish the best digitizing procedure for the other trials. The top, centre and bottom of the disc were digitized throughout the trial (43 fields, from release to past the peak of the rebound) and the differences in position between the mean of the top and bottom points and the centre of the disc were calculated. There was little difference: RMS difference of 3.8 mm horizontally (maximum 7.4 mm) and 2.3 mm vertically (maximum 5.6 mm). In practice the disc centre was more difficult to locate than the top and bottom, and since taking the mean of the two points to represent the centre reduces the error, it was decided to omit the disc centre from future digitizations and to rely on the top and bottom points. In some trials the disc tended to rotate about the horizontal axis perpendicular to the camera's optical axis during the rebound; taking the mean of these two points reduced the problem that this rotation might have introduced.

A total of 78 trials out of the 90 were digitized: all ten trials of three conditions and eight trials of the remaining six conditions. Twelve trials could not be digitized due to difficulties with the video frame grabbing in those trials. Approximately 15 fields were digitized before disc impact with the springboard (ensuring that release of the disc had occurred before digitization commenced), and approximately 12 fields after the disc left the board (stopping before the disc had been arrested by the rope).

Analysis

For each trial two separate quadratic curves were fitted by the method of least squares to the disc centre vertical position data: one during the drop (before touchdown) and one during the rebound (after takeoff). The curve fitting smoothed the position data and the first derivatives of the equations of the curves were used to estimate the disc velocities immediately after the point of release and approaching the peak of the rebound. The disc velocities at touchdown and takeoff from the board could not be calculated in the same way because the times of touchdown and takeoff were unknown. Therefore the position and velocity data at the beginning of the drops and the positions of the disc centre at springboard touchdown (measured height of the board surface plus disc radius, not from digitization), were substituted into equations of constantly accelerated motion to calculate the times of first contact with the board and then the disc velocities at springboard touchdown. A similar process was used to calculate times at springboard takeoff and the disc velocities. From these data, the durations of contact with the springboard were determined for each trial.

The disc-board interaction was modelled as a simple one dimensional mass-spring-damper system. The equation of motion for such a system is:

$$\ddot{z} = \frac{\left(-k.z - c.\dot{z}\right)}{m} - g \qquad 5.10$$

where z is the spring length change (compression taken to be negative), $\dot{z}$ and $\ddot{z}$ are respectively the first and second derivatives of z with respect to time, k is the spring stiffness coefficient, c is the damping coefficient, m is the mass of the disc and g is the acceleration due to gravity.

A program was written in Maple™ V (Waterloo Maple Software; Appendix C.3) to solve Equation 5.10 and hence to find the stiffness and damping values which satisfied the touchdown and takeoff velocity, and time of contact data. In doing this, the time of contact was used as the criterion for the stiffness estimate (too stiff and the mass leaves the spring too soon and vice versa) and the disc velocity at takeoff was used as the criterion for the damping estimate (too much damping leads to a low takeoff velocity and vice versa).

The stiffness and damping were calculated for each trial digitized, from which the mean and standard deviation of the two values were calculated for each of the nine combinations of springboard contact positions and springboard adjustment knob positions.

5.3.2. SERVO JACK TEST

An estimate of the mean vertical forces involved during vaulting and in the drop tests was made using the impulse-momentum relationship:

$$\overline{F} = \frac{M.(v-u)}{t_c} \qquad 5.11$$

Here $\overline{F}$ is the mean vertical force, M the gymnast's mass, t_c is the duration of contact with the springboard, and v and u are the mass centre vertical velocities at springboard takeoff and touchdown respectively.

From the first five vaulting trials analysed (normal approach speed and the stiffest springboard setting) the mean change in vertical momentum and the mean springboard contact time were approximately 350 $kg.m.s^{-1}$ and 0.121 s respectively, which indicated a mean force of approximately 2890 N. This is in agreement with the results of a study by Takei (1989) who found a mean vertical force of 2970 N for the same style of vault, using the same type of estimation procedure, for elite male gymnasts with a mean body mass of 61.93 kg. Modelling the force history as the positive half of a sinusoid (a good approximation to the vertical GRF in activities like running and jumping, see for example Chapter Three, Figure 3.3) gave a peak force of approximately 4540 N (Appendix C.4). An identical analysis of the trials from the softest springboard setting gave a mean force estimate of 2590 N, suggesting a peak force of 4070 N. Using the same technique, data from the drop tests suggested peak forces of 2610 N at the stiffest setting and 2140 N at the softest setting. Kreighbaum (1974) used a calibrated springboard and estimated the initial peak vertical forces during handspring vaults by eight women gymnasts to be between 5260 and 9630 N and the secondary peak vertical forces to be between 2450 and 4680 N. These secondary peak figures agree with the estimates from this study, while the initial peak values are somewhat higher, but this was expected since the method of estimating peak forces used here would not reproduce any initial transient forces.

From these data it appeared that the forces applied to the springboard during the tests using the FIG protocol would not have been representative of the forces applied during vaults. The servo jack test on the springboard was an attempt to apply forces more like those estimated to have been applied during the vaulting.

In the Department of Civil and Building Engineering at Loughborough University a servo jacking system (R.D.P.-Howden Ltd) was arranged so that the piston of the system was positioned over the mid-longitudinal axis of the springboard which was placed flat on a solid concrete floor. The control unit for the servo jacking system enabled the excursion of the piston to be pre-set, up to a maximum of 100 mm, and the position over time to be

output to a recording system. Between the piston and the springboard surface was a 10 kN f.s.d. load cell (W.H. Mayes & Son (Windsor) Ltd) which was wired through a bridge circuit to provide a 2 mV/kN output. The load cell rested on a 100 mm plywood disc to provide a contact area the same as used in the FIG springboard testing procedures (FIG, 1994), and was coupled to the piston through a steel ball and cup arrangement. Figure 5.3 shows the testing rig set up.

The outputs from the servo jack and the load cell were recorded on a chart recorder displaying the load-deflection graph. The system was calibrated by the workshop technician and the scaling arranged so that there were 0.5 mm springboard deflection and 50 N compressive load per millimetre on the graph. A pilot test revealed that at the stiffest springboard setting, 100 mm compression resulted in a load of between 5 and 6.8 kN depending upon the load position along the longitudinal axis of the springboard. Similarly at the softest springboard setting 100 mm compression resulted in a load of between 3.5 and 4.4 kN. These forces were comparable with those estimated for the vaulting trials.

The piston control allowed a variety of load-unload rates but it was found that the fastest rate at which the full 100 mm excursion could be achieved without a noticeable judder of the piston was six seconds per cycle. Comparing tests at cycle lengths of between six and twenty seconds revealed less than a 1% change in peak load-deflection ratio. The fastest rate was chosen for the subsequent testing.

Ten repeated cycles at the same position and setting revealed a variation between any two cycles of no more than 100 N at any point in the cycle and so it was decided only to repeat each setting three times. The tests were conducted using the same nine combinations of load application point and springboard adjustment setting as in the drop testing (section 5.3.1), and finally two of the combinations conducted at the beginning of testing were repeated to assess whether any springboard fatigue was evident. This showed a change of less than 3% in the peak load-deflection ratio, suggesting that the order of testing was unlikely to have affected the results.

The results from a typical test can be seen in Figure 5.4 (an example from each of the nine test combinations is in Appendix C.5). The graphs were slightly non-linear, showing a gradual increase in slope and therefore stiffness. Given the lack of a sudden change in slope, an estimate of the average or overall stiffness for each trial was made by dividing the peak load by the springboard deflection at that load. These values were determined by scaling measures taken manually from the graphs. The resulting uncertainty in the stiffness estimates was calculated based on the resolution of the readings taken from the graphs.

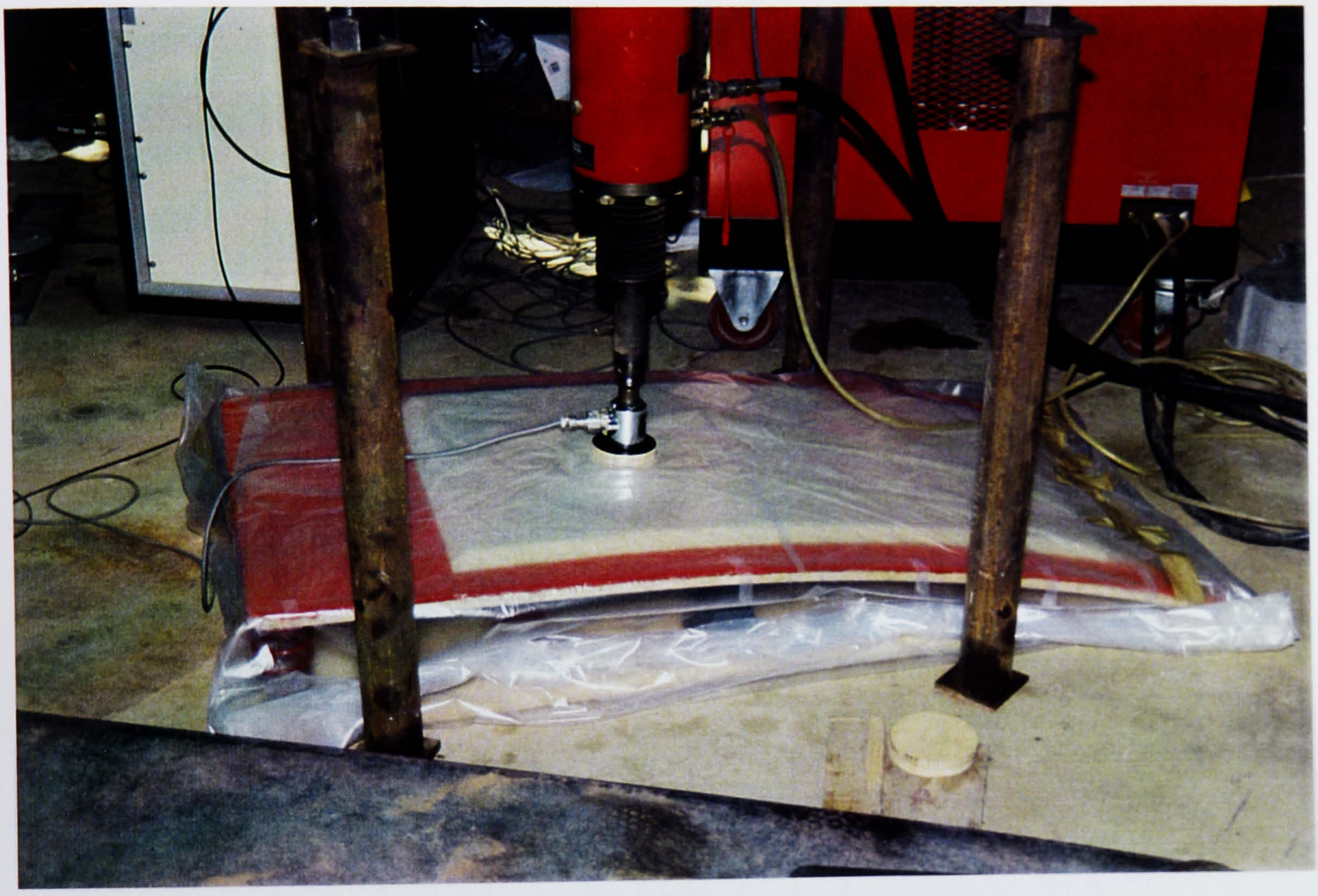

Figure 5.3. The servo jack springboard testing rig.

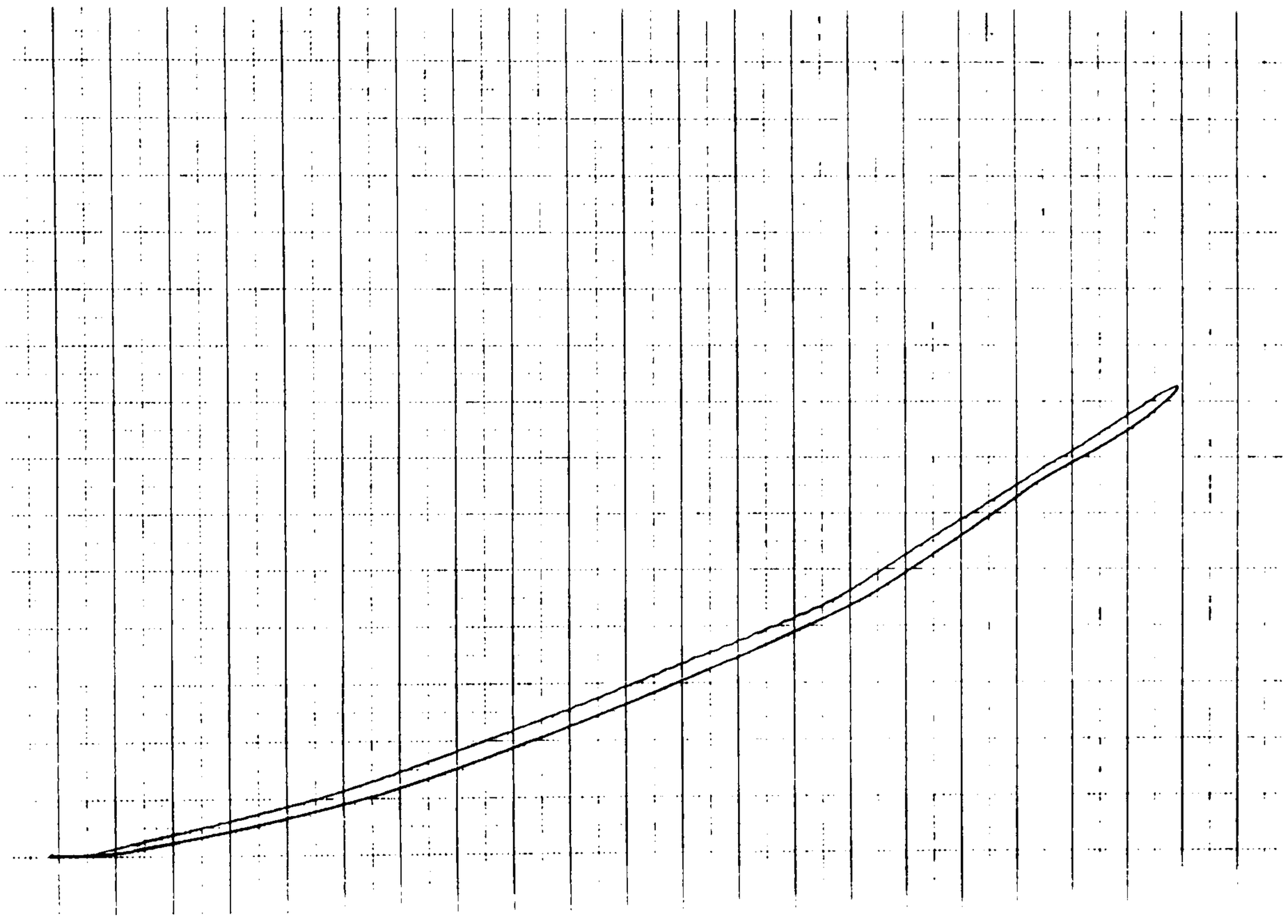

Figure 5.4. An example load-deflection graph from the servo jack springboard testing. N.B. Reduced in size from the original by 60% such that 6 mm (one bold division) represents 5 mm springboard deflection (horizontal axis) and 500 N compressive load (vertical axis).

5.4. RESULTS AND DISCUSSION

5.4.1. VAULTING

Table 5.1 contains the details of the digitization of the springboard adjustment knob position and gymnast's foot contact point on the springboard's surface, along with the calculated lengths of the vaulting area on the springboard. The foot contact position and adjuster position are given with respect to the near end of the springboard. The gymnast's contact point with the board displays some variability but is always within 60 to 90 percent of the vaulting area's length (from the near end) corresponding to the flatter, higher part of the surface. The adjuster position can be seen to have moved gradually between trials 3 and 9 before it was positioned at the softest setting for vaults 10, 11 and 12. From these data the contact and adjuster positions for the springboard testing were chosen to be 0.75, 0.90 and 1.05 m (contact) and 0.96, 1.04 and 1.28 m (adjuster). Comparing the actual vaulting area length (1.20 m) with the calculated values a transformation accuracy of 7 mm was estimated, which is of the same order of magnitude as the RMS error of the DLT calibration check (approximately 5 mm; see section 5.2.2 above).

Based on the repeated digitization of one trial, the standard errors of the mass centre and segment endpoint locations in Table 5.2 showed little improvement in precision as a result of increasing the number of digitizations from 2 to 3 to 4. The precision with which segment endpoints on the right side of the body were located was up to 3 mm better than on the left side. This was probably due to the unobstructed view of the right side of the gymnast's body throughout the trials. The precision of the mass centre location was the same (to three decimal places) regardless of the number of digitizations and it was better than that with which the segment endpoints could be located due to the fact that it is the result of a weighted mean of all the segment endpoints. The accuracies calculated were also of the same order of magnitude as the transformation accuracy.

The estimated uncertainties in the kinematic data obtained from the analysis of the video were small. At touchdown the mean relative error in mass centre velocity was 0.2% horizontally and 1.3% vertically; while at takeoff it was 0.2% horizontally and 0.3% vertically. For trials one to five these approximated to 0.016 $m.s^{-1}$ horizontally and 0.017 $m.s^{-1}$ vertically at touchdown, and 0.011 $m.s^{-1}$ horizontally and 0.012 $m.s^{-1}$ vertically at takeoff. The mean relative error in both the spring length and angle was 0.5%, and for the whole body moment of inertia it was 0.9%. Errors in the angular momentum and angular velocity were calculated in absolute terms since the very small angular momentum and velocity at springboard touchdown made relative errors rather meaningless. The standard

Table 5.1. Vaulting area length, foot contact position and springboard adjuster position with respect to the near end of the springboard at foot-board contact (m).

Trial	Vaulting area length	Foot position	Adjuster position
1	1.206	0.707	0.952
2	1.204	0.965	0.962
3	1.205	0.912	0.963
4	1.208	0.848	0.989
5	1.206	0.781	1.012
6	1.210	1.019	1.030
7	1.210	1.105	1.040
8	1.213	0.966	1.057
9	1.205	0.879	1.081
10	1.201	0.796	1.274
11	1.209	0.905	1.280
12	1.208	0.721	1.291
RMSE	0.0069	---	---

Table 5.2. Standard error estimates for the mass centre and all digitized landmarks, calculated from two, three and four digitizations (m).

	2 Digitizations		3 Digitizations		4 Digitizations	
	y	z	y	z	y	z
left wrist	0.006	0.004	0.006	0.004	0.004	0.003
left elbow	0.010	0.005	0.009	0.005	0.006	0.004
left shoulder	0.006	0.005	0.006	0.004	0.005	0.003
left hip	0.007	0.006	0.006	0.005	0.005	0.004
left knee	0.007	0.007	0.006	0.006	0.006	0.005
left ankle	0.006	0.005	0.005	0.005	0.004	0.004
left toes	0.009	0.007	0.007	0.007	0.007	0.005
right wrist	0.007	0.004	0.006	0.003	0.005	0.003
right elbow	0.007	0.005	0.007	0.004	0.006	0.004
right shoulder	0.007	0.004	0.007	0.003	0.005	0.003
right hip	0.005	0.004	0.005	0.004	0.004	0.003
right knee	0.005	0.005	0.004	0.004	0.004	0.003
right ankle	0.005	0.005	0.004	0.004	0.004	0.004
right toes	0.008	0.006	0.007	0.006	0.006	0.004
neck	0.005	0.005	0.005	0.004	0.004	0.004
top of head	0.005	0.005	0.004	0.004	0.004	0.003
mass centre	0.002	0.002	0.002	0.002	0.002	0.002

error in angular momentum was 0.79 $kg.m^2.s^{-1}$ in hurdle and 1.01 $kg.m^2.s^{-1}$ in preflight, and for the angular velocity it was 0.09 $rad.s^{-1}$ at both touchdown and takeoff from the board.

Tables 5.3 and 5.4 contain the model input values for the one spring and two spring models respectively, calculated from the video data as described in section 5.2.4 (Appendix C.6 contains the data from which the model input velocities were calculated). Note that the angle and angular velocity were measured clockwise from the negative horizontal such that they increase from touchdown to takeoff. Trials 1 to 5, 11 and 12 were performed at what the gymnast considered to be his normal approach speed which was calculated from the video analysis to be 7.91 ± 0.12 $m.s^{-1}$. This corresponded closely with Takei (1989) who found a mean and standard deviation of 7.50 ± 0.51 $m.s^{-1}$ in a study of 40 elite gymnasts performing handspring vaults in competition. The values for the other variables in these trials showed good consistency. Trials 6 and 7 were performed with progressively slower approaches (6.21 and 5.55 $m.s^{-1}$ respectively), trial 7 being the slowest at which the gymnast was comfortable. At these slow speeds the gymnast adopted a more upright body position and reduced his moment of inertia at touchdown. As expected there were corresponding reductions in the radial and angular velocities. The differences in body orientation and configuration between the normal approach speed and the intermediate approach speeds in trials 8, 9 and 10 (6.57, 7.14 and 7.36 $m.s^{-1}$ respectively) were less pronounced, however the radial and angular velocities were lower at the intermediate approach speeds than at the normal approach speed. The feet mass velocities (Table 5.4) did not vary in a systematic way as the approach speed changed because there was no systematic variation in the mass centre vertical velocity and the angular velocity immediately before touchdown.

Table 5.5 contains the kinematic data at springboard takeoff that formed the criteria against which the output of both models were later evaluated. The takeoff angles showed no systematic variation dependent upon the approach speed, while the horizontal and angular velocities were lower for the slower approach speeds. Vertical velocity at takeoff was less clearly related to the approach speed, but there is some indication that slower approaches resulted in lower vertical velocities at takeoff.

5.4.2. SPRINGBOARD TESTING

In the drop tests, the least squares quadratic curves fitted the vertical position data very closely. In only one trial was the mean coefficient of determination (r^2) less than 1.000 and even then it was 0.998. The greatest standard error of the position estimate was 0.003 m with the mean being 0.001 m. The time of springboard contact and touchdown and takeoff

Table 5.3. Touchdown input values for the one spring model.

Trial	Approach speed	I_G (kg.m^2)	L (m)	θ (rad)	v_t (m.s^{-1})	v_r (m.s^{-1})	$\dot{\theta}_1$ (rad.s^{-1})
1	Normal	9.64	1.049	1.151	6.48	-4.36	5.44
2	Normal	8.95	1.010	1.124	6.57	-4.69	5.73
3	Normal	9.20	1.044	1.100	6.40	-4.75	5.42
4	Normal	9.64	1.059	1.114	6.50	-4.79	5.43
5	Normal	9.46	1.067	1.085	6.47	-4.76	5.35
6	Slow	8.86	0.990	1.209	5.28	-3.58	4.66
7	Slow	8.30	0.973	1.245	4.80	-3.14	4.30
8	Intermed.	9.19	1.033	1.176	5.45	-3.98	4.65
9	Intermed.	9.11	1.057	1.117	5.82	-4.36	4.90
10	Intermed.	9.04	1.042	1.125	6.11	-4.30	5.20
11	Normal	9.50	1.078	1.091	6.34	-4.82	5.23
12	Normal	9.06	1.091	1.085	6.59	-4.84	5.43

N.B. I_G is the moment of inertia of the system about its mass centre, L and θ are the spring length and angle, v_r is the mass centre radial velocity, and $\dot{\theta}_1$ is the angular velocity of the system. v_t is the mass centre transverse velocity immediately *before* touchdown and is not actually a model input but it is included for completeness as it is used in the calculation of $\dot{\theta}_1$.)

Table 5.4. Touchdown input values for the two spring model.

Trial	Approach speed	I_G (kg.m^2)	L (m)	θ (rad)	v_t (m.s^{-1})	v_r (m.s^{-1})	$\dot{y}$ (m.s^{-1})	$\dot{\theta}_1$ (rad.s^{-1})
1	Normal	9.64	0.888	1.147	6.46	-3.21	-1.29	6.12
2	Normal	8.95	0.888	1.123	6.56	-3.45	-1.39	6.30
3	Normal	9.20	0.901	1.096	6.38	-3.63	-1.28	6.03
4	Normal	9.64	0.881	1.175	6.78	-3.07	-1.43	6.48
5	Normal	9.46	0.912	1.105	6.56	-3.68	-1.07	6.09
6	Slow	8.86	0.880	1.196	5.24	-2.36	-1.38	5.03
7	Slow	8.30	0.858	1.261	4.85	-1.80	-1.33	4.76
8	Intermed.	9.19	0.876	1.172	5.44	-2.61	-1.52	5.22
9	Intermed.	9.11	0.889	1.170	6.04	-2.78	-1.38	5.79
10	Intermed.	9.04	0.888	1.127	6.12	-3.17	-1.24	5.87
11	Normal	9.50	0.910	1.108	6.42	-3.51	-1.34	6.00
12	Normal	9.06	0.897	1.106	6.69	-3.60	-1.23	6.39

N.B. I_G is the moment of inertia of the system about its mass centre, L and θ are the spring length and angle, v_r is the mass centre radial velocity, $\dot{y}$ is the vertical velocity of the feet mass and $\dot{\theta}_1$ is the angular velocity of the system. v_t is the mass centre transverse velocity immediately *before* touchdown and is not actually a model input but it is included for completeness as it is used in the calculation of $\dot{\theta}_1$.

Table 5.5. Takeoff criteria for both the one and two spring models.

Trial	Approach speed	θ_{one} (rad)	θ_{two} (rad)	v_h ($m.s^{-1}$)	v_v ($m.s^{-1}$)	$\dot{\theta}$ ($rad.s^{-1}$)
1	Normal	1.820	1.894	5.43	3.89	6.09
2	Normal	1.766	1.809	5.29	4.10	6.72
3	Normal	1.749	1.789	5.11	4.16	6.59
4	Normal	1.784	1.907	5.39	3.96	6.14
5	Normal	1.790	1.852	5.51	3.94	6.21
6	Slow	1.753	1.792	4.23	4.01	5.35
7	Slow	1.806	1.841	4.20	3.80	4.38
8	Intermed.	1.774	1.852	4.50	3.82	5.49
9	Intermed.	1.801	1.876	5.13	3.92	5.74
10	Intermed.	1.785	1.857	5.38	3.97	5.46
11	Normal	1.803	1.883	5.48	3.94	6.19
12	Normal	1.825	1.905	5.86	3.89	5.93

N.B. Only the takeoff angles (θ_{one} and θ_{two}) are different between the two models owing to the different definitions for the base of the spring. v_h and v_v are the mass centre horizontal and vertical velocities, and $\dot{\theta}$ is the system angular velocity.

velocity estimates for each of the trials in the nine combinations of springboard contact position and springboard adjustment are summarized in Table 5.6. The mean and standard deviation of the stiffness and damping values calculated by the Maple™ V model for each trial are presented in Table 5.7.

The uncertainty in the stiffness estimates from the servo jack tests was calculated as follows:

1. The graphs could be read to the nearest 0.5 mm, therefore the largest error in any reading was 0.25 mm, which equated to 25 N and 0.25×10^{-3} m in the load and deflection dimensions respectively.

2. This gave a relative deflection error of 0.25×10^{-3} m per 0.1 m (maximum deflection of the springboard) which is 0.25%.

3. The relative load error was 25 N in 3500 N at the softest springboard setting which is 0.71%, and 25 N in 6800 N or 0.37% at the stiffest setting.

4. The combined relative error in the calculated stiffness was therefore 0.75% (equivalent to 263 $N.m^{-1}$) at the softest setting and 0.44% (equivalent to 302 $N.m^{-1}$) at the stiffest setting.

Hence confidence in the calculated stiffness values was better than 500 $N.m^{-1}$. (It was not possible to estimate springboard damping using this equipment). Table 5.8 summarizes the results of the servo jack tests of the springboard stiffness.

In both drop and servo jack tests the springboard stiffness increased as the contact position moved towards the far end of the board and as the adjuster position moved towards the near end of the board. As can be seen in Figure 5.5, the stiffness estimates from the servo jack test (filled symbols) were consistently greater than those from the drop test (open symbols). On average the difference was 66%, ranging from 48% to 94%. However the results from both tests conformed to the expectations that the 'competition' setting (adjuster 0.96 m from the near end) would be the stiffest, regardless of springboard contact point and *vice versa*.

Since the servo jack test was estimated to have reproduced more closely the magnitude of the typical peak forces applied to the springboard during the vaulting (see section 5.3.2 above), it was decided that the stiffness estimates derived from these tests would be most suitable as model inputs.

Table 5.6. A summary of the springboard contact times (T_c), touchdown velocities (V_{td}) and takeoff velocities (V_{to}) in the drop test (mean ± sd).

		Contact position		
Adjuster position		0.75	0.90	1.05
0.96	T_c (s)	0.079±0.0007	0.077±0.0009	0.075±0.0008
	V_{td} ($m.s^{-1}$)	-3.698±0.018	-3.685±0.057	-3.694±0.027
	V_{to} ($m.s^{-1}$)	2.621±0.020	2.691±0.028	2.765±0.031
1.04	T_c (s)	0.083±0.0014	0.080±0.0008	0.077±0.0009
	V_{td} ($m.s^{-1}$)	-3.677±0.018	-3.677±0.022	-3.701±0.026
	V_{to} ($m.s^{-1}$)	2.533±0.020	2.679±0.017	2.776±0.015
1.28	T_c (s)	0.094±0.0005	0.092±0.0011	0.088±0.0011
	V_{td} ($m.s^{-1}$)	-3.687±0.023	-3.679±0.027	-3.676±0.027
	V_{to} ($m.s^{-1}$)	2.581±0.025	2.550±0.039	2.438±0.034

Table 5.7. Drop test stiffness and damping estimates for each contact and springboard adjuster combination (mean ± sd).

		Contact position		
Adjuster position		0.75	0.90	1.05
0.96	stiffness ($kN.m^{-1}$)	31.1±0.612	32.6±0.804	35.1±0.741
	damping ($N.s.m^{-1}$)	163±4	156±3	153±4
1.04	stiffness ($kN.m^{-1}$)	28.1±0.929	30.5±0.583	33.3±0.839
	damping ($N.s.m^{-1}$)	170±3	152±3	147±4
1.28	stiffness ($kN.m^{-1}$)	22.3±0.224	23.2±0.512	24.7±0.583
	damping ($N.s.m^{-1}$)	142±4	156±4	184±6

Table 5.8. Servo jack test stiffness parameter estimates for each contact and springboard adjuster combination (mean ± sd).

		Contact position		
Adjuster position		0.75	0.90	1.05
0.96	stiffness ($kN.m^{-1}$)	49.2±0.251	56.4±0.274	68.2±0.222
1.04	stiffness ($kN.m^{-1}$)	41.6±0.000	47.7±0.078	60.4±0.181
1.28	stiffness ($kN.m^{-1}$)	34.5±0.130	35.7±0.051	42.3±0.063

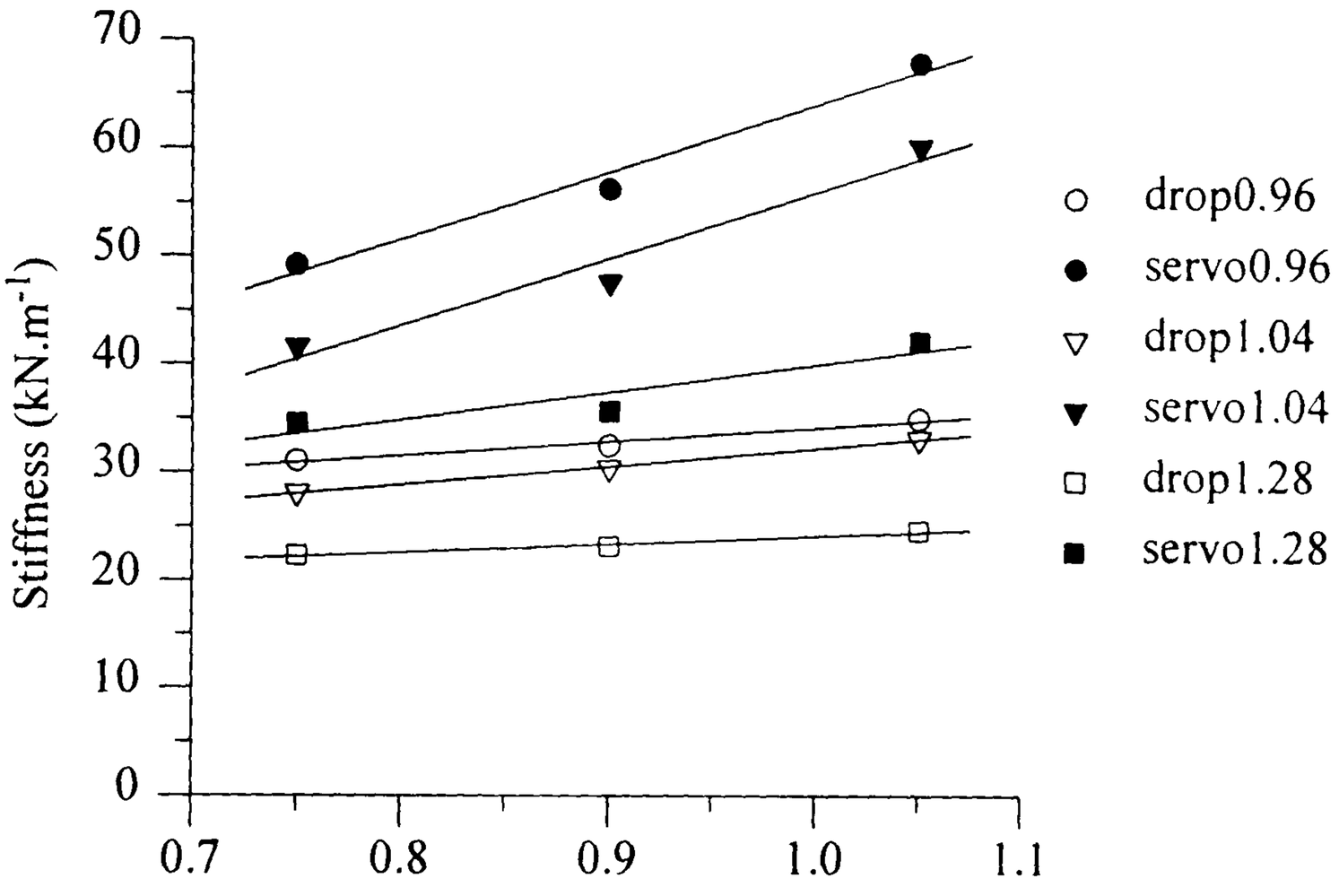

Figure 5.5. Springboard stiffness estimates from the drop test and servo jack test at each of the three board adjuster positions.

Figure 5.6 illustrates the springboard damping estimated from the drop test. In general, the damping did not vary greatly between springboard settings and test locations, with the greatest variation being for the softest springboard setting (adjuster 1.28 m from the near end of the board). In damped mass-spring systems the degree of damping is characterized by the relationship between the damping, c, the mass, m, and the stiffness, k; in particular, if $c^2 < 4.m.k$ the system is described as *underdamped* (Bolton, 1994). In the case of the drop test data (m = 20 kg), even taking the greatest damping estimate (184 N.s.m^{-1}) and the corresponding stiffness (24.7 kN.m^{-1}), c^2 was less than 2% of $4.m.k$, suggesting that the effect of the damping would be negligible over one half of an oscillation (equivalent to the foot contact phase). However, the inability to calculate the damping at higher loads and the uncertainty over the precise equivalent mass of the springboard-feet component of the model meant that this estimate was subject to some doubt. Further investigation of the effect of springboard damping was therefore necessary as part of the model evaluation (Chapter Six).

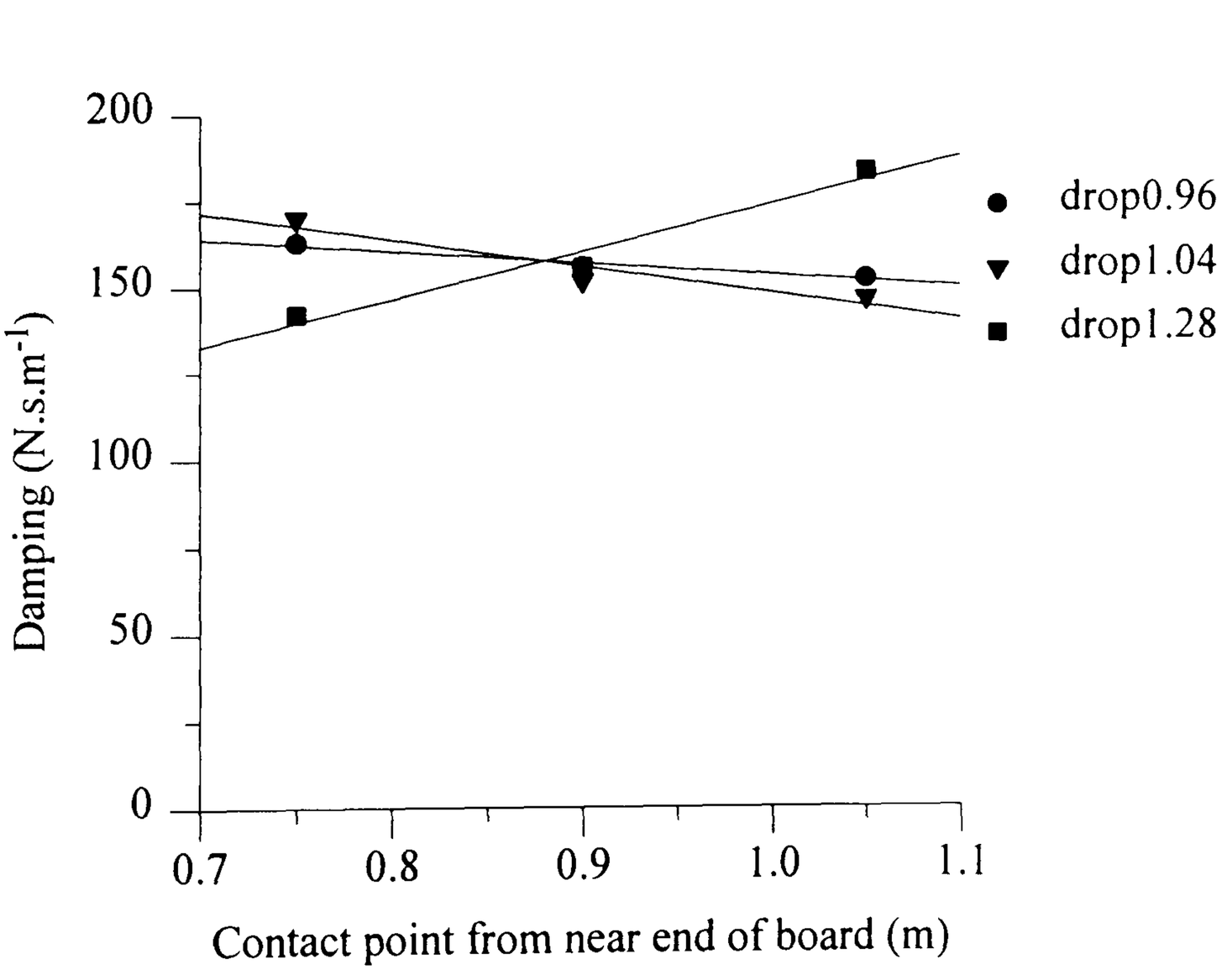

Figure 5.6. Springboard damping estimates from the drop test at each of the three board adjuster positions.

The foot contact positions with the springboard in the vaulting did not correspond exactly with the tested springboard positions. In order to estimate the springboard stiffness and damping values for each specific contact position, linear regressions were calculated using Microsoft Excel for stiffness and damping against springboard contact position at each of the springboard adjuster settings, based on the measured values from the springboard testing. Only the data from the servo jack test were used for the stiffness regressions. While these stiffness estimates appeared (Figure 5.5) to increase in a less linear fashion than the stiffness and damping estimates from the drop test, linear approximation does not differ from the actual results by more than 5% (mean 2.6%). The regression lines were of the form $y = a.x + c$ where a was the slope, c the intercept and x the foot contact position with respect to the near end of the springboard. Table 5.9 summarizes the regression equation results.

Table 5.9. Linear regression parameters for stiffness and damping calculation on the basis of foot contact position.

Adjuster position		slope (a)	intercept (b)	r^2	SE_y
0.96	stiffness	63.333	0.933	0.98	1.878
	damping	-33	187	0.95	1.63
1.04	stiffness	62.667	-6.500	0.96	2.694
	damping	-77	225	0.90	5.31
1.28	stiffness	26.000	14.100	0.86	2.205
	damping	140	35	0.96	5.72

N.B. For the stiffness the slope has units of $kN.m^{-2}$ and the intercept and standard error of the estimate have units of $kN.m^{-1}$. For damping the slope has units of $N.s.m^{-2}$ and the intercept and standard error of the estimate have units of $N.s.m^{-1}$.

5.5 SUMMARY

This chapter described the determination of kinematic data relating to the inputs to the models developed in Chapter Four, and the uncertainties associated with these data. Video of an elite British male gymnast performing a series of 12 handspring vaults from an adjustable springboard was collected and analysed to provide kinematic data on the gymnasts performances. These data were the mass centre velocity, whole body angular velocity and moment of inertia about a transverse axis through the mass centre, spring length and spring angle. These data were required at springboard touchdown and takeoff. For the two spring model, an estimate of the vertical velocity of the feet at touchdown was also needed. The springboard was subjected to a drop test and a servo jack test over a range of contact positions and board adjustments. The drop test was based on FIG testing procedures and, in conjunction with a mass-spring model, enabled the estimation of springboard stiffness and damping. However, the estimated peak vertical forces applied during the drop test were substantially lower than those estimated to have been applied during the actual vaults by the gymnast. The servo jack test applied forces more consistent with the vault trials and allowed the springboard stiffness to be calculated but did not enable the calculation of springboard damping. From the drop test data, it was estimated that the damping during one half of a cycle would be negligible, but it was felt that further investigation was warranted during model evaluation. Altogether, the results from the studies described in this chapter enable the models developed in Chapter Four to be evaluated and applied.

CHAPTER SIX
MODEL EVALUATION AND APPLICATION

6.1 INTRODUCTION

As described in Chapter Four, both the one spring and two spring models were formulated with two modes of operation: where the spring stiffness is unknown the models will determine a stiffness which ensures that the angle of the spring at takeoff matches a specified takeoff angle, while a second mode predicts the takeoff velocities and spring angle if the spring stiffness is provided. This chapter describes the evaluation and application of the models, and explores the utility of the models as a means of understanding the mechanics of vault takeoffs and of answering the questions posed in Chapter One. The analysis of the handspring vaults described in Chapter Five provided the input data for the simulations of specific vaults. Mean values from the first five vaults, those where the gymnast approached the springboard in his usual way and where the springboard was at its competition setting (hereafter known as the normal approach trials) were used where an average vault was required. These data, in conjunction with values from the literature, also provided information on the realistic ranges for the model inputs for other simulations.

6.2 METHOD

6.2.1 STIFFNESS ESTIMATION AND MODEL EVALUATION

The models predict takeoff velocities based on the assumption of a simple rebound. In order to determine what proportion of the gymnast's takeoff linear and angular velocities can be accounted for by a simple rebound, the models were used to determine the spring stiffness required to achieve the correct takeoff angle and then to output the takeoff velocities. The twelve vaults discussed in Chapter Five were simulated with both models and the outputs were compared with the results of the video analysis by calculating the percentage of the actual takeoff velocities the models predicted. The calculated spring stiffnesses were noted for each simulation to provide a basis for further simulations and for comparison with other studies that have used mass-spring systems to investigate human locomotion. The durations of the rebounds were also calculated and compared with the times of contact of the gymnast with the springboard from the analyses of the actual vaults. Since the time of contact of the gymnast with the springboard was not used in the models, this comparison provided an indirect but independent evaluation of the fit of the models to the vaults.

To determine how sensitive the spring stiffness estimates and predicted takeoff velocities were to the uncertainty in the input data, a sensitivity analysis was conducted on both models. One at a time, each model input (with the exception of the moment of inertia) from trial one was increased by twice the standard error estimated from the video analysis (Chapter Five, section 5.4.1) and a new simulation executed. For the two spring model the board parameters were also perturbed by twice the uncertainty estimated from the board tests (Chapter Five, section 5.4.2) and the feet mass proportion was doubled. Doubling the feet mass was chosen as a rigorous test since it was not possible to be precise with the estimate of how much mass to apportion to the base of the spring. Since the moment of inertia of the gymnast increased from springboard touchdown to takeoff (by 39%), the sensitivity of both models to using the takeoff value rather than the touchdown value was also determined. Where sensitivity to an increase in an input was noted, a further simulation was performed with that input reduced by the same amount. The takeoff angle was held constant in these simulations. The outputs from these simulations were compared with the outputs from the original simulation to determine the differences the perturbations had caused.

6.2.2 BOARD STIFFNESS VARIATIONS

A series of simulations using the two spring model was performed in order to determine the extent to which board stiffness variations affected the model outputs. The mean values from the five normal approach trials were used as inputs, including a representative leg spring stiffness of 125 $kN.m^{-1}$. The board damping was set to 155 $N.s.m^{-1}$, representing a mid-board contact, while the board stiffness was varied from 35 to 75 $kN.m^{-1}$, covering a range of realistic values (calculated using the regression equations and actual board contact positions determined in Chapter Five, section 5.4.2). With the leg spring stiffness being preset, the model calculated the takeoff velocities and leg spring angle for each board stiffness.

To determine whether a gymnast might be able to compensate for springboard stiffness variations by adjusting his leg stiffness, a series of simulations were performed using the two spring model. These simulations demonstrated how the leg spring stiffness would need to vary as the board stiffness was altered, whilst the touchdown conditions and takeoff angle were held constant. The mean values from the five normal approach trials were used as inputs, including the desired spring takeoff angle, while the leg spring stiffness was recalculated for each of the board stiffnesses. Again the board stiffness was varied over a range of realistic values and the board damping set at 155 $N.s.m^{-1}$. Board damping was not varied as the board testing had shown that this value did not change greatly between board settings and contact positions (always between 142 and 184 $N.s.m^{-1}$; see Chapter Five, section 5.4.2). Furthermore, preliminary simulations had shown that this range of damping

variations made a negligible difference to the outcomes, which was also supported by the sensitivity analyses.

To investigate compensating for springboard stiffness variations in some way other than by changing leg stiffness, a series of simulations were conducted in which the leg spring stiffness was held constant, the board stiffness was altered and the touchdown horizontal velocity or touchdown spring angle was adjusted. Using the regression equations determined from the board testing (Chapter Five, section 5.4.2), a stiff board setting of 58 $kN.m^{-1}$ was calculated, equivalent to board contact 0.90 m from the near end with the stiffest board adjustment, and similarly a soft setting of 37.5 $kN.m^{-1}$ was calculated, equivalent to board contact at the same place but with the softest board adjustment. Two scenarios were analysed: one in which the board stiffness was changed from being stiff to soft and one where the change was in the opposite direction. In each case an initial simulation using the mean inputs and takeoff spring angle from the five normal approach trials was executed in order to calculate the required leg spring stiffness. The board stiffness was then changed (to either the stiffer or softer value) while the leg spring stiffness was kept at the previously calculated value and simulations were then conducted in which the touchdown horizontal velocity or spring angle was systematically adjusted. Each new simulation was compared with the original board stiffness simulation by calculating the square root of the mean squared differences between the takeoff spring angle and velocities.

6.2.3 APPROACH AND CONTACT STRATEGIES

One of the issues raised in Chapter One concerned suggesting strategies which gymnasts could adopt in order to achieve a particular takeoff. To investigate this, the horizontal touchdown velocity, touchdown spring angle and (leg) spring stiffness were each separately varied over a range of realistic values, while the other touchdown variables were kept to the mean values from the five normal approach trials.

The range of horizontal velocities investigated was from 6.30 to 8.67 $m.s^{-1}$ and the range of touchdown spring angles was from 0.90 to 1.24 radians for the two spring model and 0.89 to 1.23 radians for the one spring model.[1] These ranges approximately covered the range of approach speeds and touchdown body angles found by Takei (1988, 1989, 1991) and Takei

---

[1] Note that all angles are given with respect to the left (negative) horizontal and in a clockwise direction, matching the gymnast's direction of rotation. Positive horizontal velocity is from left to right and positive vertical velocity is upwards.

and Kim (1990) for Handspring and Handspring Salto Forward Tucked vaults by national and international competitors, and included all but the slowest two vaults analysed in Chapter Five (trials six and seven). For these simulations with the one spring model the stiffness was set at 41.523 $kN.m^{-1}$, the predicted stiffness for the mean touchdown and takeoff inputs. For the two spring model simulations the board stiffness was set at 58.000 $kN.m^{-1}$ and the damping at 155 $N.s.m^{-1}$, representing the gymnast contacting the board 0.90 m from the near end with the stiffest board adjustment. The leg spring stiffness was held at 103.125 $kN.m^{-1}$, the predicted stiffness for the mean touchdown and takeoff inputs with these board settings. Further simulations were conducted to explore the effects of altering the touchdown spring angle and horizontal velocity simultaneously.

Where the spring stiffness was varied, the range of stiffnesses for the one spring model was 30 to 50 $kN.m^{-1}$ and for the two spring model the range of leg spring stiffnesses was 80 to 290 $kN.m^{-1}$. Thus the range of predicted stiffnesses for the twelve analysed trials was covered. The board stiffness and damping were again set to 58 $kN.m^{-1}$ and 155 $N.s.m^{-1}$ for the two spring model simulations (the influence of board stiffness variations due to feet contact position and board adjustment had already been investigated).

6.3 RESULTS

6.3.1 STIFFNESS ESTIMATION AND MODEL EVALUATION

A summary of the results of the simulations of the twelve analysed trials are presented for the one and two spring models in Tables 6.1 and 6.2 respectively (the raw model output can be found in Appendix D.1 and D.2). These simulations calculated the spring stiffness required to produce the criterion takeoff spring angle given the measured touchdown inputs. Each table contains the estimated spring stiffnesses, the rebound durations as a percentage of the gymnast's contact times with the springboard and the percentage of the measured takeoff velocities accounted for by the simulations.

The simple rebound of the one spring model lasted an average of 87% of the actual contact time and accounted for the majority of the takeoff velocities, though the model underestimated the angular and mass centre vertical velocities at takeoff, while overestimating the mass centre horizontal velocity at takeoff (Table 6.1). The mean percentage of the angular velocity accounted for was 87% (range 81-97%), of the vertical velocity was 78% (range 54-88%) and of the horizontal velocity was 119% (range 113-123%). Simulations of trials 6 and 7, the slowest approach speeds, produced the poorest

Table 6.1. Estimates of spring stiffness, percentage of contact time and the percentage of takeoff velocities accounted for by one spring model simulations.

Trial	K (kN.m^{-1})	t_c (%)	$\dot{\theta}$ (%)	v_h (%)	v_v (%)
1	38.945	86	88	120	72
2	48.906	86	84	123	84
3	44.102	86	81	123	88
4	40.938	85	87	122	87
5	35.547	90	85	118	86
6	47.969	86	86	121	67
7	39.063	88	97	113	54
8	40.234	85	83	121	76
9	33.086	90	84	116	77
10	38.125	88	94	114	76
11	34.023	87	83	119	85
12	32.031	87	90	117	81
mean	-	87	87	119	78
r^2	-	0.85	0.80	0.94	0.46
p	-	<0.001	<0.001	<0.001	0.015

N.B. Inputs to the simulations were from the analysis of the twelve vault trials in Chapter Five (Table 5.3) and outputs were compared with the takeoff data from the same trials (Table 5.5). Spring stiffnesses were estimated by the model using the measured takeoff angle as the criterion. r^2 indicates the coefficient of determination between the model output and the criterion values from Chapter Five, and p the probability of this being by chance.

Table 6.2. Estimates of leg spring stiffness, percentage of contact time and the percentage of takeoff velocities accounted for by two spring model simulations.

Trial	K ($kN.m^{-1}$)	t_c (%)	$\dot{\theta}$ (%)	v_h (%)	v_v (%)
1	110.156	90	107	108	57
2	135.156	90	95	110	73
3	121.094	88	92	111	76
4	111.719	84	112	115	53
5	139.063	89	105	108	64
6	121.875	91	94	107	60
7	94.531	88	110	103	48
8	79.688	92	96	108	65
9	106.250	86	105	107	55
10	293.750	92	116	102	55
11	129.688	89	104	107	62
12	242.969	86	119	105	55
mean	-	89	105	108	60
r^2	-	0.68	0.51	0.92	0.67
p	-	0.001	0.009	<0.001	0.001

N.B. Inputs to the simulations were from the analysis of the twelve vault trials in Chapter Five (Table 5.4) and outputs were compared with the takeoff data from the same trials (Table 5.5). Leg spring stiffnesses were estimated by the model using the measured takeoff angle as the criterion. r^2 indicates the coefficient of determination between the model output and the criterion values from Chapter Five, and p the probability of this being by chance.

agreement with the vertical velocity at takeoff, but otherwise the proportions of the takeoff velocities accounted for were reasonably consistent. There did not appear to be a particular trend in the spring stiffness estimates, though those from the three trials at the softest board setting (trials ten to twelve) were lower than for most of the other trials, reflecting the influence of the board on the overall stiffness.

Using the two spring model the rebound duration was an average of 89% of the actual contact time. The results of the simulations again showed a good degree of consistency in the proportion of the takeoff velocities accounted for by a simple rebound (Table 6.2) and demonstrated that a simple rebounding model is able to account for the majority of the actual takeoff velocities. The mean percentage of the angular velocity predicted was 105% with a range from 92 to 119% and for the horizontal velocity the mean was 108% (range 102-115%). The proportion of the vertical velocity accounted for was 60% on average with a range from 48 to 76%, still generally more than half but not as good as for the other velocities. As with the one spring model, the simulation of the slowest approach speed trial (trial 7) generated the smallest proportion of the vertical takeoff velocity. Leg spring stiffness estimates did not show a very clear pattern, indeed the estimates for trials 11 and 12, both with normal approach speeds but the softest board setting, were almost at the two extremes of the range of stiffnesses found (the board stiffnesses were very similar despite different feet contact points).

Tables 6.3 and 6.4 summarize the results of the sensitivity analyses performed on the one and two spring models respectively. Each table shows the percentage difference between the outputs using the perturbed inputs and the original simulation results from trial one, and indicates the amount by which each input was perturbed (equivalent to twice the estimated uncertainty in each case except the moment of inertia, where the takeoff value was used, and the feet mass, which was doubled). Generally the takeoff velocity estimates from neither model were particularly sensitive to input uncertainties: both models showed some sensitivity to the uncertainty in the horizontal velocity at touchdown, but the sensitivities of the vertical velocities at takeoff to the spring angles at touchdown were greatest. Similarly, the spring stiffness estimates were most sensitive to the touchdown angle of the system, with some degree of sensitivity also to the touchdown horizontal velocity and spring length at touchdown. The two spring model results showed that the leg spring stiffness estimate was somewhat sensitive to the board stiffness, but distinctly insensitive to the board damping and feet mass parameters (which was helpful since it was not possible to estimate these parameters with as much confidence as the other inputs). While the velocity changes in

Table 6.3. Sensitivity of outputs from the one spring model simulation of trial 1 to perturbations of model inputs.

Input (perturbation)	$\dot{\theta}$ (% diff.)	v_h (% diff.)	v_v (% diff.)	K (% diff.)
v_h (0.4%)	1	1	0	1
v_v (2.6%)	0	0	1	0
θ (±1.0%)	1/-1	1/0	-3/3	4/-4
L (1.0%)	-1	0	0	-2
I_G (39%)	-4	-4	6	-4
$\dot{\theta}$ (0.18 rad.s^{-1})	0	0	0	0

N.B. Differences are by comparison with the results of the original trial one simulation.

Table 6.4. Sensitivity of outputs from the two spring model simulation of trial 1 to perturbations of model inputs.

Input (perturbation)	$\dot{\theta}$ (% diff.)	v_h (% diff.)	v_v (% diff.)	K (% diff.)
v_h (0.4%)	1	0	0	2
v_v (2.6%)	0	0	1	1
θ (±1.0%)	1/-1	0/0	-4/4	+12/-9
L (1.0%)	-1	0	0	-4
I_G (39%)	-7	-6	10	-4
$\dot{\theta}$ (0.18 rad.s^{-1})	0	0	0	0
K_b (±8.1%)	-1/1	0/0	2/-3	-12/+21
C_b (2.0%)	0	0	0	0
Feet mass (100%)	-1	0	-2	-5

N.B. Differences are by comparison with the results of the original trial one simulation.

response to the perturbation of the moment of inertia may seem quite large, the 39% increase in the moment of inertia to bring these about puts them into perspective. Both models were insensitive to the uncertainties in the vertical velocity and angular velocity at touchdown.

6.3.2 BOARD STIFFNESS VARIATIONS

The effects of altering the board stiffness in the two spring model, while all the other inputs were held constant is illustrated in Figure 6.1. For consistency, the range on the ordinate of each of the graphs is from 70% to 130% of the value of the dependent variable at a board stiffness of 55 $kN.m^{-1}$. The results showed that each of the takeoff variables were affected: over the full range of board stiffness perturbation the vertical velocity varied from 1.99 to 3.12 $m.s^{-1}$, the angular velocity from 6.87 to 6.19 $rad.s^{-1}$, the horizontal velocity from 6.07 to 5.75 $m.s^{-1}$ and the takeoff angle from 1.94 to 1.78 radians. These ranges are comparable with or greater than the variations in the takeoff values from the five trials which were used to calculate the mean inputs (Chapter Five section 5.4.1 and Table 6.5 below) and the differences between means of the eleven best and eleven worst handspring and forward salto performances reported by Takei (1991), which indicated that the effect of board stiffness variation was likely to be of importance. The increase in vertical velocity was particularly great, this being due mainly to the takeoff angle getting closer to vertical, thereby reducing the negative contribution of the angular velocity and increasing the positive contribution of the mass centre's radial velocity.

Simulations in which the leg spring stiffness was recalculated to compensate for board stiffness variations (while other inputs remained unchanged) showed that as the board stiffness was increased the estimated leg spring stiffness reduced in a non-linear fashion (Figure 6.2). For the inputs used in these simulations the leg spring stiffness reached a stiffness of about 77 $kN.m^{-1}$ at the top end of the feasible board stiffness range; it should be remembered though that the actual required leg spring stiffnesses are dependent on the individual inputs to the simulation, so the leg spring stiffness would not always tend towards 77 $kN.m^{-1}$. No account was taken of the variations in takeoff velocities induced by these stiffness changes but over the whole range the angular, horizontal and vertical takeoff velocities only varied by ±3.3%, ±1.0% and ±7.5% from the mean respectively (the leg spring angle at takeoff was used as the criterion in the selection of the leg spring stiffness and so did not vary).

Altering something other than the leg stiffness in order to compensate for board stiffness variations was also investigated. Figures 6.3 and 6.4 summarize the results of simulations exploring the effects of altering the horizontal velocity and spring angle at touchdown. Adjusting the board stiffness from a stiff to soft value while keeping the leg spring stiffness

(a)

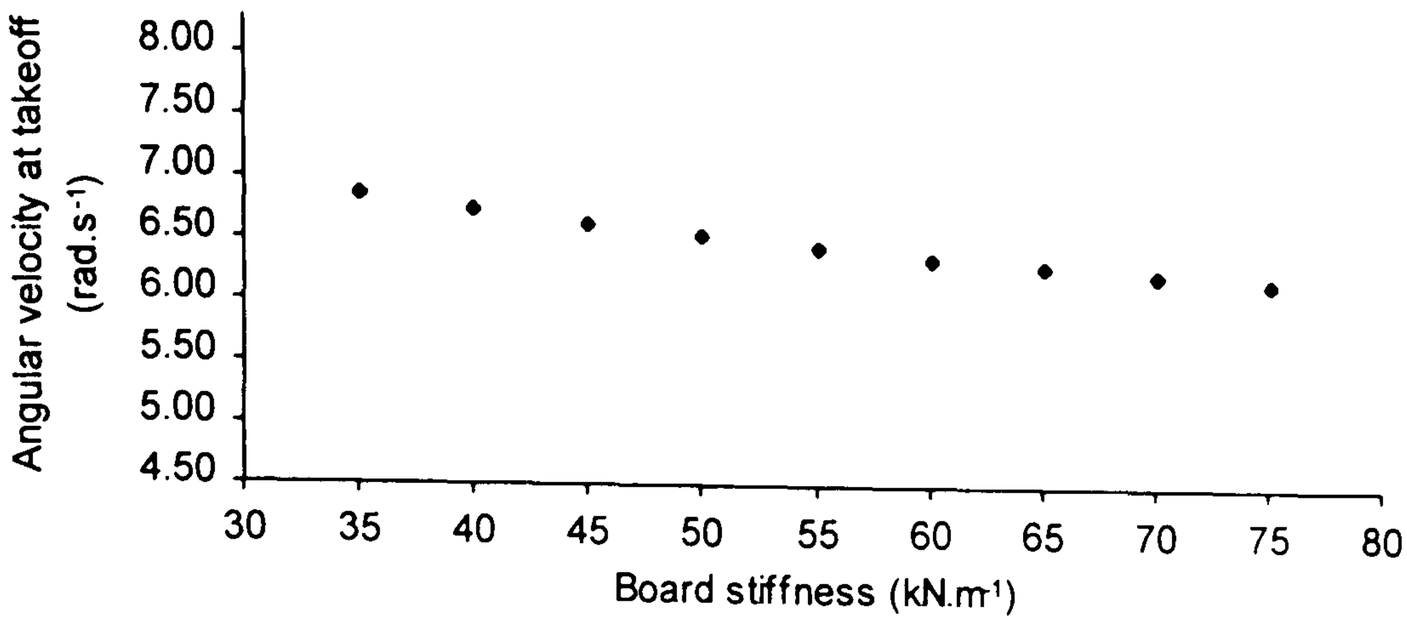

(b)

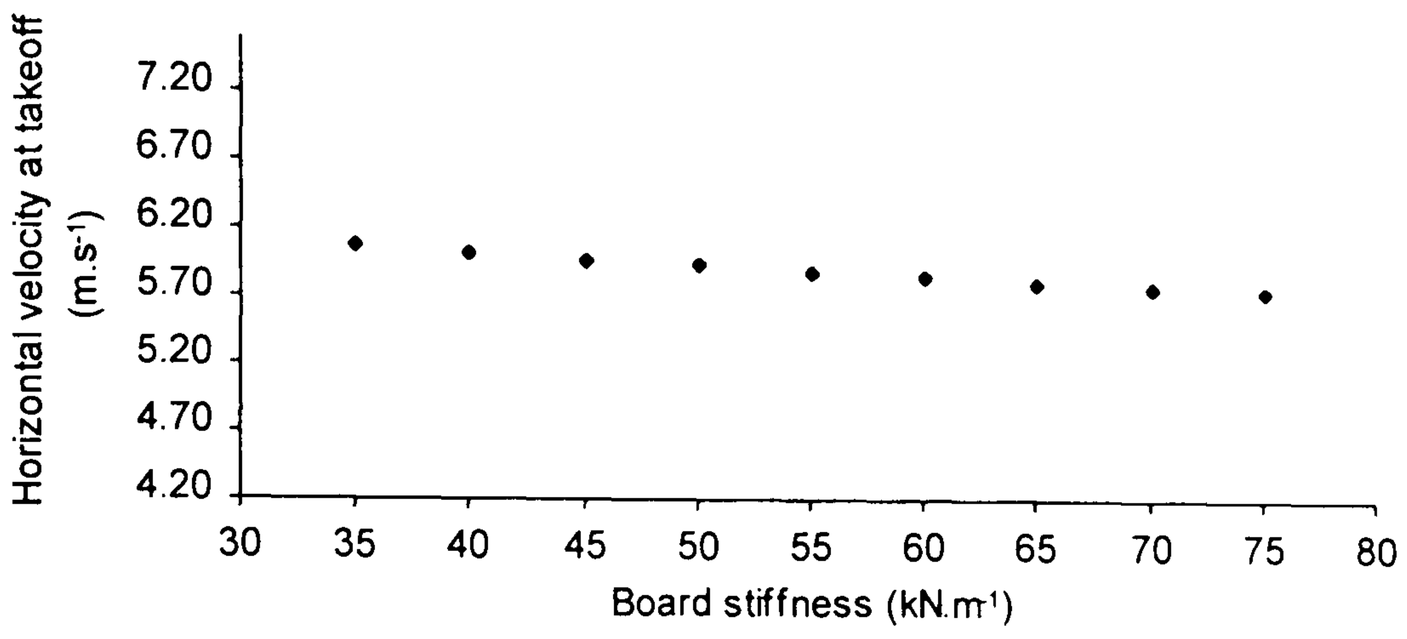

(c)

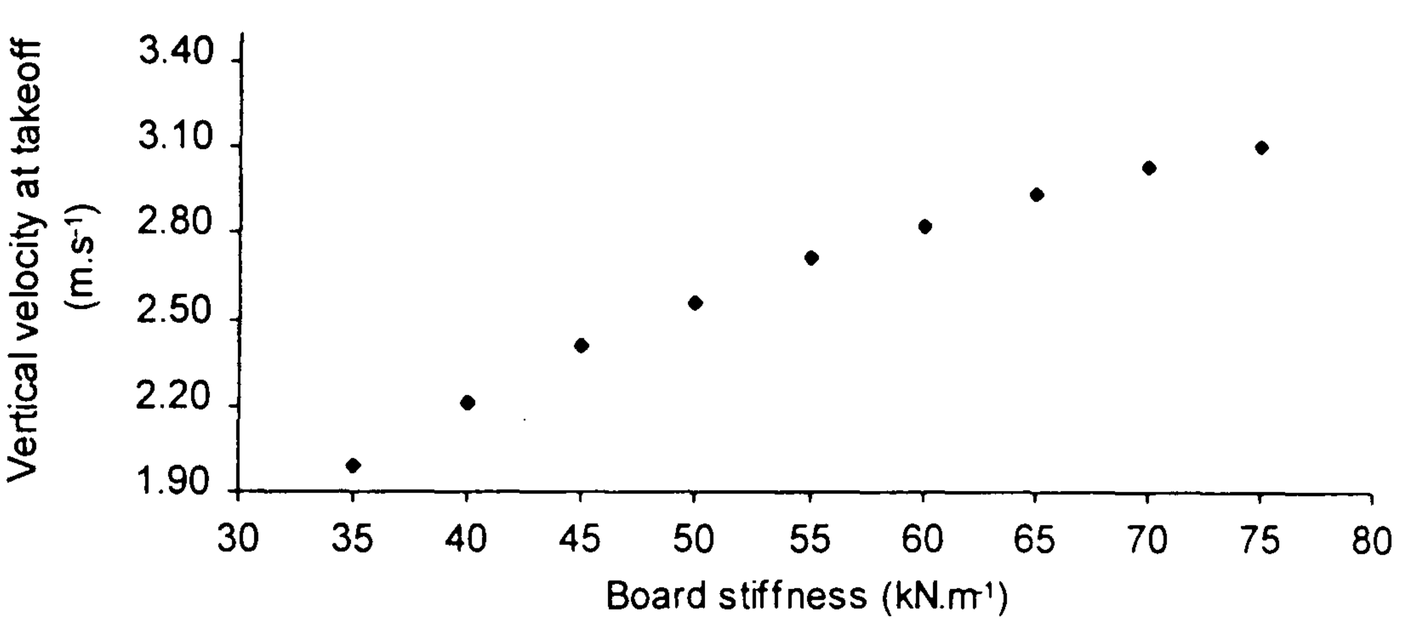

(d)

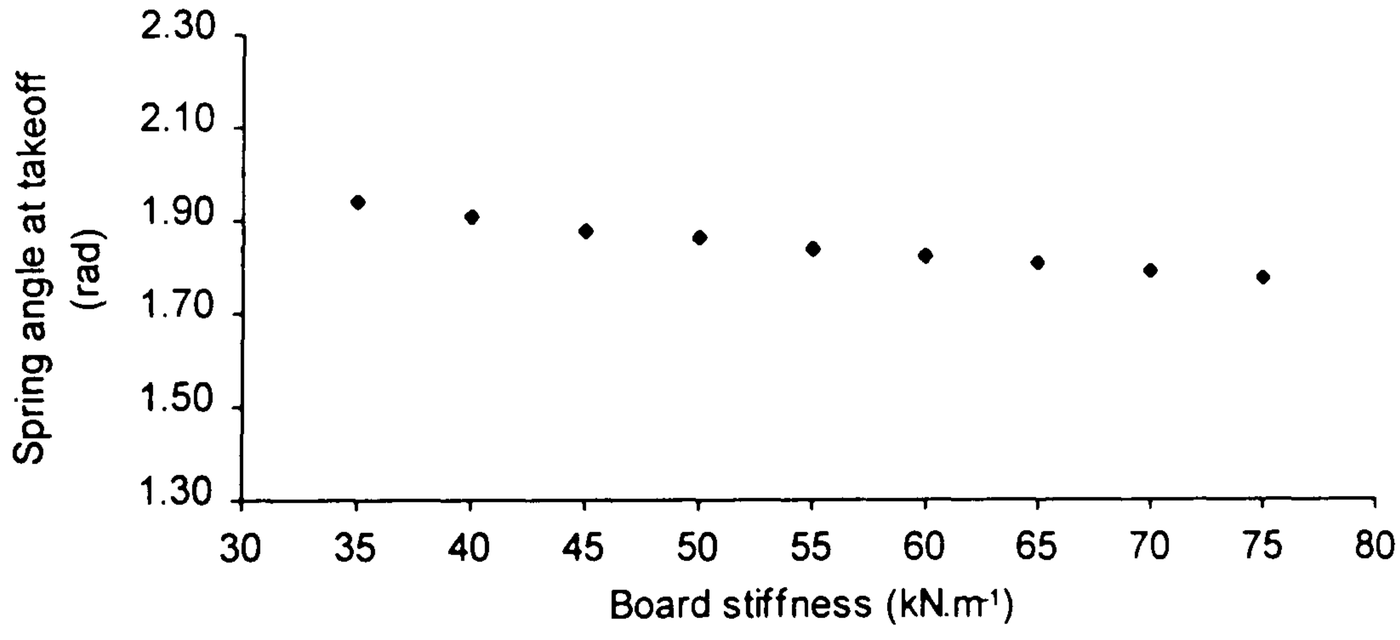

Figure 6.1. The effect of altering board stiffness on the takeoff conditions of the two spring model.
(Leg stiffness: 125 $kN.m^{-1}$; board damping: 155 $N.s.m^{-1}$; other inputs: mean of trials one to five).

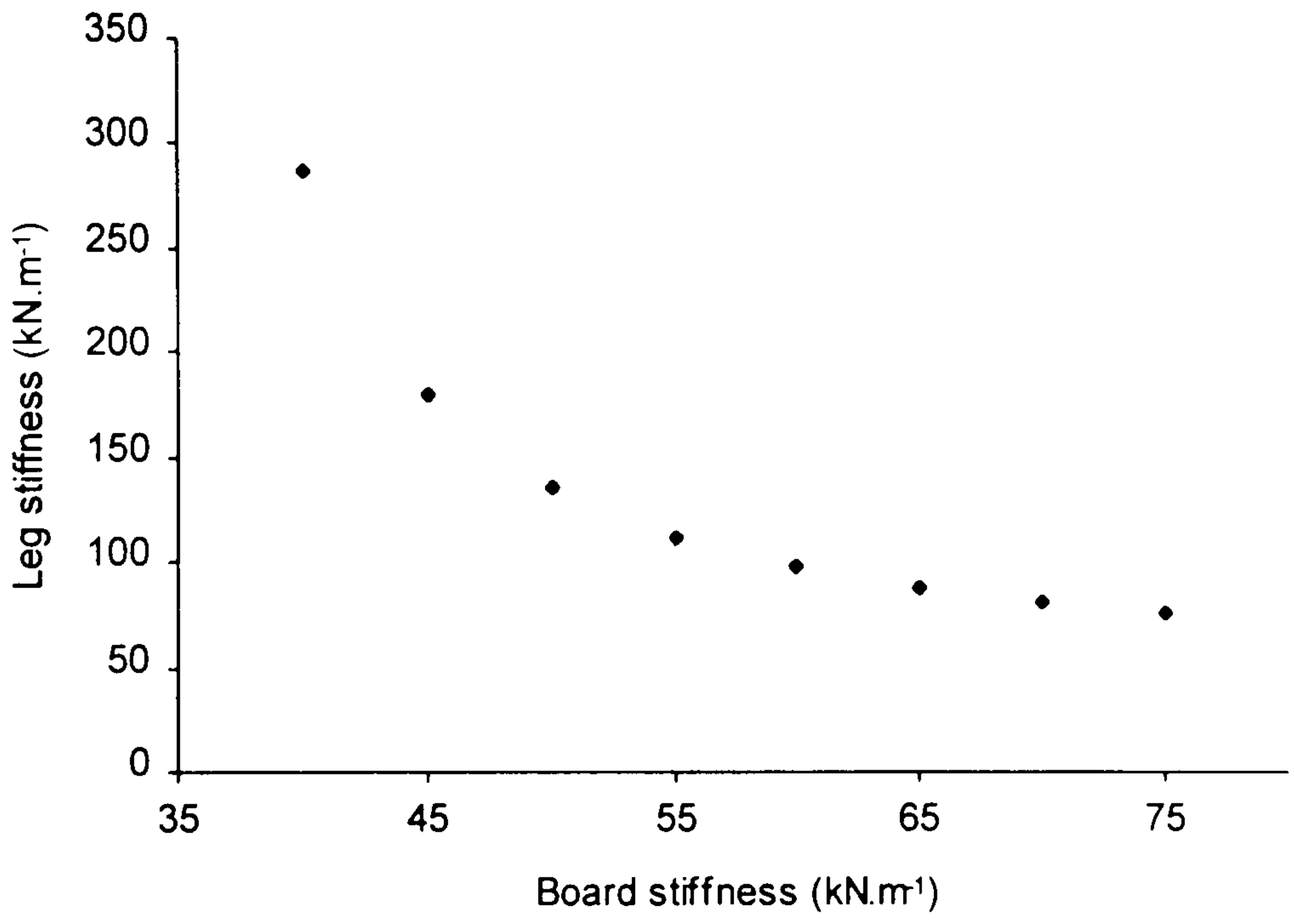

Figure 6.2. Changes to leg spring stiffness in order to compensate for board stiffness alterations.
(Board damping: 155 N.s.m^{-1}; other inputs: mean of trials one to five).

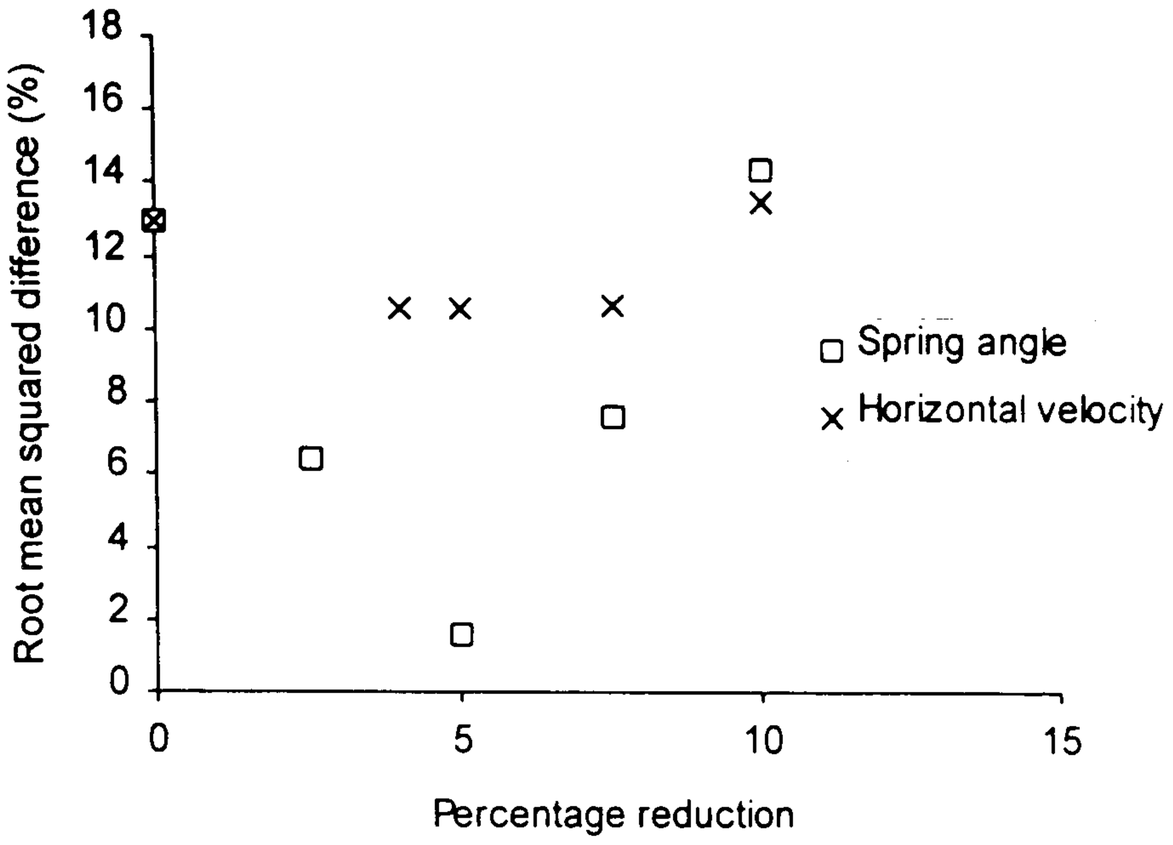

Figure 6.3. The effect on takeoff conditions of reducing the touchdown spring angle or horizontal velocity to compensate for a board stiffness reduction from 58 $kN.m^{-1}$ to 37.5 $kN.m^{-1}$.

(Root mean squared difference calculated with respect to the original simulation with board stiffness of 58 $kN.m^{-1}$. Leg stiffness: 103.125 $kN.m^{-1}$; board damping: 155 $N.s.m^{-1}$; other inputs: mean of trials one to five).

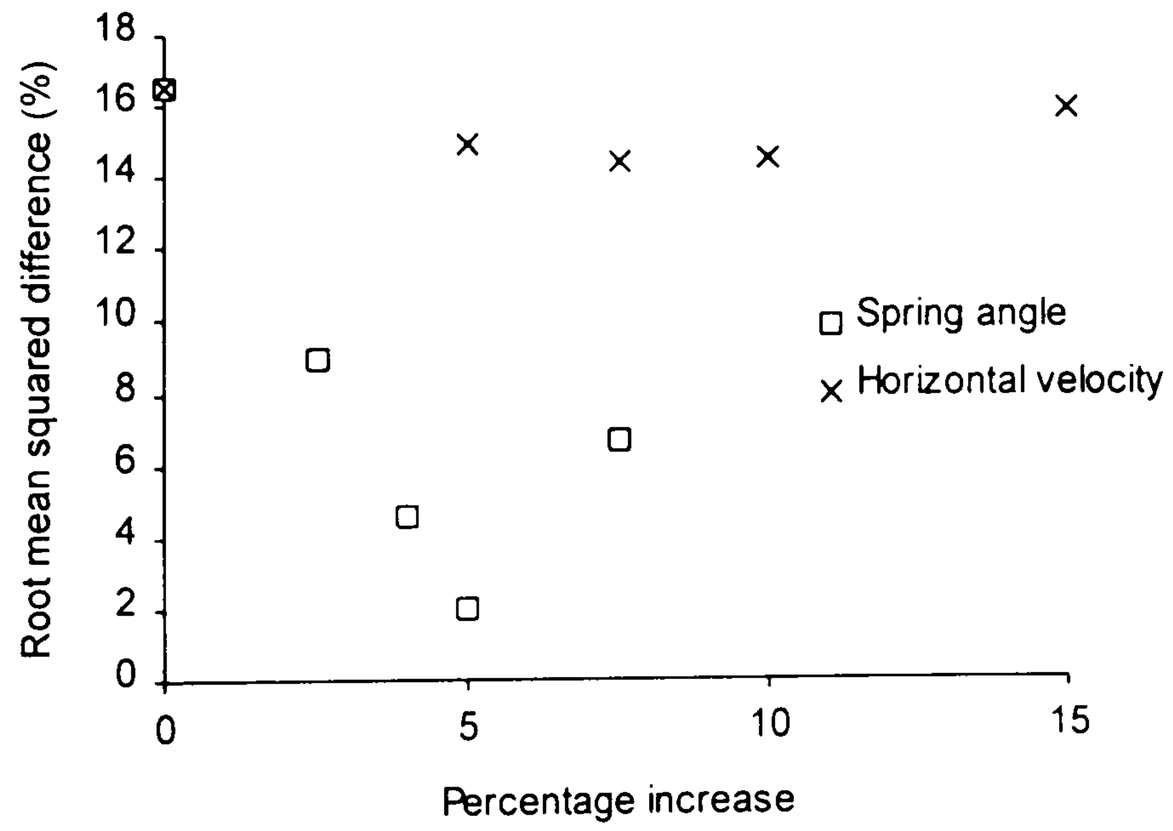

Figure 6.4. The effect on takeoff conditions of increasing the touchdown spring angle or horizontal velocity to compensate for a board stiffness increase from 37.5 $kN.m^{-1}$ to 58 $kN.m^{-1}$.

(Root mean squared difference calculated with respect to the original simulation with board stiffness of 37.5 $kN.m^{-1}$. Leg stiffness: 475.000 $kN.m^{-1}$; board damping: 155 $N.s.m^{-1}$; other inputs: mean of trials one to five).

the same as was required for the stiff board setting meant that in order to approach the same takeoff conditions a reduction in the touchdown horizontal velocity or spring angle was necessary. In a similar manner, increasing the board stiffness (from soft to stiff) required an increase in the touchdown velocity or angle to reduce the difference between the takeoffs. Figures 6.3 and 6.4 clearly illustrate that altering the touchdown spring angle has a much more marked effect on the takeoff conditions than alterations to the touchdown horizontal velocity. In both cases altering the touchdown spring angle by 5% resulted in the root mean squared difference (between these and the original simulation takeoff conditions) being reduced to less than 2%, while altering the touchdown horizontal velocity had only a minor effect. The comparatively small influence of touchdown velocity alterations meant that in any combined alteration of touchdown angle and velocity, the angle effect would dominate and therefore the findings would not differ substantially from those when only the angle was altered.

6.3.3 APPROACH AND CONTACT STRATEGIES

The approach and contact strategies which could be adopted by gymnasts were investigated for both the one and two spring models. The effects of adjusting the horizontal velocity at touchdown (from 6.30 to 8.67 $m.s^{-1}$), the spring angle at touchdown (from 0.89 to 1.23 radians for the one spring model and 0.90 to 1.24 radians for the two spring model) and the (leg) spring stiffness (from 30 to 50 $kN.m^{-1}$ for the one spring model and 80 to 290 $kN.m^{-1}$ for the two spring model) are summarized in Figures 6.5 to 6.10. In each case inputs other than the one of interest were held constant (at the mean values from trials one to five), including the board stiffness (58 $kN.m^{-1}$) and damping (155 $N.s.m^{-1}$) for the two spring model. To assist comparisons between the same dependent variable in each different figure, the scaling of the ordinate of the graphs is consistent for each dependent variable. With the exception of Figures 6.6c and 6.9c, the range on the ordinate of each of the graphs is (to one decimal place) from 50% to 100% of the maximum value found across all six sets of data for each dependent variable. For example the maximum takeoff angular velocity was 7.29 $rad.s^{-1}$ (in Figure 6.8a) so the range on all six angular velocity graphs is from 3.6 to 7.3 $rad.s^{-1}$. Figures 6.6c and 6.9c are exceptions due to the much greater variation in the vertical velocity at takeoff as a result of touchdown spring angle adjustments, therefore three times the range of the other vertical velocity graphs was used.

Comparing the effects of the adjustments between the one and two spring models it was immediately apparent that the influence of each input was broadly similar whether the one or two spring model was used (compare Figures 6.5 and 6.8, 6.6 and 6.9, 6.7 and 6.10). The

(a)

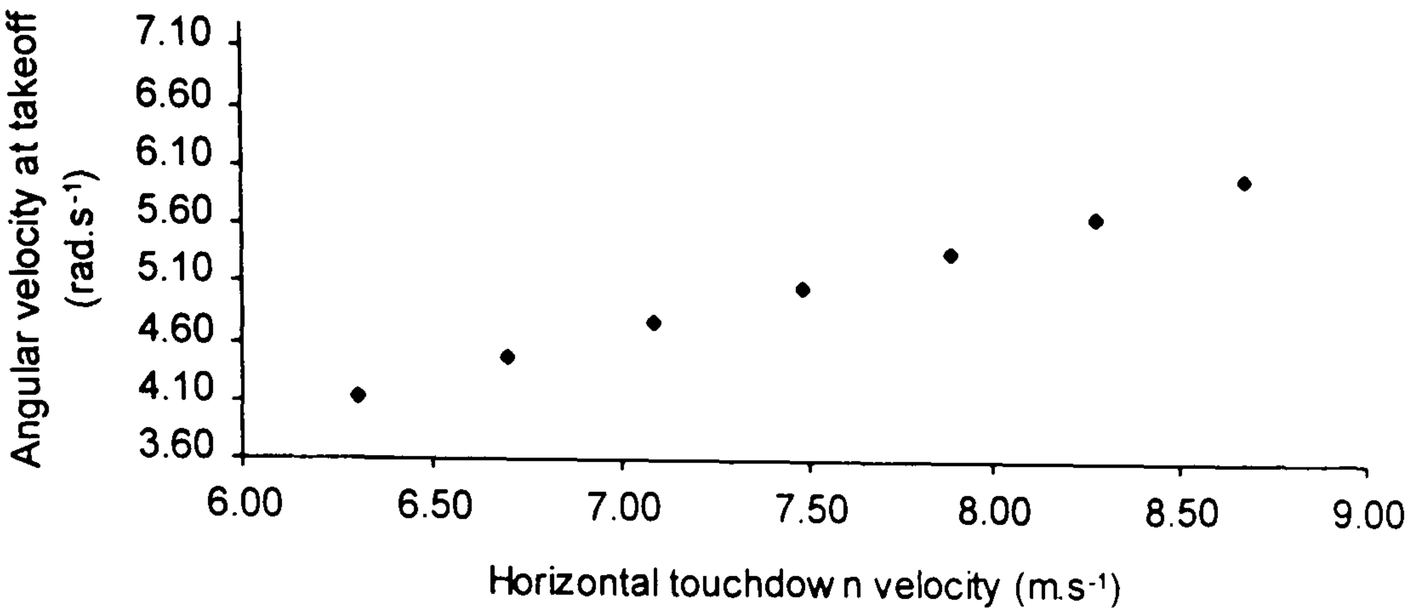

(b)

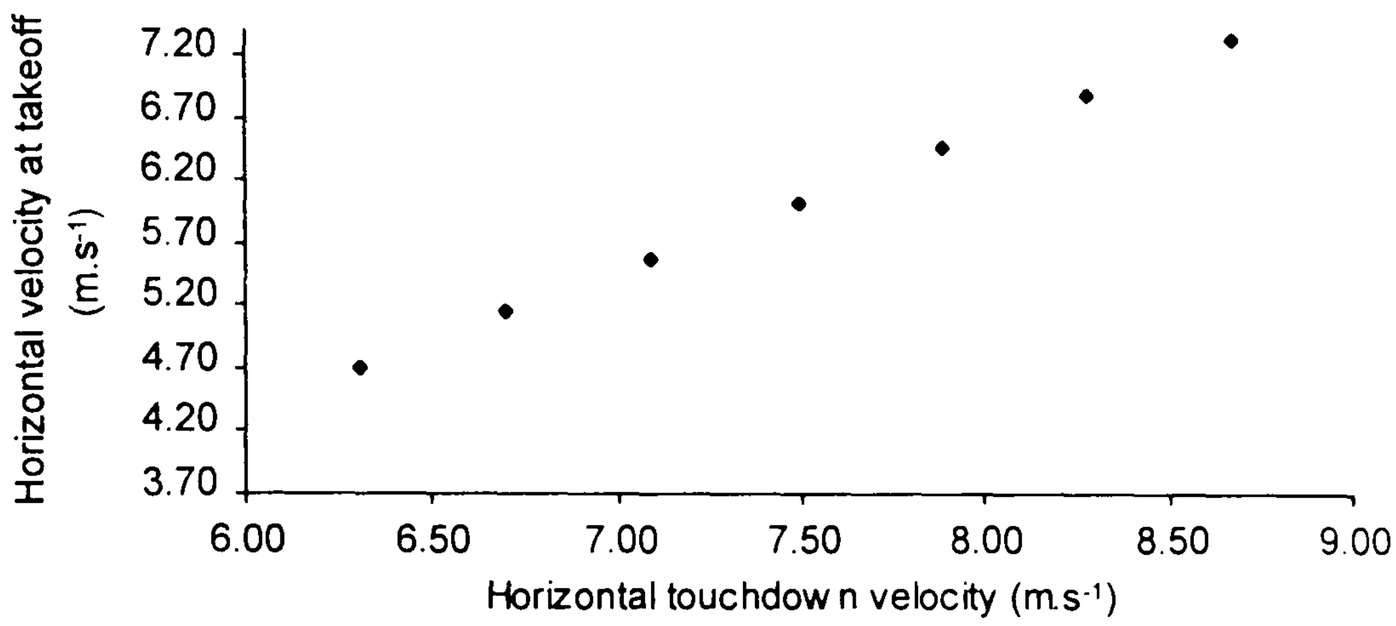

(c)

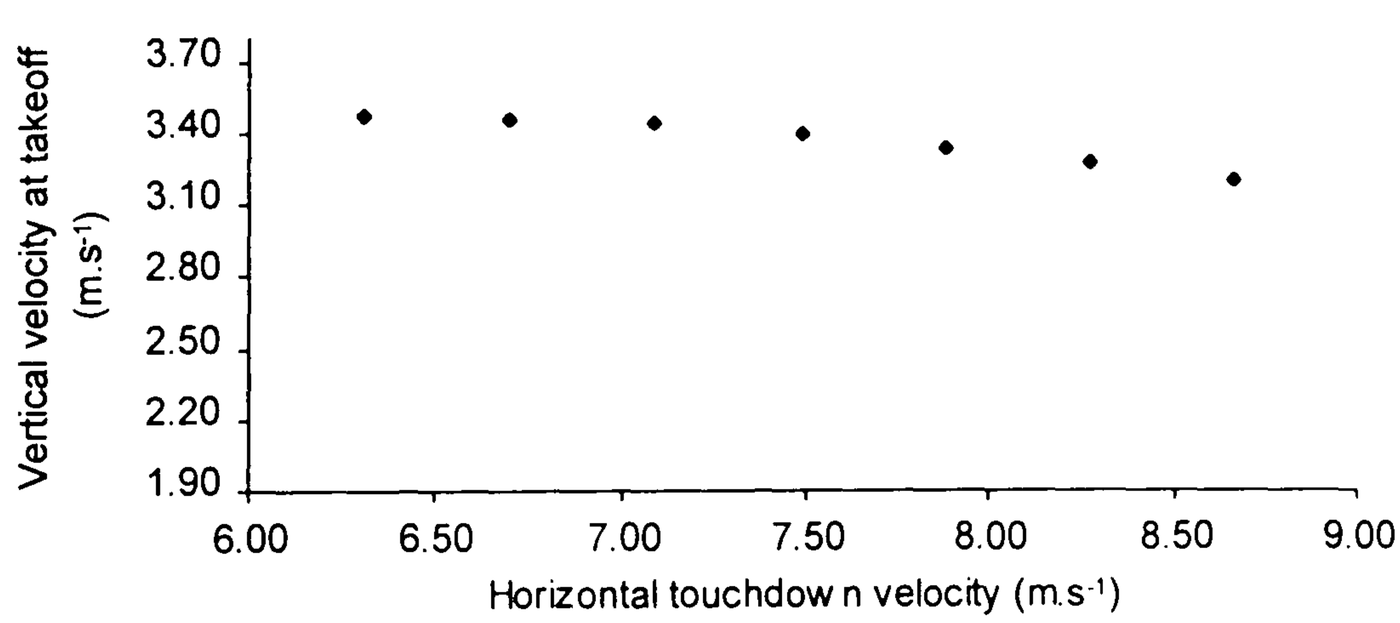

(d)

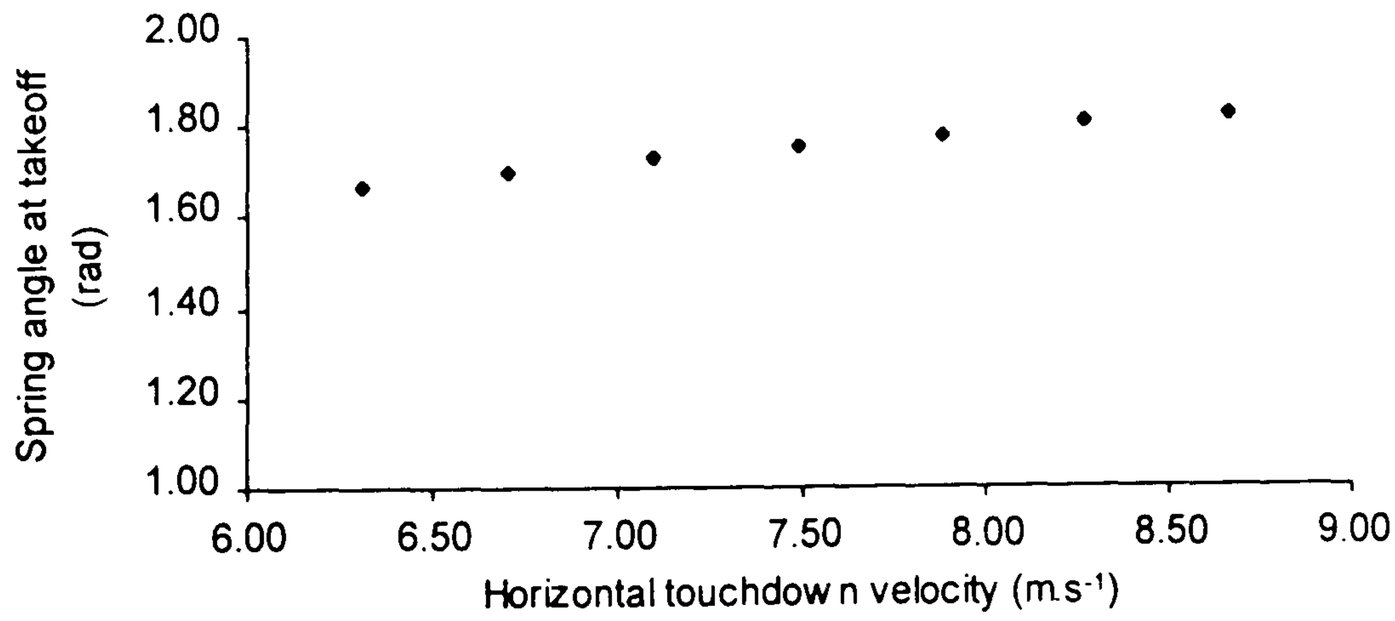

Figure 6.5. The effect of varying the touchdown horizontal velocity on the takeoff conditions of the one spring model.

(a)

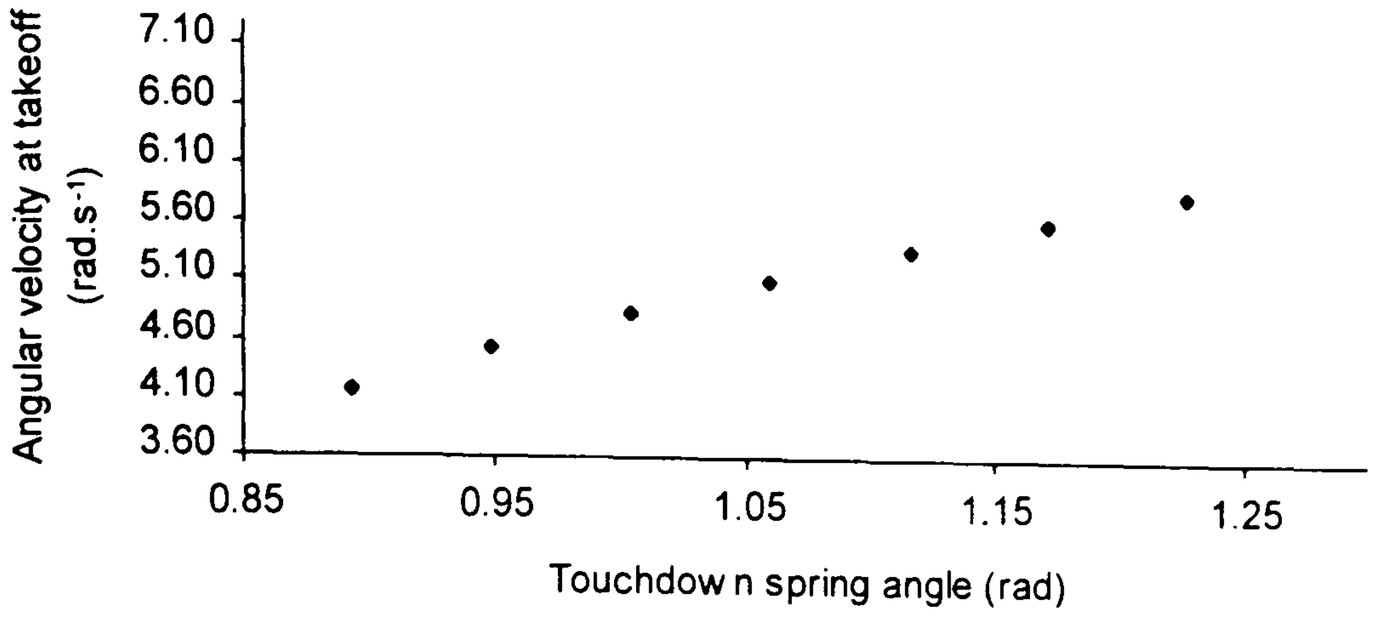

(b)

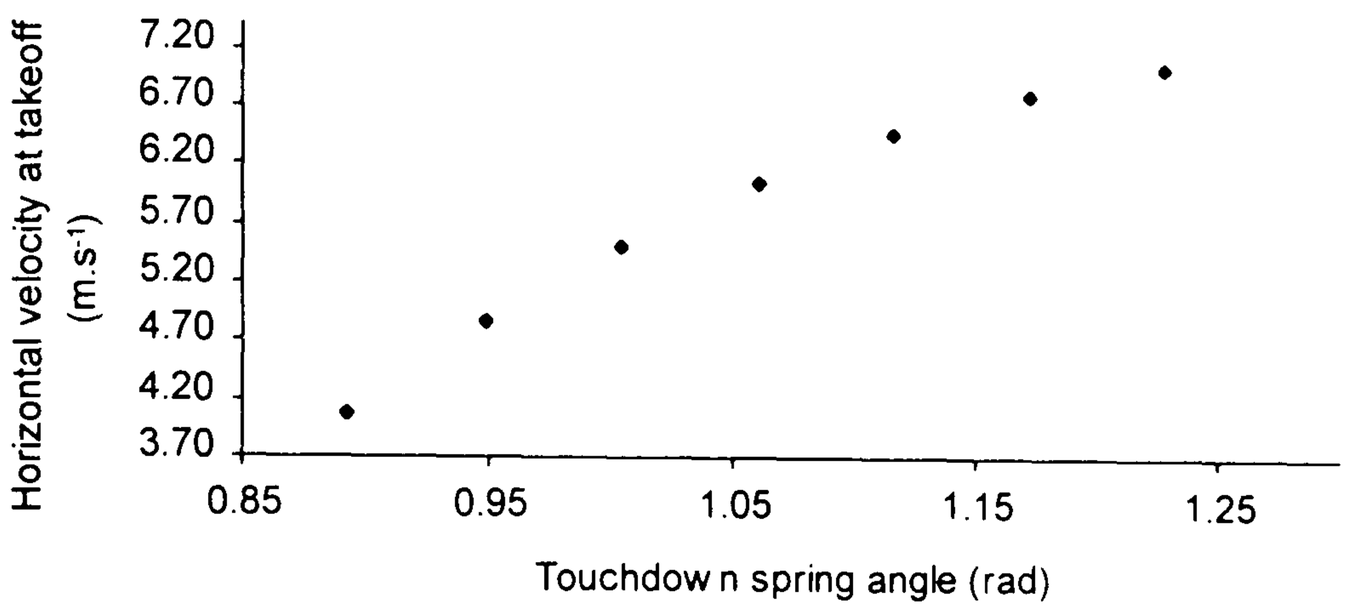

(c)

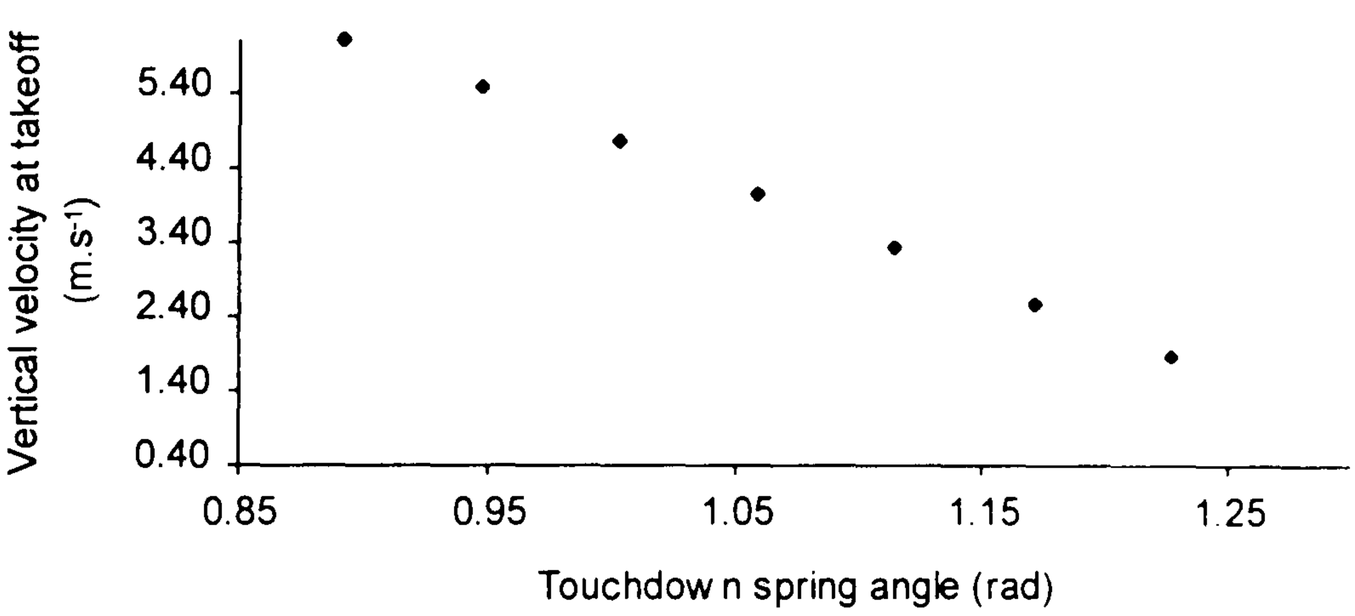

(d)

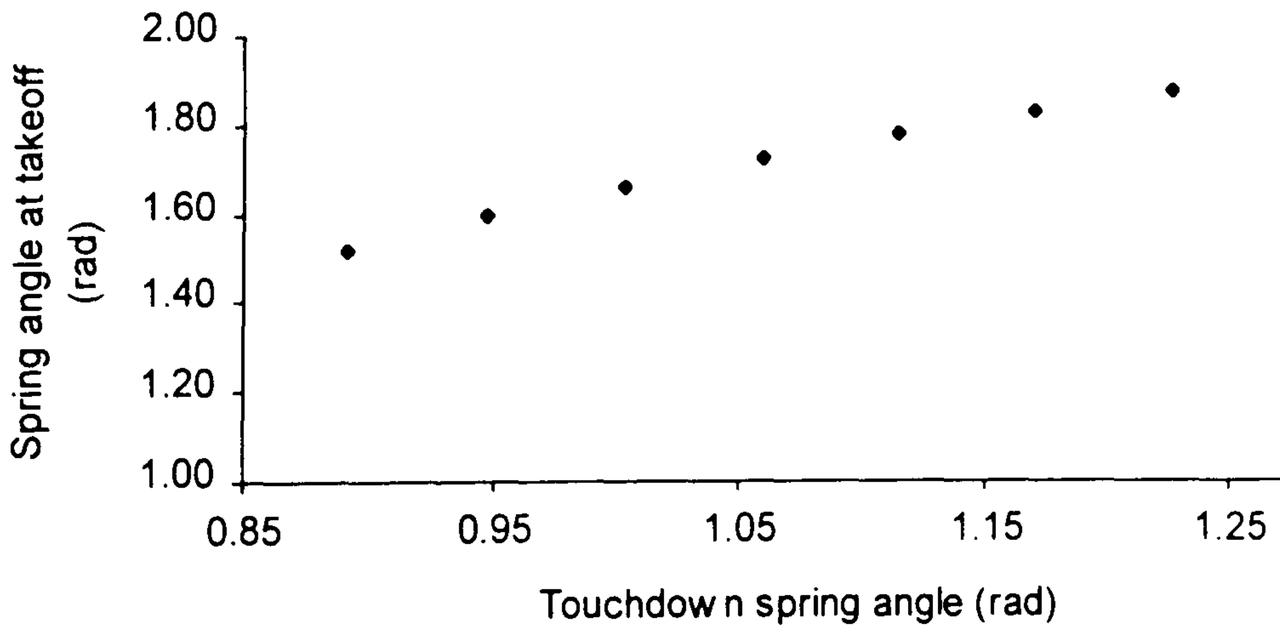

Figure 6.6. The effect of varying the touchdown spring angle on the takeoff conditions of the one spring model.
N.B. In relation to the other graphs, the ordinate scale in graph (c) is three times larger.
A larger spring angle at touchdown indicates a more upright position.

(a)

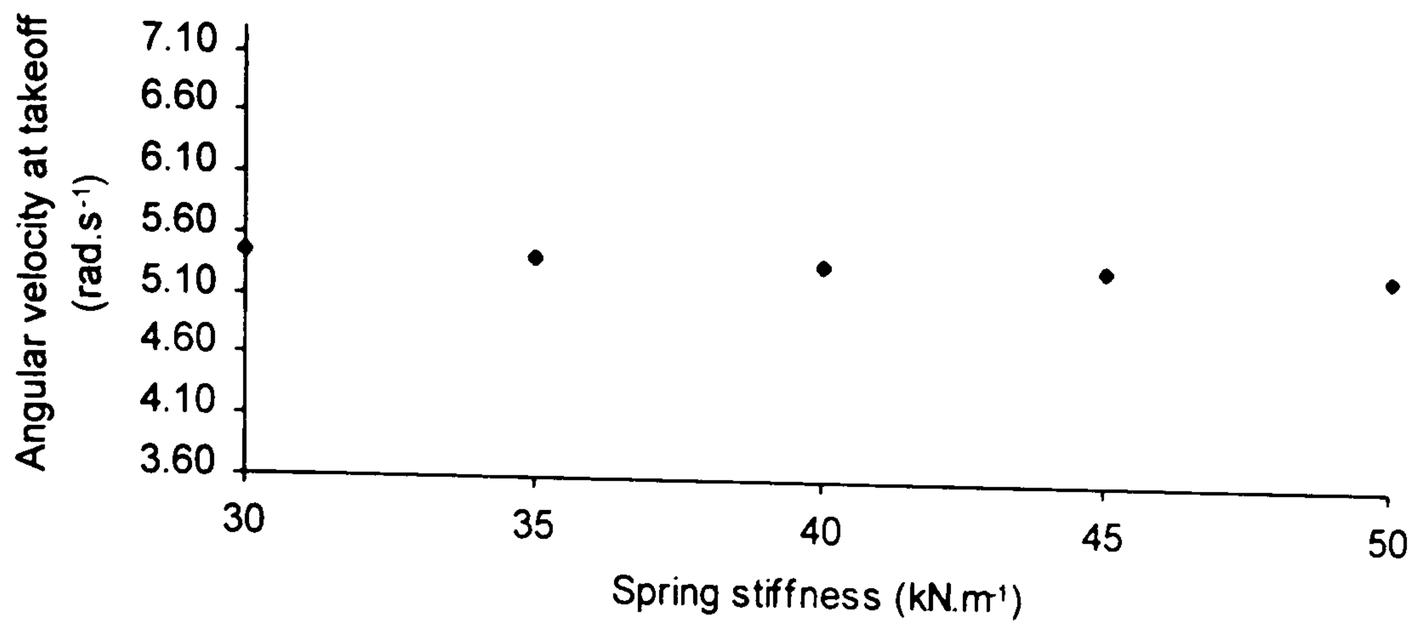

(b)

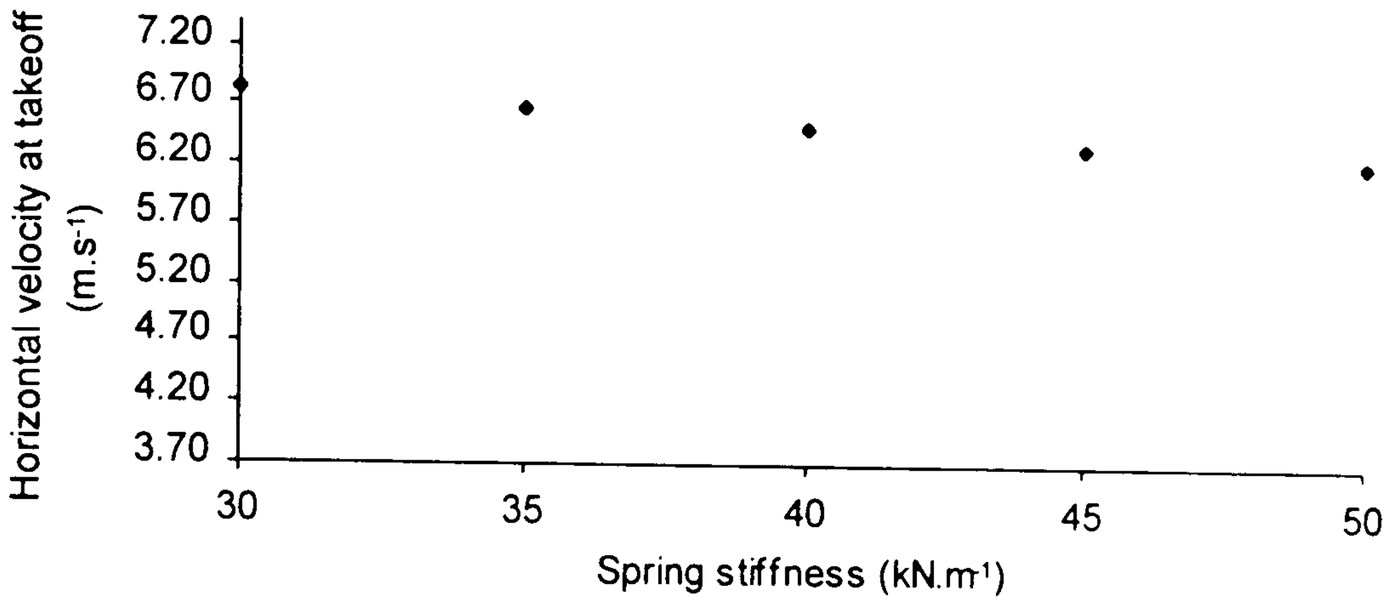

(c)

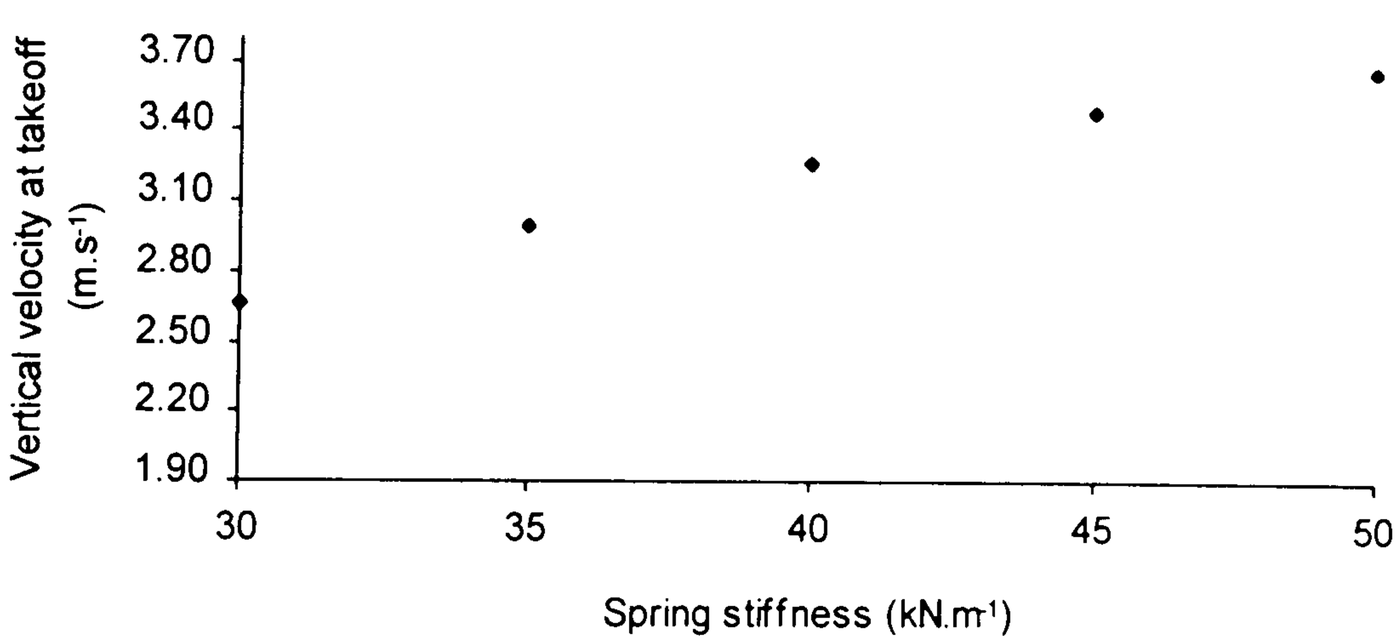

(d)

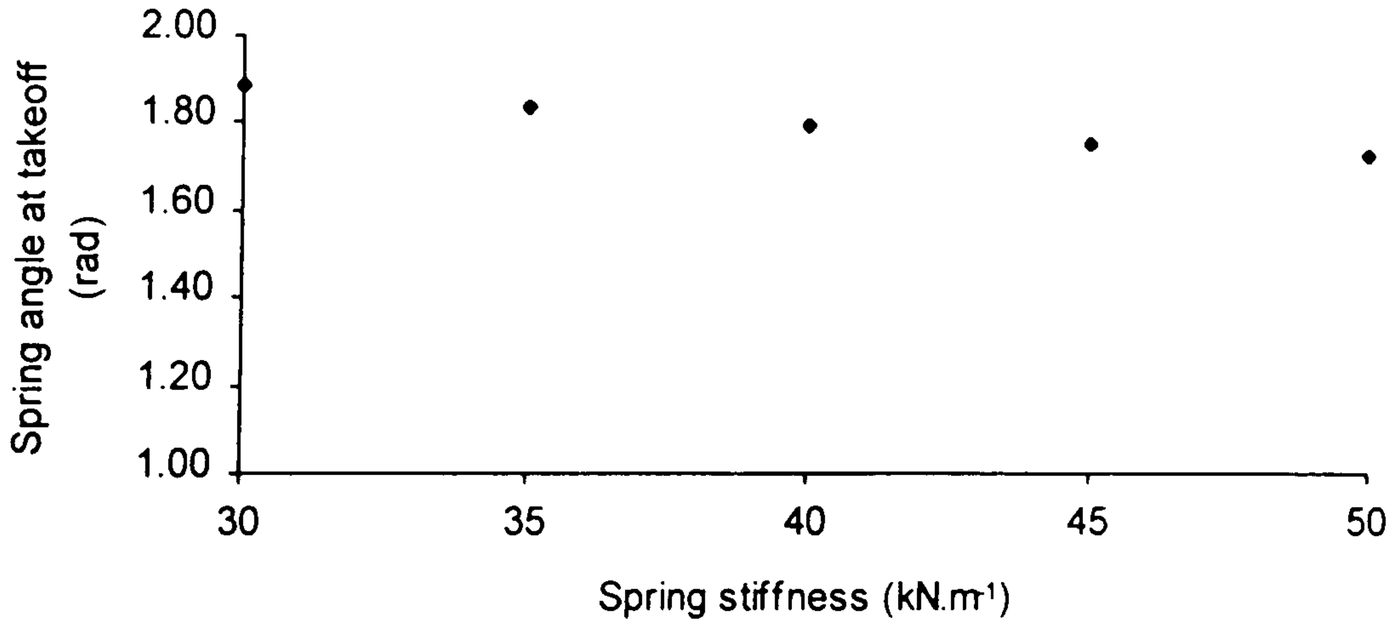

Figure 6.7. The effect of varying the spring stiffness on the takeoff conditions of the one spring model.

(a)

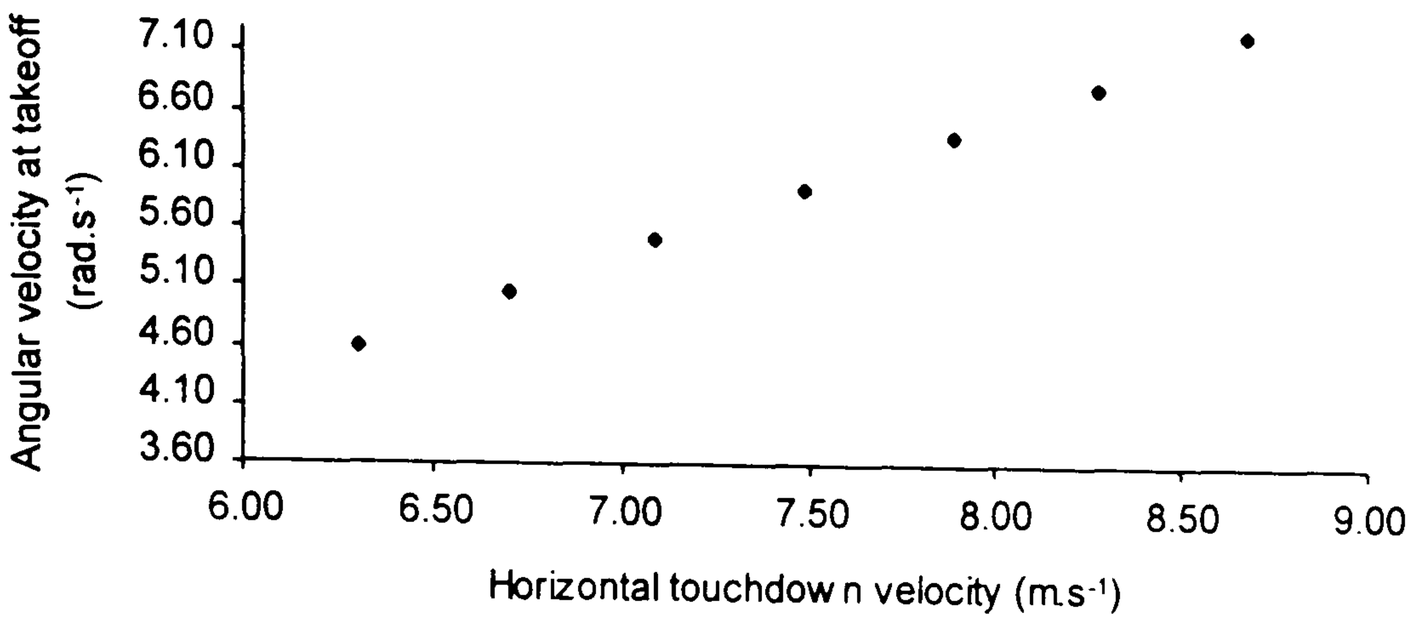

(b)

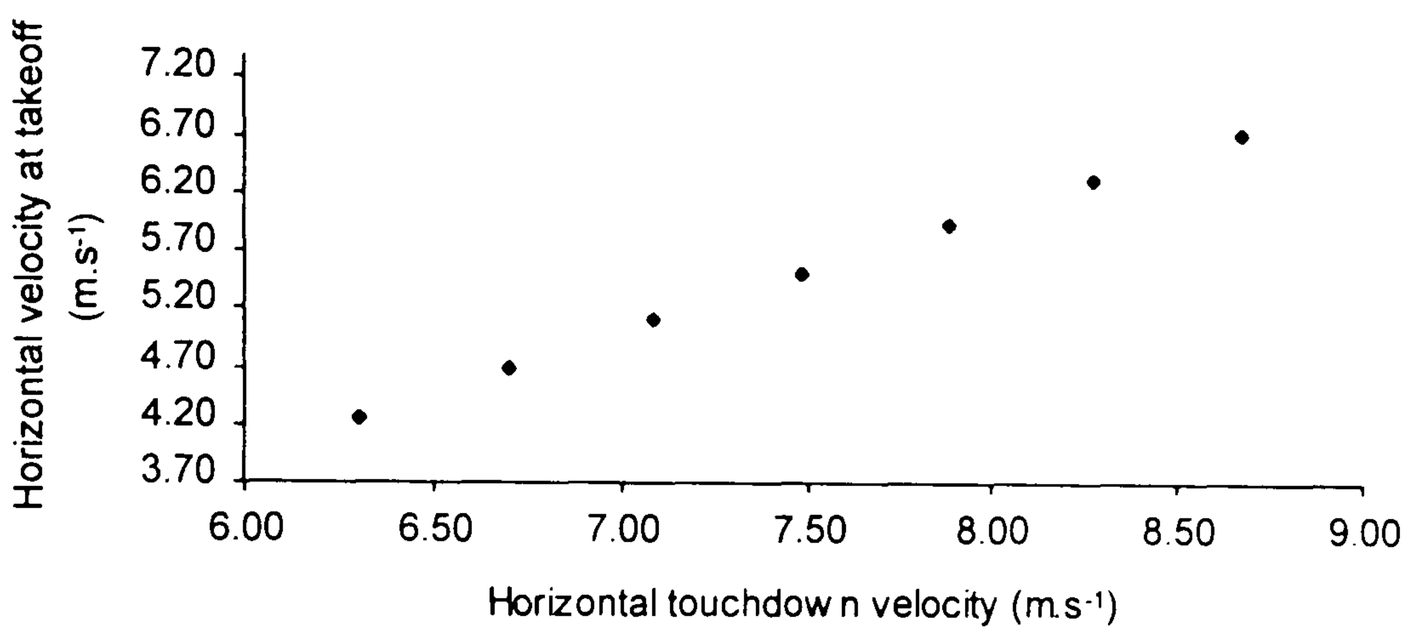

(c)

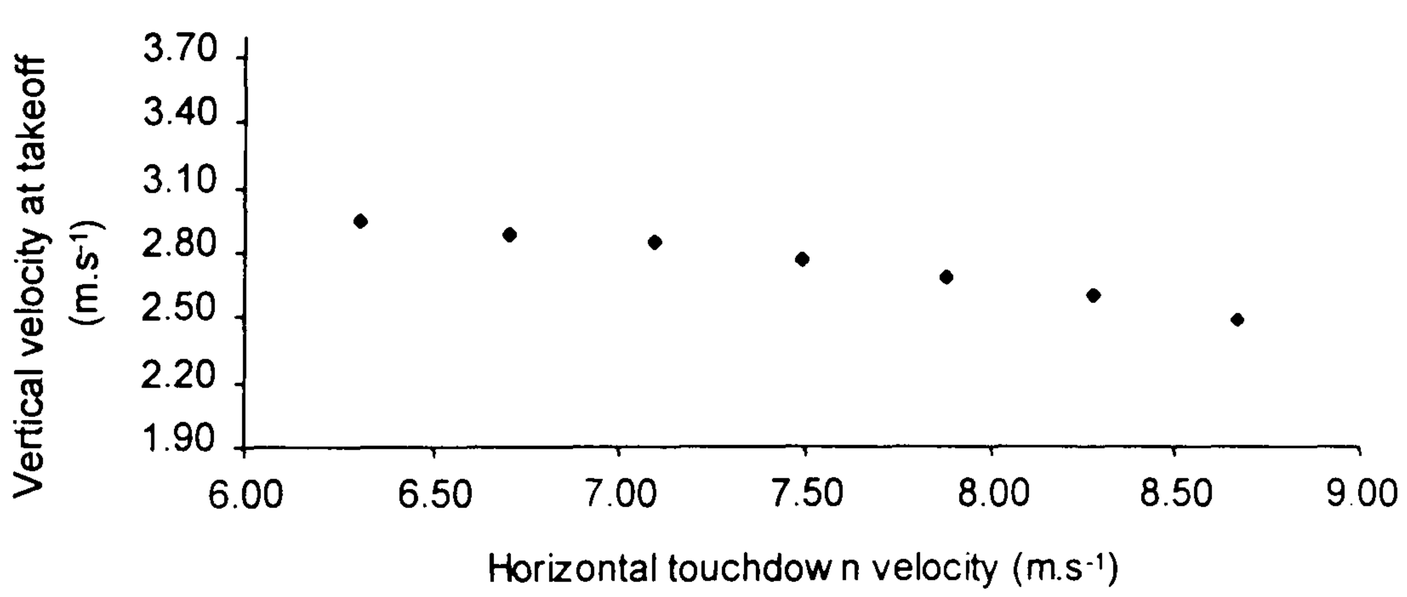

(d)

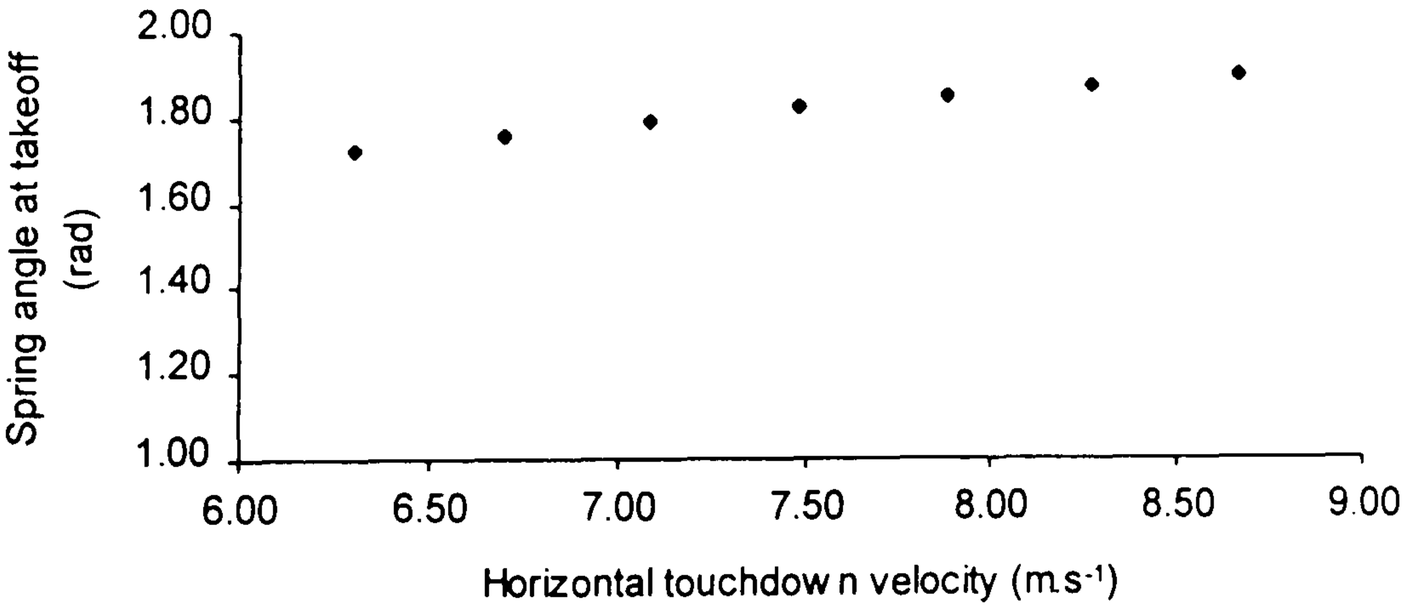

Figure 6.8. The effect of varying the touchdown horizontal velocity on the takeoff conditions of the two spring model.

(a)

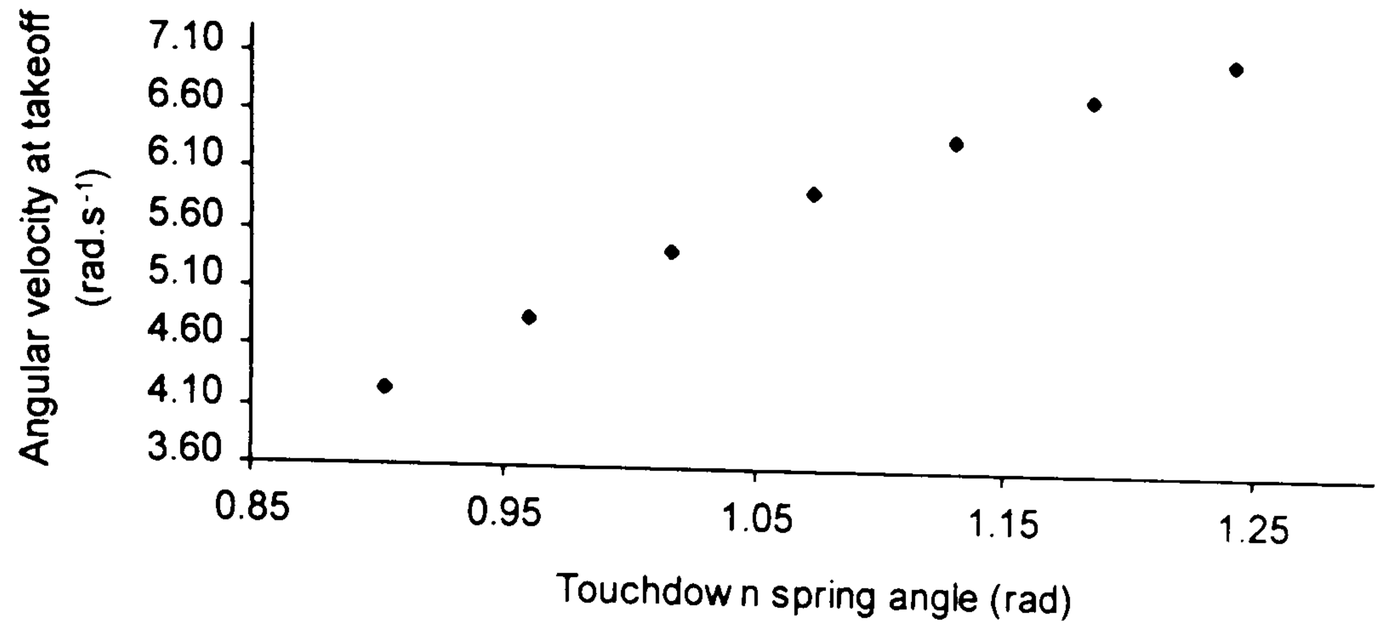

(b)

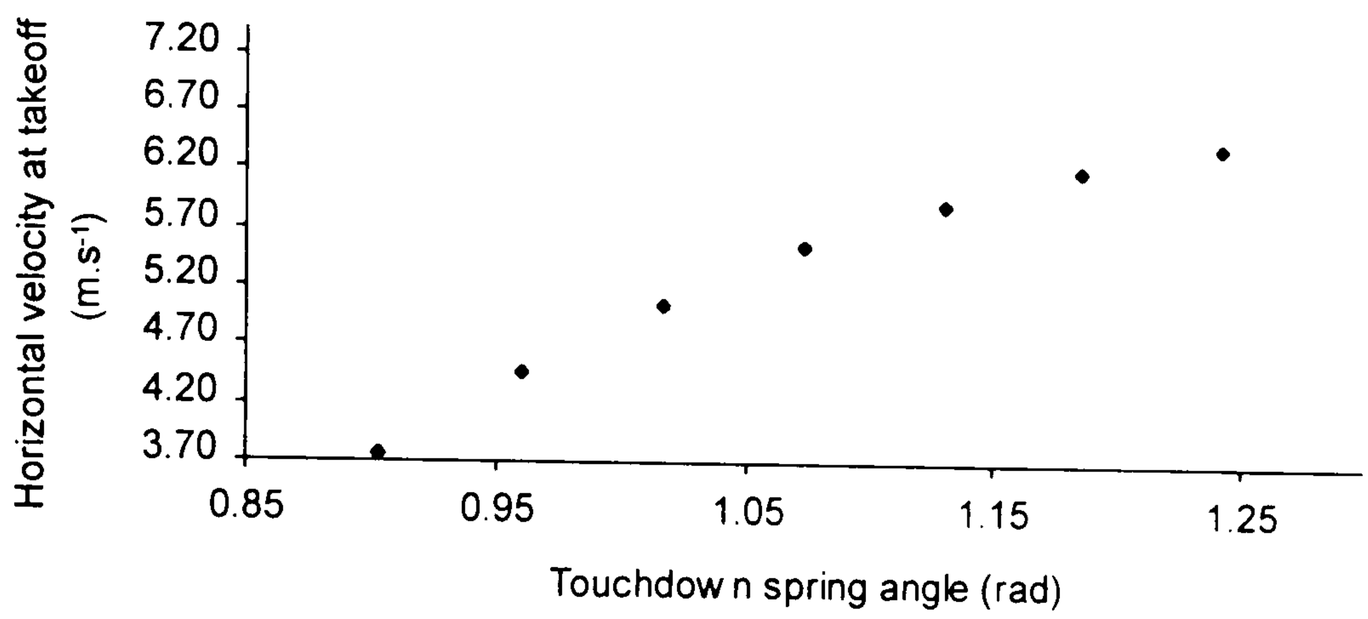

(c)

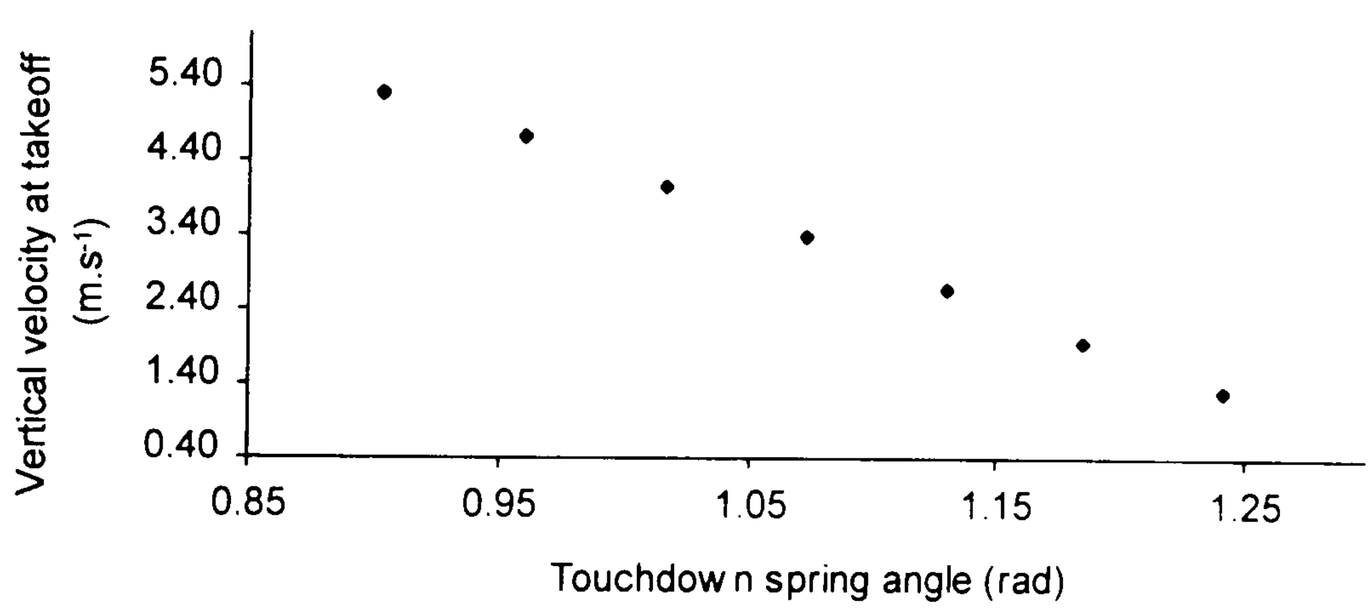

(d)

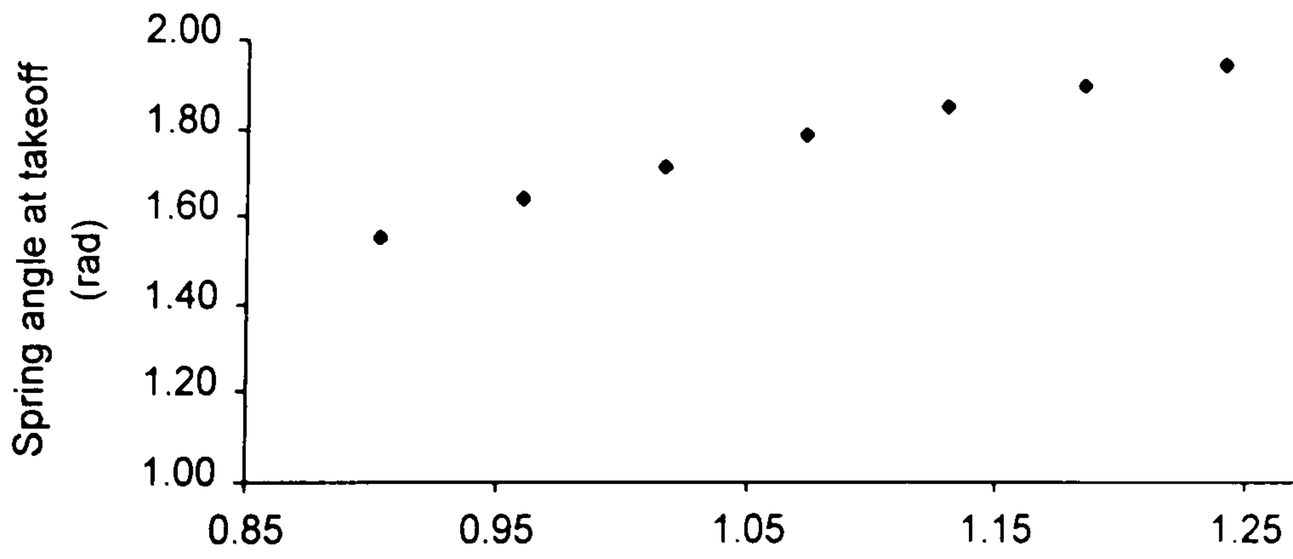

Figure 6.9. The effect of varying the touchdown spring angle on the takeoff conditions of the two spring model.
N.B. In relation to the other graphs, the ordinate scale in graph (c) is three times larger.
A larger spring angle at touchdown indicates a more upright position.

(a)

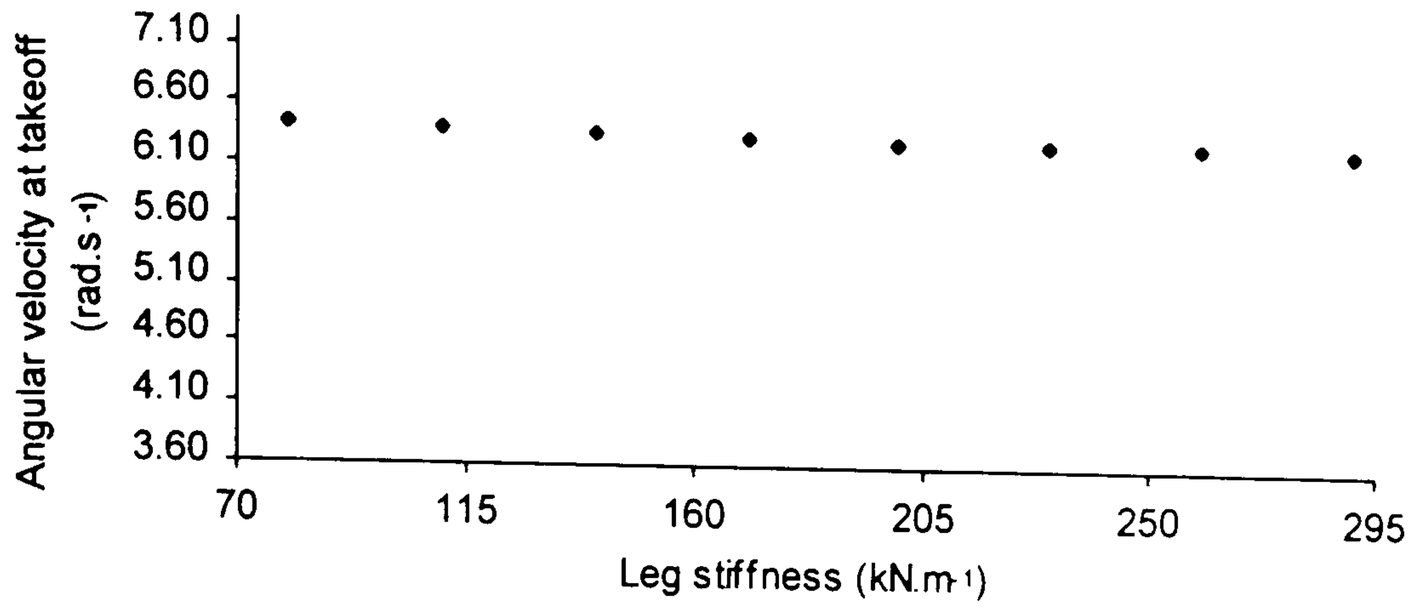

(b)

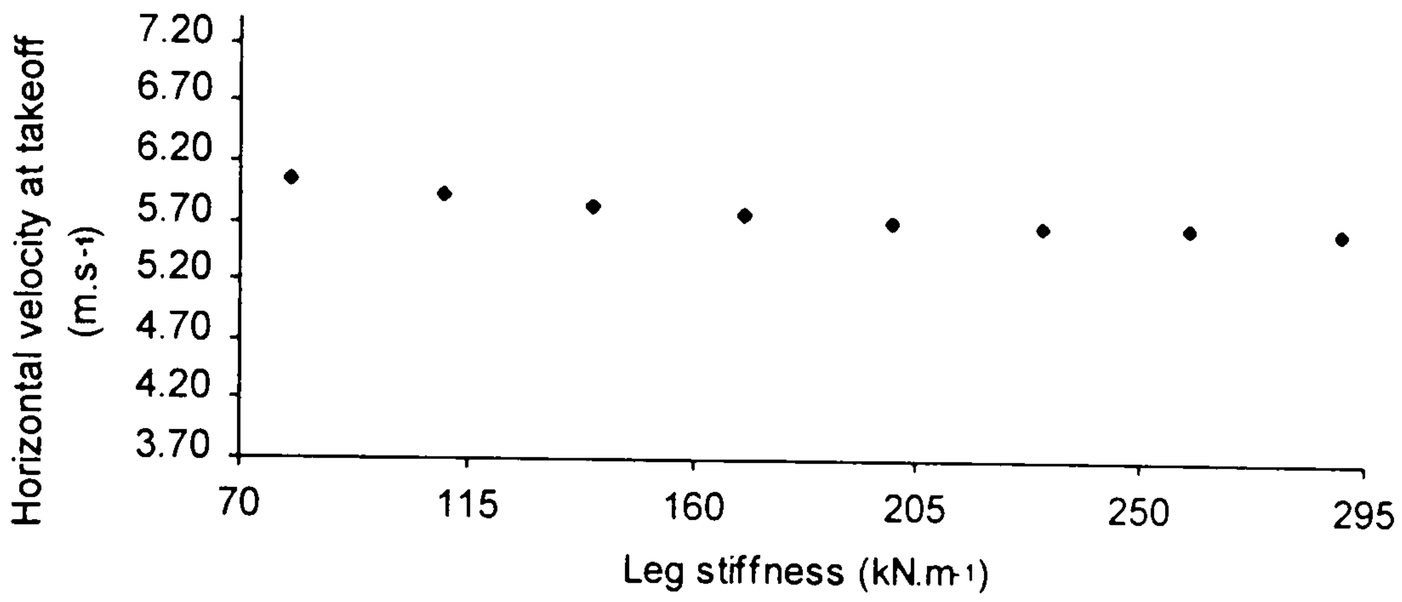

(c)

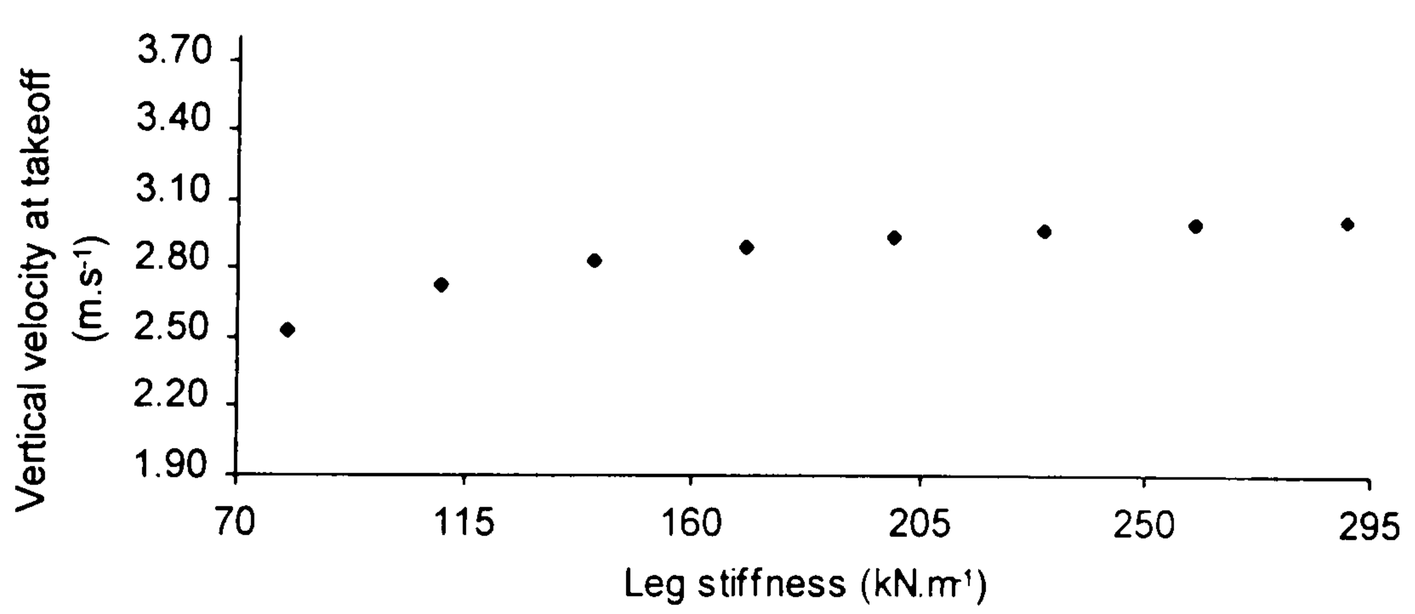

(d)

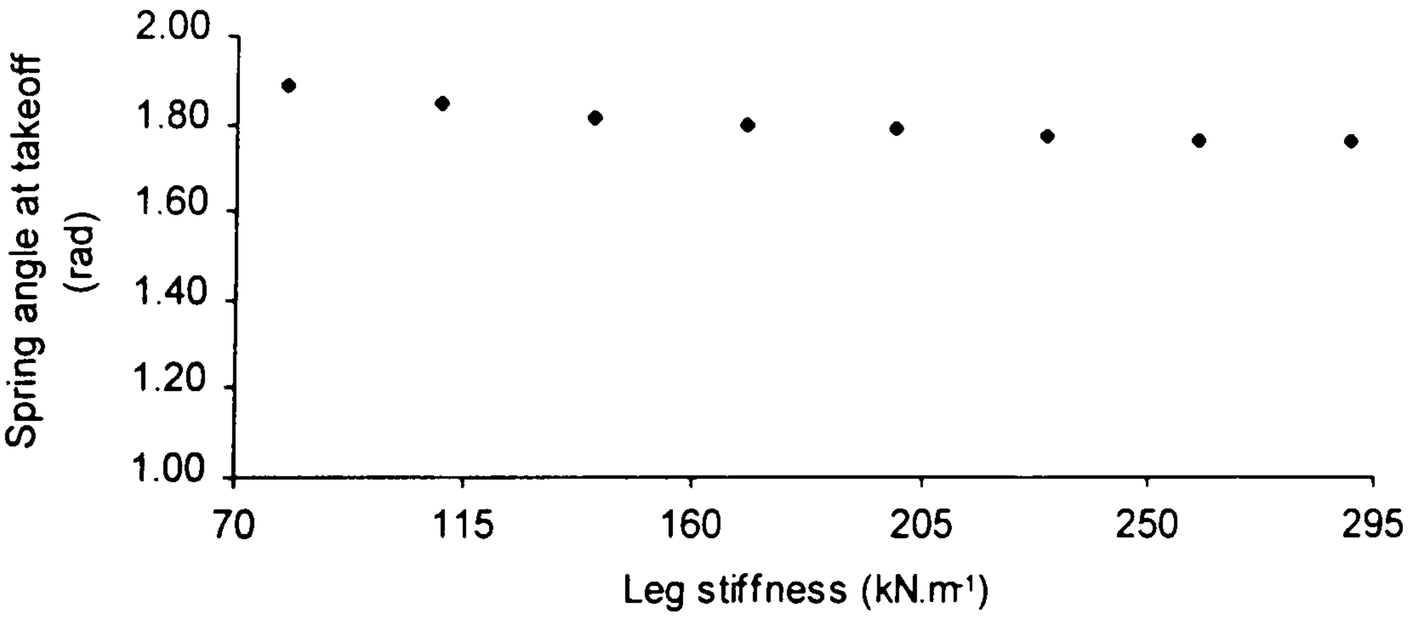

Figure 6.10. The effect of varying the leg spring stiffness on the takeoff conditions of the two spring model.

direction, rate and general magnitudes of the effects of the variations were remarkably similar between models. The vertical velocity at takeoff began to plateau at high leg stiffnesses in the two spring model, otherwise the differences between models were in the precise magnitudes of the angular and linear velocities at takeoff: the one spring model produced greater horizontal and vertical velocities, while the two spring model produced greater angular velocities.

For both models, altering the (leg) spring stiffness produced the smallest effects of the three inputs on the takeoff conditions, with only vertical velocity of the one spring model at takeoff showing a really noticeable change (Figure 6.7c). Even then, the size of the increase in vertical velocity was not as great as when the touchdown spring angle was altered, vertical velocity being greatest for the smallest touchdown spring angles (Figure 6.6c). This inverse relationship between touchdown spring angle and vertical velocity at takeoff was also apparent in the two spring model simulations (Figure 6.9c). Increases to the horizontal velocity and touchdown spring angle markedly increased both the angular and horizontal velocities at takeoff for the one spring and two spring models alike (graphs a and b in Figures 6.5, 6.6, 6.8 and 6.9). Only the touchdown spring angle had a very noticeable effect on the takeoff spring angle, but for neither model was this as great as the effect on other variables (Figures 6.6d and 6.9d).

Having found that the horizontal velocity and spring angle at touchdown showed the greatest potential for modifying takeoff, the effects of varying these inputs simultaneously was examined. The touchdown spring angle was again varied from 0.90 to 1.24 radians for the two spring model and 0.89 to 1.23 radians for the one spring model, and three touchdown horizontal velocities were used: 7.88 $m.s^{-1}$, 7.09 $m.s^{-1}$ (7.88-10%) and 8.67 $m.s^{-1}$ (7.88+10%). In Figures 6.11 and 6.12, the takeoff variables are plotted against the touchdown spring angle, with the results for each of the three touchdown horizontal velocities represented on each graph. The range on the ordinate of each of the graphs is (to one decimal place) from 15% to 100% of the maximum value found across the results from both models for each dependent variable. Once again great similarity was apparent between the results of the one and two spring model simulations and again the magnitudes of the takeoff angular velocities were slightly greater for the two spring model while the takeoff linear velocities were slightly greater for the one spring model. For both models the takeoff horizontal velocity was on average 17-18% different for each 10% change in touchdown horizontal velocity over the range of touchdown spring angles (Figures 6.11b and 6.12b). This was almost matched by the average 16% changes in takeoff angular velocity for the two spring model (Figure 6.12a), but for the one spring model the changes averaged 12% (Figure

(a)

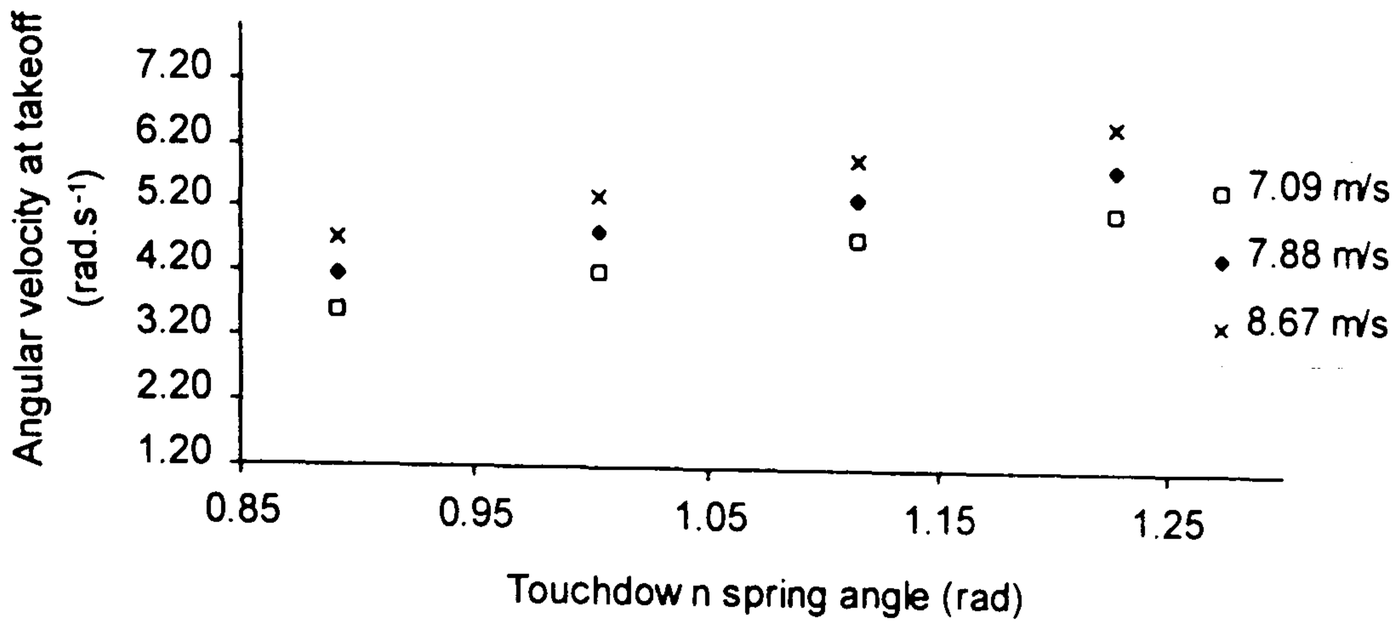

(b)

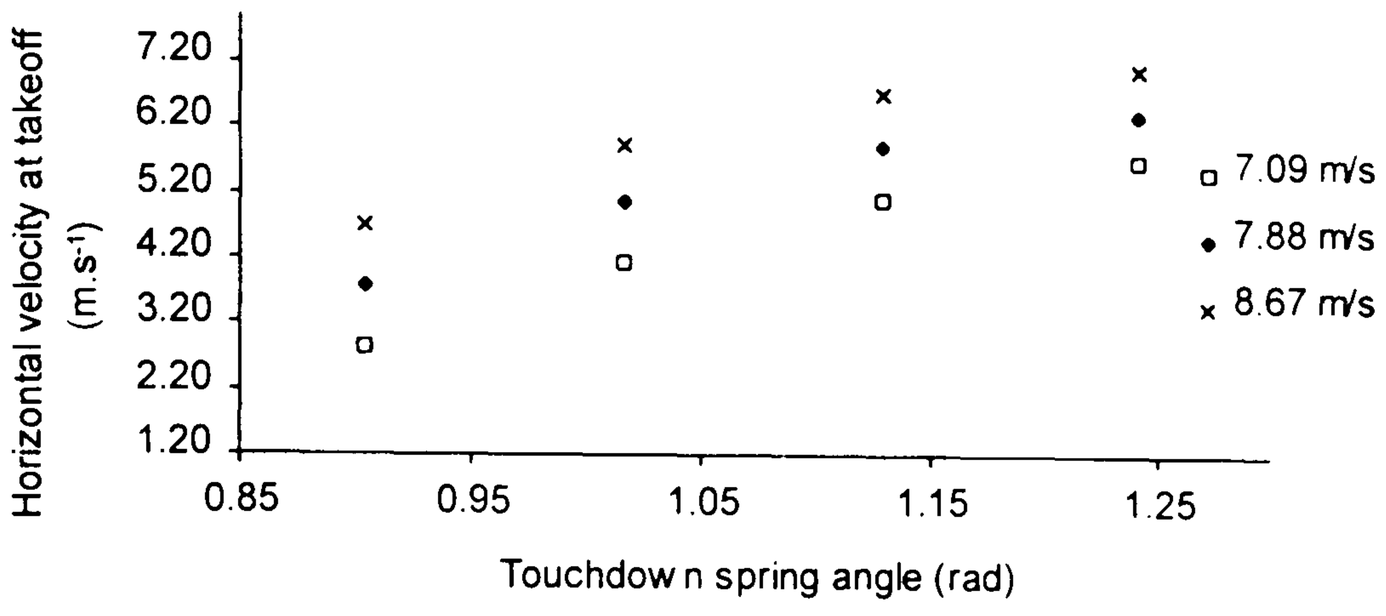

(c)

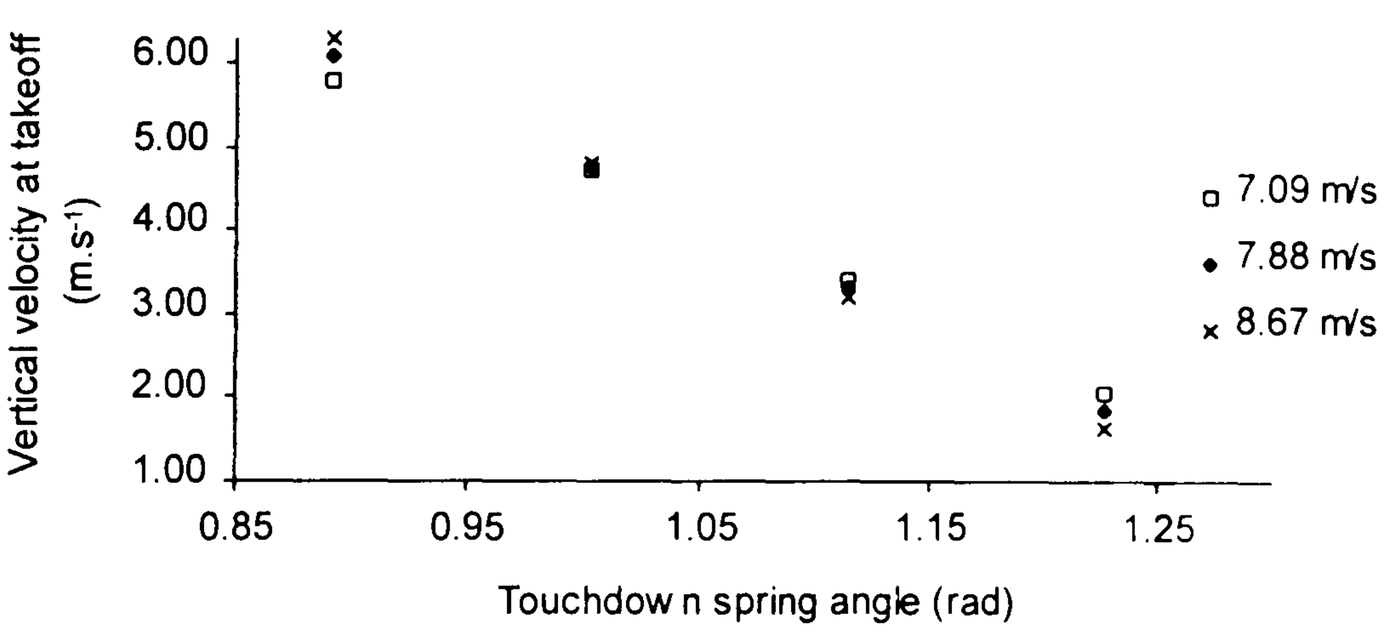

(d)

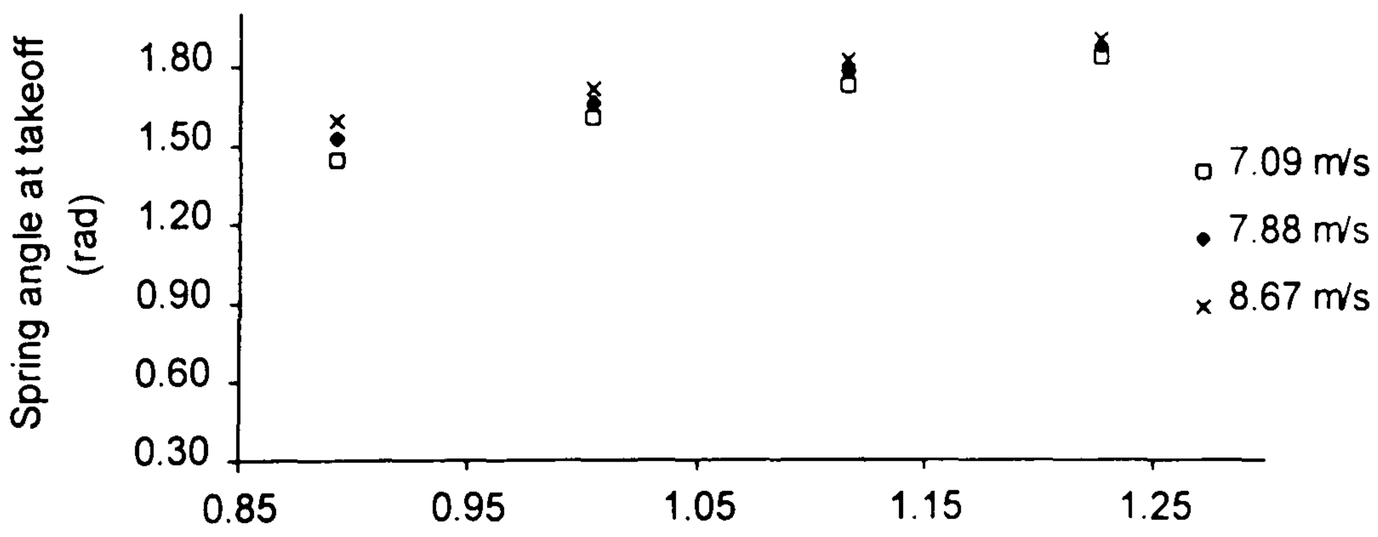

Figure 6.11. The effect of varying the spring angle and horizontal velocity at touchdown on the takeoff conditions of the one spring model.
N.B. A larger spring angle at touchdown indicates a more upright position.

(a)

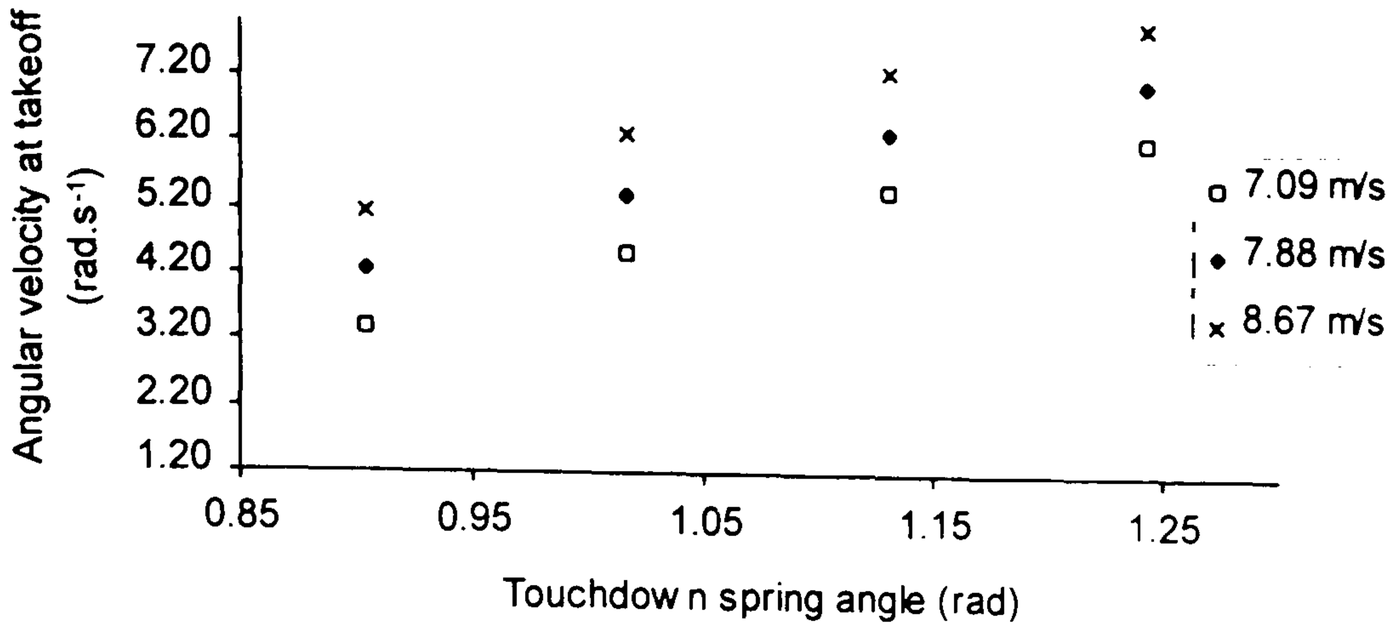

(b)

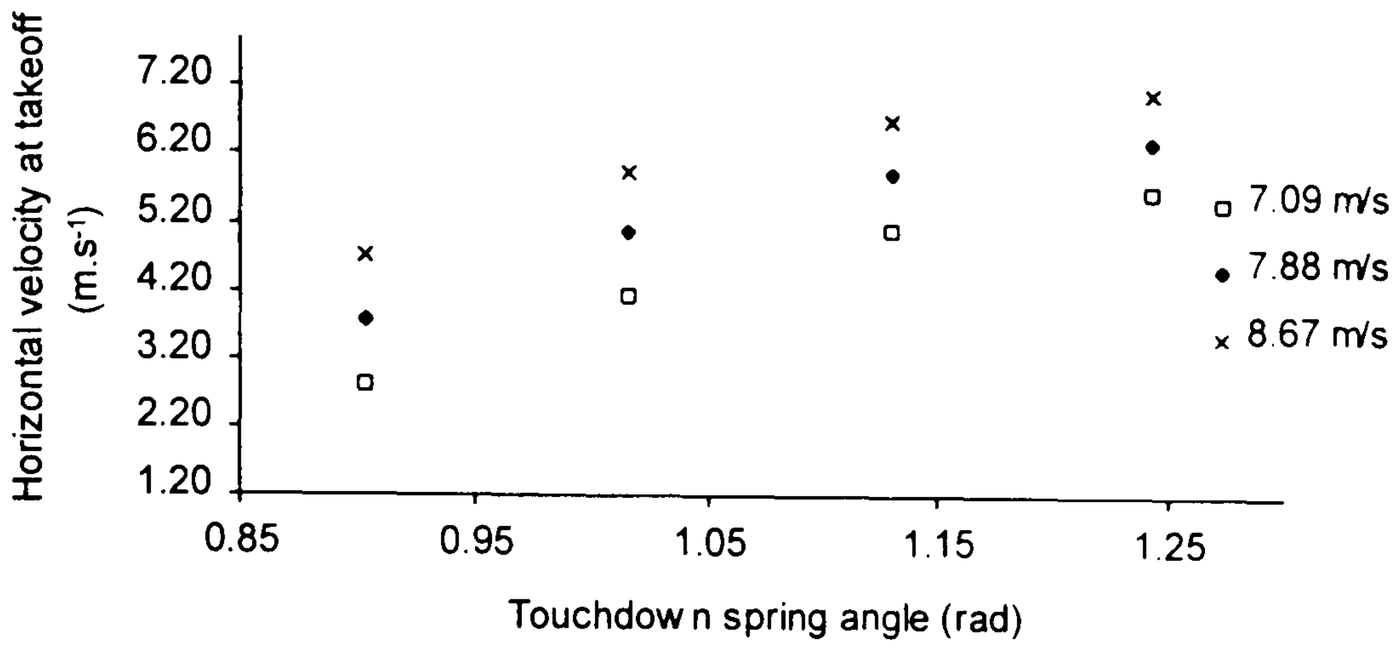

(c)

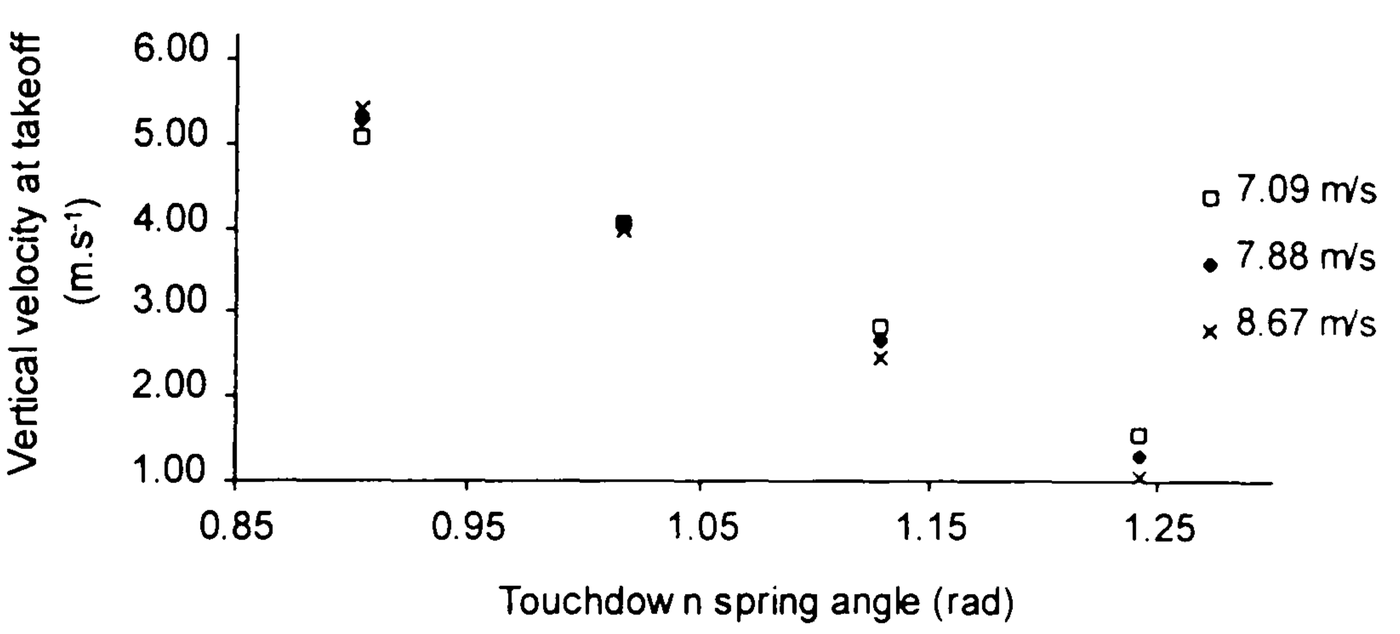

(d)

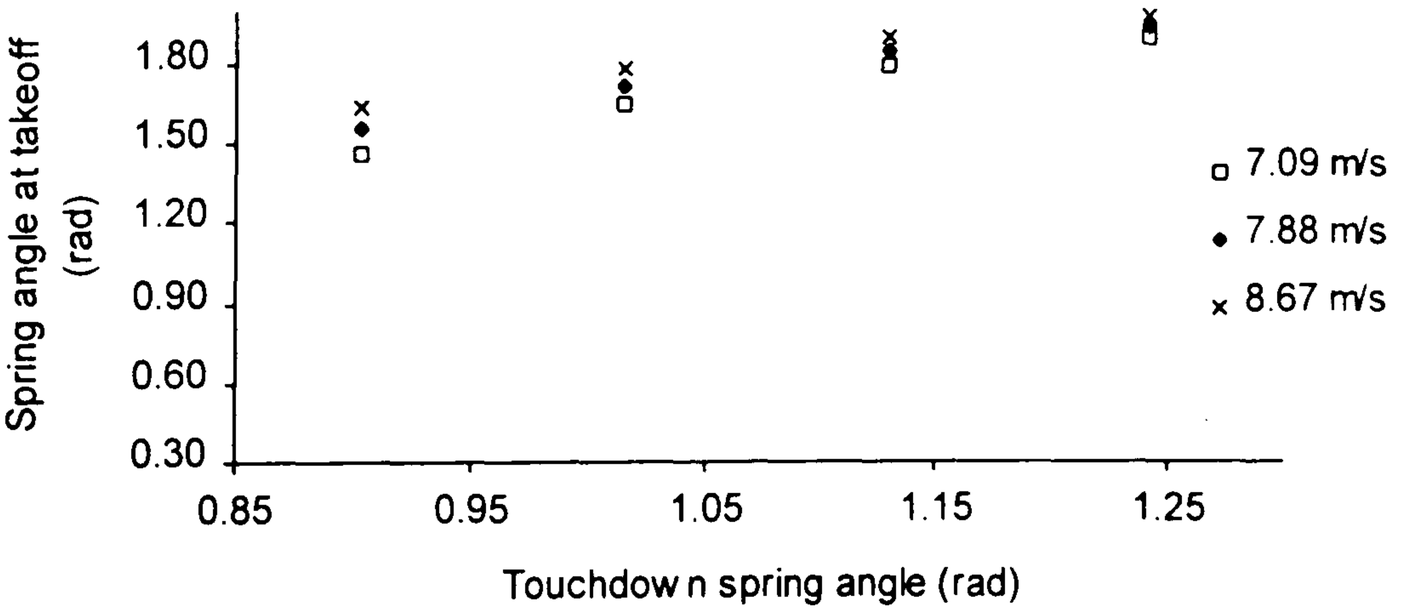

Figure 6.12. The effect of varying the spring angle and horizontal velocity at touchdown on the takeoff conditions of the two spring model.
N.B. A larger spring angle at touchdown indicates a more upright position.

6.11a). Graphs c and d in Figures 6.11 and 6.12 illustrate the effects on takeoff vertical velocity and spring angle: for each 10% change in touchdown horizontal velocity, vertical velocity was on average 6-7% different for the one spring model and 10% different for the two spring model, while altering the touchdown horizontal velocity made only an average 3-4% difference to the takeoff spring angle for both models.

A further strategy which gymnasts might be able to adopt was suggested by the results presented previously in Figure 6.1. This related to simulations where the approach speed, touchdown angle and leg spring stiffness were kept the same while the board spring stiffness was varied. While the stiffness of the springboard used for the data collection in Chapter Five was mechanically adjustable, the results of the board tests (section 5.4.2) showed that the contact point on the board surface also affected the board stiffness. With the springboard adjuster set to the stiffest position, contacting the board 0.70 m from the near end gave a stiffness of 45 $kN.m^{-1}$, while contacting 1.10 m from the near end resulted in a stiffness of 71 $kN.m^{-1}$. At these two extremes, simulations showed that the takeoff angle, angular velocity and horizontal velocity were only slightly affected (reduced by 8%, 7% and 4% respectively), but that at the stiffer position the vertical velocity at takeoff was increased by 38%, from 2.21 to 3.04 $m.s^{-1}$.

6.4 DISCUSSION

6.4.1 STIFFNESS ESTIMATION AND MODEL EVALUATION

The results of the simulations of the twelve vaults analysed in Chapter Five gave an indication of the fit of the models to the actual performances. The rebound durations were slightly underestimated by the models, averaging 87% (range 85-90%) and 89% (range 84-92%) of the gymnast's contact times with the springboard for the one and two spring models respectively. The fact that the models underestimated the contact times is consistent with the nature of the models in that they do not account for any net extension of the legs and arms (i.e. beyond that at springboard touchdown). This extension by the gymnast increases the depression of the board and hence the contact time (compared with a vault without this extension), though whether all of the difference between the models and reality would be accounted for by this is not clear.

The results from both models showed that a simple rebound can produce the majority of the linear and angular velocities required at takeoff from the board in handspring vaulting. The two spring model matched the takeoff horizontal and angular velocities more closely than the one spring model, however the one spring model showed better agreement with the vertical velocity at takeoff.

When considering the ability of the models to account for the vertical velocity at takeoff it can be tempting to be heartened by the findings of Takei (1988, 1989) and Takei and Kim (1990). In none of these papers was the vertical velocity at takeoff from board found to be significantly correlated with score. However this should not be taken to indicate that vertical velocity at springboard takeoff was unimportant to achieving success and therefore perhaps that the poorer ability of the models to predict vertical velocity at takeoff is inconsequential. Nevertheless it is likely that vertical velocity is less important than horizontal velocity at springboard takeoff since gymnasts are able to increase their vertical velocity during horse contact, but their horizontal velocity is reduced (e.g. Takei, 1988, 1989; Takei and Kim, 1990).

The vertical velocity which a simple rebounding model *cannot* represent is probably due to the extension of the hips, knees and ankles, and to some extent the shoulders, during springboard contact. Figures 6.13 a and b illustrate the points of touchdown and takeoff from the springboard respectively in a typical vault analysed in Chapter Five and show the net extension during contact. It is worth noting that at touchdown the arms are already substantially extended at the shoulder, having been swung forward and upward during the hurdle step, prior to springboard contact. Therefore the contribution of the arms to the vertical velocity at takeoff was not as great as might be imagined, or has been implied in the coaching literature (e.g. Readhead, 1987), and was unlikely to have approached the 12.7% contribution to vertical momentum found by Lees and Barton (1996) for vertical jumping. Kreighbaum (1974) also observed that the contribution of the arms to springboard takeoff 'appeared to be negligible' (page 142).

The leg spring stiffnesses calculated for the two spring model over the twelve vaults analysed in Chapter Five ranged from 79.69 to 293.75 $kN.m^{-1}$, with ten of the twelve falling between 94 and 140 $kN.m^{-1}$. Ferris and Farley (1997) reported leg stiffness values up to about 120 $kN.m^{-1}$ for two footed hopping in place at 3.2 Hz on a compliant surface (stiffness 26.1 $kN.m^{-1}$). Their activity has some obvious similarities with vault springboard takeoffs but the 'effective' frequency, forces and surface stiffness for vault takeoffs are higher than for hopping. The higher frequency and forces would indicate that greater leg stiffnesses would be required, while a stiffer surface would indicate that a lower leg stiffness would be appropriate, so overall all that can be said is that their results indicate that the stiffnesses found in this study are reasonable.

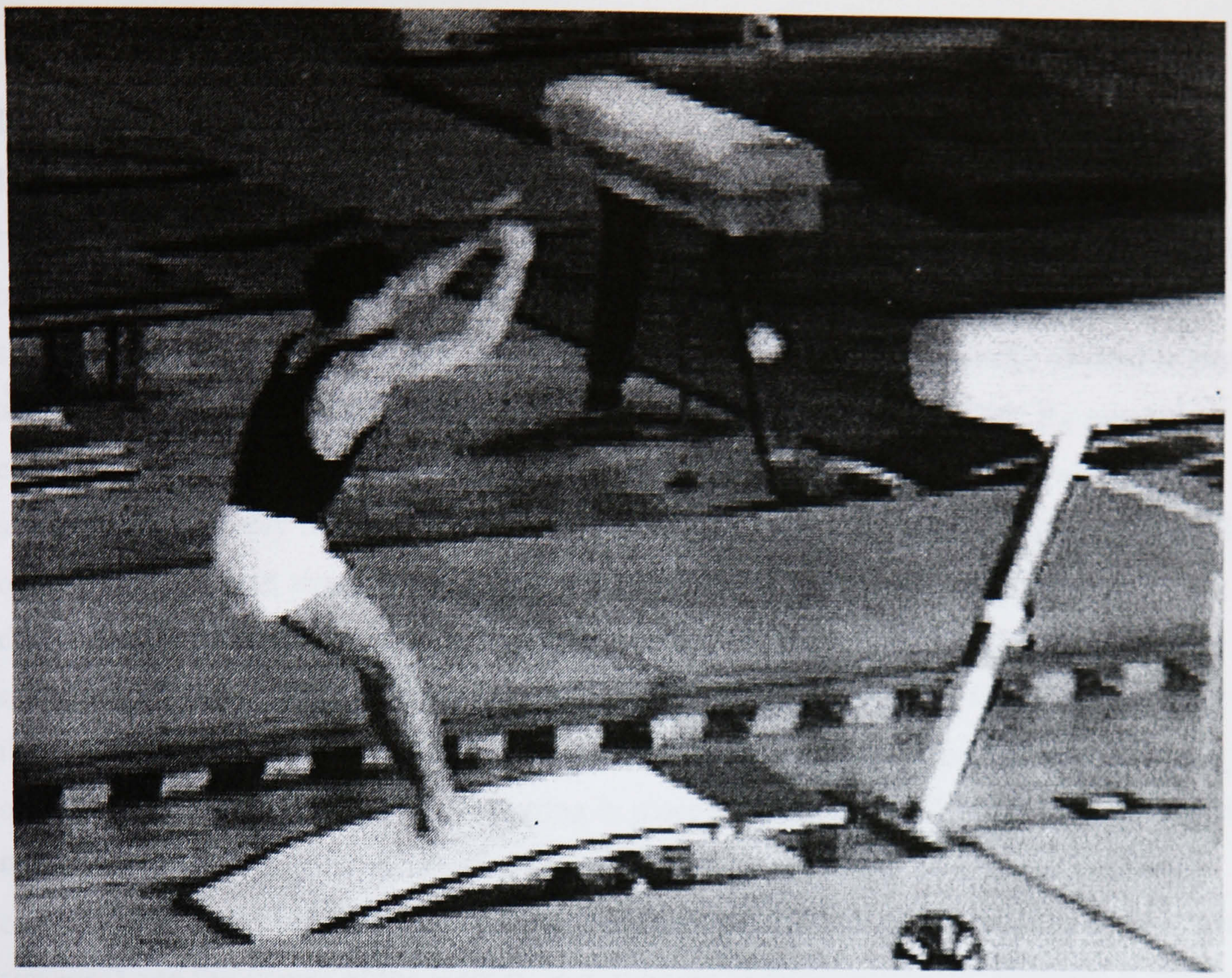

Figure 6.13a. Touchdown with the springboard for a typical vault.

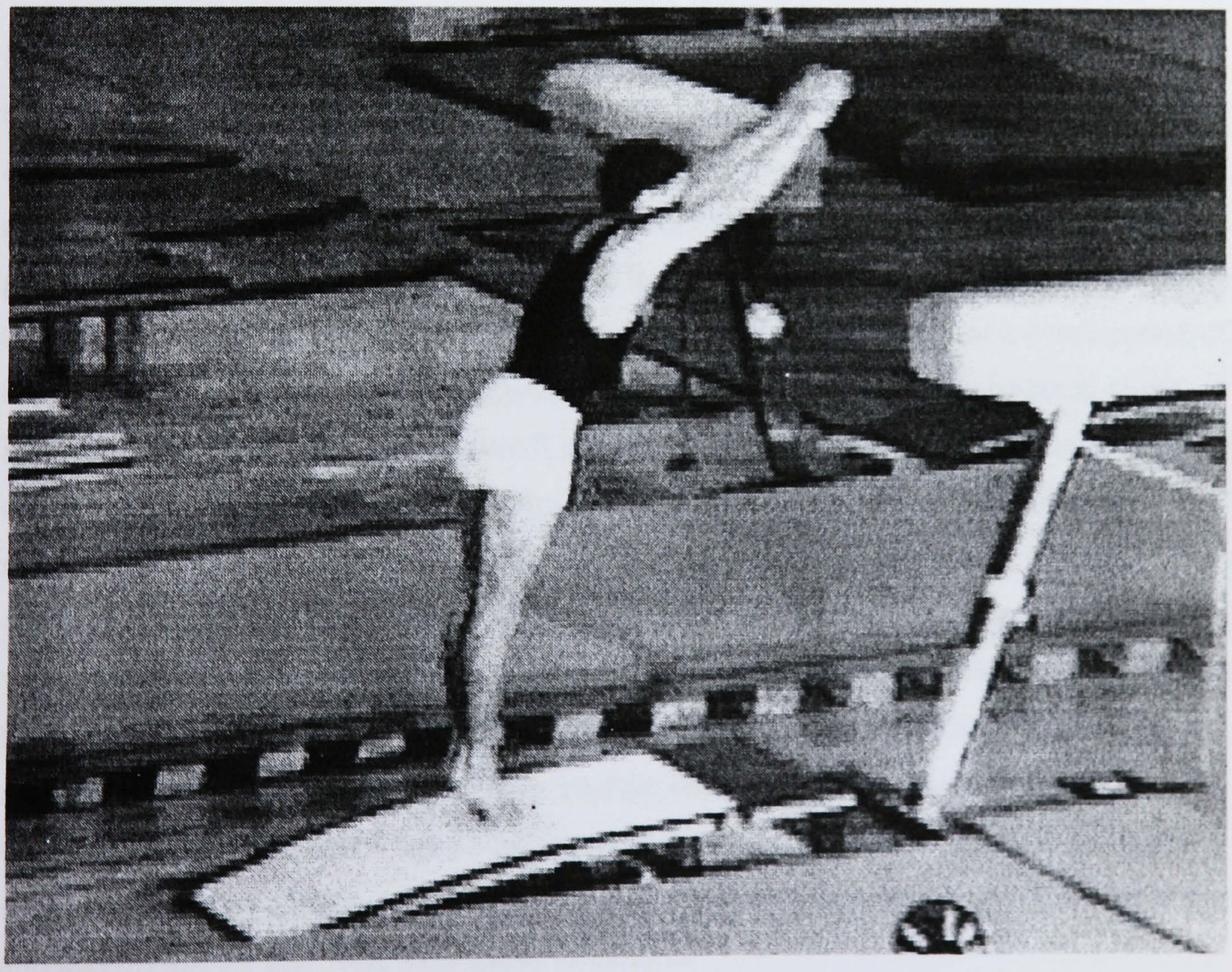

Figure 6.13b. Takeoff from the springboard for a typical vault.

The majority of the other stiffness estimates found in the literature range between 7 and 112 $kN.m^{-1}$ (see Chapter Two, Table 2.2) but comparisons with these data are not straightforward for a number of reasons. For example, stiffnesses calculated for running are obviously for one leg not two, but it might be assumed that the legs act as two parallel springs with the same stiffness, so the stiffness of both legs together would be double that of a single leg. However, Cavagna (1970) and Greene and McMahon (1979). for example. estimated two-legged stiffness only to be an average of 153% and 123% of one-legged stiffness respectively in a given situation; this may be related to the bilateral deficit noted in one versus two limb strength comparisons (e.g. Howard and Enoka, 1991). Another difficulty when comparing stiffness estimates is that most studies have estimated vertical stiffnesses not leg stiffnesses: vertical stiffness should be greater than leg stiffness since for the same peak force in the leg spring the vertical deflection is less than the change in length of the leg spring (the exception is hopping in place where these stiffnesses are identical since the mass centre motion is assumed to be one dimensional). Other factors confounding comparisons include the nature of the surface (most studies are of locomotion on very stiff surfaces) and the nature of the activity (e.g. running at different speeds, hopping at different frequencies). Nevertheless, while the stiffnesses estimated in this study are higher than most in the literature they are certainly feasible.

In the simulations which were conducted in order to estimate the spring stiffnesses, the takeoff angle of the gymnast's body was used as the criterion (as also adopted by McMahon and Cheng (1990) for their model for running). In this way the spring angle at takeoff is always correct in those simulations, while the takeoff velocities are unconstrained and generally do not match the values calculated from the recorded vaults. In principle, any of the takeoff velocities could have been chosen instead as the criterion, or a combination of the outputs could have been used. The spring angle was chosen principally because of the intrinsic logic of associating the takeoff angle with the stiffness, i.e. too soft and the takeoff occurs past the desired angle, too stiff and takeoff occurs before it. The choice was reinforced by conducting a number of simulations in which the takeoff spring angle was not constrained and the 'correct' stiffness was chosen on the basis of an error score based on a variety of combinations from the four outputs. For the two spring model these simulations failed to find optima: increasing the leg stiffness kept reducing the error score while the rebound duration became progressively shorter, leading to what were deemed to be unrealistic stiffnesses and rebound durations. The one spring model simulations found an optimum for some trials but again produced very short rebound durations, high stiffnesses and takeoff angles that were very close to vertical.

6.4.2 BOARD STIFFNESS VARIATIONS

The results of the simulations with the two spring model clearly showed that different springboard stiffnesses did affect the takeoff (Figure 6.1) and therefore to achieve the same takeoff the gymnast would need to effect some sort of compensation. One way in which compensation could be achieved is by altering the leg stiffness. This stiffness would have to be predetermined by the gymnast since springboard contact lasts less than 150 ms (e.g. Takei, 1988, 1989; Takei and Kim, 1990), too brief to enable modification to the movement to take place during contact (Melvill Jones and Watt, 1971). For a fixed approach, but with a variety of springboard stiffnesses, it was speculated that in order to produce the same takeoff, the combined stiffness of the gymnast and the springboard would remain constant.

The results of the simulations in which the leg spring stiffness of the model was recalculated to accommodate board stiffness variations, showed the leg spring stiffness decreasing non-linearly as the board stiffness was increased linearly (Figure 6.2). Ferris and Farley (1997) found a similar relationship for leg stiffness as the surface stiffness was increased while hopping in place at a fixed frequency. The non-linear relationship can be explained by considering the theoretical interaction of springs in series. When springs are arranged linearly in series, the overall stiffness is the reciprocal of the sum of the compliances of the individual springs, compliance being the reciprocal of stiffness. This is shown in Equation 6.1, where k_o, k_l and k_s are the overall, leg spring and surface stiffnesses respectively. Equation 6.1 can be rearranged to enable the leg spring stiffness to be predicted (Equation 6.2) and from this equation it can be seen that if the overall stiffness in a two spring system is held constant while the stiffnesses of the two springs are varied, a non-linear relationship between the two spring stiffnesses results.

$$\frac{1}{k_o} = \frac{1}{k_l} + \frac{1}{k_s} \qquad 6.1$$

$$k_l = \frac{k_o . k_s}{k_s - k_o} \qquad 6.2$$

Figure 6.14 shows the model calculated leg spring stiffnesses against board stiffness data (as in Figure 6.2) along with the theoretical leg spring stiffnesses calculated based the assumption that the combined stiffness of the two springs was 37.122 $kN.m^{-1}$ (for the mean touchdown conditions and takeoff angle for trials one to five, and based on a representative board stiffness of 58 $kN.m^{-1}$ with a corresponding leg spring stiffness of 103.125 $kN.m^{-1}$). This graph shows that, except for the softest board setting, the theoretical relationship is very close to that found in the simulations, despite the fact that the springs in the two spring

model are not arranged in a straight line. In other words it does appear that the leg and board springs combine to produce an overall stiffness which is approximately constant for all but the softest board stiffness.

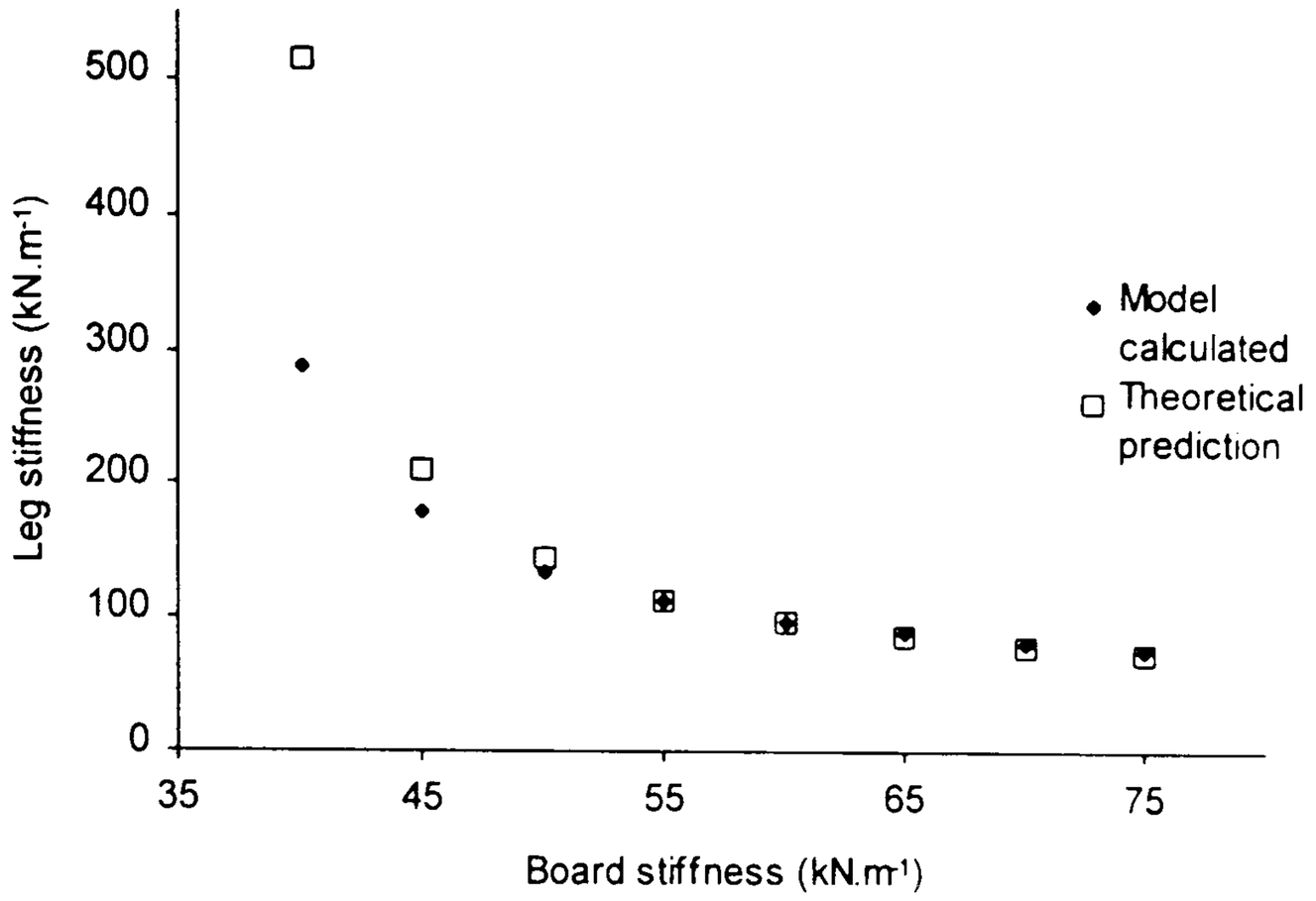

Figure 6.14. Model calculated and theoretically predicted changes to leg spring stiffness in order to compensate for board stiffness alterations.

The discrepancy between the model calculated and theoretical leg spring stiffnesses at the softer board stiffnesses may indicate that for softer board settings the non-aligned arrangement of the two springs has a greater effect. At the stiffer board settings, the levelling off of the graphs gives an indication of the leg spring stiffness that would be expected for the same vault from a very stiff surface (if it were possible). For example, for the same inputs, assuming a surface stiffness of 35 000 $kN.m^{-1}$ (as estimated for a force plate by Ferris and Farley, 1997) produces a leg spring stiffness of just over 37 $kN.m^{-1}$. This value is approximately the same as the overall stiffness used in the simulation and would tend towards the overall stiffness if the surface stiffness was increased further (this is clear from Equation 6.2 since the surface stiffness is in the numerator and the denominator).

The possibility of compensating for springboard stiffness changes by adjusting the touchdown horizontal velocity or spring angle rather than the leg spring stiffness showed that touchdown spring angle adjustments were most effective. This is consistent with the findings that the models tended to be most sensitive to spring angle. The alterations in leg spring stiffness required to make the same compensations were also much greater in relative magnitude than the spring angle adjustments.

This raises the issue of what gymnasts should do or should be advised to do when faced with a springboard that is stiffer or softer than that to which they are accustomed. Compensating by making small changes to touchdown angle seemed to be effective but Figures 6.3 and 6.4 show quite sharp minima, which mean that if the gymnast does not have an ability to modify touchdown angle precisely the result could be overcompensation. Modifying the horizontal velocity at touchdown had only a small compensatory effect. Using leg spring stiffness adjustment to compensate required a larger relative change (particularly when compensating for a reduction in board stiffness, see Figure 6.2) but it was more effective than modifying horizontal velocity and less sensitive than adjusting touchdown angle. Adjusting touchdown angle or leg stiffness would appear to be the most promising methods of coping with springboard stiffness variations, but deciding which would be most effective in practice is not straightforward. The answer would depend upon a gymnast's ability to achieve either precise, small changes in touchdown angle, or large changes in leg stiffness, but without the need to be so precise. The coaching literature does not address this topic and discussions with gymnasts and coaches have not identified any consensus.

In order to be able to establish which of the possible methods of compensation for board changes gymnasts actually adopt, it would be necessary to have vaults for which the board stiffness varies while the takeoff kinematics remain the same. It would then be possible to see which of the inputs were altered. The vaults analysed in this study did not however result in any trials where all of the takeoff velocities and the takeoff angle were the same and furthermore it was usually the case that the gymnast had changed more than one touchdown variable at a time, which complicates the attempt to identify his strategy. Alternatively it may be that adjusting more than one touchdown parameter is necessary in some circumstances. For example, when vaulting from the springboard at its softest setting, if no other input was varied the two spring model would predict a takeoff with slightly increased angular and horizontal velocities but greatly reduced vertical velocity. To maintain vertical velocity at takeoff the results of the simulations showed that reducing the spring angle at touchdown would be the most effective strategy (Figure 6.9); however this in turn reduces the horizontal and angular velocities at takeoff. A possible solution would be to increase the horizontal velocity *and* reduce the spring angle at touchdown to help to maintain all three velocities despite the reduction in board stiffness (Figure 6.12). Furthermore, an increase in leg spring stiffness would help to maintain the vertical velocity at takeoff, while not being too detrimental to the horizontal and angular velocities at takeoff (Figure 6.10).

Table 6.5 draws together the leg spring stiffness estimates from the simulations of the twelve vault trials and key data from the analysis of these trials, as described in Chapter Five. In

trials 11 and 12 (where the springboard was at its softest setting and the gymnast approached it at his preferred speed), the gymnast had a reduced touchdown angle in comparison with most of the normal stiffness and approach speed trials (trials 1 to 5). In trial 12 his horizontal velocity at touchdown was greater and his leg spring stiffness was also estimated to have increased, all of which conforms with the strategy suggested above. The takeoff velocities achieved in trial 12 were close to those in trials 1 to 5, so the gymnast did seem to compensate for the board changes in a way that could be proposed using the model.

Trials 5 and 11 come closest to having the same takeoff kinematics, but while the board setting in each of these vaults was different, the effect of the point of contact with the board on its stiffness resulted in quite similar board stiffnesses for the two trials. This may account for the lack evidence of a clear strategy having been adopted to achieve the similar takeoff. However in comparison with trial 5, the slightly larger angle and lower angular and

Table 6.5. Key data for the twelve vault trials.

Trial	K_b (kN.m^{-1})	K_{leg} (kN.m^{-1})	θ_{td} (rad)	v_{htd} (m.s^{-1})	θ_{tof} (rad)	v_{htof} (m.s^{-1})	v_{vtof} (m.s^{-1})	$\dot{\theta}_{tof}$ (rad.s^{-1})
1	45.9	110.156	1.15	7.70	1.89	5.43	3.89	6.09
2	62.4	135.156	1.12	7.95	1.81	5.29	4.10	6.72
3	58.6	121.094	1.10	7.86	1.79	5.11	4.16	6.59
4	54.8	111.719	1.18	7.95	1.91	5.39	3.96	6.14
5	42.4	139.063	1.11	7.94	1.85	5.51	3.94	6.21
6	57.4	121.875	1.20	6.21	1.79	4.23	4.01	5.35
7	62.4	94.531	1.26	5.55	1.84	4.20	3.80	4.38
8	54.3	79.688	1.17	6.57	1.86	4.50	3.82	5.49
9	48.6	106.250	1.17	7.14	1.88	5.13	3.92	5.74
10	34.9	293.750	1.13	7.36	1.91	5.38	3.97	5.46
11	37.8	129.688	1.11	7.85	1.88	5.48	3.94	6.19
12	32.8	242.969	1.11	8.09	1.91	5.86	3.89	5.93

N.B. K_b and K_{leg} are the board stiffness and the calculated leg spring stiffness respectively. θ_{td} and v_{htd} are the spring angle and mass centre horizontal velocity at touchdown. θ_{tof}, v_{htof}, v_{vtof} and $\dot{\theta}_{tof}$ are the takeoff spring angle and the takeoff horizontal, vertical and angular velocities respectively. K_{leg} values were calculated using the model, while the other data were determined from the analyses in Chapter Five.

horizontal velocities at takeoff in trial 11 are consistent with the model predictions for lower board and leg stiffnesses, along with the slower approach (Figures 6.8 and 6.10). Similarly, Figures 6.8 and 6.10 illustrate that lower horizontal velocity at touchdown and lower leg stiffness have opposite effects on vertical velocity at takeoff, so the combination of the two could result in the same vertical velocity, as was found in trial 11 compared with trial 5.

The fact that board stiffness varies quite appreciably due to foot contact position could have important implications for gymnasts. Trials 1 to 5 were conducted with the board at the same stiffness setting, yet Table 6.5 shows that the board stiffness varied appreciably between trials. The results from the board stiffness testing (Chapter Five, section 5.4.2) combined with the actual range of foot contact positions found in the vaults analysed revealed that the board stiffness can vary by 32% (32.3 to 42.7 $kN.m^{-1}$) with the board at its softest setting and 56% (45.3 to 70.6 $kN.m^{-1}$) with the board at its stiffest setting. If gymnasts are aware of this variability and are able to control their approach such that they can contact the board at a precise point on its surface, they may have another way in which the takeoff can be controlled and possibly a method of compensating for board variations between venues. Conversely, if gymnasts are unaware of this variability and do not achieve consistency of foot placement this could adversely affect their performance.

An indication of the consistency of foot placement that might be achievable comes from studies of long jumping. In terms of assessing this aspect, perhaps the most important difference between long jump and vault takeoffs is the fact that long jumpers have up to six jumps, only the best of which counts. Therefore they may try to get at least one legal jump (takeoff behind the board) early in the competition with the takeoff foot well behind the board, thus 'artificially' increasing the apparent variability of the final foot placement. Despite this, the majority of the elite long jumpers analysed by Hay (1988; 20 women, 18 men) and Lees, Graham-Smith and Fowler (1994; 7 men) achieved standard deviations of the position of the foot at takeoff of 0.05 m or less. Of the six women long jumpers analysed by Lees, Fowler and Derby (1993) only two had standard deviations of less than 0.05 m, but all were less than 0.07 m (though only the best three or four jumps per athlete were reported). These figures compare with a standard deviation for foot placement on the springboard of 0.10 m for the first five trials by the gymnast analysed in Chapter Five, which, if the gymnast was not consciously changing his foot placement, would indicate that greater consistency is achievable.

6.4.3 APPROACH AND CONTACT STRATEGIES

The results from simulations in which inputs were changed systematically to assess the effects on the takeoff conditions showed that the touchdown spring angle and horizontal velocity were much more influential than spring stiffness. Increasing either the spring angle or the horizontal velocity resulted in increased angular and horizontal velocities at takeoff, while increasing the spring angle also led to a large reduction in vertical velocity at takeoff. This last finding can be explained by considering the spring angle at takeoff:

- only the touchdown spring angle had a really noticeable effect on the takeoff spring angle in that a larger angle at contact (i.e. closer to vertical) resulted in a spring angle at takeoff which was further past vertical,
- the vertical velocity at takeoff is the sum of the vertical components of the spring extension rate and the transverse velocity of the mass centre (plus the board spring extension rate in the two spring model),
- if the takeoff occurs further past vertical then the vertical components of both the spring extension rate and the transverse velocity of the mass centre are reduced.

Thus in order to increase the vertical velocity at takeoff, both models indicated that smaller touchdown spring angles were required, but this also reduced the horizontal and angular velocity at takeoff. The men's artistic gymnastics Code of Points (FIG,1997) indicates that gymnasts should strive for both postflight horizontal distance and height. Postflight horizontal distance is due to horizontal velocity and time in the air (which in turn is largely due to vertical velocity at horse takeoff). Since gymnasts performing continuous rotation vaults like handsprings generally gain vertical velocity but lose horizontal velocity during contact with the horse (Dillman, Cheetham and Smith, 1985; Takei, 1988, 1989; Takei and Kim, 1990; Takei, Blucker, Dunn, Myers and Fortney, 1996) it is necessary for them to achieve a high horizontal velocity during their approach to the springboard and not to lose too much of it during the springboard and horse contacts if they are to maximize their postflight distance. Hence, it could be argued that during springboard contact the maintenance of horizontal velocity is more important than gaining vertical velocity. When greater pre- and postflight angular velocity is also required (in handspring and forward salto vaults for example) it would make even more sense to sacrifice gaining vertical velocity during springboard contact. Some of the loss in vertical velocity might be offset by making the legs stiffer or contacting a stiffer part of the board, although these changes would also tend to reduce the takeoff horizontal and angular velocities slightly.

Altering both the horizontal velocity and the spring angle at touchdown produced takeoff angle and vertical velocity results which were virtually identical to those from simulations where only the spring angle was changed. This was anticipated due to the minimal influence of the horizontal velocity on these two takeoff variables as already noted. The effect on the takeoff horizontal and angular velocities of increasing the horizontal velocity as well as the spring angle at touchdown was also as expected: increasing the horizontal velocity at touchdown shifted the curves up by consistent amounts.

The effects of board stiffness variation over the length of the board surface were explored in a series of simulations using the two spring model (see Figure 6.1) and found to affect all of the takeoff velocities but to have least effect on horizontal velocity. The effect on takeoff vertical velocity was the most notable. At the higher board stiffnesses the takeoff vertical velocity was increased, which can be ascribed once again to the influence of spring angle at takeoff: a stiffer board meant that the model lost board contact sooner (not so far past the vertical), therefore the vertical component of the leg spring extension velocity was greater and the negative contribution of the mass centre transverse velocity was reduced. Under conditions in which the predicted vertical velocity at takeoff was low (large touchdown spring angles), the effect on vertical velocity of contacting the board in different places could approach 60%, though typically it was around 20%.

In trials 6, 7 and 8 the gymnast was required to approach the board more slowly than normal but still to perform the same handspring vault. The simulation results indicated that this would lead to lower angular and horizontal velocities at takeoff, therefore to compensate a larger touchdown angle (more upright at contact) should be used. This was indeed found to be the case, although the gymnast still did not manage to achieve the same takeoff velocities as in the normal approach trials. The drawback of increasing the touchdown angle is that the vertical velocity at takeoff is predicted to be reduced, however, as noted above, it may be possible for gymnasts to achieve adequate vertical velocity by contacting a stiffer part of the springboard or making their legs stiffer. Alternatively, gymnasts might adopt a more jump-like takeoff to increase vertical velocity, for example by using arm swing and greater than normal hip, knee and ankle extension. The results from the trials analysed for this study and inspection of the video do not lead to a clear conclusion as to whether one or more of these options were chosen by the gymnast.

Looking at handspring and forward salto vaults, Takei (1991) found that the best vaulters approached the springboard with high horizontal velocity (a mean of 8.19 $m.s^{-1}$ for the best 11 of 51 gymnasts compared with 7.69 $m.s^{-1}$ for the worst 11) but otherwise their touchdown kinematics were very similar to the poorer vaulters. From this, the models would predict

greater takeoff horizontal and angular velocities for the better vaulters, however Takei (1991) found that only their horizontal velocity was substantially greater. This does not necessarily detract from the model predictions since it is possible that by running up faster the better vaulters do not achieve (and presumably do not need) greater angular velocity in preflight, but they get more of their angular velocity from the simple rebound. Simulations using inputs estimated from Takei's data supported this suggestion and reiterated the ability of the models to account for the majority of the velocities at springboard takeoff.

Since both touchdown horizontal velocity and spring angle had similar effects on takeoff (with the exception of vertical velocity at takeoff) it would be of interest to discover whether adjusting one is preferable to the other. Takei (1991) found that horizontal velocity at springboard contact, not touchdown angle, was different between the best and worst vaulters. Takei stressed the importance of the approach speed by stating that 'gymnasts should develop a large horizontal velocity in the hurdle and preflight by vigorously sprinting the approach run' (p. 74). In his 1989 paper, Takei presented information for handspring vaults which when compared with his 1991 paper on handspring and forward salto vaults showed that gymnasts had much greater horizontal velocities at board touchdown for the latter vault. In preflight, the major difference between the two vaults was the greater angular momentum for the handspring and forward salto. Unfortunately Takei (1989) did not report body angles at touchdown, but the difference between horizontal velocities at board touchdown does provide some support for the notion that this was the preferred input to adjust in order to increase takeoff angular momentum. Further support for the contention that horizontal velocity may be the best input to vary, comes from the simulations which showed that to increase angular velocity at board takeoff by increasing the touchdown angle, would result in an accompanying reduction in vertical velocity, which would be unhelpful to the gymnast. This problem could be alleviated to some extent by increasing the leg spring stiffness and/or the board stiffness. While altering two or three variables as opposed to just one is more complex, the results from the analysed vaults did show that more than one input at a time was varied.

The discussion has concentrated on handspring type vaults but it is interesting to assess whether the models might work for other types of vault. Brüggemann (1994) stated that vaults with twists are essentially the same at springboard takeoff as those without twists, which implies that the models should be suitable for these vaults. However, Brüggemann was presumably considering only continuous rotation vaults rather than Hecht vaults, in which the direction of rotation of the body is reversed during horse contact and therefore less angular momentum at springboard takeoff would be expected. Few data have been published

on the kinematics of the Hecht, but sufficient are available to enable a simple evaluation. Sprigings and Yeadon (1997) suggested that mass centre horizontal velocities at takeoff from the springboard in excess of 5.6 $m.s^{-1}$ would be optimal, which was supported by King (1998) who found horizontal velocities between 5.73 and 6.28 $m.s^{-1}$. These velocities are greater than all but one of the handspring trials analysed in this study and the great majority of the handspring and handspring and forward salto vaults reported by Takei (1988, 1989, 1991) and Takei and Kim (1990). The results of the simulations with the models indicated that achieving high horizontal velocities at springboard takeoff could be achieved by approaching the board faster and/or contacting the board at a larger angle. Both of these strategies also result in low vertical velocities and high angular velocities at takeoff. The latter would be particularly detrimental to the reversal of rotation necessary during horse contact (angular velocities of around 3 to 4 $rad.s^{-1}$ have been suggested by Sprigings and Yeadon (1997) and found by King (1998), compared with values in excess of 6 $rad.s^{-1}$ for the five normal approach handspring vaults analysed in Chapter Five, see Table 6.7). Again by comparison with the normal approach handspring vaults, the Hecht vaults analysed by King (1998) did reveal larger touchdown angles, but lower horizontal velocities at touchdown. At takeoff the vertical velocities *were* lower than for the handspring vaults, but so too were the angular velocities. In the light of this it can be seen that the models developed in this study give some indication of suitable approach strategies for gymnasts performing Hecht vaults, but that springboard contact for the Hecht vault involves more than a simple rebound from the springboard, in order to limit the gain of angular velocity.

6.4.4 MODEL SELECTION

Both models have shown that, for the trials analysed, the majority of the angular and linear velocities at springboard takeoff can be accounted for by a simple rebound. The two spring model gave angular and horizontal velocities which were always within 20% of the measured values and in the majority of cases predicted them to within 10%, however it predicted the takeoff vertical velocity much less well. The one spring model generally did not get as close to the measured angular and horizontal velocities, but was better able to account for the vertical velocity. Little difference was found between the models in terms of rebound durations as a percentage of the gymnast's actual contact time with the springboard. Therefore, based on the closeness of fit to the analysed vaults it is difficult to choose between the models. The sensitivity of the models to the uncertainties in the input estimates was also very similar, with only the sensitivity to the touchdown spring angle being of note. This sensitivity to the spring angle data must be kept in mind when using the models, particularly when trying to utilize kinematic data reported in the literature since the way in which body angle at touchdown is defined would affect the simulation results.

One way in which the results of the two models noticeably differed was in their estimates of spring stiffness; for the same vaults the two spring model predicted considerably greater stiffnesses than the one spring model. This can be explained if the two spring model is approximated as a two spring system with the springs constrained to move in a straight line (as mentioned previously, the combined stiffness of the two springs can be calculated by adding the compliances of the two springs and taking the reciprocal). For any trial, if the one spring model stiffness is assumed to be the same as the combined stiffness of the two springs in the two spring model and given that the directly measured springboard stiffnesses (Chapter Five) are similar in magnitude to the estimated stiffnesses from the one spring model simulations, the leg spring would need to be much stiffer than the one spring model stiffness. For example, if the one spring model stiffness was 40 $kN.m^{-1}$ and the board spring stiffness was 55 $kN.m^{-1}$, the leg spring stiffness would be approximately 146.7 $kN.m^{-1}$. With the springs not arranged linearly the actual values are naturally different but a similar pattern emerges. The geometry of the two spring system means that the touchdown angle is smaller and the takeoff angle greater than the one spring simulation, therefore the actual leg spring stiffnesses predicted by the two spring model are somewhat lower than the approximation above would suggest, but still much greater than the one spring model stiffness estimates. In addition, the trends in stiffness estimates did not match exactly, for example the trial which produced the stiffest spring estimate for the one spring model did not result in the stiffest leg spring estimate with the two spring model.

When using the models to identify possible strategies which gymnasts might use in their approach to and contact with the springboard, both models produced remarkably similar results. The magnitudes of the takeoff velocities and spring angle were slightly different, but the trends in the data were consistent. However, one distinct advantage of the two spring model is its ability to enable the effects of the stiffness of the surface to be investigated directly. In the simulations performed in this study, the board stiffness affected the vertical velocity at takeoff more than the other velocities (Figure 6.1) and it had a considerable influence on the leg spring stiffness estimates. The leg spring stiffness was affected more at lower board stiffnesses, which suggests that the benefit of having a two spring model is greatest for relatively soft surfaces.

Both models are simple to use and the additional complexity of the two spring model does not add substantially to the computation time of the simulations. However obtaining the inputs for the two spring model is somewhat simpler since it does not require detailed knowledge of the feet position during springboard contact; the one spring model requires a 'base of the spring' point to be determined (which was taken to be the mean position of the

mid-metatarso-phalangeal joints of the two feet at the lowest point during board contact). In addition, the spring angle in the two spring model matches more closely what gymnasts and coaches would understand as 'blocking angle' which adds to the attractiveness of the two spring model.

To summarize model selection, the one spring model is adequate for the tasks it can perform (it cannot be used to investigate surface and leg stiffnesses separately) and in those cases produces similar results to those of the two spring model. On balance however, the two spring model has a wider range of uses, making it the preferred model for the majority of the analyses in this study.

6.5 SUMMARY

In this chapter it was demonstrated that both the one and two spring models fit the analysed vaults in terms of the duration of the rebound and that the majority of the takeoff velocities can be accounted for by simple rebounds. The spring stiffness values estimated by the models show reasonably good agreement with the stiffnesses found by other investigators, although it was highlighted that direct comparisons are not always possible. On balance the two spring model was more useful than the one spring model, owing to its ability to model surface stiffness separately from the leg spring stiffness, though otherwise the models' predictions agreed very closely.

The influence of springboard stiffness on takeoffs from the board was appreciable and a number of ways of accommodating board stiffness changes were suggested, including adjusting the leg spring stiffness. Furthermore, agreement between model derived strategies and actual performances was found. Although adjusting leg spring stiffness to cope with changes in springboard stiffness was shown to be feasible, it was suggested that a combination of modifications to the approach and board contact might be required. It was also demonstrated that the models enable strategies to be suggested which could be used to achieve particular changes to springboard takeoff. Although the takeoff velocities predicted by the models do not exactly match the actual data from the vaults analysed, it was possible to investigate the influence of different approach variables and springboard stiffnesses on the subsequent takeoff. Hence, an insight into the mechanisms operating during board contact was gained.

CHAPTER SEVEN
DISCUSSION AND SUMMARY

7.1 INTRODUCTION

While the springboard contact in gymnastic vaulting is not judged in competition, it underpins the rest of the vault. The research literature supports its importance, but the coaching literature lacks a consensus on the subject and sometimes contradicts detailed analyses of the activity. In addition to the approach to the springboard and the way the body is controlled during contact with the springboard, conversations with gymnasts suggested that springboards also vary in their response to the gymnast's contact, though no mention is made of this in the literature. Even with skilled and willing subjects, systematically investigating the influence of each of the variables involved in springboard contact by direct intervention would be unlikely to be successful, particularly since springboard contact is physically very demanding, so the number of vaults a gymnast could perform would be limited. Using a suitable mathematical model however, offered a means of investigation.

The purpose of this study was to develop an understanding of the mechanics of the springboard contact phase of gymnastic vaulting. The method adopted to achieve this involved analysing real vaults and modelling the gymnast-springboard contact using a mass-spring system. The aim was to explore the relationships between hurdle and preflight kinematics as modified by the springboard contact, and to determine the strategies a gymnast might employ to achieve the desired springboard takeoff conditions. To provide a focus for the study the following questions were raised:

- What proportion of a gymnast's linear and angular velocities at takeoff from the springboard can be accounted for by a simple rebound?
- To what extent does springboard stiffness affect takeoff kinematics?
- How does changing the kinematics at springboard touchdown affect the takeoff from the board?
- What effect does the gymnast's stiffness during springboard contact have on the takeoff from the board?
- How can gymnasts compensate for springboard stiffness differences?

- What modifications to a gymnast's approach to and contact with the springboard are most effective for achieving specific changes to preflight?

This chapter reviews the two models developed and the results from the investigations performed, leading to the answers to these questions. The chapter concludes with suggestions for future studies.

7.2 THE MODELS

Previous mass-spring models of human hopping, running and jumping have been concerned solely with the linear motion of the mass centre and the duration of ground contact, and have therefore been able to treat the body as a point mass on a spring (e.g. Blickhan, Friedrichs, Rebhan, Schmalz and Wank, 1995; Farley, Blickhan, Saito and Taylor, 1991; McMahon and Cheng, 1990). To be able to investigate the angular motion of the gymnast in vault springboard contacts, the two models developed for this thesis treated the body as a uniform, rigid cylinder supported by a spring constrained to maintain alignment with the cylinder. The cylinder was defined as having the same mass as the gymnast being modelled (less the mass of the feet for the two spring model) and a fixed moment of inertia equivalent to the moment of inertia of the gymnast at springboard touchdown. In reality, a gymnast's moment of inertia increases up to the point of takeoff from the springboard, but the lack of sensitivity of the simulation results to moment of inertia perturbations was taken as an indication that using a constant value for each simulation was reasonable. The two spring model was also insensitive to the feet mass between the leg and board springs, and it was argued, on the basis of previous research (McMahon and Greene, 1979; Sprigings, Stilling and Watson, 1989), that no mass representing the effective mass of the springboard was required since its influence was likely to be negligible.

Results from the hopping and running jump study reported in Chapter Three indicated that using a linear spring to represent the legs was a good approximation. Linear springs have previously been used for mass-spring models of human hopping and running (e.g. Blickhan, 1989; McMahon and Cheng, 1990), but in these cases the ground contact was assumed to be symmetrical whereas in vaulting it clearly is not (for example the horizontal velocity is much lower at takeoff from the springboard than at touchdown). The vertical ground reaction force-mass centre displacement graphs presented by Cavagna, Franzetti, Heglund and Willems (1988) were used by McMahon and Cheng (1990) to justify using a linear spring for hopping and running; the running jump analysis in Chapter Three of this thesis used the same type of analysis to extend the leg spring linearity justification to asymmetrical ground

contacts. Tests conducted on the springboard (Chapter Five, sections 5.3 and 5.4.2) showed that the board could also be modelled as a linear spring and that the board damping was low.

The one spring model treated the springboard and the gymnast's legs as a single spring, while the two spring model kept them separate and constrained the spring representing the springboard to move vertically. Both models could be used in two ways: either to estimate the spring stiffness required to best fit a particular vault, or to predict the takeoff kinematics given the touchdown kinematics and spring stiffness. The first of these modes of operation required a criterion against which the fit of the model (and therefore the suitability of the stiffness) could be judged. The angle of the line joining the middle of the feet to the mass centre of the gymnast at takeoff from the springboard (takeoff angle) was used. McMahon and Cheng (1990) had used this method of choosing the spring stiffness in their model of running and hopping, although because they assumed perfect symmetry of ground contact, the takeoff velocity of their model also fitted exactly. While forcing the takeoff angle to be correct might appear to favour that variable arbitrarily over the takeoff velocities, there is an appealing logic to associating the takeoff angle with spring stiffness. That is to say, a spring which is too stiff causes takeoff to occur too close to vertical, while a spring which is too soft causes takeoff to occur too far past vertical or not at all. Furthermore, simulations in which the spring stiffness was sought on the basis of optimizing a combination of the takeoff variables (without constraining the spring angle), either did not manage to find an optimum, or resulted in unrealistically high spring stiffnesses and short contact times. The leg spring stiffness estimates found using the two spring model were somewhat higher than the majority of the previously published stiffness estimates but, given the difficulty of making exact comparisons between estimates from different activities and methods of estimation, they were sensible.

In order to estimate the leg spring stiffness with the two spring model it was necessary to determine the stiffness of the springboard. Springboard tests (Chapter Five, sections 5.3 and 5.4.2) found that board stiffness varied not just in response to adjustments to the board setting but also to the point of contact with the board. However springboard damping was low and did not vary greatly from one contact point to another, or between board settings. Subsequent sensitivity analyses (Chapter Six, section 6.3.1) found that the two spring model leg stiffness estimates were only slightly sensitive to board stiffness, but otherwise the model was insensitive to both board stiffness and damping. Being able to alter the board and leg spring stiffnesses separately is a distinctive feature of the two spring model and enabled strategies involving board and leg spring stiffnesses to be investigated independently.

7.3 RESEARCH QUESTIONS

The results of the simulations conducted in which the approach and board contact variables were systematically adjusted to see their effects on the board takeoff are summarized as the questions posed in Chapter One are addressed.

What proportion of a gymnast's linear and angular velocities at takeoff from the springboard can be accounted for by a simple rebound?

Both models showed that a simple rebound can produce the majority of the linear and angular velocities required at takeoff from the board in handspring vaulting. The two spring model matched the takeoff horizontal and angular velocities calculated from the vaults analysed in Chapter Five more closely than the one spring model, however the one spring model showed better agreement with the vertical velocity at takeoff. The vaults analysed were all handsprings, but simulations using inputs estimated from data on handspring and front salto vaults (Takei, 1991) indicated that the majority of the takeoff velocities were still accounted for using the one and two spring models. Comparing the Hecht vault data presented by King (1998) with the normal approach handspring vaults analysed in this study, showed that the approach to the springboard for Hecht vaults was slower than for the handspring vaults, but that the Hecht touchdown angles were larger (closer to vertical). At takeoff from the board however, the horizontal velocity was greater for Hechts than handsprings while the Hecht angular and vertical velocities were lower. The simulation results in Chapter Six showed that the models would indicate increasing the touchdown angle to limit the loss of horizontal velocity during springboard contact and that this would also reduce the vertical velocity at takeoff, thereby matching the general pattern for Hecht vaults. However the simulations also showed that achieving a high horizontal velocity in preflight would be accompanied by high angular momentum, which is not found in Hecht vaults, therefore gymnasts performing Hechts cannot *just* rebound from the springboard but must be doing something to limit the angular momentum.

The proportion of vertical velocity at takeoff produced by both models was lower than for the horizontal and angular velocities. In a real vault the mass centre of the gymnast is further from the feet at takeoff than at touchdown, because of flexion of the shoulders and the extension of the ankles, knees, and hips. This movement mainly contributes to the vertical velocity because the body angle at takeoff is only just past vertical. The models in this study were deliberately kept straightforward to explore the simple rebound influence and therefore do not include this additional component of vertical velocity. To improve the fit of the models while retaining a mass-spring structure would entail contrivances such as variable

stiffnesses or negative damping, thus adding to their complexity, making their use and interpretation more difficult (e.g. Blickhan, Friedrichs, Rebhan, Schmalz and Wank, 1995).

It is interesting to note that Alexander (1992) has criticized mass-spring models of jumping on the basis that models with springy legs would jump too high. This is contrary to the finding that the models in this study take off with less vertical velocity than the gymnast. However, Alexander does not consider a number of important factors: the initial impact with the ground, rotational kinetic energy and the possible upper limit to leg stiffness. In calculating the initial conditions for the models in this study, an instantaneous impact was assumed, one consequence of which was the generation of angular momentum. Thus not all of the linear kinetic energy of the approach can be converted into potential energy following takeoff, since much has been transferred to rotational kinetic energy. Furthermore, Alexander (1992, page 7) states that 'a model with a spring instead of a muscle would suggest falsely that high jumpers should run up as fast as possible', which ignores the fact that in order to maximize vertical velocity at takeoff, the model would need to be vertical. This would demand increasing leg stiffness as the horizontal velocity of the approach increased (see Figures 6.5d and 6.7d) and it seems reasonable to assume a physical upper limit to leg stiffness (e.g. Blickhan, 1989) which would mean that running up faster would at some point fail to increase the height achieved (as predicted by Alexander (1990b) and found empirically by Greig, Yeadon and Kerwin (1996)). Seen in this light, mass-spring models *would* be useful for the investigation of the mechanics of jumping.

To what extent does springboard stiffness affect takeoff kinematics?

In Chapter Five it was found that by a combination of foot contact position and adjustment of the springboard, the springboard stiffness ranged from approximately 35 to 75 $kN.m^{-1}$. Results from the two spring model simulations in which the leg spring stiffness was held constant while the board spring stiffness was increased throughout this range, showed that each of the takeoff variables were affected, with the vertical velocity being affected most. The vertical velocity varied from 1.99 to 3.12 $m.s^{-1}$, the angular velocity from 6.87 to 6.19 $rad.s^{-1}$, the horizontal velocity from 6.07 to 5.75 $m.s^{-1}$ and the takeoff angle from 1.94 to 1.78 radians. Comparison of these variations with the data on handspring vaults in Chapter Five and with data in the literature indicated that the effect of board stiffness variation was likely to be of importance.

The fact that the point of contact with the springboard surface varied the board's stiffness (in fact by a similar amount to when the springboard adjuster was moved through its full range for a fixed point of contact) has implications for the way in which gymnasts should practise

their approach to the springboard. Gymnasts need to appreciate the influence on springboard stiffness of the contact point with the board and it would be sensible for them to aim to be as precise as possible with their foot placement. Gymnasts vaulting without being aware of this could have to make adjustments during preflight and horse contact if the point of contact, and therefore the board stiffness, varies from vault to vault. Conversely, a gymnast who understands the effect of foot placement on the springboard's characteristics and who can strike the board precisely, could use this to adjust the takeoff.

Kreighbaum (1979) highlighted the fact that gymnasts' foot placements on the springboard were inconsistent and the results in Chapter Five (Table 5.1) confirmed this: however it is possible that these variations in foot placement were deliberate. In discussion, gymnasts have commented that while they target a certain region of the springboard, they do not think about where to contact the board during the approach, especially for more difficult vaults. The variability in the foot placements would therefore seem unlikely to be deliberate attempts to utilize the differences in springboard stiffness. On the other hand, observations reveal that gymnasts *can* modify their vaults to accommodate unexpected takeoff conditions: for example at the 1991 World Student Games a gymnast missed the springboard but vaulted successfully from the foam safety pad surrounding the board. However, not contacting in a favourable position would be a bigger problem for more difficult vaults.

How does changing the kinematics at springboard touchdown affect the takeoff from the board?

In Chapter Six simulations were reported in which the horizontal velocity and the spring angle at springboard touchdown were varied, separately and in combination, over a range of realistic values. Other inputs were held constant during these trials. The results from the one and two spring models were remarkably similar, so no distinction between models needs to be made when addressing the question.

Increasing the horizontal velocity or the spring angle at touchdown increased appreciably both the angular and horizontal velocities at takeoff. Only the increase in touchdown spring angle had much of an effect on the spring angle at takeoff, causing it to increase, but not to the extent to which the angular and horizontal velocities had been increased. The touchdown spring angle had a much greater effect than the touchdown horizontal velocity on the vertical velocity at takeoff; though increases in each led to reductions in vertical velocity at takeoff.

The very similar influences on the takeoff horizontal and angular velocities of increasing the horizontal velocity or the spring angle at touchdown, led to a combined effect which was to amplify consistently the increases either one on its own produced. For example in addition to

the increase in horizontal velocity at takeoff due to increasing the touchdown spring angle, a ten percent increase in touchdown horizontal velocity resulted in an average further increase in horizontal velocity at takeoff of 17-18%. The smaller effect of the horizontal velocity at touchdown on the vertical velocity and spring angle at takeoff, meant that when both the horizontal velocity and the spring angle at touchdown were altered, the results were virtually identical to those when only the touchdown angle was changed.

What effect does the gymnast's stiffness during springboard contact have on the takeoff from the board?

The results of two spring model simulations in which the leg stiffness was adjusted to cover a range of realistic values showed that only the vertical velocity at takeoff was appreciably altered. Increasing the leg stiffness tends to make the takeoff occur earlier when the spring angle is not so far past the vertical and therefore the contribution to vertical velocity of the radial velocity of the mass centre is increased, while the negative contribution of the angular velocity of the model is reduced. The net result is therefore that stiffer legs produce a higher vertical velocity at takeoff.

Although the effect of leg stiffness variation on vertical velocity at takeoff is relatively small by comparison with the influence other inputs have on takeoff, it could still have a role. High horizontal and angular velocities at takeoff from the springboard are desirable for handspring type vaults and can be achieved by increasing the horizontal velocity and/or spring angle at touchdown, however these both reduce vertical velocity at takeoff. Increasing the leg stiffness can help to maintain vertical velocity and combining this with using a stiff springboard setting and contacting at a stiff part of the board would help further. This would be likely to increase the stress on the gymnasts' legs, but in competition gymnasts do not perform many vaults and if they are well conditioned this is unlikely to be a great concern.

How can gymnasts compensate for springboard stiffness differences?

Evidence was presented in Chapter Six which showed that for the same approach to the board, changes in board stiffness could be compensated for by alterations to leg spring stiffness, such that at takeoff the angular, horizontal and vertical velocities were within 3.3%, 1.0% and 7.5% respectively of the original values. The relationship between board and leg spring stiffnesses was non-linear, with the leg spring stiffness reducing as the board spring stiffness was increased. Others (e.g. Ferris and Farley, 1997) have also found that humans compensate for surface stiffness changes by altering their leg stiffness to produce an overall stiffness of leg and surface which is constant. However it has been pointed out (Alexander, 1997; Ferris and Farley, 1997) that this is only likely to be feasible when surface and subject

stiffnesses are 'similar' (due to the fact that the overall stiffness is the reciprocal of the sum of the constituent compliances, therefore the most compliant component will dominate the result if there is much difference between components). Results from this study show that this is the case in vault springboard contacts.

Modifying the horizontal velocity or spring angle at touchdown, instead of the leg spring stiffness, were also investigated as possible ways of achieving nearly the same takeoff from the board if the board stiffness was altered. Only the spring angle at touchdown proved to be effective, with a lower board stiffness requiring a reduced spring angle, while a higher board stiffness required an increased spring angle. However the results showed quite sharp minima (at a 5% change to spring angle) for the root mean squared differences between the original and board adjusted simulations. This means that gymnasts would have to have precise control over their body angle at touchdown in order to make use of this method of compensation.

Leg spring stiffness or spring angle adjustments were therefore found to be the effective ways to compensate for board spring stiffness changes. To compensate for the same board stiffness alteration, large leg spring stiffness changes were necessary compared with small spring angle adjustments. The ability to achieve small, precise changes to spring angle, or large changes to leg stiffness, might determine which would be the preferred strategy. While changes to horizontal velocity were not as effective, the possibility that adjusting more than one input at a time could be a useful strategy meant that horizontal velocity alterations could still have a function. An example of how a combination of adjustments could be used was proposed and results from the trials analysed in Chapter Five provided evidence that this strategy had been adopted.

What modifications to a gymnast's approach to and contact with the springboard are most effective for achieving specific changes to preflight?

Considering each of the takeoff variables, the results from Chapter Six (section 6.3.3) revealed that:

- increases to angular velocity and horizontal velocity at takeoff were produced most effectively by increasing either the spring angle or the horizontal velocity at touchdown, or both;

- vertical velocity at takeoff was increased most effectively by *reducing* the spring angle at touchdown (i.e. leaning back more); increasing board stiffness (by board adjustment or point of contact with the board) was also effective;

- increasing the spring angle at takeoff (i.e. taking off with a greater forward lean) was best achieved by increasing the spring angle at touchdown.

In deciding upon the input to alter in order to achieve a particular change to takeoff, the other effects of alterations to that input must be considered. For example, if more angular velocity at takeoff is desired, increasing either the horizontal velocity or spring angle at touchdown would be effective. However (to achieve the same increase in angular velocity) increasing the spring angle at touchdown leads to a much greater reduction in vertical velocity at takeoff than increasing horizontal velocity at touchdown. Horizontal velocity increases still lead to slight reductions in vertical velocity, but this could be compensated for by striking a stiffer part of the springboard and/or making the leg spring stiffer. This is another example (see also Chapter Six, section 6.4.2) which indicates that a combination of adjustments may be a preferable strategy.

In addition to looking at the effectiveness of a particular input in altering some aspect of the takeoff, consideration must also be given to the ability of a gymnast to control each variable. Adjusting the spring angle at touchdown may be effective in principle, but the simulations show that the takeoff is quite sensitive to this input, therefore the ability of the gymnast to make small modifications to the angle would be critical. Similarly, the variation in springboard stiffness, as a function of the point of contact with its surface, could be used to alter the takeoff if the point of contact could be accurately controlled. This possibility has not been discussed in the coaching literature, though some gymnasts have reported taking it into consideration. Adjustments to horizontal velocity at touchdown and leg spring stiffness would not require such precision and so may be more useful in practice. Evidence from the literature which lent some support to the use of horizontal velocity to alter the angular velocity at takeoff was discussed in Chapter Six.

The identification of several ways in which to alter the takeoff from the springboard has implications for training and conditioning. To make use of the influence of the touchdown angle or foot contact position, gymnasts would clearly have to train to achieve the necessary control over these factors. Furthermore, although achieving approach speeds higher than 7.5 to 8 $m.s^{-1}$ should be relatively straightforward, maintaining control of the other inputs at the same time is more difficult. This and other studies (e.g. Ferris and Farley, 1997) have found that humans can change their leg stiffnesses, but it has not been established that leg stiffness is consciously controlled. Farley and Gonzalez (1996) suggested that leg stiffness may be adjusted through limb posture changes (e.g. McMahon and Greene, 1979; McMahon, Valiant and Frederick, 1987) and by changing the activation of muscles acting about the leg joints. Komi (1983) also expected training to influence viscoelastic behaviour of muscle. Therefore

appropriate conditioning should enable gymnasts to achieve greater leg stiffnesses and to increase their awareness of and control over this factor.

7.4 FUTURE STUDIES

Having developed the models, the most obvious direction for the future is to extend the application of the models. As discussed in Chapter Six, the way in which two springs in series combine to act like a single spring, means that where the two springs have very different stiffnesses, the influence of the softer spring will dominate. Although the springs in the two spring model are not constrained to be in line, the same general principle of combined stiffness was demonstrated. The implication is that the two spring model would be more beneficial for exploring the mechanics of rebounds from relatively low stiffness surfaces such as tumbling, than it would for investigating running on hard surfaces, for example, where the one spring model would be adequate.

The results of the simulations in Chapter Six led to a number of strategies for altering the springboard contact being identified. However, it was also noted that to be able to use some of these strategies gymnasts would have to be able to adjust their approach to and contact with the springboard precisely. It would therefore be informative to explore the approach and contact to determine consistency and the precision with which adjustments can be made (e.g. to contact point with the springboard). This would identify those inputs which could be utilized and indicate the effects on takeoff of any inconsistencies found. Using a difficult vault would encourage the subjects to be as consistent as possible.

This and other studies have shown that leg stiffness varies (e.g. when asked to hop at different frequencies, on different surfaces or run with varying amounts of knee flexion) but the ability of subjects specifically to control leg stiffnesses has not been explored. If leg stiffness cannot be controlled consciously, then it cannot be used as a direct way to alter springboard contact or any other surface interaction. This could be investigated for an activity, such as stationary hopping, which has a minimum number of extraneous factors for the subject(s) to consider.

Allied to the ability to change leg stiffness is the question of the source of the stiffness. Alexander and Vernon (1975) differentiated between the true elasticity of materials such as tendon and the way that muscles can act like elastic structures ('pseudoelasticity'), while others have suggested that joint angles and muscle activation may be used to affect leg stiffness (e.g. Blickhan, 1989; Farley and Gonzalez, 1996; Greene and McMahon, 1979). Calculating leg stiffness for subjects performing small oscillations over a constrained range

of joint angles at a specified frequency while carrying varying additional loads (similar to Greene and McMahon, 1979) would enable the true elastic and pseudoelastic components of stiffness to be investigated. Similarly, comparing one legged and two legged stiffnesses for the same activities would also shed light on the sources of the stiffness. In these situations the stiffness component due just to (linearly) elastic materials should vary in a predictable way whereas the pseudo-elastic components probably would not. For example the component due to linearly elastic materials should be doubled for two legs, whereas pseudoelastic components might not double, in the way that two legs together are not normally twice as strong as an individual leg (Howard and Enoka, 1991).

An indication of the range of leg stiffnesses which are possible was identified in this study and by others (see Tables 2.2 and 6.2). The extent to which the range might be extended through conditioning, would help to determine practical limits to the changes the simulations indicated would be achievable. Leg stiffness limitations affect not only changes which the stiffness itself can bring about, but also the effectiveness of other alterations (e.g. increasing horizontal velocity at touchdown beyond the point where leg stiffness can produce a takeoff at the correct angle). The influence of conditioning on leg stiffness depends to some extent on the source of leg stiffness, for example increased muscle strength would imply an increase in the number of actin-myosin cross-bridges used, with each one contributing to the overall stiffness of the muscle.

7.5 SUMMARY

This study investigated the mechanics of the springboard contact phase of gymnastic vaulting by using mathematical models in combination with data from vaults performed by an elite gymnast. It has demonstrated the utility of mass-spring models which incorporate angular motion for exploring the influence of touchdown kinematics and spring stiffnesses on the takeoff from the springboard. In addition to improving the mechanical understanding of springboard contact, the results of the study may be useful for identifying performance strategies for gymnasts. Possible avenues for future research involving the application of the mass-spring models and the investigation of the physical underpinning of the leg spring stiffness have been identified.

REFERENCES

Abdel-Aziz, Y. I. and Karara, H. M. (1971) Direct linear transformation from comparator coordinates into object space coordinates in close-range photogrammetry. In *Proceedings of the Symposium on Close-Range Photogrammetry*, pp. 1-18. American Society of Photogrammetry, Falls Church, VA.

Ackland, T. R., Blanksby, B. A. and Bloomfield, J. (1988) Inertial characteristics of adolescent male body segments. *Journal of Biomechanics*, **21**, 319-327.

Ackland, T. R., Henson, P. W. and Bailey, D. A. (1988) The uniform density assumption: Its effect upon the estimation of body segmental intertial parameters. *International Journal of Sport Biomechanics*, **4**, 146-155.

Alexander, R. McN. (1974) The mechanics of jumping by a dog (*Canis familiaris*). *Journal of Zoology*, **173**, 549-573.

Alexander, R. McN. (1984) Walking and running. *American Scientist*, **72**, 348-354.

Alexander, R. McN. (1988) The spring in your step: The role of elastic mechanisms in human running. In *Biomechanics XI-A* (Edited by de Groot, G., Hollander, A. P., Huijing, P. A. and van Ingen Schenau, G.J.), pp. 17-25. Free University Press, Amsterdam.

Alexander, R. McN. (1989) Sequential joint extension in jumping. *Human Movement Science*, **8**, 339-345.

Alexander, R. McN. (1990a) Three uses for springs in legged locomotion. *International Journal of Robotics Research*, **9**, 53-61.

Alexander, R. McN. (1990b) Optimum take-off techniques for high and long jumps. *Philosophical Transactions of the Royal Society*, **329**, 3-10.

Alexander, R. McN. (1991a) Optimum timing of muscle activation for simple models of throwing. *Journal of Theoretical Biology*, **150**, 349-372.

Alexander, R. McN. (1991b) Energy-saving mechanisms in walking and running. *Journal of Experimental Biology*, **160**, 55-69.

Alexander, R. McN. (1992) Simple models of walking and jumping. *Human Movement Science*, **11**, 3-9.

Alexander, R. McN. (1997) Invited editorial on "Interaction of leg stiffness and surface stiffness during human hopping". *Journal of Applied Physiology*, **82**, 13-14.

Alexander, R. McN. and Bennet-Clark, H. C. (1977) Storage of elastic strain energy in muscle and other tissues. *Nature*, **265**, 114-117.

Alexander, R. McN. and Vernon, A. (1975) The mechanics of hopping by kangaroos (Macropodidae). *Journal of Zoology*, **177**, 265-303.

Angulo, R. M. and Dapena, J. (1992) Comparison of film and video techniques for estimating three-dimensional coordinates within a large field. *International Journal of Sport Biomechanics*, **8**, 145-151.

Bahlsen, H. A. and Nigg, B. M. (1987) Estimation of impact forces using the idea of an effective mass. In *Biomechanics X-B* (Edited by Jonsson, B.), pp. 837-841. Human Kinetics Publishers, Champaign.

Ball, K. A. and Pierrynowski, M. R. (1988) A modified direct linear transformation (DLT) calibration procedure to improve the accuracy of 3D reconstruction for large volumes. In *Biomechanics XI-B* (Edited by de Groot, G., Hollander, A. P., Huijing, P. A. and van Ingen Schenau, G. J.), pp. 1045-1050. Free University Press, Amsterdam.

Barford, N. C. (1985) *Experimental measurements: Precision, error and truth* (Second edition). John Wiley & Sons, Chichester.

Barter, J. T. (1957) *Estimation of the mass of body segments. WADC Technical Report 57-260*. Wright-Patterson Air Force Base, OH.

Bartlett, R. M. (1997) *Introduction to Sports Biomechanics*. E & FN Spon, London.

Bartlett, R. M., Messenger, N. and Lindsay, M. (1997) Force platform. In *Biomechanical Analysis of Movement in Sport and Exercise* (Edited by Bartlett, R. M.), pp. 31-36. The British Association of Sport and Exercise Sciences, Leeds.

Bergemann, B. W. (1974) Three-dimensional cinematography: a flexible approach. *Research Quarterly*, **45**, 302-309.

Berme, N. (1990) Measurement of force, pressure, and muscle activity: 8.1 Load transducers. In *Biomechanics of Human Movement: applications in rehabilitation, sports and ergonomics* (Edited by Berme, N. and Cappozzo, A.), pp. 140-149. Bertec Corporation, Worthington, OH.

Blickhan, R. (1989) The spring-mass model for running and hopping. *Journal of Biomechanics*, **22**, 1217-1227.

Blickhan, R., Friedrichs, A., Rebhan, F., Schmalz, T. and Wank, V. (1995) Influence of speed, stiffness, and angle of attack on jumping distance. In *Proceedings of the XIVth International Society of Biomechanics Congress*, pp. 108-109. Gummerus, Finland.

Bobbert, M. F. and Schamhardt, H. C. (1990) Accuracy of determining the point of force application with piezoelectric force plates. *Journal of Biomechanics*, **23**, 705-710.

Bolton, W. (1994) *Ordinary Differential Equations.* Longman Scientific and Technical, Harlow.

Borse, G. J. (1991) *FORTRAN 77 and numerical methods for engineers* (Second edition). PWS-KENT, Boston.

Bouisset, S. and Pertuzon, E. (1968) Experimental determination of the moment of inertia of limb segments. In *Biomechanics I, 1st International Seminar Zurich*, pp. 106-109. Karger, Basel/New York.

Bratley, P., Fox, B. L. and Schrage, L. E. (1987) *A Guide to Simulation* (Second edition). Springer-Verlag New York Inc., New York.

Braune, W. and Fischer, O. (1889) Über den Schwerpunkt des menschlichen Körpers, mit Rücksicht auf die Aüsrustung des deutschen Infanteristen. *Abhandlung der Königl. Sächsischen Gesellschaft der Wissenschaften*, **26**, 561-672. (Cited by Barter, 1957).

Brooks, C. B. and Jacobs, A. M. (1975) The gamma mass scanning technique for inertial anthropometric measurement. *Medicine and Science in Sports*, 7, 290-294.

Brüggemann, G.-P. (1987) Biomechanics in Gymnastics. In *Medicine and Sport Science: 25. Current Research in Sports Biomechanics* (Edited by van Gheluwe, B. and Atha, J.), pp. 142-176. Karger, Basel.

Brüggemann, G.-P. (1994) Biomechanics of gymnastic techniques. *Sport Science Review*, **3**, 79-120.

Brüggemann, G.-P. and Nissinen, M. A. (1981) Analyse kinematischer Merkmale des Handstützüberschlags beim Pferdsprung. *Leistungssport*, **11**, 537-547. (Cited by Brüggemann, 1987)

Cappozzo, A. and Berme, N. (1990) Subject-specific segmental inertia parameter determination - a survey of current methods. In *Biomechanics of Human Movement: Application in Rehabilitation, Sports and Ergonomics* (Edited by Berme, N. and Cappozzo, A.), pp. 179-185. Bertec Corporation, Worthington, OH.

Cavagna, G. A. (1970) Elastic bounce of the body. *Journal of Applied Physiology*, **29**, 279-282.

Cavagna, G. A., Franzetti, P., Heglund, N. C. and Willems, P. (1988) The determination of the step frequency in running, trotting and hopping in man and other vertebrates. *Journal of Physiology*, **399**, 81-92.

Cavagna, G. A. and Kaneko, M. (1977) Mechanical work and efficiency in level walking and running. *Journal of Physiology*, **268**, 467-481.

Cavagna, G. A., Saibene, F. P. and Margaria, R. (1964) Mechanical work in running. *Journal of Applied Physiology*, **19**, 249-256.

Cavanagh, P. R. and Gregor, R. J. (1974) The quick-release method for estimating the moment of inertia of the shank and foot. In *Biomechanics IV* (Edited by Nelson, R. C. and Morehouse, C. A.), pp. 524-530. Macmillan Press Ltd, London.

Cavanagh, P. R. and Kram, R. (1985) The efficiency of human movement- a statement of the problem. *Medicine and Science in Sports and Exercise*, **17**, 304-308.

Challis, J. H. (1995) A multiphase calibration procedure for the direct linear transformation. *Journal of Applied Biomechanics*, **11**, 351-358.

Challis, J. H. (1996) Accuracy of human limb moment of inertia estimations and their influence on resultant joint moments. *Journal of Applied Biomechanics*, **12**, 517-530.

Challis, J. H. (1997) Estimation and propagation of experimental errors. In *Biomechanical Analysis of Movement in Sport and Exercise* (Edited by Bartlett, R. M.), pp. 105-124. The British Association of Sport and Exercise Sciences, Leeds.

Challis, J. H. and Kerwin, D. G. (1988) An evaluation of splines in biomechanical analysis. In *Biomechanics XI-B* (Edited by de Groot, G., Hollander, A. P., Huijing, P. A. and Ingen Schenau GJ), pp. 1057-1061. Free University Press, Amsterdam.

Challis, J. H. and Kerwin, D. G. (1989) An evaluation of cine-photogrammetric techniques. *Journal of Sports Sciences*, **7**, 72.

Challis, J. H. and Kerwin, D. G. (1992) Accuracy assessment and control point configuration when using the DLT for photogrammetry. *Journal of Biomechanics*, **25**, 1053-1058.

Challis, J. H., Bartlett, R. M. and Yeadon, M. R. (1997) Image-based motion analysis. In *Biomechanical Analysis of Movement in Sport and Exercise* (Edited by Bartlett, R. M.), pp. 7-30. The British Association of Sport and Exercise Sciences, Leeds.

Challis, J. H., Yeadon, M. R. and Kerwin, D. G. (1991) A comparison of numerical differentiation techniques. In *Proceedings of the Sports Biomechanics Section of the British Association of Sports Sciences* (Vol. 16) (Edited by Yeadon, M. R.). The British Association of Sports Sciences, Leeds.

Chandler, R. F., Clauser, C. E., McConville, J. T., Reynolds, H. M. and Young, J. W. (1975) *Investigation of inertial properties of the human body. AMRL-TR-74-137*. Wright-Patterson Air Force Base, OH.

Cheetham, P. J. (1982) The men's handspring front 1½ somersault vault: relationship of early phase to postflight. Unpublished MSc Thesis, Arizona State University.

Chen, L., Armstrong, C. W. and Raftopoulos, D. D. (1994) An investigation on the accuracy of three-dimensional space reconstruction using the direct linear transformation technique. *Journal of Biomechanics*, **27**, 493-500.

Clarke, T. E., Frederick, E. C. and Cooper, L. B. (1982) The effects of shoe cushioning upon selected force and temporal parameters in running. *Medicine and Science in Sports*, **14**, 144.

Clarke, T. E., Frederick, E. C. and Cooper, L. B. (1983) The effects of shoe cushioning upon ground reaction forces in running. *International Journal of Sports Medicine*, **4**, 247-251. (Cited by Frederick, 1986).

Clauser, C. E., McConville, J. T. and Young, J. W. (1969) *Weight, volume and centre of mass of segments of the human body. AMRL-TR-69-70*. Wright-Patterson Air Force Base, OH.

Dainis, A. (1979) Cinematographic analysis of the handspring vault. *Research Quarterly*, **50**, 341-349.

Dainis, A. (1981) A model for gymnastics vaulting. *Medicine and Science in Sports and Exercise*, **13**, 34-43.

Dapena, J., Harman, E. A. and Miller, J. A. (1982) Three-dimensional cinematography with control object of unknown shape. *Journal of Biomechanics*, **15**, 11-19.

Dawson, T. J. and Taylor, C. R. (1973) Energetic cost of locomotion in kangaroos. *Nature*, **246**, 313-314.

Dempster, W. T. (1955) *Space requirements of the seated operator. WADC Technical Report (TR-55-159)*. Wright-Patterson Air Force Base, OH.

Dillman, C. J., Cheetham, P. J. and Smith, S. L. (1985) A kinematic analysis of men's Olympic long horse vaulting. *International Journal of Sport Biomechanics*, **1**, 96-110.

Draper, J. A. (1981) The biomechanical determinants of post-flight performance in side-horse vaulting. Unpublished M.Phil Thesis, Loughborough University of Technology.

Drillis, R. and Contini, R. (1966) *Technical Report No 1166.03*. N.Y.U., New York.

Edwards, D. and Hamson, M. (1989) *Guide to Mathematical Modelling*. Macmillan Education Ltd, Basingstoke.

Farley, C. T., Blickhan, R., Saito, J. and Taylor, R. (1991) Hopping frequency in humans: a test of how springs set stride frequency in bouncing gaits. *Journal of Applied Physiology*, **71**, 2127-2132.

Farley, C. T., Blickhan, R. and Taylor, C. R. (1985) Mechanics of human hopping: model and experiments. *American Zoologist*, **25**, 54A.

Farley, C. T., Glasheen, J. and McMahon, T. A. (1993) Running Springs: speed and animal size. *Journal of Experimental Biology*, **185**, 71-86.

Farley, C. T. and González, O. (1996) Leg stiffness and stride frequency in human running. *Journal of Biomechanics*, **29**, 181-186.

Fédération Internationale de Gymnastique (1994) *Norm-testing of functional properties of FIG gymnastic equipment and FIG mats*. Fédération Internationale de Gymnastique, Switzerland.

Fédération Internationale de Gymnastique (1997) *The code of points: artistic gymnastics for men*. Fédération Internationale de Gymnastique, Switzerland.

Ferris, D. P. and Farley, C. T. (1997) Interaction of leg stiffness and surface stiffness during human hopping. *Journal of Applied Physiology*, **82**, 15-22.

Fischer, O. (1906) *Theoretische Grundlagen für eine Mechanik der lebenden Körper*. Teubner, Berlin. (Cited by Barter, 1957).

Forsythe, G. E., Malcolm, M. A. and Moler, C. B. (1977) *Computer methods for mathematical computations*. Prentice-Hall Inc., Englewood Cliffs.

Frederick, E.C. (1986) Kinematically mediated effects of sport shoe design: a review. *Journal of Sports Sciences*, **4**, 169-184.

Fukuda, H., Miyashita, M. and Fukuoka, M. (1987) Unconscious control of impact force during landing. In *Biomechanics X-A* (Edited by Jonsson, B.), pp. 301-305. Human Kinetics Publishers Inc, Champaign.

Gagnon, Y. and Bourassa, P. (1987) Simulation and experiment of a running motion over deformable visco-elastic surfaces. In *Abstracts of the XIth International Congress of Biomehcanics* (Edited by Whiting, H.T.A., Hollander, A.P., van Campen, D.H., Clarijs, J.P., de Groot, G., van Ingen Schenau, G.J., Huijing, P.A., Huiskes, R. and Rozendal, R.H.), p. 95. Free University Press, Amsterdam.

Gajdos, A. (1997) *Artistic Gymnastics: a history of development and Olympic competition*. Loughborough University, Loughborough.

George, G. S. (1971) Long horse angles of incidence specific to reuter board contact. *Modern Gymnast*, **12**, 22.

George, G. S. (1980) *Biomechanics of Women's Gymnastics*. Prentice-Hall Inc, Englewood Cliffs.

Gheluwe, B. van (1974) A new three-dimensional filming technique involving simplified alignment and measuring procedures. In *Biomechanics IV* (Edited by Nelson, R. C. and Morehouse, C. A.), pp. 476-481. Macmillan Press Ltd, London.

Greene, P. R. and McMahon, T. A. (1979) Reflex stiffness of man's anti-gravity muscles during kneebends while carrying extra weights. *Journal of Biomechanics*, **12**, 881-891.

Greig, M. P., Yeadon, M. R. and Kerwin, D. G. (1996) The influence of approach parameters on high jumping performance. In *Proceedings of the Biomechanics Section of the British Association of Sport and Exercise Sciences No. 21*, 25-28. BASES, Loughborough.

Griffiths, R. I. (1989) The mechanics of the medial gastrocnemius muscle in the freely hopping wallaby (Thylogale billardierii). *Journal of Experimental Biology*, **147**, 439-456.

Griffiths, R. I. (1991) Shortening of muscle fibres during stretch of the active cat medial gastrocnemius muscle: the role of tendon compliance. *Journal of Physiology*, **436**, 219-236.

Hall, M. G., Fleming, H. E., Dolan, M. J., Millbank, S. F. D. and Paul, J. P. (1996) Static in situ calibration of force plates. *Journal of Biomechanics*, **29**, 659-665.

Hanavan, E.P. (1964) *A mathematical model of the human body. AMRL-TR-64-102*. Wright-Patterson Air Force Base, OH. (Cited by Nigg, 1994a).

Hatze, H. (1980) A mathematical model for the computational determination of parameter values of anthropomorphic segments. *Journal of Biomechanics*, **13**, 833-843.

Hatze, H. (1981) A comprehensive model for the human motion simulation and its application to the take-off phase of the long jump. *Journal of Biomechanics*, **14**, 135-142.

Hatze, H. (1981) The use of optimally regularized Fourier series for estimating higher-order derivatives of noisy biomechanical data. *Journal of Biomechanics*, **14**, 13-18.

Hatze, H. (1990) Data conditioning and differentiation techniques. In *Biomechanics of human movement: applications in rehabilitation, sports and ergonomics* (Edited by Berme, N. and Cappozzo, A.), pp. 237-248. Bertec Corporation, Worthington, OH.

Hay, J. G. (1988) Approach strategies in the long jump. *International Journal of Sport Biomechanics*, **4**, 114-129.

Hay, J. G. (1993) *The Biomechanics of Sports Techniques* (Fourth edition). Prentice-Hall International, Inc., Englewood Cliffs.

Hay, J. G. and Reid, J. G. (1982) *The anatomical and mechanical bases of human motion*. Prentice-Hall, Inc., Englewood Cliffs.

Hay, J. G., Wilson, B. D., Dapena, J. and Woodworth, G. G. (1977) A computational technique to determine the angular momentum of a human body. *Journal of Biomechanics*, **10**, 269-277.

He, J., Kram, R. and McMahon, T. A. (1991) Mechanics of running under simulated low gravity. *Journal of Applied Physiology*, **71**, 863-870.

Hill, A. V. (1950) The series elastic component of muscle. *Proceedings of the Royal Society*, **Series B 137**, 273-280.

Hinrichs, R. N. (1985) Regression equations to predict segmental moments of inertia from anthropometric measurements: an extension of the data of Chandler et al (1975). *Journal of Biomechanics*, **18**, 621-624.

Hinrichs, R. N. (1990) Adjustments to the segment center of mass proportions of Clauser et al(1969). *Journal of Biomechanics*, **23**, 949-951.

Hinrichs, R. N. and McLean, S. P. (1995) NLT and extrapolated DLT: 3-D cinematography alternatives for enlarging the volume of calibration. *Journal of Biomechanics*, **28**, 1219-1223.

Howard, J. D. and Enoka, R. M. (1991) Maximum bilateral contractions are modified by neurally mediated interlimb effects. *Journal of Applied Physiology*, **70**, 306-316.

Huang, H. K. and Suarez, F. R. (1983) Evaluation of cross sectional geometry and mass density distributions of humans and laboratory animals using computerized tomography. *Journal of Biomechanics*, **16**, 821-832.

Huang, H. K. and Wu, S. C. (1976) The evaluation of mass densities of the human body in vivo from CT scans. *Computers in Biology and Medicine*, **6**, 337-343.

Ingen Schenau, G. J. van (1984) An alternative view of the concept of utilisation of elastic energy in human movement. *Human Movement Science*, **3**, 301-336.

Jackson, K. M. (1979) Fitting of mathematical functions to biomechanical data. *IEEE Transactions on Biomedical Engineering*, **BME-26**, 122-124.

Jensen, R. K. (1978) Estimation of biomechanical properties of three body types using a photogrammetric method. *Journal of Biomechanics*, **11**, 349-358.

Jensen, R. K. (1986) Body segment mass, radius and radius of gyration proportions of children. *Journal of Biomechanics*, **19**, 359-368.

Jensen, R. K. and Fletcher, P. (1994) Distribution of mass to the segments of elderly males and females. *Journal of Biomechanics*, **27**, 89-96.

Jensen, R. K. and Nassas, G. (1988) Growth of segmental princpal moments of inertia between four and twenty years. *Medicine and Science in Sport and Exercise*, **20**, 594-604.

Jones, I. C. and Miller, D. I. (1996) Influence of fulcrum position on springboard response and takeoff performance in the running approach. *Journal of Applied Biomechanics*, **12**, 383-408.

Kennedy, P. W., Wright, D. L. and Smith, G. A. (1989) Comparison of film and video techniques for three-dimensional DLT repredictions. *International Journal of Sport Biomechanics*, **5**, 457-460.

Ker, R. F., Bennett, M. B., Alexander, R. McN. and Kester, R. C. (1989) Foot strike and the properties of the human heel pad. *Journal of Engineering Medicine*, **203**, 191-196.

Ker, R. F., Bennett, M. B., Bibby, S. R., Kester, R. C. and Alexander, R. McN. (1987) The spring in the arch of the human foot. *Nature*, **235**, 147-149.

Kerwin, D. G. (1994) Video and cinefilm digitisation accuracy. In *Proceedings of the Biomechanics Section of The British Association of Sport and Exercise Sciences* (Vol. 19) (Edited by Watkins, J.), pp. 21-24. The British Association of Sport and Exercise Sciences. Leeds.

Kerwin, D. G. and Chapman, G. M. (1988a) Resonant mode shapes of a force plate and its mounting. In *Biomechanics XI-B* (Edited by de Groot, G., Hollander, A. P., Huijing, P. A., and van Ingen Schenau, G. J.), pp. 978-983. Free University Press, Amsterdam.

Kerwin, D. G. and Chapman, G. M. (1988b) The frequency content of hurdling and running. In *Biomechanics in Sport* (Edited by the Institute of Mechanical Engineers), pp. 107-111. Institute of Mechanical Engineers, London.

Kerwin, D. G. and Littlechild, K. M. (1989) Energy storage characteristics of a gymnastic reuther board. *Journal of Sports Sciences*, **7**, 70-71.

Kerwin, D. G., Harwood, M. J. and Yeadon, M. R. (1993) Hand placement techniques in long horse vaulting. *Journal of Sports Sciences*, **11**, 329-335.

Kerwin, D. G., Yeadon, M. R. and Harwood, M. J. (1993) High bar release in triple somersault dismounts. *Journal of Applied Biomechanics*, **9**, 279-286.

Kim, W., Voloshin, A. S. and Johnson, S. H. (1994) Modeling of heel strike transients during running. *Human Movement Science*, **13**, 221-244.

King, M. A. (1998) Contributions to performance in dynamic jumps. Unpublished doctoral dissertation, Loughborough University.

Komi, P. V. (1983) Elastic potentiation of muscle and its influence on sport performance. In *Biomechanics and Performance in Sport* (Edited by Baumann, W.), pp. 59-70. Verlag Karl Hofmann, Schorndorf.

Kreighbaum, E. (1974) The mechanics of the use of the Reuther board during side horse vaulting. In *Biomechanics IV* (Edited by Nelson, R. C. and Morehouse, C. A.), pp. 137-143. Macmillan Press Ltd, London.

Kreighbaum, E. (1979) Qualitative descriptions of the lower leg and board movements during gymnastics vaulting. In *Science in Gymnastics* (Edited by Terauds, J. and Daniels, D. B.), pp. 25-30. Academic Publishers, Del Mar.

Kwon, Y.-H. (1996) Effects of the method of body segment parameter estimation on airborne angular momentum. *Journal of Applied Biomechanics*, **12**, 413-430.

Kwon, Y.-H., Fortney, V. L. and Shin, I.-S. (1990) 3-D analysis of Yurchenko vaults performed by female gymnasts during the 1988 Seoul Olympic Games. *International Journal of Sport Biomechanics*, **6**, 157-176.

Lees, A. (1980) An optimised film analysis method based on finite difference techniques. *Journal of Human Movement Studies*, **6**, 165-180.

Lees, A., Fowler, N. and Derby, D. (1993) A biomechanical analysis of the last stride, touch-down and take-off characteristics of the women's long jump. *Journal of Sports Sciences*, **11**, 303-314.

Lees, A., Graham-Smith, P. and Fowler, N. (1994) A biomechanical analysis of the last stride, touchdown, and takeoff characteristics of the men's long jump *International Journal of Sport Biomechanics*, **10**, 61-78.

Lees, A. and Barton,G. (1996). The interpretation of relative momentum data to assess the contribution of the free limbs to the generation of vertical velocity in sports activities. *Journal of Sports Sciences*, **14**, 503-511.

Loken, N. C. and Willoughby, R. J. (1977) *The Complete Book of Gymnastics*. Prentice-Hall Inc., Englewood Cliffs.

Luhtanen, P. and Komi, P. V. (1980) Force-, power-, and elasticity-velocity relationships in walking, running, and jumping. *European Journal of Applied Physiology*, **44**, 279-289.

Martin, P. E., Mungiole, M., Marzke, M. W. and Longhill, J. M. (1989) The use of magnetic resonance imaging for measuring segment inertial properties. *Journal of Biomechanics*, **22**, 367-376.

Martin, T. P. and Pongratz, M. B. (1974) Mathematical correction for photographic perspective error. *Research Quarterly*, **45**, 318-323.

Matsuo, A., Ozawa, H., Goda, K. and Fukunaga, T. (1995) Moment of inertia of whole body using an oscillating table in adolescent boys. *Journal of Biomechanics*, **28**, 219-223.

McLaughlin, T. M., Dillman, C. J. and Lardner, T. J. (1977) Biomechanical analysis with cubic spline. *Research Quarterly*, **48**, 569-581.

McMahon, T. A. (1985) The role of compliance in mammalian running gaits. *Journal of Experimental Biology*, **115**, 263-283.

McMahon, T. A. and Cheng, G. C. (1990) The mechanics of running: How does stiffness couple with speed? *Journal of Biomechanics*, **23**, Supplement 1, 65-78.

McMahon, T. A. and Greene, P. R. (1979) The influence of track compliance on running. *Journal of Biomechanics*, **12**, 893-904.

McMahon, T. A., Valiant, G. and Frederick, E. C. (1987) Groucho running. *Journal of Applied Physiology*, **62**, 2326-2337.

McNitt-Gray, J. L., Yokoi, T. and Millward, C. (1993) Landing strategy adjustments made by female gymnasts in response to drop height and mat composition. *Journal of Applied Biomechanics*, **9**, 173-190.

McNitt-Gray, J. L., Yokoi, T. and Millward, C. (1994) Landing strategies used by gymnasts on different surfaces. *Journal of Applied Biomechanics*, **10**, 237-252.

Medley, D.G. (1982) *An Introduction to Mechanics and Modelling*. Heinemann Educational Books Ltd, London.

Meerschaert, M. M. (1993) *Mathematical Modelling*. Academic Press Inc., London.

Melvill Jones, G. and Watt, D. G. D. (1971) Observations on the control of stepping and hopping movements in man. *Journal of Physiology*, **219**, 709-727.

Mihram, G. A. (1972) The Modeling Process. *IEEE Transactions on Systems, Man and Cybernetics*, **SMC-2**, 621-629.

Miller, D. I. (1975) Computer simulation of human motion. In *Techniques for the Analysis of Human Motion* (Edited by Grieve, D. W., Miller, D. I., Mitchelson, D., Paul, J. and Smith, A. J.), pp. 69-105. Lepus Books, London.

Miller, D. I. and Morrison, W. E. (1975) Prediction of segmental parameters using the Hanavan human body model. *Medicine and Science in Sports*, **7**, 207-212.

Morgan, D. L., Proske, U. and Warren, D. (1978) Measurement of muscle stiffness and the mechanism of elastic storage of energy in hopping kangaroos. *Journal of Physiology*, **282**, 253-261.

Mungiole, M. and Martin, P. E. (1990) Estimating segment inertial properties: comparison of magnetic resonance imaging with existing methods. *Journal of Biomechanics*, **23**, 1039-1046.

Murthy, D. N. P., Page, N. W. and Rodin, E. Y. (1990) *Mathematical modelling: a tool for problem solving in engineering, physical, biological and social sciences*. Pergamon Press, Oxford.

Nelson, R. C., Gross, T. S. and Street, G. M. (1985) Vaults performed by female olympic gymnasts: a biomechanical profile. *International Journal of Sport Biomechanics*, **1**, 111-121.

Nigg, B. M. (1994a) Inertial properties of the human or animal body. In *Biomechanics of the Musculo-Skeletal System* (Edited by Nigg, B. M. and Herzog, W.), pp. 337-364. John Wiley and Sons Ltd, Chichester.

Nigg, B. M. (1994b) Force. In *Biomechanics of the Musculo-Skeletal System* (Edited by Nigg, B. M. and Herzog, W.), pp. 200-224. John Wiley and Sons Ltd, Chichester.

Nigg, B. M. (1994c) General comments about modelling. In *Biomechanics of the Musculo-Skeletal System* (Edited by Nigg, B. M. and Herzog, W.), pp. 367-379. John Wiley and Sons Ltd, Chichester.

Nigg, B. M., Herzog, W. and Read, J. L. (1988) Effect of viscoelastic shoe insoles on vertical impact forces in heel-toe running. *The American Journal of Sports Medicine*, **16**, 70-75.

O'Connor, B. J., Yack, H. J. and White, S. C. (1995) Reducing errors in kinetic calculations: improved synchronization of video and ground reaction force records. *Journal of Applied Biomechanics*, **11**, 216-223.

Panjabi, M. (1979) Validation of mechanical models. *Journal of Biomechanics*, **12**, 238.

Pflughoeft, M. (1989) Men's vaulting: learning to contact the board correctly. *International Gymnast*, **April**, 53.

Phillips, S. J. and Roberts, E. M. (1983) Spline solution to terminal zero acceleration problems in biomechanical data. *Medicine and Science in Sports and Exercise*, **15**, 382-387.

Plagenhoef, S., Evans, F. G. and Abdelnour, T. (1983) Anatomical data for analyzing human motion. *Research Quarterly for Exercise and Sport*, **54**, 169-178.

Reid, J. G. and Jensen, R. K. (1990) Human Body Segmental Inertia Parameters: A Survey and Status Report. In *American College of Sports Medicine Series. Exercise and Sport Science Reviews* (Vol. 18) (Edited by Pandolf, K. B. and Holloszy, J. O.). pp. 225-241. Williams & Wilkins, Baltimore.

Reinsch, C. H. (1967) Smoothing by spline functions. *Numerische Mathematik*, **10**, 177-183.

Reinsch, C. H. (1971) Smoothing by spline functions,II. *Numerische Mathematik*, **16**, 451-454.

Roberts, T. J., Marsh, R. L., Weyand, P. G. and Taylor, C. R. (1997) Muscular force in running Turkeys: the economy of minimizing work. *Science*, **275**, 1113-1115.

Rome, L. C. (1995) A device for synchronizing biomechanical data with cine film. *Journal of Biomechanics*, **28**, 333-338.

Sanders, R. H. and Allen, J. B. (1993) Changes in net joint torques during accommodation to change in surface compliance in a drop jumping task. *Human Movement Science*, **12**, 299-326.

Sanders, R. H. and Wilson, B. D. (1988) Factors contributing to maximum height of dives after takeoff from the 3m springboard. *International Journal of Sport Biomechanics*, **4**, 231-259.

Sanders, R. H. and Wilson, B. D. (1992) Comparison of static and counter movement jumps of unconstrained movement amplitude. *The Australian Journal of Science and Medicine in Sport*, **24**, 79-85.

Sands, W. A. (1982) *Modern Women's Gymnastics*. Sterling Publishing Co. Inc, New York.

Santschi, W. R., du Bois, J. and Omoto, C. (1963) Moments of inertia and centres of gravity of the living human body. AMRL-TDR-63-36.

Schweizer, L. (1985) *Testing procedures for landing mats, surfaces for floor exercises and vaulting boards*. Fédération Internationale de Gymnastique, Freiburg.

Seyfarth, A., Friedrichs, A., Wank, V. and Blickhan, R. (1996) Extended spring-mass model for the take-off phase of long jump. In *Proceedings of the First Annual Congress Frontiers in Sport Science* (Edited by Marconnet, P., Gaulard, J., Margaritis, I. and Tessier, F.), pp. 466-467. University of Nice Sophia-Antipolis, Nice.

Siegler, S., Seliktar, R. and Hyman, W. (1982) Simulation of human gait with the aid of a simple mechanical model. *Journal of Biomechanics*, **15**, 415-425.

Smith, A. J. (1975) The kinetic energy of the human body. *Journal of Human Movement Studies*, **1**, 13-18.

Smith, G. (1989) Padding point extrapolation techniques for the Butterworth digital filter. *Journal of Biomechanics*, **22**, 967-971.

Smith, T. (1982) *Gymnastics: A Mechanical Understanding*. Hodder and Stoughton, London.

Soest, A. J. van , Schwab, A. L., Bobbert, M. F. and van Ingen Schenau, G. J. (1992) SPACAR: a software subroutine package for simulation of the behaviour of biomechanical systems. *Journal of Biomechanics*, **25**, 1219-1226.

Sprigings, E. J. and Yeadon, M. R. (1997) An insight into the reversal of rotation in the Hecht vault. *Human Movement Science*, **16**, 517-532.

Sprigings, E. J., Burko, D. B., Watson, L. G. and Laverty, W. H. (1987) An evaluation of three segmental methods used to predict the location of the total body CG for human airborne movements. *Journal of Human Movement Studies*, **13**, 57-68.

Sprigings, E. J., Stilling, D. S. and Watson, L. G. (1989) Development of a model to represent an aluminium spring board in diving. *International Journal of Sport Biomechanics*, **5**, 297-307.

Sprigings, E. J., Stilling, D. S., Watson, L. G. and Dorotich, P. D. (1990) Measurement of the modeling parameters for a Maxiflex "B" springboard. *International Journal of Sport Biomechanics*, **6**, 325-335.

Sprigings, E.J. and Watson, L.G. (1985) A mathematical search for the optimal timing of the armswing during springboard diving take-offs. In *Biomechanics IX-B* (Edited by Winter, D.A., Norman, R.W., Wells, R.P., Hayes, K.C. and Patla, A.E.), pp. 389-394. Human Kinetics Publishers, Champaign.

Stuart, N. and Sommerville, A. (1980) *Tackle Gymnastics*. Stanley Paul & Co, London.

Swearingen, J. J. (1962) *Determination of centers of gravity of man. Report 62-14*. Civil Aeromedical Research Institute, Federal Aviation Agency, OK.

Takei, Y. (1988) Techniques used in performing handspring and salto forward tucked in gymnastic vaulting. *International Journal of Sport Biomechanics*, **4**, 260-281.

Takei, Y. (1989) Techniques used by elite male gymnasts performing a handspring vault at the 1987 Pan American Games. *International Journal of Sport Biomechanics*, **5**, 1-25.

Takei, Y. (1991) A comparison of techniques used in performing the men's compulsory gymnastic vault at the 1988 Olympics. *International Journal of Sport Biomechanics*, 7, 54-75.

Takei, Y. and Kim, E. J. (1990) Techniques used in performing the handspring and salto forward tucked vault in the 1988 Olympic Games. *International Journal of Sport Biomechanics*, **6**, 111-138.

Takei, Y., Blucker, E. P., Dunn, J. H., Myers, S. A. and Fortney, V. L. (1996) A three-dimensional analysis of the men's compulsory vault performed at the 1992 Olympic Games. *Journal of Applied Biomechanics*, **12**, 237-257.

Tan, J., Kerwin, D. G. and Yeadon, M. R. (1995) Evaluation of the Apex video digitisation system. In *Proceedings of the Biomechanics Section of The British Association of Sport and Exercise Sciences* (Vol. 20) (Edited by Watkins, J.), pp. 5-8. The British Association of Sport and Exercise Sciences, Leeds.

Taylor, B., Bajin, B. and Zivic, T. (1972) *Olympic Gymnastics for Men and Women*. Prentice-Hall Inc, Englewood Cliffs.

Thys, H., Faraggiana, T. and Margaria, R. (1972) Utilization of muscle elasticity in exercise. *Journal of Applied Physiology*, **32**, 491-494.

de Vahl Davis, G. (1986) Numerical methods in engineering and science. Allen and Unwin (Publishers) Ltd, London.

Vaughan, C. L. (1980) A kinetic analysis of basic trampoline stunts. *Journal of Human Movement Studies,* **6**, 236-251.

Vaughan, C. L. (1984) Computer simulation of human motion in sports biomechanics. In *Exercise and Sports Science Reviews* (Volume 12) (Edited by Terjung, R. T.), pp. 373-416. Collamore Press, Lexington.

Vint, P. F. and Hinrichs, R. N. (1996) Endpoint error in smoothing and differentiating raw kinematic data: an evaluation of four popular methods. *Journal of Biomechanics*, **29**, 1637-1642.

Wahba, G. and Wold, S. (1975) A completely automatic french curve: fitting spline functions by cross validation. *Communicatons in Statistics*, **4**, 1-17.

Warren, M. (1972) *The Book of Gymnastics*. Arthur Baker Ltd., London.

White, J. (1989) *Gymnastics in Action*. Stanley Paul, London.

Wilkie, D. R. (1956) Measurement of the series elastic component at various times during a single muscle twitch. *Journal of Physiology*, **134**, 527-530.

Willems, P. A., Cavagna, G. A. and Heglund, N. C. (1995) External, internal and total work in human locomotion. *Journal of Experimental Biology*, **198**, 379-393.

Williams, K. R. and Cavanagh, P. R. (1983) A model for the calculation of mechanical power during distance running. *Journal of Biomechanics*, **16**, 115-128.

Winter, D. A. (1990) *Biomechanics and Motor Control of Human Movement* (Second edition). John Wiley and Sons Inc., New York, NY.

Winter, D. A., Sidwall, H. G. and Hobson, D. A. (1974) Measurement and reduction of noise in kinematics of locomotion. *Journal of Biomechanics*, **7**, 157-159.

Wold, S. (1974) Spline functions in data analysis. *Technometrics*, **16**, 1-11.

Woltring, H. J. (1980) Planar control in multi-camera calibration for three-dimensional gait studies. *Journal of Biomechanics*, **13**, 39-48.

Woltring, H. J. (1986) A Fortran package for generalized, cross-validatory spline smoothing and differentiation. *Advances in Engineering Software*, **8**, 104-113.

Wood, G. A. (1982) Data smoothing and differentiation procedures in biomechanics. In *Exercise and Sport Sciences Reviews*, Volume 10, (Edited by Terjung, R.L.), pp. 308-362. Franklin Institute Press, New York.

Wood, G. A. and Jennings, L. S. (1979) On the use of spline functions for data smoothing. *Journal of Biomechanics*, **12**, 477-479.

Wood, G. A. and Marshall, R. N. (1986) The accuracy of DLT extrapolation in three-dimensional film analysis. *Journal of Biomechanics*, **19**, 781-785.

Yeadon, M. R. (1989) A method for obtaining three-dimensional data on ski jumping using pan and tilt cameras. *International Journal of Sport Biomechanics*, **5**, 238-247.

Yeadon, M. R. (1990a) The simulation of aerial movement - I. The determination of orientation angles from film data. *Journal of Biomechanics*, **23**, 59-66.

Yeadon, M. R. (1990b) The simulation of aerial movement - II. A mathematical inertia model of the human body. *Journal of Biomechanics*, **23**, 67-74.

Yeadon, M. R. (1994) Computer simulation and sport biomechanics. In *Proceedings of the VIIth Biennial Conference of the Canadian Society for Biomechanics* (Edited by Herzog, W., Nigg, B. and van den Bogert, T.), pp. 156-157. Calgary, Alberta.

Yeadon, M. R. and Challis, J. H. (1994) The future of performance-related sports biomechanics research. *Journal of Sports Sciences*, **12**, 3-32.

Yeadon, M. R. and Morlock, M. (1989) The appropriate use of regression equations for the estimation of segmental inertia parameters. *Journal of Biomechanics*, **22**, 683-689.

Yeadon, M. R., Challis, J. H. and Ng, R. (1994) Personalised segmental inertia parameters. *Journal of Biomechanics*, **27**, 770.

Yokoi, T., Shibukawa, K., Ae, M., Ishijama, S. and Hashihari, Y. (1985) Body-segment parameters of Japanese children. In *Biomechanics IX-B* (Edited by Winter, D. A., Norman, R. W., Wells, R. P., Hayes, K. C. and Patla, A. E.), pp. 227-232. Human Kinetics Publishers Inc, Champaign.

Zatsiorsky, V. M. and Seluyanov, V. (1983) The mass and inertia characteristics of the main segments of the human body. In *Biomechanics VIII-B* (Edited by Matsui, H. and Kobayashi, K.), pp. 1152-1159. Human Kinetics Publishers Inc, Champaign.

Zatsiorsky, V. M. and Seluyanov, V. (1985) Estimation of the mass and inertia characteristics of the human body by means of the best predictive regression equations. In *Biomechanics IX-B* (Edited by Winter, D. A., Norman, R. W., Wells, R. P., Hayes, K. C. and Patla, A. E.), pp. 233-239. Human Kinetics Publishers Inc, Champaign.

Zatsiorsky, V. M., Seluyanov, V. and Chugunova, L. (1990) Body Segment Inertial Parameters:9.2 In vivo body segmental inertial parameters determination using a gamma-scanner method. In *Biomechanics of Human Movement: applications in rehabilitation, sports and ergonomics* (Edited by Berme, N. and Cappozzo, A.), pp. 186-202. Bertec Corporation, Worthington, OH.

Zernicke, R. F., Caldwell, G. and Roberts, E. M. (1976) Fitting biomechanical data with cubic spline functions. *Research Quarterly*, **47**, 9-19.

APPENDIX A

This appendix contains information related to the hopping and running jump study reported in Chapter Three.

Appendix A.1 Informed consent.

Appendix A.2 Subject segment masses and proximal ratios derived from Yeadon's (1990b) geometric solid model and Dempster's (1955) ratio data (summarized by Winter, 1990).

APPENDIX A.1

Loughborough University of Technology

INFORMED CONSENT FORM

PURPOSE To obtain anthropometric, kinematic and kinetic data of a subject during hopping and jumping, in order to determine the ground reaction force-mass centre displacement relationship.

PROCEDURES Cine cameras and a force plate will be used to collect information while performing two footed stationary and forward hopping and two footed running jumps. A number of trials will be requested, with suitable breaks to minimize fatigue and boredom.
Anthropometric data will be collected using tape measures and specialist anthropometers.

QUESTIONS The researcher will be pleased to answer any questions which you may have at any time.

WITHDRAWAL You are free to withdraw from the study at any time for whatever reason without prejudice.

CONFIDENTIALITY Your identity will remain confidential in any material resulting from this work.

I have read and understood the information on this form and agree to participate in this study. As far as I am aware I do not have any injury nor infirmity which would be affected by the procedures outlined.

Name _____

Signed _____(subject)

In the presence of:

Name _____

Signed _____

Date _____

APPENDIX A.2

Subject segment masses and proximal ratios derived from Yeadon's (1990b) geometric solid model and Dempster's (1955) ratio data (summarized by Winter, 1990).

	Model		Ratio	
	Mass (kg)	Proximal ratio	Mass (kg)	Proximal ratio
Head	4.187	0.84	5.702	1.000
Trunk	33.027	0.51	34.989	0.500
Upper arm	1.911	0.44	1.971	0.436
F'arm & hand	1.618	0.64	1.549	0.682
Thigh	8.616	0.44	7.040	0.433
Shank	4.616	0.44	3.274	0.433
Foot	0.807	0.35	1.021	0.500
Whole Body	72.35		70.40	
Actual	70.40			

APPENDIX B

APPENDIX B.1

Maple code to determine spring stiffness using the one spring model.

```
> #Iterating one spring model. All mass at mass centre.

> #Finds stiffness using spring angle at takeoff as criterion.

> #Takeoff is when vertical contact force falls to <1 N.

> radial:=diff(diff(x(t),t),t)=(L+x(t))*diff(theta(t),t)^2-(k/m)*x(t)-g*sin(theta(t));
```

$$radial := \frac{\partial^2}{\partial t^2}\,\mathrm{x}(t) = (L + \mathrm{x}(t))\left(\frac{\partial}{\partial t}\,\theta(t)\right)^2 - \frac{k\,\mathrm{x}(t)}{m} - g\,\sin(\theta(t))$$

```
> angular:=diff(diff(theta(t),t),t)=(-m*(L+x(t))*(2*diff(x(t),t)*diff(theta(t),t)+g*cos(theta(t)))-i
> dot*diff(theta(t),t))/(MI+m*(L+x(t))^2);
```

$$angular := \frac{\partial^2}{\partial t^2}\,\theta(t) = \frac{-m\,(L + \mathrm{x}(t))\,2\,\frac{\partial}{\partial t}\,\mathrm{x}(t)\,\frac{\partial}{\partial t}\,\theta(t) + g\,\cos(\theta(t)) - idot\,\frac{\partial}{\partial t}\,\theta(t)}{MI + m\,(L + \mathrm{x}(t))^2}$$

```
> dequs:={radial,angular}:

>

> alpha:=proc(tee)

> #Calculate angular acceleration

>    local t;

>    t:=tee;

>    (-m*(L+fx(t))*(2*fxdot(t)*fthetadot(t)+g*cos(ftheta(t)))-idot*fthetadot(t))/(MI+m*(L+fx(t))
> ^2);

> end:

>

> Rz:=proc(tee)

> #Calculate vertical reaction force

>    local t;

>    t:=tee;

>    (m*(2*fxdot(t)*fthetadot(t)+(L+fx(t))*alpha(t)+g*cos(ftheta(t))))*cos(ftheta(t))-k*fx(t)*si
> n(ftheta(t));

> end:

>
```

```
> takeoffs:=proc(tee,intvl,IMAX)

> #Uses secant iteration to find time of takeoff based on Rz falling to within Rztol(eranc
> e) of zero

>    local t0, dt0, F0, I, t1, dt1, F1;

>    t0:=tee: dt0:=intvl: F0:=Rz(t0): print (`toffs`);

>    if abs(F0)<Rztol then RETURN (eval (t0)) fi;

>    for I from 1 to IMAX do

>      t1:=t0+dt0: F1:=Rz(t1):

>      if abs(F1)<Rztol then RETURN (eval(t1)) fi;

>      dt1:=(dt0*F1)/(F0-F1):

>      if abs(dt1)>(2*intvl) then ERROR(`Probably diverging`)

>        elif abs(dt1)>(2*abs(dt0)) then ERROR(`dt values not decreasing`);

>        else t0:=t1: dt0:=dt1: F0:=F1

>      fi:

>    od:

> ERROR(`Takeoff time solution not found`);

> end:

>

> takeoffb:=proc(tee,intvl,IMAX)

> #Uses bisection method to find time of takeoff based on Rz falling to within Rztol(eran
> ce) of zero

>    local I, dt, t1,t2,t3, F1,F2,F3, count;

>    t1:=tee: dt:=intvl: F1:=Rz(t1): count:=0: print (`toffb`);

>    t3:=t1+dt:

>    F3:=Rz(t3):

>      while (F3*F1)>0 do

>        print(`No root in force interval- adjusting interval`);

>        if F1>0 then t3:=t3+dt: F3:=Rz(t3): else t1:=t1-dt: F1:=Rz(t1): fi:
```

```
>       count:=count+1: print(count);
>     od;
>     for I from 1 to IMAX do
>       print(F3,F1);
>       if abs(F1)<Rztol then RETURN (eval(t1));
>       elif abs(F3)<Rztol then RETURN (eval(t3));
>         else
>           t2:=0.5*(t1+t3):
>           F2:=Rz(t2):
>           if F1*F2<0 then   t3:=t2:   F3:=F2:
>           else t1:=t2:   F1:=F2 fi:
>       fi:
>     od;
> ERROR (`Takeoff time solution not found`);
> end:
>
> angerr:=proc(ky)
> #Calculates the difference between the spring angle at takeoff and takeoff angle criteri
> on
>     global k, f1, fx, fxdot, ftheta, fthetadot, toff1;
>     k:='k': toff1:='toff1':  f1:='f1': fx:='fx': fxdot:='fxdot': ftheta:='ftheta': fthetadot:='ft
> hetadot':
>     k:=ky: print (`aerr`);
>     f1:= dsolve(dequs union initcons,{x(t),theta(t)},type=numeric,output=listprocedure)
> :
>     fx:=subs(f1,x(t)): fxdot:=subs(f1,diff(x(t),t)): ftheta:=subs(f1,theta(t)): fthetadot:=su
> bs(f1,diff(theta(t),t)):
>     toff1:=takeoffs(0.09,0.04,20):
```

```
>       ftheta(toff1)-thetaoff;

> end:

>

> findk:=proc(kay,intvl,IMAX)

> #Finds k using the spring angle at takeoff as a criterion

> #Uses bisection method because of divergence problems with secant & regula falsi m
> ethods

>    local l, dk, k1, k2, k3, angerr1, angerr2, angerr3, count;

>       k1:=kay:   dk:=intvl:   angerr1:=angerr(k1):   count:=0: print (`fndk`);

>       if abs(angerr1)<angtol then RETURN (eval(k1)) fi;

>       k3:=k1+dk:

>       angerr3:=angerr(k3):

>       if abs(angerr3)<angtol then RETURN (eval(k3)) fi;

>       while (angerr3*angerr1)>0 do

>          print(`No root in angerr interval- adjusting interval`);

>          if angerr1>0 then k3:=k3+dk: angerr3:=angerr(k3): else k1:=k1-dk: angerr1:=ange
> rr(k1): fi:

>          count:=count+1: print(count);

>       od;

>       for l from 1 to IMAX do

>          print (`in loop`); print(angerr3,angerr1);

>          if abs(angerr1)<angtol then RETURN (eval(k1));

>          elif abs(angerr3)<angtol then RETURN (eval(k3));

>          else

>             k2:=0.5*(k1+k3):

>             angerr2:=angerr(k2):

>             if angerr1*angerr2<0 then   k3:=k2:   angerr3:=angerr2:

>             else k1:=k2:   angerr1:=angerr2 fi:
```

```
>         fi:
>       od;
> ERROR (`No stiffness solution found`);
> end:
>
> ###ASSIGN PARAMETERS, TOUCHDOWN VARIABLES AND TAKEOFF CRITERIA###
> # Data from Trial 1
>       m:=65.8: L:=1.049: MI:=9.64: g:=9.81:
>       initcons:= {x(0)=0, theta(0)=1.151, D(x)(0)=-4.36, D(theta)(0)=5.44}:
>       xdotoff:=1: thetaoff:=1.820: Rztol:=1: angtol:=0.0005:
> # # # # # # # MAIN PROGRAM # # # # # # #
> #Can choose between secant and bisection methods in takeoff time calculation,
> #need to alter call in angerr to 'takeoffs' or 'takeoffb' respectively.
> t:='t': k:='k': idot:='idot': k:=25000: idot:=0:
>    k:=findk(k,15000,15);
> print(`Final stiffness estimate is`,k);
> f1(toff1);
> restart;
>
```

APPENDIX B.2

Maple code to determine the takeoff kinematics using the one spring model.

```
> #One spring model. All mass at mass centre.

> #Finds takeoff conditions if spring stiffness is known.

> #Takeoff is when vertical contact force falls to <1 N.

> radial:=diff(diff(x(t),t),t)=(L+x(t))*diff(theta(t),t)^2-(k/m)*x(t)-g*sin(theta(t));
```

$$radial := \frac{\partial^2}{\partial t^2}\,\mathrm{x}(t) = (L + \mathrm{x}(t))\left(\frac{\partial}{\partial t}\,\theta(t)\right)^2 - \frac{k\,\mathrm{x}(t)}{m} - g\sin(\theta(t))$$

```
> angular:=diff(diff(theta(t),t),t)=(-m*(L+x(t))*(2*diff(x(t),t)*diff(theta(t),t)+g*cos(theta(t)))-i
> dot*diff(theta(t),t))/(MI+m*(L+x(t))^2);
```

$$angular := \frac{\partial^2}{\partial t^2}\,\theta(t) = \frac{-m\,(L + \mathrm{x}(t))\left(2\,\frac{\partial}{\partial t}\,\mathrm{x}(t)\right)\left(\frac{\partial}{\partial t}\,\theta(t)\right) + g\cos(\theta(t)) - idot\,\frac{\partial}{\partial t}\,\theta(t)}{MI + m\,(L + \mathrm{x}(t))^2}$$

```
> dequs:={radial,angular}:

>

> alpha:=proc(tee)

> #Calculate angular acceleration

>    local t;

>    t:=tee;

>    (-m*(L+fx(t))*(2*fxdot(t)*fthetadot(t)+g*cos(ftheta(t)))-idot*fthetadot(t))/(MI+m*(L+fx(t))
> ^2);

> end:

>

> Rz:=proc(tee)

> #Calculate vertical reaction force

>    local t;

>    t:=tee;

>    (m*(2*fxdot(t)*fthetadot(t)+(L+fx(t))*alpha(t)+g*cos(ftheta(t))))*cos(ftheta(t))-k*fx(t)*si
> n(ftheta(t));

> end:

>
```

```
> takeoffs:=proc(tee,intvl,IMAX)

> #Uses secant iteration to find time of takeoff based on Rz falling to within Rztol(eranc
> e) of zero

>    local t0, dt0, F0, I, t1, dt1, F1;

>    t0:=tee: dt0:=intvl: F0:=Rz(t0): print (`toffs`);

>    if abs(F0)<Rztol then RETURN (eval (t0)) fi;

>    for I from 1 to IMAX do

>      t1:=t0+dt0: F1:=Rz(t1):

>      if abs(F1)<Rztol then RETURN (eval(t1)) fi;

>      dt1:=(dt0*F1)/(F0-F1):

>      if abs(dt1)>(2*intvl) then ERROR(`Probably diverging`)

>        elif abs(dt1)>(2*abs(dt0)) then ERROR(`dt values not decreasing`);

>        else t0:=t1: dt0:=dt1: F0:=F1

>      fi:

>    od:

> ERROR(`Takeoff time solution not found`);

> end:

>

> takeoffb:=proc(tee,intvl,IMAX)

> #Uses bisection method to find time of takeoff based on Rz falling to within Rztol(eran
> ce) of zero

>    local I, dt, t1,t2,t3, F1,F2,F3, count;

>    t1:=tee: dt:=intvl: F1:=Rz(t1): count:=0: print (`toffb`);

>    t3:=t1+dt:

>    F3:=Rz(t3):

>      while (F3*F1)>0 do

>        print(`No root in force interval- adjusting interval`);

>        if F1>0 then t3:=t3+dt: F3:=Rz(t3): else t1:=t1-dt: F1:=Rz(t1): fi:
```

```
>         count:=count+1: print(count);
>       od;
>       for I from 1 to IMAX do
>         print(F3,F1);
>         if abs(F1)<Rztol then RETURN (eval(t1));
>       elif abs(F3)<Rztol then RETURN (eval(t3));
>           else
>             t2:=0.5*(t1+t3):
>             F2:=Rz(t2):
>             if F1*F2<0 then   t3:=t2:   F3:=F2:
>             else t1:=t2:   F1:=F2 fi:
>         fi:
>       od;
> ERROR (`Takeoff time solution not found`);
> end:
>
> ###ASSIGN PARAMETERS, TOUCHDOWN VARIABLES AND TAKEOFF CRITERIA###
> # Data from 'average trial'
>       m:=65.8: L:=1.046: MI:=9.38: g:=9.81:
>       initcons:= {x(0)=0, theta(0)=1.227, D(x)(0)=-4.19, D(theta)(0)=6.51}:
>       Rztol:=1:
> ###### MAIN PROGRAM ######

> #Can choose between secant and bisection methods in takeoff time calculation, need
> to alter call in velerr and angerr to 'takeoffs' or takeoffb' respectively

> t:='t': k:='k': idot:='idot': k:=41523: idot:=0:

> f1:= dsolve(dequs union initcons,{x(t),theta(t)},type=numeric,output=listprocedure):

> fx:=subs(f1,x(t)): fxdot:=subs(f1,diff(x(t),t)): ftheta:=subs(f1,theta(t)): fthetadot:=subs(f
```

```
> 1,diff(theta(t),t)):
> toff1:=takeoffs(0.09,0.04,20):
> f1(toff1);
> Rz(toff1);
> restart;
>
```

APPENDIX B.3

Maple code to determine leg spring stiffness using the two spring model.

```
> #Iterating two spring two mass model. One mass at mass centre, second at feet.

> #Require stiffness and damping in board.

> #Finds Kleg using spring angle at takeoff as criterion.

> #Takeoff is when vertical contact force falls to <1 N.

> radial:=diff(diff(x(t),t),t)=(L+x(t))*diff(theta(t),t)^2-(Kl/m)*x(t)-g*sin(theta(t))-diff(diff(y(t),t
> ),t)*sin(theta(t));
```

$$radial := \frac{\partial^2}{\partial t^2}\,\mathrm{x}(t) = (L + \mathrm{x}(t))\left(\frac{\partial}{\partial t}\,\theta(t)\right)^2 - \frac{Kl\,\mathrm{x}(t)}{m} - g\sin(\theta(t)) - \frac{\partial^2}{\partial t^2}\,\mathrm{y}(t)\,\sin(\theta(t))$$

```
> angular:=diff(diff(theta(t),t),t)=((L+x(t))*sec(theta(t))*(Kb*y(t)+Cb*diff(y(t),t)-Kl*x(t)*sin(t
> heta(t))+Mf*(diff(diff(y(t),t),t)+g))-idot*diff(theta(t),t))/Ml;
```

$$angular := \frac{\partial^2}{\partial t^2}\,\theta(t) = \frac{(L + \mathrm{x}(t))\sec(\theta(t))\left(Kb\,\mathrm{y}(t) + Cb\,\frac{\partial}{\partial t}\,\mathrm{y}(t) - Kl\,\mathrm{x}(t)\sin(\theta(t)) + Mf\left(\frac{\partial^2}{\partial t^2}\,\mathrm{y}(t) + g\right)\right) - idot\left(\frac{\partial}{\partial t}\,\theta(t)\right)}{MI}$$

```
> vertical:=diff(diff(y(t),t),t)=(-2*diff(x(t),t)*diff(theta(t),t)-(L+x(t))*diff(diff(theta(t),t),t)-g*co
> s(theta(t))-(Ml*diff(diff(theta(t),t),t)+idot*diff(theta(t),t))/(m*(L+x(t))))*sec(theta(t));
```

$$vertical := \frac{\partial^2}{\partial t^2}\,\mathrm{y}(t) = -2\left(\frac{\partial}{\partial t}\,\mathrm{x}(t)\right)\left(\frac{\partial}{\partial t}\,\theta(t)\right) - (L + \mathrm{x}(t))\,\frac{\partial^2}{\partial t^2}\,\theta(t) - g\cos(\theta(t)) - \frac{MI\left(\frac{\partial^2}{\partial t^2}\,\theta(t)\right) + idot\left(\frac{\partial}{\partial t}\,\theta(t)\right)}{m\,(L + \mathrm{x}(t))}\sec(\theta(t))$$

```
> dequs:={radial,angular,vertical}:

>

> alpha:=proc(tee)

> #Calculate angular acceleration

>    local t;

>    t:=tee;
```

```
>    -(sin(ftheta(t))*Kl*(fx(t)^2)*cos(ftheta(t))*m-fx(t)*Kb*fy(t)*cos(ftheta(t))*m+2*fx(t)*Mf*fx
> dot(t)*fthetadot(t)*m-fx(t)*Cb*fydot(t)*cos(ftheta(t))*m+L*sin(ftheta(t))*Kl*fx(t)*cos(fthet
> a(t))*m-L*Kb*fy(t)*cos(ftheta(t))*m-L*Cb*fydot(t)*cos(ftheta(t))*m+idot*fthetadot(t)*(cos
> (ftheta(t))^2)*m+2*L*Mf*fxdot(t)*fthetadot(t)*m+Mf*idot*fthetadot(t))/(Mf*(L^2)*m+2*L*M
> f*fx(t)*m+Ml*m*(cos(ftheta(t))^2)+Mf*(fx(t)^2)*m+Mf*Ml);

> end:

>

> Rz:=proc(tee)

> #Calculate vertical reaction force

>    local t;

>    t:=tee;

>    -Kl*fx(t)*sin(ftheta(t))+((-Ml*alpha(t)/(L+fx(t)))-(-Kb*fy(t)-Cb*fydot(t))*cos(ftheta(t)))*co
> s(ftheta(t));

> end:

>

> takeoffs:=proc(tee,intvl,IMAX)

> #Uses secant iteration to find time of takeoff based on Rz falling to within Rztol(eranc
> e) of zero

>    local t0, dt0, F0, I, t1, dt1, F1;

>    t0:=tee: dt0:=intvl: F0:=Rz(t0):

>    if abs(F0)<Rztol then RETURN (eval(t0)) fi;

>    for I from 1 to IMAX do

>      t1:=t0+dt0: F1:=Rz(t1):     print(`F0,F1`,F0,F1,I);

>      if abs(F1)<Rztol then RETURN (eval(t1)) fi;

>      dt1:=(dt0*F1)/(F0-F1):

>      if abs(dt1)>(2*intvl) then ERROR(`Probably diverging`)

>        elif abs(dt1)>(2*abs(dt0)) then ERROR(`dt values not decreasing`);

>        else t0:=t1: dt0:=dt1: F0:=F1

>      fi:

>    od:
```

```
> ERROR(`Takeoff time solution not found`);

> end:

>

> takeoffb:=proc(tee,intvl,IMAX)

> #Uses bisection method to find time of takeoff based on Rz falling to within Rztol(eran
> ce) of zero

>   local I, dt, t1,t2,t3, F1,F2,F3, count;

>   t1:=tee: dt:=intvl: F1:=Rz(t1): count:=0:

>   t3:=t1+dt:

>   F3:=Rz(t3):

>     while (F3*F1)>0 do

>       print(`No root in force interval- adjusting interval`);

>       if F1>0 then t3:=t3+(2*dt): F3:=Rz(t3): else t1:=t1-(2*dt): F1:=Rz(t1): fi:

>       count:=count+1:

>     od;

>     for I from 1 to IMAX do

>       print(F3,F1);

>       if abs(F1)<Rztol then RETURN (eval(t1));

>       elif abs(F3)<Rztol then RETURN (eval(t3));

>         else

>           t2:=0.5*(t1+t3):

>           F2:=Rz(t2):

>           if F1*F2<0 then   t3:=t2:   F3:=F2:

>           else t1:=t2:   F1:=F2 fi:

>       fi:

>     od;

> ERROR (`Takeoff time solution not found`);
```

```
> end:

>

> angerr:=proc(kleg)

> #Calculates the difference between the spring angle at takeoff and takeoff angle criteri
> on

>       global Kl, f1, fx, fxdot, ftheta, fthetadot, fy, fydot, toff1;

>       Kl:='Kl': toff1:='toff1':  f1:='f1':  fx:='fx':  fxdot:='fxdot':  ftheta:='ftheta':  fthetadot:=
> 'fthetadot': fy:=`fy`: fydot:=`fydot`:

>       Kl:=kleg:   print(`aerr`);

>       f1:= dsolve(dequs union initcons,{x(t),y(t),theta(t)},type=numeric,output=listproced
> ure):

>       fx:=subs(f1,x(t)):  fxdot:=subs(f1,diff(x(t),t)):  fy:=subs(f1,y(t)):  fydot:=subs(f1,diff
> (y(t),t)):  ftheta:=subs(f1,theta(t)):  fthetadot:=subs(f1,diff(theta(t),t)):


>       toff1:=takeoffs(0.10,0.04,20):

>       ftheta(toff1)-thetaoff;

> end:

>

> findk:=proc(kay,intvl,IMAX)

> #Finds k using the spring angle at takeoff as a criterion

> #Uses bisection method because of divergence problems with secant & regula falsi m
> ethods

> #See Borse pages 141-145

>    local l, dk, k1, k2, k3, angerr1, angerr2, angerr3, count;

>       k1:=kay:  dk:=intvl:  angerr1:=angerr(k1):  count:=0:  print(`fndk`);

>       if abs(angerr1)<angtol then RETURN (eval(k1)) fi;

>       k3:=k1+dk:

>       angerr3:=angerr(k3):

>       if abs(angerr3)<angtol then RETURN (eval(k3)) fi;
```

```
>      while (angerr3*angerr1)>0 do

>        print(`No root in angerr interval- adjusting interval`);

>        if angerr1>0 then k3:=k3+dk: angerr3:=angerr(k3): else k1:=k1-dk: angerr1:=ange
> rr(k1): fi:

>        count:=count+1: print(count);

>      od;

>      for I from 1 to IMAX do

>        print(angerr3,angerr1);

>        if abs(angerr1)<angtol then RETURN (eval(k1));

>        elif abs(angerr3)<angtol then RETURN (eval(k3));

>          else

>            k2:=0.5*(k1+k3):

>            angerr2:=angerr(k2):

>            if angerr1*angerr2<0 then   k3:=k2:   angerr3:=angerr2:

>              else k1:=k2:   angerr1:=angerr2 fi:

>        fi:

>      od;

> ERROR (`No stiffness solution found`);

> end:

>

> ###ASSIGN PARAMETERS, TOUCHDOWN VARIABLES AND TAKEOFF CRITERIA###

> # Data from 'average' trial

>      m:=64.2: L:=0.894: Ml:=9.38: g:=9.81: Mf:=1.6:

>      initcons:= {x(0)=0, y(0)=0, theta(0)=1.129, D(x)(0)=-3.24, D(y)(0)=-1.30 , D(theta)(0)=
> 5.86}:

>      thetaoff:=1.850: Rztol:=1: angtol:=0.0005:

> ####### MAIN PROGRAM #######

> #Can choose between secant and bisection methods in takeoff time calculation,
```

```
> #need to alter call in angerr to 'takeoffs' or 'takeoffb' respectively.
> t:='t': Kl:='Kl': idot:='idot': Kl:=100000: Kb:=50000: Cb:=155: idot:=0:
>    Kl:=findk(Kl,25000,15);
>    print(`Final leg stiffness estimate is`,Kl);
> f1(toff1);
> Rz(toff1);
> restart;
>
```

APPENDIX B.4

Maple code to determine the takeoff kinematics using the two spring model.

```
> #Two spring two mass model. One mass at mass centre, second at feet.

> #Finds takeoff condtions if Kleg known.

> #Require stiffness and damping in board.

> #Takeoff is when vertical contact force falls to <1 N.

> radial:=diff(diff(x(t),t),t)=(L+x(t))*diff(theta(t),t)^2-(Kl/m)*x(t)-g*sin(theta(t))-diff(diff(y(t),t
> ),t)*sin(theta(t));
```

$$radial := \frac{\partial^2}{\partial t^2}\,\mathrm{x}(t) = (L + \mathrm{x}(t))\left(\frac{\partial}{\partial t}\,\theta(t)\right)^2 - \frac{Kl\,\mathrm{x}(t)}{m} - g\sin(\theta(t)) - \frac{\partial^2}{\partial t^2}\,\mathrm{y}(t)\,\sin(\theta(t))$$

```
> angular:=diff(diff(theta(t),t),t)=((L+x(t))*sec(theta(t))*(Kb*y(t)+Cb*diff(y(t),t)-Kl*x(t)*sin(t
> heta(t))+Mf*(diff(diff(y(t),t),t)+g))-idot*diff(theta(t),t))/Ml;
```

$$angular := \frac{\partial^2}{\partial t^2}\,\theta(t) = \frac{(L + \mathrm{x}(t))\sec(\theta(t))\left(Kb\,\mathrm{y}(t) + Cb\,\frac{\partial}{\partial t}\,\mathrm{y}(t) - Kl\,\mathrm{x}(t)\sin(\theta(t)) + Mf\left(\frac{\partial^2}{\partial t^2}\,\mathrm{y}(t) + g\right) - idot\left|\frac{\partial}{\partial t}\,\theta(t)\right|\right)}{MI}$$

```
> vertical:=diff(diff(y(t),t),t)=(-2*diff(x(t),t)*diff(theta(t),t)-(L+x(t))*diff(diff(theta(t),t),t)-g*co
> s(theta(t))-(Ml*diff(diff(theta(t),t),t)+idot*diff(theta(t),t))/(m*(L+x(t))))*sec(theta(t));
```

$$vertical := \frac{\partial^2}{\partial t^2}\,\mathrm{y}(t) = -2\,\frac{\partial}{\partial t}\,\mathrm{x}(t)\,\frac{\partial}{\partial t}\,\theta(t) - (L + \mathrm{x}(t))\,\frac{\partial^2}{\partial t^2}\,\theta(t) - g\cos(\theta(t)) - \frac{\left(MI\,\frac{\partial^2}{\partial t^2}\,\theta(t) + idot\,\frac{\partial}{\partial t}\,\theta(t)\right)\sec(\theta(t))}{m\,(L + \mathrm{x}(t))}$$

```
> dequs:={radial,angular,vertical}:

>

> alpha:=proc(tee)

> #Calculate angular acceleration

>    local t;

>    t:=tee;
```

```
>    -(sin(ftheta(t))*Kl*(fx(t)^2)*cos(ftheta(t))*m-fx(t)*Kb*fy(t)*cos(ftheta(t))*m+2*fx(t)*Mf*fx
> dot(t)*fthetadot(t)*m-fx(t)*Cb*fydot(t)*cos(ftheta(t))*m+L*sin(ftheta(t))*Kl*fx(t)*cos(fthet
> a(t))*m-L*Kb*fy(t)*cos(ftheta(t))*m-L*Cb*fydot(t)*cos(ftheta(t))*m+idot*fthetadot(t)*(cos
> (ftheta(t))^2)*m+2*L*Mf*fxdot(t)*fthetadot(t)*m+Mf*idot*fthetadot(t))/(Mf*(L^2)*m+2*L*M
> f*fx(t)*m+Ml*m*(cos(ftheta(t))^2)+Mf*(fx(t)^2)*m+Mf*Ml);

> end:

>

> Rz:=proc(tee)
> #Calculate vertical reaction force

>    local t;

>    t:=tee;

>    -Kl*fx(t)*sin(ftheta(t))+((-Ml*alpha(t)/(L+fx(t)))-(-Kb*fy(t)-Cb*fydot(t))*cos(ftheta(t)))*co
> s(ftheta(t));

> end:

>

> takeoffs:=proc(tee,intvl,lMAX)
> #Uses secant iteration to find time of takeoff based on Rz falling to within Rztol(eranc
> e) of zero

>    local t0, dt0, F0, l, t1, dt1, F1;

>    t0:=tee: dt0:=intvl: F0:=Rz(t0):

>    if abs(F0)<Rztol then RETURN (eval(t0)) fi;

>    for l from 1 to lMAX do

>      t1:=t0+dt0: F1:=Rz(t1):      print(`F0,F1`,F0,F1,l);

>      if abs(F1)<Rztol then RETURN (eval(t1)) fi;

>      dt1:=(dt0*F1)/(F0-F1):

>      if abs(dt1)>(2*intvl) then ERROR(`Probably diverging`)

>        elif abs(dt1)>(2*abs(dt0)) then ERROR(`dt values not decreasing`);

>        else t0:=t1: dt0:=dt1: F0:=F1

>      fi:

>    od:
```

```
> ERROR(`Takeoff time solution not found`);

> end:

>

> takeoffb:=proc(tee,intvl,IMAX)

> #Uses bisection method to find time of takeoff based on Rz falling to within Rztol(eran
> ce) of zero

>   local I, dt, t1,t2,t3, F1,F2,F3, count;

>   t1:=tee: dt:=intvl: F1:=Rz(t1): count:=0:

>   t3:=t1+dt:

>   F3:=Rz(t3):

>     while (F3*F1)>0 do

>       print(`No root in force interval- adjusting interval`);

>       if F1>0 then t3:=t3+(2*dt): F3:=Rz(t3): else t1:=t1-(2*dt): F1:=Rz(t1): fi:

>       count:=count+1:

>     od;

>     for I from 1 to IMAX do

>       print(F3,F1);

>       if abs(F1)<Rztol then RETURN (eval(t1));

>       elif abs(F3)<Rztol then RETURN (eval(t3));

>         else

>           t2:=0.5*(t1+t3):

>           F2:=Rz(t2):

>           if F1*F2<0 then   t3:=t2:   F3:=F2:

>           else t1:=t2:   F1:=F2 fi:

>       fi:

>     od;

> ERROR (`Takeoff time solution not found`);
```

```
> end:

>

> ###ASSIGN PARAMETERS, TOUCHDOWN VARIABLES AND TAKEOFF CRITERIA###

> # Data from trial 12

>       m:=64.2: L:=0.897: MI:=9.06: g:=9.81: Mf:=1.6:

>       initcons:= {x(0)=0, y(0)=0, theta(0)=1.106, D(x)(0)=-3.60, D(y)(0)=-1.23, D(theta)(0)=6
> .39}:

>       Rztol:=1:

> # # # # # # # MAIN PROGRAM # # # # # # #

> #Can choose between secant and bisection methods in takeoff time calculation,
> #need to alter call to 'takeoffs' or 'takeoffb' respectively

> t:='t': KI:='KI': idot:='idot': KI:=500000: Kb:=32800: Cb:=136: idot:=0:

>      f1:= dsolve(dequs union initcons,{x(t),y(t),theta(t)},type=numeric,output=listproced
> ure):

>      fx:=subs(f1,x(t)):  fxdot:=subs(f1,diff(x(t),t)):  fy:=subs(f1,y(t)):  fydot:=subs(f1,diff
> (y(t),t)):  ftheta:=subs(f1,theta(t)):  fthetadot:=subs(f1,diff(theta(t),t)):

> toff1:=takeoffs(0.10,0.03,20):

> f1(toff1);

> Rz(toff1);

> restart;

>
```

APPENDIX C

APPENDIX C.1

Loughborough University of Technology
INFORMED CONSENT FORM

PURPOSE To obtain anthropometric and kinematic data of a gymnast during the hurdle step, springboard contact and pre-flight of long horse vaulting, in order to develop and evaluate a mathematical model of this activity.

PROCEDURES Video cameras will be used to collect information during the performance of handspring long horse vaults from a Gymnova 'super springboard' using a variety of run up speeds and from two board stiffness settings. A number of vaults will be requested, with suitable breaks to minimize fatigue and boredom.
Anthropometric data will be collected using tape measures and specialist anthropometers.

QUESTIONS The researcher will be pleased to answer any questions which you may have at any time.

WITHDRAWAL You are free to withdraw from the study at any time for whatever reason without prejudice.

CONFIDENTIALITY Your identity will remain confidential in any material resulting from this work.

I have read and understood the information on this form and agree to participate in this study. As far as I am aware I do not have any injury nor infirmity which would be affected by the procedures outlined.

Name _____ Date _____

Signed _____(gymnast)

In the presence of:

Name _____

Signed _____(coach)

APPENDIX C.2

Subject segment masses, proximal ratios, transverse moment of inertias and segment lengths derived from Yeadon's (1990b) geometric solid model.

	Mass (kg)	Proximal ratio	MI ($kg.m^2$)	Segment length (m)
Left forearm	1.778	0.624	0.023	0.259
Left upper arm	2.064	0.432	0.012	0.250
Left thigh	7.488	0.423	0.099	0.395
Left shank	3.185	0.425	0.038	0.400
Left foot	0.792	0.376	0.002	0.202
Right forearm	1.798	0.611	0.023	0.262
Right upper arm	2.156	0.442	0.014	0.258
Right thigh	7.924	0.426	0.113	0.411
Right shank	3.347	0.425	0.038	0.394
Right foot	0.800	0.376	0.002	0.202
Trunk	28.920	0.515	0.829	0.555
Head & neck	5.530	0.500	0.034	0.268
Whole body	65.780			

APPENDIX C.3

Maple springboard stiffness and damping estimation program.

```
> # Calculates board stiffness and damping.

> # Uses duration of contact and touchdown and takeoff velocities from drop tests as in
> puts.

> # Iterates to find the stiffness and damping which, after the known duration, result in a

> # spring-damper force of less than 0.5 N and the correct takeoff velocity.

> vmotion:=diff(diff(y(t),t),t)=-(k/20)*y(t)-(c/20)*diff(y(t),t)-g;
```

$$vmotion := \frac{\partial^2}{\partial t^2} y(t) = -\frac{1}{20} k\, y(t) - \frac{1}{20} c \frac{\partial}{\partial t} y(t) - g$$

```
> #Defines equation of motion.

>

> ypos:=dsolve({vmotion,y(0)=0,D(y)(0)=-3.698},y(t));

> #A function defining the mass position at time 't', given the initial conditions.

>

> ydot:=diff(ypos,t);

> #Defines the mass velocity at time 't'.

>

> velerr:=proc(ce)

> #Substitutes known takeoff time and current stiffness and damping estimates

> # into 'ydot' to determine velocity.

> #Calculates difference between this velocity and criterion takeoff velocity.

>    local vel;

>    subs(k=kay,c=ce,g=9.81,t=tee,rhs(ydot)):

>    vel:=evalf(''):

>    vel-voff;

> end:

>

> force:=proc(kay,ce)

> #Determines the spring-damper force at known takeoff time using current
```

```
> # stiffness and damping estimates.
>   local vel, pos;
>   subs(k=kay,c=ce,g=9.81,t=tee,rhs(ydot)):
>   vel:=evalf(''):
>   subs(k=kay,c=ce,g=9.81,t=tee,rhs(ypos)):
>   pos:=evalf(''):
>   -kay*pos-ce*vel;
> end:
>
> findc:=proc(ce)
> #Uses bisection method to find the damping value which gives a velocity
> # error of less than the tolerance, vtol.
>   local c1, c2, c3, velerr1, velerr2, velerr3, l;
>   c1:=ce: c3:=ce+25:
>   velerr1:=velerr(c1): velerr3:=velerr(c3):
>   while (velerr1*velerr3)>0 do
>     print(`No root in velerr interval-adjusting`);
>     if velerr1>0 then c3:=c3+25: velerr3:=velerr(c3): else c1:=c1-25: velerr1:=velerr(c1):
> fi:
>   od;
>   for l from 1 to 20 do
>     if abs(velerr1)<vtol then RETURN (eval(c1));
>     elif abs(velerr3)<vtol then RETURN (eval(c3));
>       else
>         c2:=0.5*(c1+c3): velerr2:=velerr(c2):
>         if velerr1*velerr2<0 then c3:=c2: velerr3:=velerr2:
>         else c1:=c2: velerr1:=velerr2  fi:
```

```
>         fi:
>    od;
>    ERROR (`No damping solution found`);
> end:
>
> findk:=proc(ky)
> #Uses bisection method to find the stiffness value which gives a spring-damper
> # force of less than the tolerance, Rztol.
>    local k1, k2, k3, f1, f2, f3, l;
>    k1:=ky: k3:=ky+5000:
>    f1:=force(k1,cee): f3:=force(k3,cee):
>    while (f1*f3)>0 do
>       print(`No root in force interval-adjusting`);
>       if f1>0 then k3:=k3+5000: f3:=force(k3,cee): else k1:=k1-5000: f1:=force(k1,cee): fi:
>    od;
>    for l from 1 to 20 do
>       if abs(f1)<Rztol then RETURN (eval(k1));
>       elif abs(f3)<Rztol then RETURN (eval(k3));
>          else
>             k2:=0.5*(k1+k3): f2:=force(k2,cee):
>             if f1*f2<0 then k3:=k2: f3:=f2:
>             else k1:=k2: f1:=f2  fi:
>          fi:
>    od;
>    ERROR (`No stiffness solution found`);
> end:
```

```
>
> # Set tolerances
> vtol:=0.0005: Rztol:=0.5:
> # Set set takeoff velocity and contact duration criteria (from drop test)
> voff:=2.681: tee:=0.0789:
> #Give initial estimates for stiffness and damping
> kay:=30000: cee:=160:
>
> ############  MAIN  PROGRAM  ###########
> # First finds damping, then stiffness. If the new stiffness estimate increases the
> # velocity error beyond the tolerance, the process repeats until the correct velocity
> # and zero force are found at the known time of takeoff.
> for n from 1 to 10 do
>    cee:=findc(cee);
>    kay:=findk(kay);
>    if abs(velerr(cee))<vtol then break fi;
> od;
> print (`Stiffness estimate `, kay); print(`Damping estimate `, cee);
> #Final checks on position, velocity and force.
> subs(k=kay,c=cee,g=9.81,t=tee,rhs(ypos)): pos:=evalf(");
> subs(k=kay,c=cee,g=9.81,t=tee,rhs(ydot)):  vel:= evalf(");
> Rz:=-kay*pos-cee*vel;
> restart;
```

APPENDIX C.4

Method to estimate peak springboard forces.

The mean vertical force exerted by the springboard can be estimated using the impulse-momentum relationship, as described in Chapter 5, section 5.3.2. In the absence of a force history, an estimate of the peak vertical force exerted by the springboard can be made by modelling the force history using a known function (in this case a sine wave) with the same mean force and duration of force (i.e. time of contact) as calculated from the actual trial. Equating the integral of the function over the time of contact to the calculated known change in momentum enables the peak force to be estimated as follows.

The equation for a sine wave is: $F(t) = F_{max}.\sin(\omega.t)$

where F_{max} is the amplitude, ω is the angular velocity and t is the time.

The duration of contact is equivalent to the first half of the sine wave, from t=0 to t=t_c, i.e. the duration of contact, t_c, is equal to the half period (T/2) of the sine wave:

Since

$$\omega = 2\pi.f$$

and

$$t_c = \frac{T}{2} = \frac{1}{2.f}$$

it follows that

$$\omega = \frac{\pi}{t_c}$$

Equating the integral of the sine function to the change in momentum from the actual trial, $m.v$-$m.u$:

$$\int_{t=0}^{t_c} F(t).dt = m.v - m.u$$

$$\int_{t=0}^{t_c} F_{max}.\sin(\omega.t).dt = m.v - m.u$$

$$F_{max}.\left[\frac{-\cos(\omega.t)}{\omega}\right]_0^{t_c} = m.v - m.u$$

$$\frac{2}{\omega}.F_{max} = m.v - m.u$$

Therefore $$F_{max} = \frac{\pi}{2}.\frac{(m.v - m.u)}{t_c}$$

Hence the peak force is equal to the mean force multiplied by $\pi/2$.

APPENDIX C.5

An example of the load-deflection graphs from each of the nine combinations of load application point and springboard adjustment setting.

(a) Load applied 0.75 m from near end, springboard at stiffest setting (adjuster 0.96 m from near end).

(b) Load applied 0.75 m from near end, springboard at intermediate setting (adjuster 1.04 m from near end).

(c) Load applied 0.75 m from near end, springboard at softest setting (adjuster 1.28 m from near end).

(d) Load applied 0.90 m from near end, springboard at stiffest setting (adjuster 0.96 m from near end).

(e) Load applied 0.90 m from near end, springboard at intermediate setting (adjuster 1.04 m from near end).

(f) Load applied 0.90 m from near end, springboard at softest setting (adjuster 1.28 m from near end).

(g) Load applied 1.05 m from near end, springboard at stiffest setting (adjuster 0.96 m from near end).

(h) Load applied 1.05 m from near end, springboard at intermediate setting (adjuster 1.04 m from near end).

(i) Load applied 1.05 m from near end, springboard at softest setting (adjuster 1.28 m from near end).

These graphs have been reduced in size from the originals by 60%. Originally each millimetre on the graph represented 0.5 mm springboard deflection (horizontal axis) and 50 N compressive load (vertical axis). On the reduced graphs 6 mm (one bold division) represents 5 mm springboard deflection (horizontal axis) and 500 N compressive load (vertical axis).

(a)

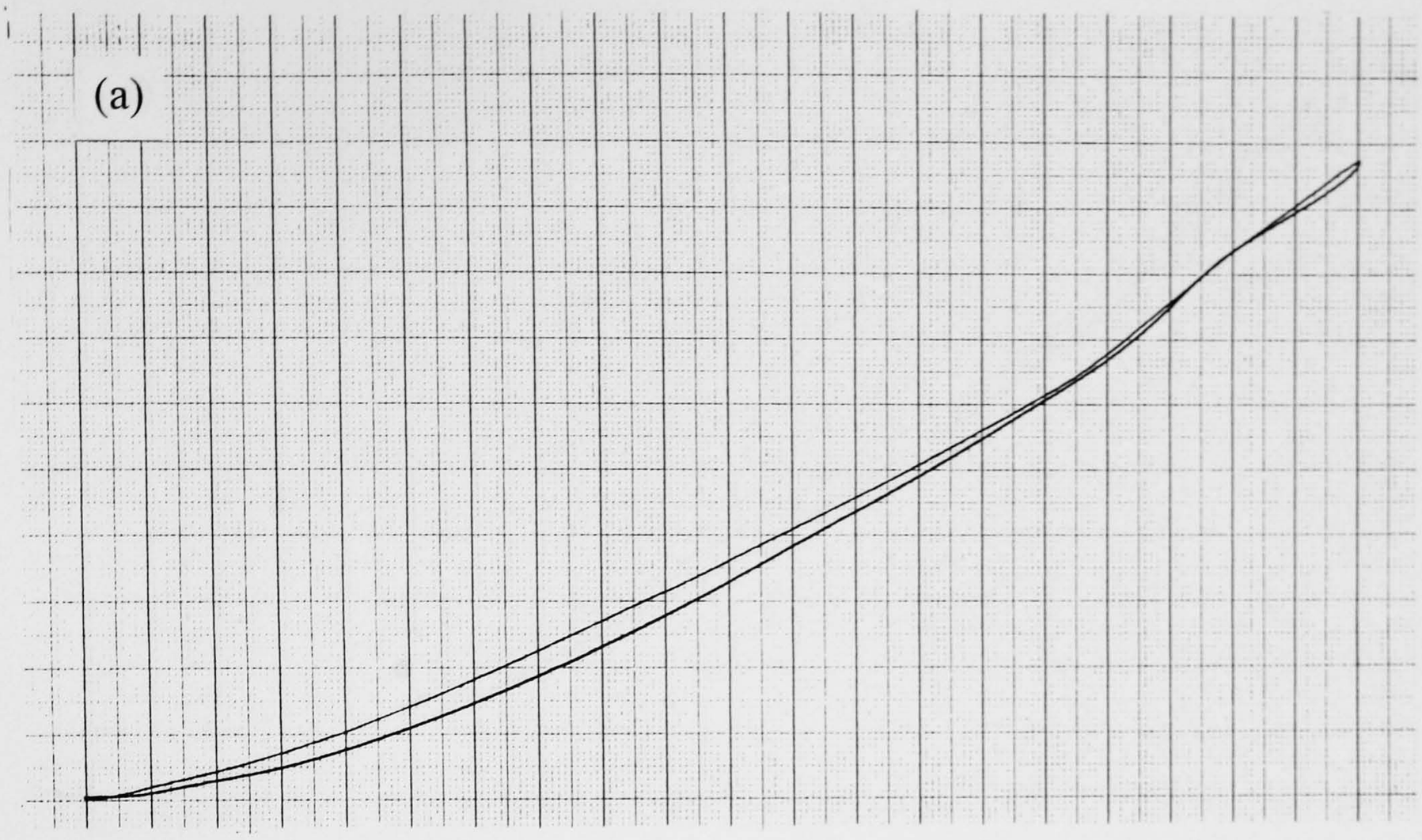

(b)

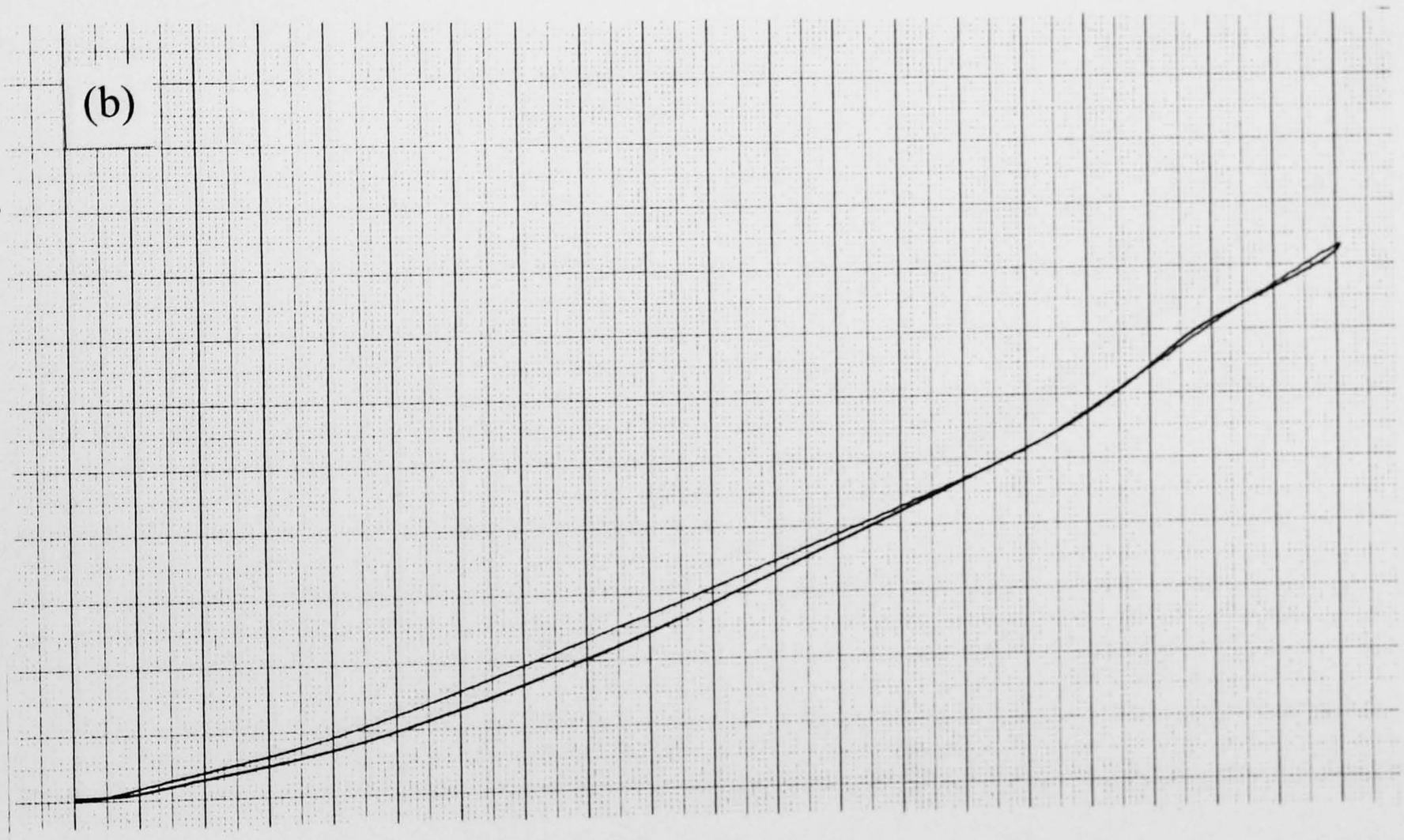

(c)

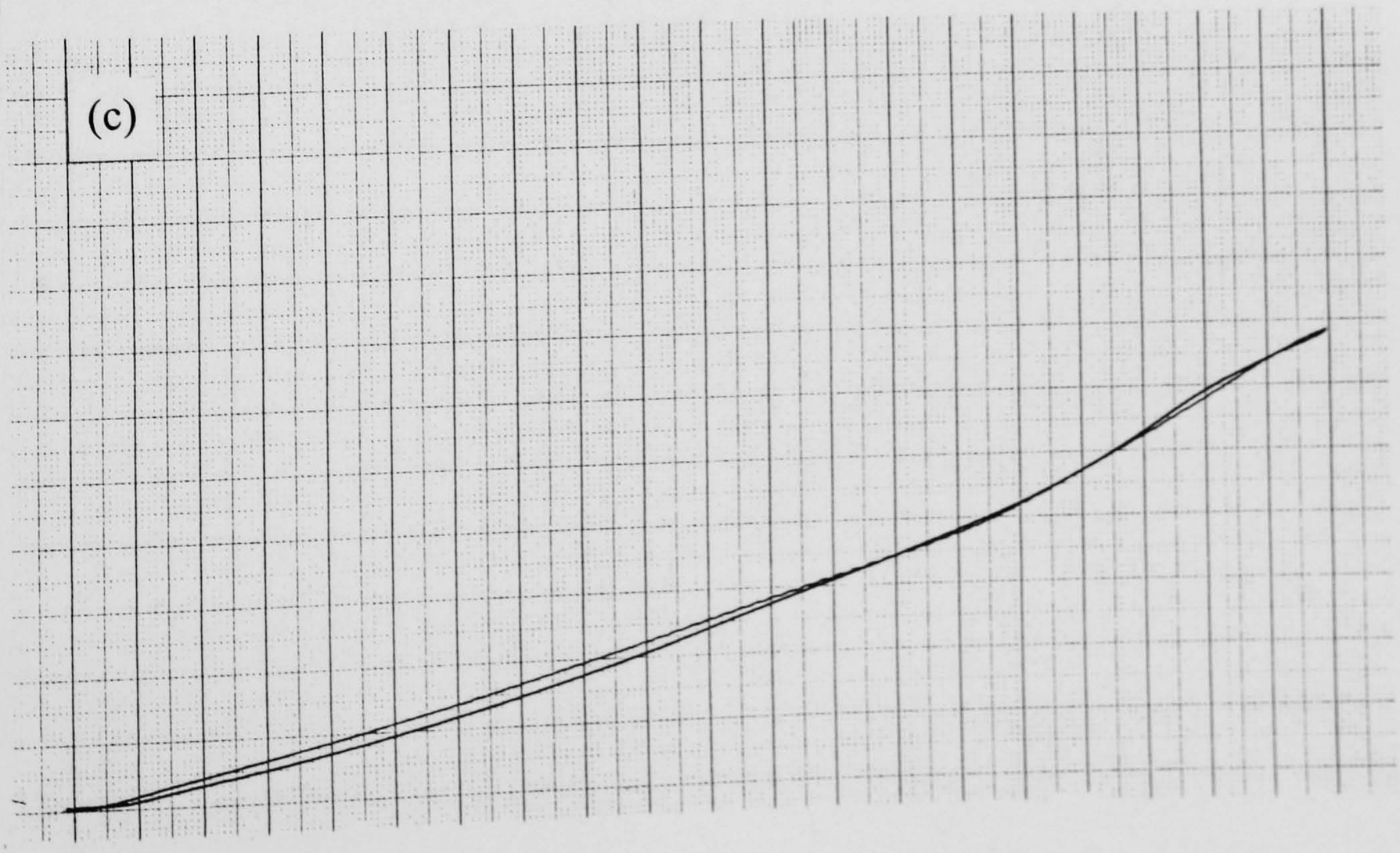

(d)

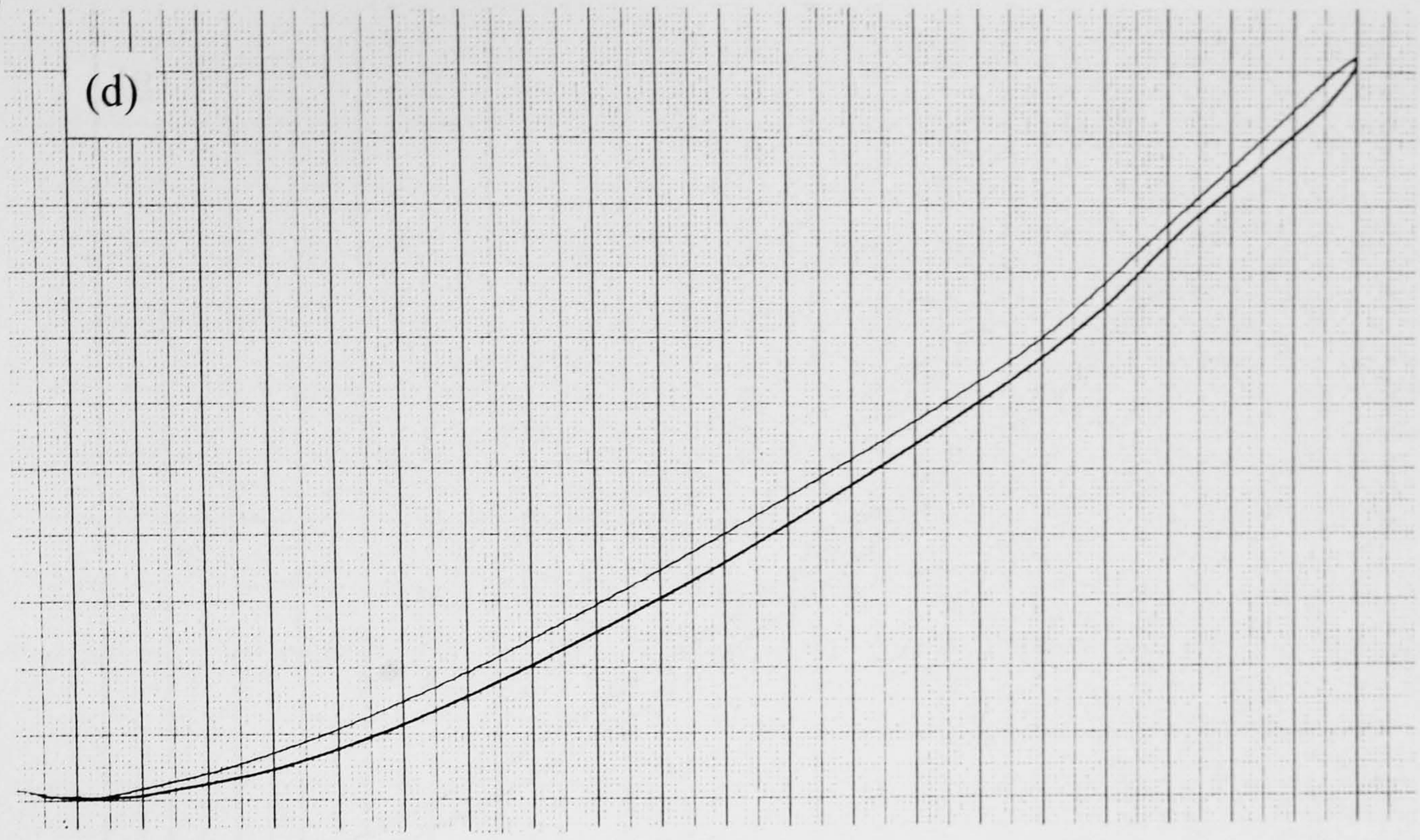

(e)

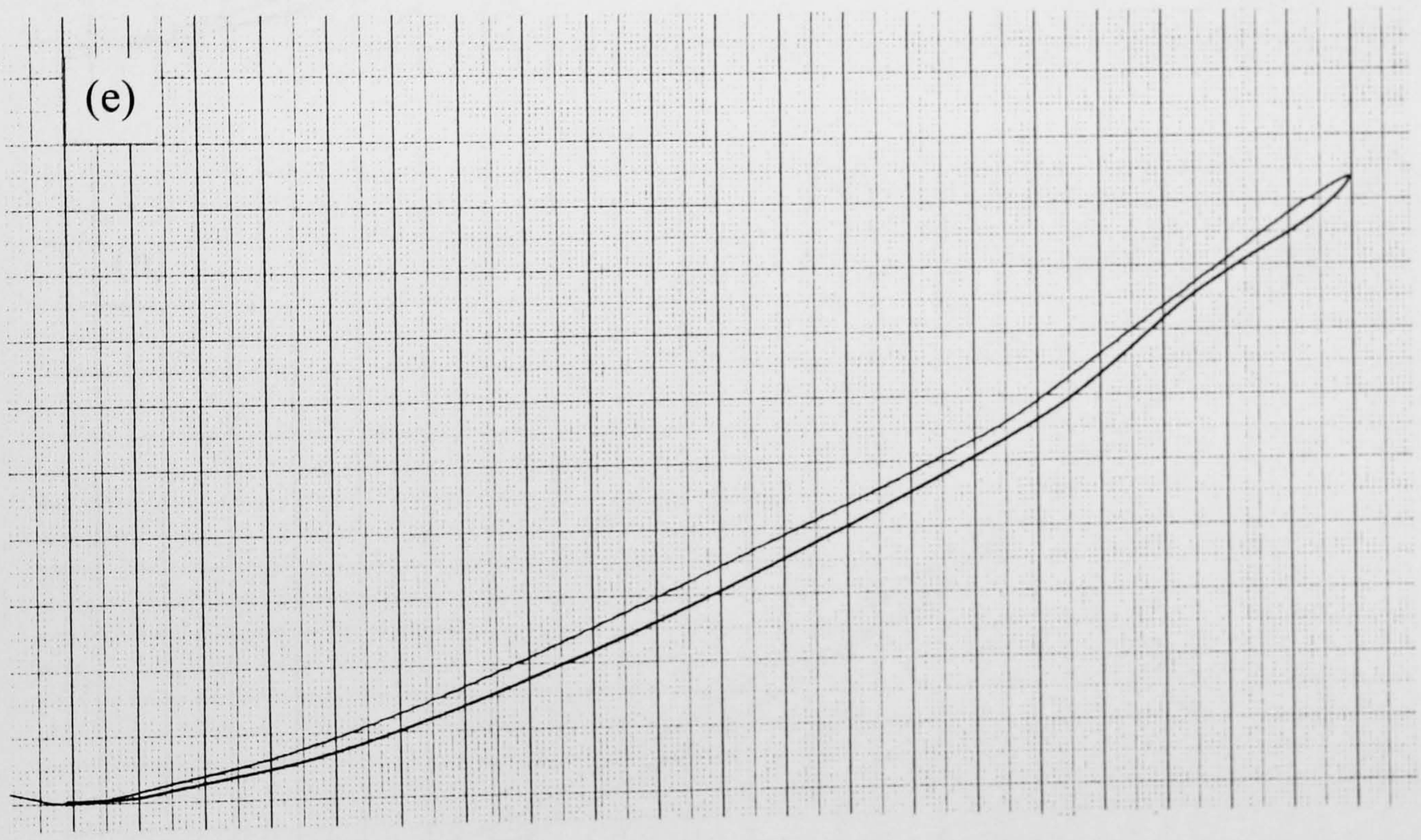

(f)

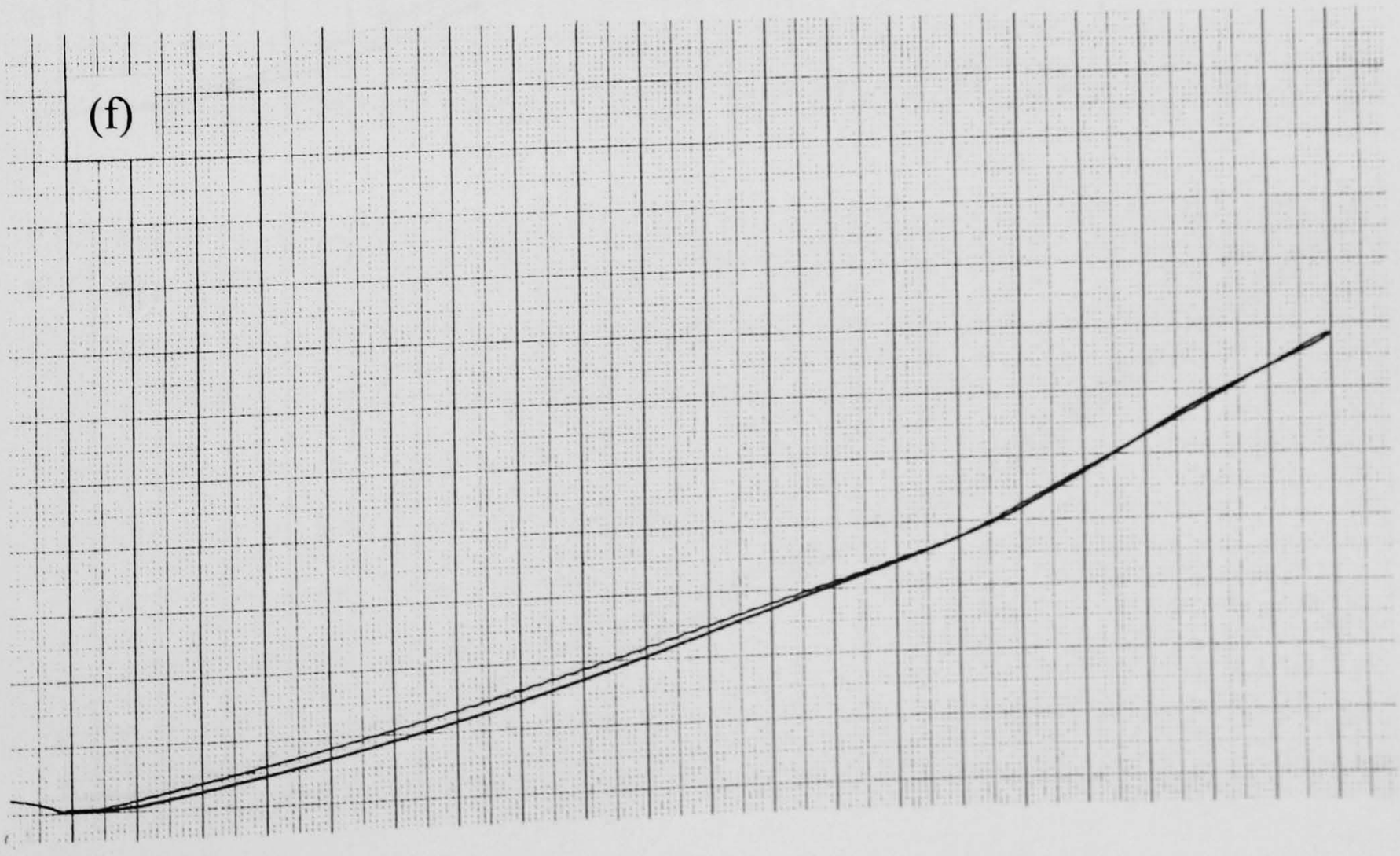

(g)

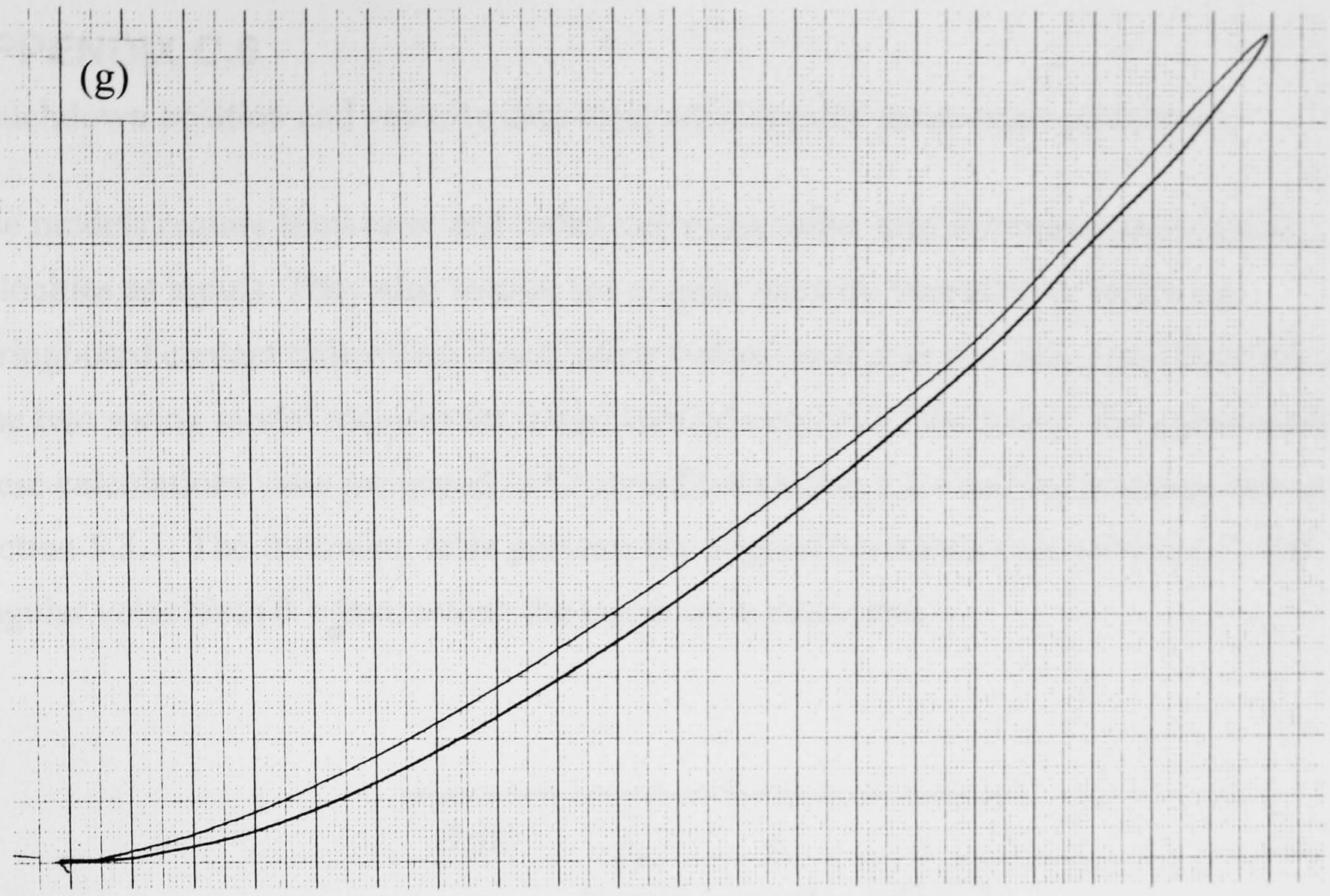

(h)

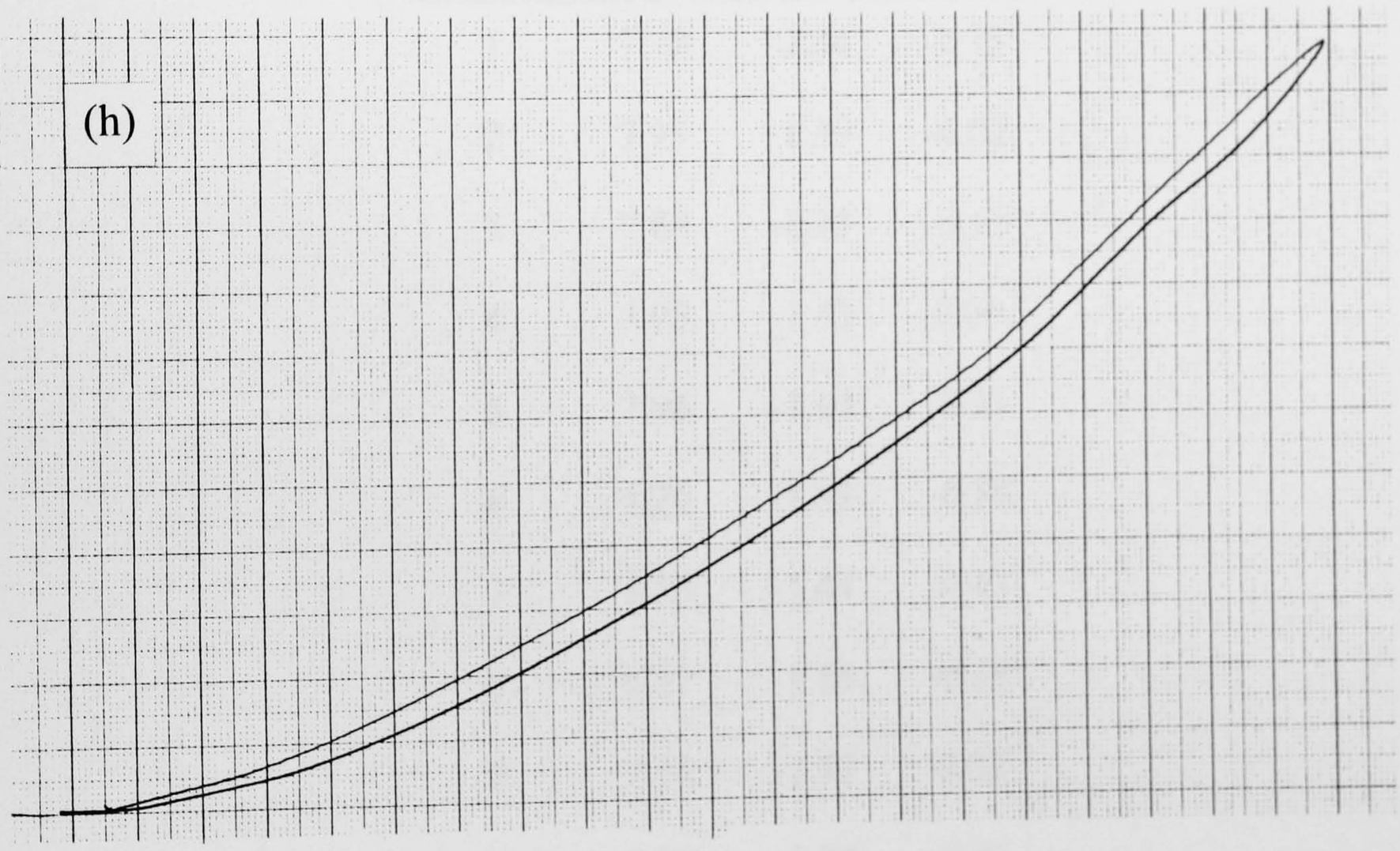

(i)

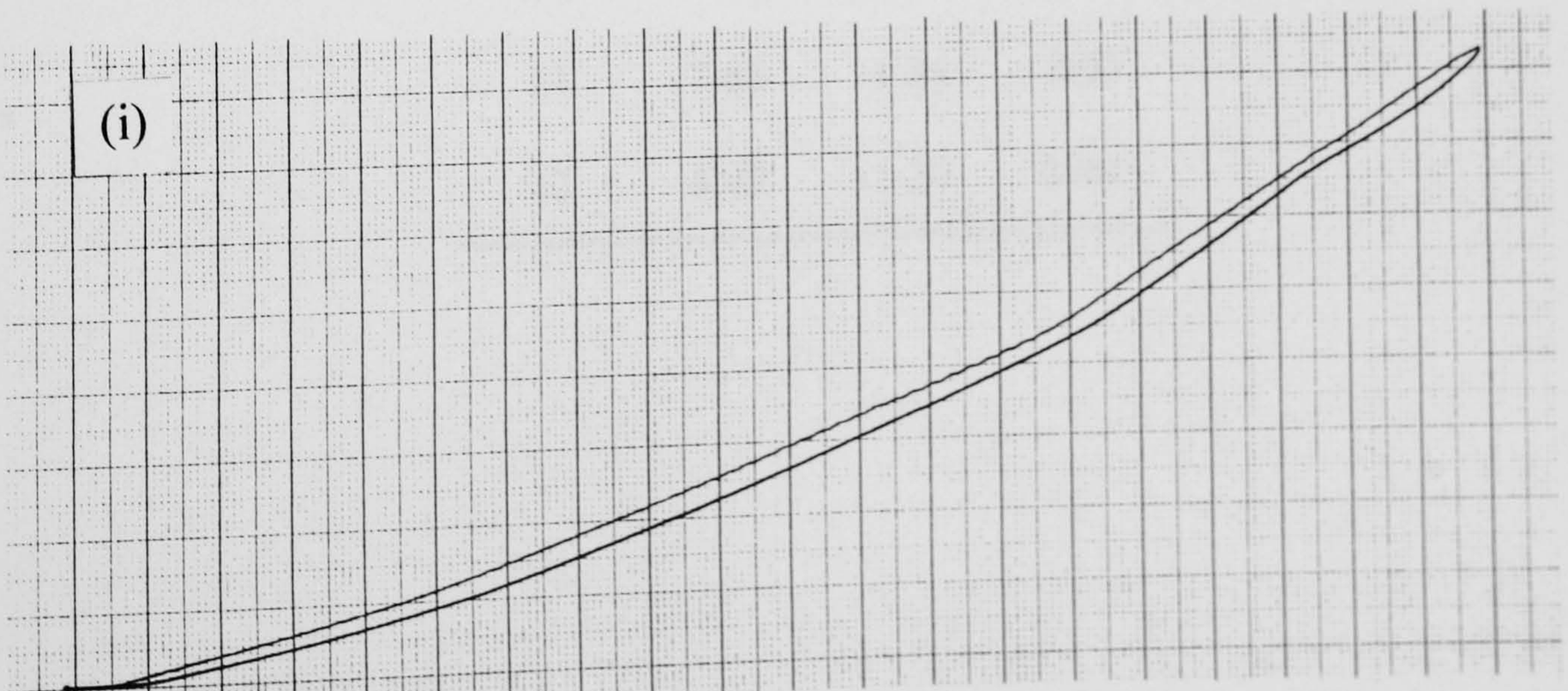

APPENDIX C.6

Touchdown position and velocity data from which model inputs were calculated.

The models require transverse and radial velocities rather than horizontal and vertical velocities as inputs. They also require the angular velocity immediately following springboard contact rather than immediately before contact as was calculated from the video. The two spring model requires the initial vertical velocity of the board. The equations for these calculations were presented in Chapter Five section 5.2.4 and the resulting data in section 5.3.1. The following table presents the original horizontal (v_h), vertical (v_v) and angular velocities ($\dot{\theta}$) from which the inputs were calculated.

Trial	v_h ($m.s^{-1}$)	v_v ($m.s^{-1}$)	$\dot{\theta}$ ($rad.s^{-1}$)
1	7.70	-1.34	-0.13
2	7.95	-1.39	-0.02
3	7.86	-1.33	-0.11
4	7.95	-1.43	0.00
5	7.94	-1.19	-0.31
6	6.21	-1.48	-0.30
7	5.55	-1.44	-0.43
8	6.57	-1.58	-0.19
9	7.14	-1.37	0.02
10	7.36	-1.24	-0.01
11	7.85	-1.35	-0.03
12	8.09	-1.20	0.08

APPENDIX D

Appendix D.1 Time of contact and takeoff velocity outputs from the one spring model simulations of vaults one to twelve, the basis for Table 6.1.

Appendix D.1 Time of contact and takeoff velocity outputs from the two spring model simulations of vaults one to twelve, the basis for Table 6.2.

APPENDIX D.1

Time of contact and takeoff velocity outputs from the one spring model simulations of vaults one to twelve, the basis for Table 6.1.

Trial	t_c (s)	$\dot{\theta}$ (rad.s^{-1})	v_h (m.s^{-1})	v_v (m.s^{-1})
1	0.106	5.39	6.54	2.79
2	0.097	5.65	6.50	3.45
3	0.103	5.32	6.30	3.64
4	0.105	5.36	6.55	3.43
5	0.112	5.26	6.50	3.37
6	0.104	4.59	5.11	2.67
7	0.116	4.27	4.77	2.06
8	0.112	4.58	5.43	2.90
9	0.119	4.82	5.94	3.03
10	0.110	5.12	6.12	3.02
11	0.115	5.15	6.50	3.35
12	0.115	5.36	6.86	3.16

APPENDIX D.2

Time of contact and takeoff velocity outputs from the two spring model simulations of vaults one to twelve, the basis for Table 6.2.

Trial	t_c (s)	$\dot{\theta}$ (rad.s^{-1})	v_h (m.s^{-1})	v_v (m.s^{-1})
1	0.112	6.52	5.88	2.21
2	0.101	6.41	5.85	3.00
3	0.106	6.08	5.65	3.18
4	0.104	6.87	6.19	2.11
5	0.111	6.50	5.97	2.50
6	0.113	5.01	4.54	2.42
7	0.116	4.83	4.31	1.81
8	0.122	5.26	4.86	2.49
9	0.113	6.05	5.49	2.15
10	0.115	6.31	5.50	2.20
11	0.117	6.43	5.87	2.44
12	0.113	7.06	6.19	2.13